THESIS FOR THE DEGREE OF DOCTOR OF PHILOSOPHY

Voltage Dip (Sag) Estimation in Power Systems based on Stochastic Assessment and Optimal Monitoring

by

GABRIEL OLGUIN

Department of Energy and Environment
Division of Electric Power Engineering
CHALMERS UNIVERSITY OF TECHNOLOGY

Göteborg, Sweden 2005

Voltage Dip (Sag) Estimation in Power Systems based on Stochastic Assessment and Optimal Monitoring
GABRIEL OLGUIN

ISBN 91-7291-594-3
Doktorsavhandlingar vid Chalmers Tekniska Högskola
Ny serie nr 2276
ISSN 0346-718x

Department of Energy and Environment
Division of Electric Power Engineering
Chalmers University of Technology
SE-412 96 Göteborg
SWEDEN
Telephone: +46 - 31 – 772 1000
Fax: +46 - 31 – 772 1633
E-mail: gabriel.olguin@ieee.org
http://www.chalmers.se

Chalmers Bibliotek, Reproservice
Göteborg, Sweden 2005

To my parents
Maria Yolanda and Manuel
My wife
Valeria
And my children
Manuel and Paola

Abstract

This dissertation deals with the statistical characterization of the performance of power systems in terms of voltage dips (sags). It presents a method named voltage dip estimation that extends monitoring results to buses not being monitored.
Statistical dip characterization of power networks is essential to decide about mitigation methods as well as for regulatory purposes. Statistics on voltage dip may be obtained by means of 1) monitoring of the power supply, and/or 2) stochastic assessment of voltage dips. Monitoring is expensive and requires long monitoring periods. Stochastic assessment is a simulation method that combines stochastic data concerning the fault likelihood with deterministic data regarding the residual voltages during the occurrence of faults. The method of fault positions is used in this work to assess the dip performance of an existing power system. An alternative analytic approach to the method of fault positions that addresses the question of the suitable number of fault positions is proposed.
It is shown that despite being able to provide a description of the long-term expected performance of the network, the method of fault positions cannot predict the performance during a particular year. Comparisons of pseudo measurements with the prediction via the method of fault positions show discrepancies and therefore the need for adjustment. A Monte Carlo simulation approach is proposed to better describe the performance of the network, and an optimal monitoring program is suggested to accomplish the adjustment of the method of fault positions. An integer optimisation model is introduced in order to determine the optimal number and location of monitors, so that every fault triggers at least a given number of power quality meters. The results of the monitoring program are then used to perform voltage dip estimation, adjusting the stochastic assessment and extending monitoring results to non-monitored buses. The dissertation shows that it is possible to profile the dip performance of the entire power system without the need for power quality monitors at every load bus of the power network.

Keywords:
power systems, power quality, voltage dips, voltage sags, stochastic methods, short-circuit faults, symmetrical components, impedance matrix, integer optimisation.

Acknowledgements

The work reported in this dissertation would not have been possible without the support from many organizations and individuals. The research work was carried out at the Department of Energy and Environment, Division of Electric Power Engineering, Chalmers University of Technology. Elforsk, Energimyndigheten, and ABB have provided the funding for this research project. Thanks are due to these institutions for their financial support.

Mats Häger (STRI AB), Ulf Grape (Vattenfall), Gunnar Ridell (Sydkraft), Mikael Dahlgren (ABB Power Technology), and Erik Thunberg (Svenska Kraftnät) participated in the industrial steering group. Thanks to all them for their active role in discussions and careful reading of the first draft of this dissertation.

Professor Jaap Daalder, examiner of this work, carefully read the manuscript and gave me helpful comments and suggestions. Gratitude is also expressed for the constant support and encouragement.

Dr. Daniel Karlsson (Gothia Power) provided supervision of this work during the second stage of the project. Professor Math Bollen (STRI AB - LTU) introduced me into the research field and gave me the opportunity to undertake the PhD program at the Department of Electric Power Engineering, Chalmers University of Technology. Both did an excellent job in guiding me through the path connecting practical engineering and scientific research.

My stay at The University of Manchester was a fruitful experience for which I would like to thank professor Daniel Kirschen (The University of Manchester, UK) and my financial sponsors. Appreciation is extended to the members of the research group, in particular to Dr. Gupta, Dr. Djokic, and Dr. Aung for interesting discussions about various aspects regarding voltage dips. Thanks also to Dr. Ivana Kockar and Ms. Ding for their friendship and interesting discussions regarding integer optimisation.

I wish to thank the researchers that have collaborated in some of the joint papers at international conferences. Roberto Leborgne has been my nearest collaborator in studying voltage dips. Ms. Marcia Martins

helped me to understand the effect of voltage dips on wind power installations. Professor Paola Verde (U. Casino, Italy) and her student Di Perna made possible our joint publication on voltage dip system indices at PMAPS 2004. Professor Jorge Coelho (UFSC, Brazil), my supervisor during my MSc at Federal University of Santa Catarina, made possible my participation at Induscon 2004. Professor Miguel Arias (USACH, Chile) and his student Marcelo Aedo helped me to finish the paper on Monte Carlo simulation submitted to IEEE T&D Asia. Dr Vuinovich (U. Palermo, Italy) helped me to understand genetic algorithms and actively participated in our joint publication at IEEE TPWRS. Professor Juan A. Martinez (ETSEIB, Spain) let me get involved in the CIGRE TF on Voltage Dips Evaluation and Predictions Techniques. They have all contributed to the success of this project.

Gabriel Olguin
Gothenburg, May 2005

Contents

1 Introduction

This chapter contains a general introduction to power quality with special emphasis on voltage dips or sags. Effects of voltage dips are presented for a selected number of equipment types. Voltage dips from a perspective of electromagnetic compatibility are discussed. The need for voltage dip statistics for decision-making regarding mitigation methods as well as for regulatory purposes is highlighted. A literature review has been done and the description of the project and the outline of this dissertation are presented. The chapter concludes with the list of publications.

1.1 Power Quality

There is an international agreement regarding the importance of reliability and power quality and several research groups work on the subject around the world. Reliability should be interpreted here as the continuity of the electric supply. This term is well understood, but there is no a real consensus about the meaning of the term power quality. According to the Standard IEEE 1100 (IEEE Std 1100, 1999) power quality is "*the concept of powering and grounding electronic equipment in a manner suitable to the operation of that equipment and compatible with the premise wiring system and other connected equipment*". This is an appropriate definition of power quality for electronic equipment, however not only electronic devices are subject to failures due to poor quality. Heydt (1991) gives another interpretation of electric power quality in his book Electric Power Quality. For this author electric power quality broadly refers to maintaining a near sinusoidal bus voltage at rated magnitude and frequency. Dugan et al. (1996) propose an even broader definition of power quality problems, stating that it is "*Any power problem manifested in voltage, current, or frequency deviations that result in failure or malfunction of customer equipment*". However not only customer equipment is subject to power quality problems. For instance the increase of the third harmonic current in the neutral of delta-wye connected distribution transformers has motivated the re-sizing of the neutral conductors to avoid overheating, losses and potential faults. Some authors use the term voltage quality and others use quality of the power supply to refer to the same concept power quality. The term clean power usually is used to refer to the supply that does not contain intolerable disturbances.

What is clear is that all these terms refer to the interaction between the load and the network supply. In this dissertation, the following

definition is adopted for being the most complete and most appropriate for the new deregulated scenario of the power industry (Bhattacharya et al. 2001).

"*Power Quality is the combination of current quality and voltage quality, involving the interaction between the system and the load. Voltage quality concerns the deviation of the voltage waveform from the ideal sinusoidal voltage of constant magnitude and constant frequency. Current quality is a complementary term and it concerns the deviation of the current waveform from the ideal sinusoidal current of constant magnitude and constant frequency. Voltage quality involves the performance of the power system towards the load, while current quality involves the behaviour of the load towards the power system*".

The work presented in this dissertation belongs to the power quality knowledge area, however it is restricted to one specific disturbance called voltage dip or voltage sag. The causes and effects of dips will be reviewed in the coming sections, but before that a discussion about general aspects of power quality is presented.

1.2 Interest in Power Quality

The main concern of consumers of electricity is the continuity of the supply, i.e. the reliability. However, nowadays consumers not only want reliability, but quality too. For example, a consumer that is connected to the same bus that supplies a large motor load may face sudden voltage depressions (dips or sags) every time the motor is started. Depending on the sensitivity of the consumer's load this voltage depression may lead to a failure or disconnection of the entire plant. Although the supply is not interrupted the consumer experiences a disturbance – a voltage dip- that causes an outage of the plant. There are also very sensitive loads such as hospitals, processing plants, air traffic control, financial institutions, etcetera that require uninterrupted and clean power.

Several reasons have been given to explain the current interest in power quality (Bhattacharya et al. 2001).

- Equipment has become less tolerant to voltage disturbances. Industrial customers are much more aware of the economical losses that power quality problems may cause in their processes.
- Equipment causes voltage disturbances. Often the same equipment that is sensitive to voltage disturbances will itself cause other voltage disturbances. This is the case with several power converters.

- The need for performance criteria. There is an increasing need for performance criteria to assess how good the power companies do their job. This is especially important for the monopolistic part of the chain formed by generation, transmission, and distribution of electricity. The natural monopoly that transmission and distribution companies possess, even in the deregulated markets, requires a quality framework where compulsory quality levels are given. Regulator bodies will have to create such a quality framework in terms of power quality indices.
- Power quality can be measured. The availability of power quality monitors means that voltage and current quality can actually be monitored on a large scale.

1.3 Voltage Sag or Voltage Dip?

According to the Standard IEEE 1346 (IEEE Std 1346, 1998) a voltage sag is "*a decrease in rms voltage or current at the power frequency for durations of 0.5 cycle to 1 minute*". To give a numerical value to a sag, the recommended usage is "a sag to X%", which means that the line voltage is reduced down to X% of the normal value.

The International Electrotechnical Commission, IEC, has the following definition for a dip (IEC 61000-2-1, 1990). "*A voltage dip is a sudden reduction of the voltage at a point in the electrical system, followed by a voltage recovery after a short period of time, from half a cycle to a few seconds*".

From the previous definitions it is evident that both voltage sag and voltage dip refer to the same disturbance. Moreover, the draft Technical Report for Electromagnetic Compatibility (IEC 61000-2-8, 2002) regarding voltage dips and short interruption on public electric power systems states, "*voltage sag is an alternative name for the phenomenon voltage dip*". In this work, both terms dip and sag are used as synonym of each other. To give a value to a voltage dip, the residual voltage will be used in this dissertation

A voltage dip is a multidimensional electromagnetic disturbance, the level of which is mainly determined by the magnitude and duration. Magnitude of a voltage dip is the value of residual voltage during the event. Duration of dip is time for which the rms voltage stays below a voltage dip threshold.

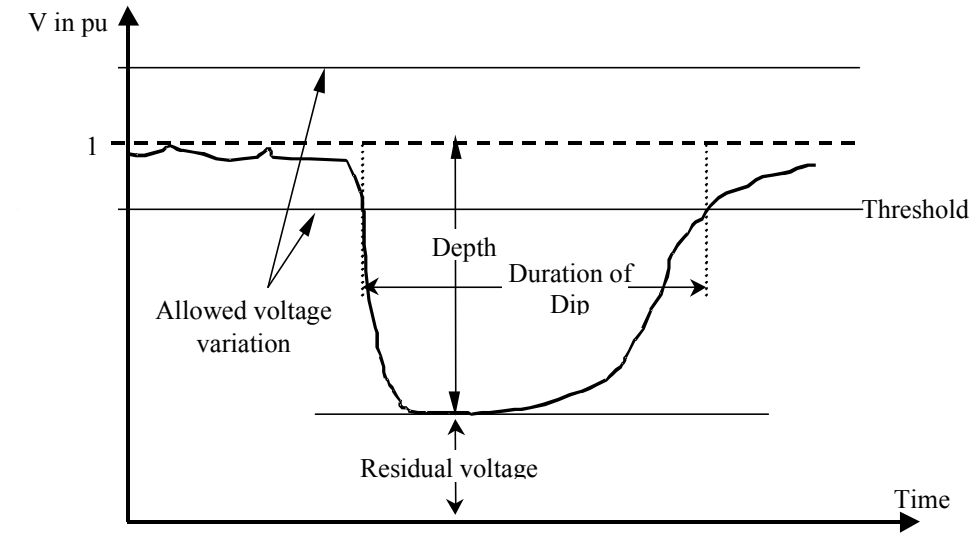

Figure 1.1: Voltage dip and its characteristics

Typically, a dip is associated with the occurrence and termination of a short-circuit fault or other extreme increase in current like motor starting, transformer energising, etc. The dip is characterised by its duration and its residual or retained voltage, which is the lowest rms voltage during the event. The duration of the dip is the time between the instant at which the rms voltage decreases at least to a value below the start threshold and the instant at which it rises above the end threshold (at a particular point of the electricity network). Figure 1.1 illustrates a single-phase dip and its basic characteristics. It should be noted that the starting and ending threshold might not be equal.

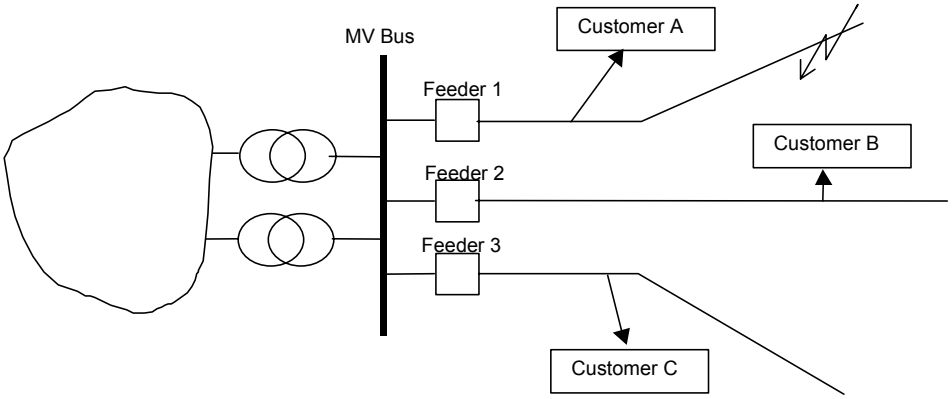

Figure 1.2: Voltage dip caused by a fault

This dissertation focuses on fault-caused dips. Figure 1.2 shows a distribution system with three feeders. Consider customer A located in feeder 1. If there is a fault downstream of the customer position, then A will experience a reduction in the voltage due to the large current flowing through the transformers and feeder followed by an interruption due to the operation of the main protection at the

beginning of the feeder. Customers B and C will not be interrupted but they will see a dip because the fault current, flowing through the transformers, will cause a voltage drop at the MV bus.

1.4 Effects of Voltage Dips

Many sensitive loads cannot discriminate between a dip and a momentary interruption. The severity of the effects of voltage dips depends not only on the direct effects on the equipment concerned, but also on how important the function carried out by that equipment is. Modern manufacturing methods often involve complex continuous processes utilising many devices acting together. A failure of one single device, in response to a voltage dip, can stop the entire process. This may be one of the most serious and expensive consequences of voltage dips. However, such damage or loss is a function of the design of the process and is a secondary effect of the voltage dip. Some of the most common direct effects are described in this section; secondary effects are discussed in relation to their economic impact in the next section.

1.4.1 IT and Process Control Equipment

The principal units of this category of equipment require direct current (dc) supplies. These dc supplies are provided by means of modules that convert the alternating current (ac) supply from the public power supply system.

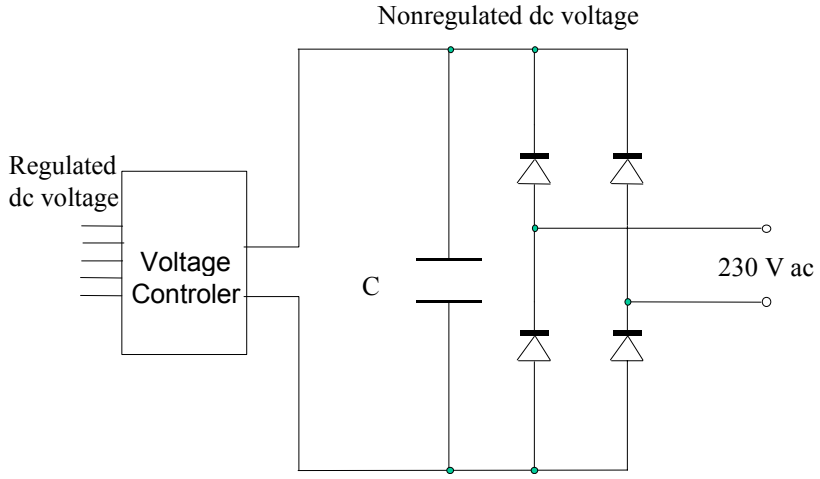

Figure 1.3: Regulated dc power supply

It is the minimum voltage reached during a voltage dip that is significant for the power supply modules. A simplified configuration of a dc power supply is shown in Figure 1.3.
The capacitor connected to the non-regulated dc bus reduces the ripple at the input of the voltage regulator. The voltage regulator converts the non-regulated dc voltage into a regulated dc voltage of a few volts and feeds sensitive digital electronics. If the ac voltage drops, so does the voltage at the dc side. The voltage regulator is able to keep its output voltage constant over a certain range of input voltage. If the dc voltage becomes too low the regulated dc voltage will start to drop and ultimately errors will occur in the digital electronics.

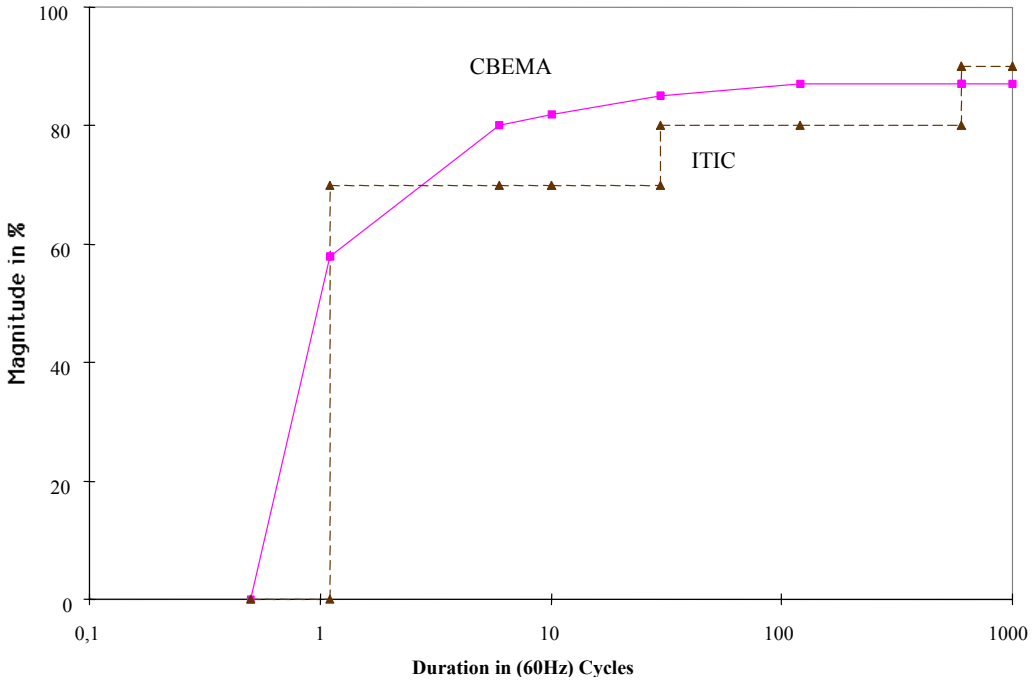

Figure 1.4: CBEMA and ITIC curve (reproduced from Bollen, 1999)

A common way to present the sensitivity of this category of equipment is by means of a voltage tolerance or power acceptability curve. The Computer Business Equipment Manufacturers Association (CBEMA) developed the most known of these curves. The purpose was to set limits to the withstanding capabilities of computers in terms of magnitude and duration of the voltage disturbances. The Information Technology Industry Council (ITIC) redesigned the CBEMA curve in the second half of the 1990s. The new curve is therefore referred to as ITIC curve and is the successor of the CBEMA curve. The work reported here focuses in dips and thus in the lower part of the ITIC and CBEMA curve, see Figure 1.4.

1.4.2 Contactors and Asynchronous Motors

Alternating current contactors (and relays) can drop out when the voltage is reduced below about 80% of the nominal for a duration of more than one cycle, i.e. a sag to 80%. A recent paper (Pohjanheimo et al., 2002) has presented test results for contactor sensitivity. The main conclusion states that most of the contactors open when the voltage drops below 50%, but the most sensitive ones tolerate only a 30% voltage depression. It is also stated that dip duration does not have a practical relevance but the point-on-wave of dip initiation affects the contactor performance significantly.
The point of operation of an asynchronous motor is governed by the balance between the torque-speed characteristic of the motor and that of the mechanical load. The torque-speed characteristic of the motor depends on the square of the voltage. During a voltage dip, the torque of the motor initially decreases, reducing the speed, and the current increases until a new point of operation can be reached. Severe dips are equivalent to short interruptions in their effect on the operation of the motor. Depending on the ratio of the total inertia to the rated torque -the mechanical time constant- two different behaviours are found:

- Mechanical time constant low compared with the duration of the dip. The speed decrease is such that the motor virtually stops.
- Mechanical time constant high compared with the duration of the dip. In this case, the motor speed decreases slightly. However, there is the possibility of the back electromotive force (emf) being in phase opposition to the supply voltage during the recovery, resulting in an inrush current greater than the normal starting current. The high inrush current at the voltage recovery can produce a second voltage drop retarding the re-acceleration of motors to normal speed.

1.4.3 Power Drives

Power drives can be very sensitive to voltage dips. Such systems generally contain a power converter/inverter, motor, control element and a number of auxiliary components. The effect on the control element can be critical, since it has the function of managing the response of the other elements to the voltage dip. The reduction in the voltage results in a reduction in the power that can be transferred to

the motor and hence to the driven equipment. Dips can lead to a loss of control (Stockman, 2003). Tripping of power drives can occur due to several phenomena (Bollen, 1999):

- The drive controller or protection detects the sudden change in operation conditions and trips the drive to prevent damage to the electronics components.
- The drop in the dc bus voltage causes failed operation or tripping of the drive controller.
- The increased ac currents during the dip or the post-dips overcurrents charging the capacitor cause an overcurrent trip or blowing of fuses protecting the electronics components.

1.5 Customer Damage Cost Due to Voltage Dips

Due to the advancement and proliferation of information technology and the widespread use of power electronic devices in recent years, utilities' customers in various industrial fields are suffering economic losses from short interruptions and voltage dips. Losses caused by a voltage dip may only be an annoyance for residential customers (as a shutdown of a personal computer) but in the industrial and commercial sectors the same event may cost millions of euros, as it will be illustrated in this section.

In contrast to the reliability of power supply, which is a well-understood and mature topic, the voltage dip phenomenon is currently being studied and the evaluation of customer damage cost due to voltage dips is still poorly explored. The assessment of customers' cost due to unreliability is a difficult but well documented task (Wacker, 1989). Customers' surveys are seen by most researchers as the most effective way to evaluate cost of unreliability. With this method customers are asked to estimate their cost or losses due to supply interruptions of varying duration and frequency, and at different times of the day and the year. It is generally accepted that the customer is in the best position to assess losses and this is the strength of this method. Similar surveys have been conducted to estimate damage cost due to voltage dips. Figure 1.5 (Pohjanheimo, 2003) summarises results from a survey in which 400 industrial customers of various categories were asked about costs due to a voltage sag to 50% lasting for 200 ms. The curve shows that 150 of those 400 customers did not have losses due to voltage dips. It also shows, however, that the same sag may lead to losses in the range of tens thousands of euros for a few industrial customers. It is evident

that certain types of industries are very sensitive to the events object of this research.

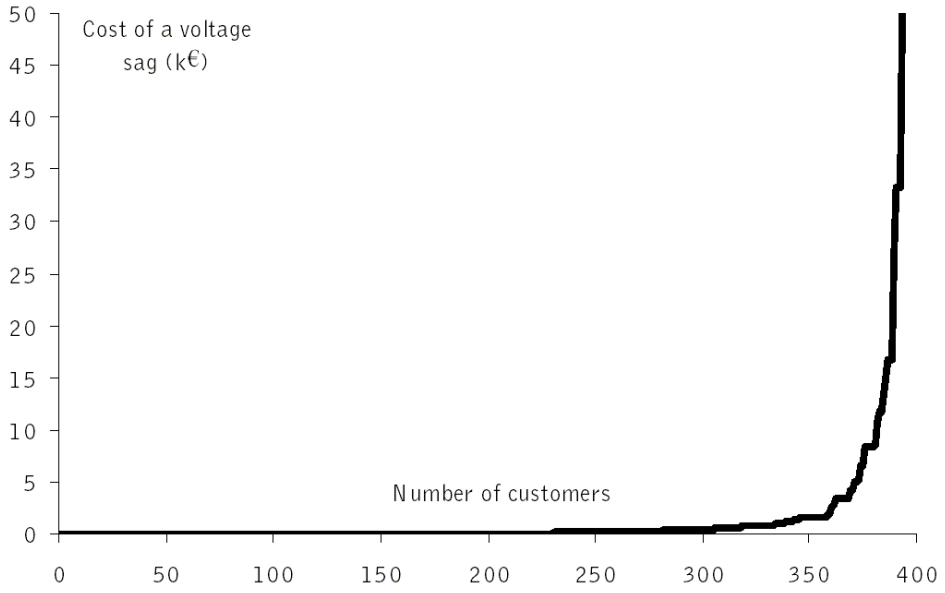

Figure 1.5: Reported industrial cost due to a voltage dip with residual voltage 50% lasting 200 ms (Pohjanheimo, 2003)

The semiconductor industry is usually mentioned as the one most sensitive to voltage dips and short interruptions. It has been reported (Shih-An Yin, 2001 and 2003) that the average interruption cost faced by the high tech industry in Taiwan ranges from about 55 000 USD for a short interruption up to 425 000 USD for a 24 hours stoppage. Many machines in a typical semiconductor factory contain power drives and control circuits that are very sensitive to voltage dips. A disturbance can cause these machines to malfunction or shut down after which a time-demanding restart procedure is needed.
The pharmaceutical industry is also sensitive to voltage dips. Production is often conducted in batches and therefore a disturbance in one process may stop the complete line leading to huge losses. Pumps, boilers, autoclaves, valves, and control device act together and are coordinated to obtain the final products. Hence a disturbance in any device may stop the entire process.
Not only high tech processes are sensitive to voltage dips. In metal processes, for example, it has been found that cost due to interruption (Carlsson, 2003) may reach as much as €100 000 per hour. The report

(Carlsson, 2003) describes three metal processes. The blast furnace, hot rolling and cold rolling processes are analysed with regard to sensitivity to voltage sags. The blast furnace and hot rolling processes are briefly reviewed here.

A blast furnace is used as one of the first steps in the production of iron and steel. Iron is produced by feeding iron-ore and coke into the top of a furnace and by blowing hot air (about 1000 ^{o}C) into the bottom of the furnace. Molten iron and slag is formed. The molten iron is drained into large containers through draining holes. The blower (fed by a synchronous machine) compresses and blows air via pipelines and heaters to the blast furnace. If the synchronous machine unexpectedly stops during production, the overpressure in the pipelines falls to zero; something that may result in production losses or worse in making the furnace unusable due to the solidification of iron and slag in the air pipes of the blast furnace. The normal case is that the furnace can still be used, however it takes about 24 hours to get the furnace in production after a stoppage and the production losses per hour may reach € 10 000.

The hot rolling mill is used in various industrial processes. A rolling mill rolls ingots of metal or alloys to make them thinner. There are many type of rolling mills, some roll hot whereas others roll cold. The hot roll mill studied by Carlsson (Carlsson, 2003) is a steel rolling mill and consists of two synchronous machines, each having a rated power of 11.2 MW. The rolls are driven individually; each one having a synchronous machine and power drive. The main problem with voltage dips in a hot rolling mill is the downtime. Since the steel slab has a temperature of about 1000 ^{o}C, the steel slab may deform the rolls due to the heating. During normal operation this does not occur because water is sprayed to cool the rolls. But when the slab gets stuck due to an unexpected stop, it is not possible to cool down the rolls at the contact area and the rolls may have to be replaced with new ones. This may cost as much as € 10 000 and take one working day.

In summary, the disruption of an industrial process, no matter the cause, can result in very substantial costs. Figure 1.6 (Andersson, 2002) illustrates the range of customers' costs due to voltage dips and short interruptions. Manufacturing facilities have interruption costs ranging up to tens millions of euros. These costs include damaged products, delays in delivery, damage in equipment and processes and reduced customer satisfaction.

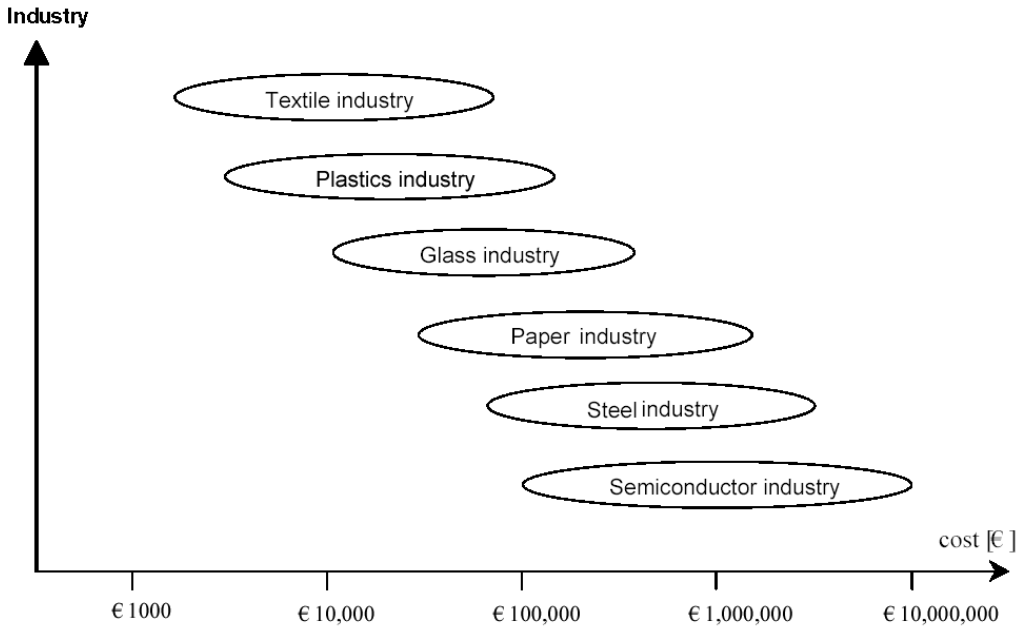

Figure 1.6: Customer's cost in different industries (Andersson, 2002)

1.6 Dips and Electromagnetic Compatibility

The International Electrotechnical Commission defines electromagnetic compatibility (IEC 61000-2-1, 1990) as "*the ability of a device, equipment or system to function satisfactorily in its electromagnetic environment without introducing intolerable electromagnetic disturbances to anything in that environment*". In the standardisation area, EMC is used in a broad sense. The aim is to ensure the compatibility through a good co-ordination of immunity levels of sensitive loads and the electromagnetic environment to which they are exposed. In the case of voltage dips, the electromagnetic environment is determined by the occurrence of events in the power network such as faults, transformer energising or motor starting.

Co-ordination between user's equipment and power supply is needed to avoid overspending on spurious outage cost (consumers cost) or network improvements (utility cost). Before connecting a sensitive device or equipment to the electrical network to get supply, it is necessary to assess the compatibility between the device and the supply. Voltage dips, as other power quality phenomena, should be treated as a compatibility problem between equipment and supply.

To assess the compatibility, it is necessary to determine the equipment's sensitivity. This information can be obtained from equipment manufacturers, doing tests or taking typical values from

the technical literature. A typical representation of this information is the voltage tolerance or power acceptability curve presented in Figure 1.4, page 6.

In addition to the description of the equipment sensitivity, it is necessary to determine the expected electrical environment. The traditional way to do this is by means of power quality monitoring. The main purpose of a motoring program is to support the description of the expected electrical environment for end-user's equipment. However, this strategy is costly and time demanding. Monitoring presents limitations when used to estimate frequencies of non-frequent events at a single site. It has been reported (Bollen, 1999) that the monitoring interval required is one year to obtain a 10% accuracy when the expected average rate is around 1 per day. If the expected event rate is 1 per month 30 years of monitoring are needed to obtain a 10% accuracy. Table 1.1 reproduces the results reported in (Bollen, 1999). Table 1.1 is based on the assumption that time-between-events is exponentially distributed, which means that the number of events within a certain period is a stochastic variable with a Poisson distribution. Under that condition for an event with a frequency of μ times per year, the monitoring period should be at least $4/(\mu.\varepsilon^2)$ to obtain an accuracy ε.

Table 1.1: Monitoring Period Needed to Obtain a Given Accuracy (Bollen, 1999)

	required accuracy		
Event Frequency	**50%**	**10%**	**2%**
1 per day	2 weeks	1 year	25 years
1 per week	4 months	7 years	200 years
1 per month	1 years	30 years	800 years
1 per year	16 years	400 years	10,000 years

Event frequencies are needed to estimate the number of expected tripping of equipment due to power quality events. Therefore, also low frequencies of one event per month or even one event per year are important.

In this work, stochastic prediction methods are proposed for the characterisation of the electrical environment, but monitoring should not be put aside. Monitoring is needed for the adjustment of the stochastic method. Stochastic prediction methods use modelling techniques to determine expected value, standard deviation and other statistics of the stochastic variable. The great advantage of these methods compared to monitoring is that results are obtained right

away and different system configurations can be studied during the planning stage.
Once the electrical environment is described and the sensitivity of the equipment is determined, the compatibility between electrical supply and equipment can be decided.

1.7 Literature Review

It is difficult to identify when a real concern for statistics on magnitude and duration of voltage dip started. Voltage dips have occurred in electrical networks since the very beginning of its time. For long the main concern was on dips caused by motor starting.
Prior to 1990, very little detailed information was available on the frequency and duration of dips. Stochastic assessment of dips was an unknown term and monitoring programs were very few.
In 1985, at the Athens Congress of the union of electricity companies in Europe UNIPEDE, (today Euroelectric), a group of experts was appointed to improve the knowledge of the severity and rates of occurrence of voltage dips in public electricity networks. A report of the study was released in 1991 (Davenport, F., 1991). Among the conclusions, the report highlights 1) that voltage depressions in the range of 0-60% and up to 500 ms arise from transient faults on higher voltage systems, mainly transmission system, and 2) the high incidence of transient events (lighting, gales) on the number of dips recorded for other than cable networks. The report was submitted to the International Electrotechnical Commission IEC to enable compatibility levels and immunity limits to be established.
In the nineties three large monitoring programs were performed in the USA and Canada with the main objective of profiling the power quality (Dorr, 1996) resulting in several papers reporting the results.
The Canadian Electrical Association began the CEA survey in 1991. Koval and Hughes (1996) report frequency of dips at industrial and commercial sites in Canada. The threshold chosen for dips was 90% of the nominal voltage and among the conclusions they highlight that the majority of the dips have their origin inside the industrial plant.
In response to the lack of information on the nature and magnitude of power disturbances at typical 120 Volts AC wall receptacles, the National Power Laboratory, NPL, initiated in 1990 a power quality study (Dorr, 1992). Hundreds of site-months of power line disturbances were accumulated. The voltage dip threshold was fixed at 104 Volts, but a decrease in voltage for more than 30 cycles (1/2 second) was considered as undervoltage. Dorr (1992) presents results

of 600 site-months and compares the recorded disturbances with the CBEMA curve. The author concludes that the large number of disturbances found at typical locations suggest the need for power conditioning or protection for computers and sensitive electronic equipment. The same author (Dorr, 1994) presents a study of 1057 site-months based on the same NPL monitoring program. Conclusions show that there is a wide variation between the best site and worst site for each event category. Seasonal variation is also highlighted showing somehow the limitation of the monitoring programs for characterisation of individual sites.

The Electric Power Research Institute EPRI commissioned a survey entitled "An Assessment of Distribution Power Quality" (Dorr, 1996). From June 1993 to September 1995 a total of 227 sites ranging from 4.16 kV to 34.5 kV were monitored. One third of the monitors were located at substations. Monitors in feeders were randomly placed along them.

A paper by Wagner et al. (1990), which focuses on industrial power quality, raised an important question regarding the incidence and consequence of dips. It states that it is surprising that manufacturers and users have not focused more attention on dips considering their incidence and consequences. The main conclusion is that dips were the most common disturbance at a typical manufacturing plant.

Conrad and co-authors (Conrad, 1991) are the pioneers in stochastic assessment of dips although they do not use this word in their paper. Their work is the foundation of Chapter 9 of the Gold Book (IEEE Std 493, 1997). Conrad and co-authors raised the importance of dips originated by faults and combine accepted analysis tools to predict important characteristics of this kind of voltage disturbances. Frequency, magnitude and duration of dips can be predicted by using three basic tools: short-circuit fault techniques, fault clearing device characteristics and reliability data. The magnitude of the dips is predicted by simulating a fault, the frequency of dips is found by considering the fault rate of lines and buses and the duration is determined by taking typical values of fault clearing time. Another issue raised in this paper is the effect of delta-wye connected power transformers on dips. It is reported that transformers alter the voltage disturbance making a dip caused by a phase-to-ground fault to appear as a dip caused by a phase-to-phase fault and vice versa.

Electricite de France (1992) developed CREUTENSI, a software that using the number of faults and reclosing was able to predict the disturbance levels in terms of dips and interruptions. The approach is

somehow similar to the one proposed by Conrad et al. (1991), but additionally it proposed the use of a statistical distribution pattern for the magnitude of dips. This pattern segments the voltage drops in four intervals: 10-20%, 20-40%, 40-60% and 60-100% of voltage depression. Less severe dips, 10-20%, are the most frequent with a 57% of occurrence whereas most severe dips, 60-100%, are the less frequent with a 6% of occurrence.

In 1991 McGranaghan and co-authors (1991) present a paper that follows the same trend shown in the previous publications: combining fault rate and fault response of the network a stochastic assessment of dips can be performed. A new concept is introduced, area of vulnerability, that relates the sensitivity of the load and the potential area where faults may cause a severe dip.

Bollen (1993 a,b) incorporates in the reliability analysis of industrial plants the effect of voltage dips. Using Monte Carlo simulation the author gets a reliability assessment of the industrial plant which includes long and short interruptions as well as voltage dips. The same author (Bollen, 1995) proposes a simple voltage divider for prediction of the magnitude of dips in radial feeders. The paper introduces the concept of "critical distance" to identify the length of the feeder exposed to faults that may cause a severe dip at the load position. It also shows that the contribution of feeder faults to the number of dips with a voltage magnitude less than V p.u. is proportional to V/(1-V). The author (Bollen, 1995) applies the voltage divider model to sub-transmission loops and combines the residual voltage during the occurrence of faults with the fault rate to determine the expected number of trips due to severe dips. Additionally the paper introduces the concept of "critical angle jump" which is the phase angle jump that may trip sensitive equipment. This angle is the difference in phase angle with respect to the phase angle of the pre-fault voltage.

Ortmeyer and Hiyama (1996 a) introduce the concept of co-ordination of time overcurrent devices with sag capability curves for radial feeders. The available short-circuit current levels are combined with the dip at the load point producing a voltage current characteristic for the load point. This characteristic is then combined with the voltage tolerance curve of the sensitive load to determine the current-time curve of the protection devices. The same author introduces the concept "footprint" of faults (Ortmeyer, 1996 b). A footprint is a plot in a voltage-time plane that shows all the potential dips caused by faults. The footprint is then combined with the fault

rate to determine frequency, duration and magnitude of dips in the load point.

Bollen and co-authors (1997) formally propose the method of critical distance for stochastic assessment of dips. The method is based on a voltage divider that gives the magnitude of the dip in terms of feeder and source impedance. Writing the distance to the fault in terms of the feeder impedance, an expression of the critical distance can be derived. Combining this expression with the fault rate, the expected number of spurious trip due to dips can be found. The method is also presented in (Bollen, 1998 a) and further developed in (Bollen, 1998 b). The latter paper presents the exact equations for the critical distance and extends the method to non-symmetrical faults. In (Bollen, 1998 c) the method of critical distances is compared with another named method of fault positions. The latter one is a straightforward method based on the simulation of short circuits through the system. Combining the voltage during the fault with the fault probability a stochastic assessment of voltage dips can be performed. The conclusions indicate that the method of fault positions is more suitable for meshed systems. The paper also raises the unsuitability of monitoring for characterisation of dip activity at individual sites, however it stresses the need for validation of the stochastic methods by means of monitoring, after which the method can be used without continuous verification.

The method of fault positions is applied by Qader (1999) to determine the expected number of dips in buses of a large transmission system. The paper introduces graphical ways of presenting the results obtained from the stochastic assessment. The exposed area (or area of vulnerability) is the area where faults will cause dips more severe than a given value. The voltage dip map is a representation of the quality of supply in terms of sags around the network. In a voltage dip map, lines enclose buses with similar number of expected sags. The conclusions raise several issues. The number of expected dips varies significantly throughout the system showing that the average number cannot be used to characterise any individual site. It also highlights the effects of the generation scheduling and the need for considering the variation in the expected number of dips in monitoring programs.

The comparison between power quality monitoring and predicted results is undertaken by Sikes (2000) and Carvalho (2002 a,b). Sikes (2000) concludes that the characteristics of the dips are very predictable, however some tuning of the stochastic method is needed. The tuning can be accomplished by using actual meter data to scale

the event rate results. If the simulation is intended to examine performance characteristics for changes in system topology, then only relative results are needed. It is argued that calibration of the predicted events to those actually experienced is the benefit of installing power quality monitoring meters. Carvalho et al. (2002 a,b) confirm the conclusions derived by Sikes (2000). The study was based on the Brazilian transmission network. A classification of the possible errors is made and some compensation factors are introduced in order to scale the stochastic results. Both deterministic results, due to short circuit simulation, and stochastic results, due to fault occurrence, show an acceptable error below 11%.

The effects of pre-fault voltage, networks topologies, embedded generation and motors are analysed by Milanovic (2000) and Gnativ (2001). These authors raise the fact that the area affected by voltage dips following a short circuit increases if the network is more interconnected. Embedded generation reduces the magnitude of dips and the same effect is reported for induction motors.

Heine and co-authors (2001) also analyse the effect of distribution system design in voltage dips. However, their work is mainly focused on comparing rural and urban networks. They conclude that urban customers seem to experience less dips compared to rural customers the main reason being shorter total feeder length of urban networks.

A paper by Carvalho (2002 c) presents an overview of methods and computational tools that are currently in use for simulation of voltage sags. The methods of fault positions and critical distances are presented and six computational tools are discussed. VSAT (EPRI/ELEKTROTEK, USA); VSAG (Pacific Gas & Energy, USA); PTI (Power Technology Inc., USA); ANAQUALI (CEPEL, Brazil); software of PUC-BH, (Catholic University of Belo Horizonte, Brazil) (Alves, 2001 and Fonseca 2002) and VISAGE (Federal University of Itajuba). Only the last two tools, developed at universities, include estimation of the duration of dips. In general all the applications use short-circuit theory to calculate the during-fault voltage. Then they combine the stochastic information given by the fault rate to get an estimation of the expected number of dips and their characteristics. The tool reported by Fonseca (2002) combines Monte Carlo simulation with a big database of during-fault voltage to incorporate the uncertainties in the fault position.

A Monte Carlo approach is reported by Martinez (2002). An EMTP based tool is assembled to a Monte Carlo module in which several

uncertainties are considered. Simulations are performed in the time domain by means of EMTP-type tools.
An analytical approach to probabilistic prediction of voltage dips in transmission networks is proposed by Lim and Strbac (Lim, Y. S., 2002). The probability density function of voltage-dips caused by faults across the network is determined. The residual voltage at an observation bus is expressed as a function of the position of a moving fault node providing a deterministic relation between two stochastic variables, fault position and residual voltage. Although powerful, the method is hard to understand and difficult to implement.
Bollen et al. propose a method to extract the phasor information from the three rms voltages only (Bollen, 2004). The method can be used to translate voltage dip statistics of the network into information for the end user or to compare voltage dip measurements realized at different voltage levels or with different monitor connections (start or delta). The phase-angle jump is recognised as a limitation of the method since for large phase angle the method may fail.
Milanovic et al. (Milanovic, 2005) analyse the influence of modelling of fault distribution along transmission line on the assessment of number and characteristics of voltage sags. Different fault distributions along a line crossing the border of the exposed area of a sensitive load are used to explore the effect on the stochastic assessment of voltage sags. The study shows that depending on the fault distribution (uniform, normal, exponential) along the line, different number of voltage dips could be expected at the selected bus.

1.8 Literature Discussion

In the previous section, a literature review has been presented. The following conclusions can be derived:

- Voltage dips are one of the most important power quality disturbances for industrial customers (Wagner et al. 1990).
- Voltage dips are caused by faults and other large increases in currents both inside the industrial plants and outside of them.
- Monitoring cannot be used to characterise individual sites due to the stochastic nature of dips. However, monitoring is needed to adjust the stochastic methods.
- Stochastic assessment of dips combines deterministic results obtained from short-circuit calculations with stochastic information about the probability of faults around the system. Two methods have been reported: method of critical distances

and method of fault positions. Considering typical fault clearing times, duration of dips can be included.

- In the method of fault positions, several faults are simulated around the system. The residual voltage during the fault is then combined with the fault rates to obtain a stochastic evaluation of dips.
- Uncertainties are taken into account by means of average values or by means of Monte Carlo simulation.
- It seems that no research has been published in which monitoring and stochastic assessment are combined to profile the performance of an entire network.

1.9 The Project

The first stage of this project started in September 2001 and ended in September 2003. During this stage stochastic methods for voltage dips characterisation of large transmission systems were introduced. The project also resulted in the definition of an optimisation problem that allows us to find the minimum number of monitors in order to describe the dip performance of a large transmission system.
The second stage started in September 2003. The main scope is the application and further development of the methods developed during the first stage of the project. The techniques for optimal location of power-quality monitors is combined with stochastic prediction methods resulting in a method for voltage dip estimation.
The results obtained from the project can be summarized in four points:

- Further knowledge on the relation between system design and voltage-dip performance.
- Better understanding of strengths and weaknesses of the method of fault positions for stochastic assessment of voltage sags.
- Better understanding of the strengths and weaknesses of different voltage-dip indices; especially as far as the relation with monitor locations is concerned.
- Methods for estimating voltage-dip frequency on busses not directly monitored.

A list of publications resulting from the first and second stage of the project is given in Section 1.9.2.

1.9.1 Industrial Relevance

Voltage dips are a serious concern for many industrial customers. For example, a sag to 50% 100 ms may lead to a 24-hour production stoppage for a paper mill. Voltage dips compete with long interruptions for the type of disturbance causing the largest annual economic impact. The recent occurrence of a number of large-scale blackouts has somewhat pushed power-quality disturbances into the background. However the average customer may experience one large-scale blackout every 10 or 20 years, but about 20 voltage dips per year.

Performance assessment of the power supply is an essential part of any well-functioning electricity market. Nowadays, the emphasis in the discussions is still too much on the collection of statistics on voltage dips. This is in part due to the lack of proper methods for prediction of the performance beforehand. Stochastic prediction of voltage dips is such a method. Discussions in various international working groups on voltage dips confirm the need for such methods. Methods in which limited monitoring results are combined with stochastic prediction techniques not only are expected to give higher accuracy in the results but also to lead to a wider acceptance of the prediction techniques.

Wind power is, next to hydro and biomass, the renewable source with the largest short-term potential. The developments in this area are clearly towards very large offshore installations. Contrary to small wind power sites, these large sites should not trip due to a voltage dip. It will however not be feasible, to make these installations immune to any disturbance. To judge the need for immunity requirements knowledge is required on the frequency of voltage dips with different characteristics, at the terminals of the wind turbines. Stochastic assessment of voltage dips may help to obtain such information without the need for expensive power quality monitoring programs.

This project contributes towards the theoretical foundations of these methods, and further develops them.

1.9.2 List of Publications

This dissertation is partially based on the work reported in the following publications.

[1] **Olguin, G.** and Bollen, M.H.J. “Stochastic Prediction of Voltage Sags: an Overview”, Proceedings of 7th International Conference on

Probabilistic Methods Applied to Power Systems, PMAPS 2002, Vol. 2, pp. 551-556, September 22-26, Naples, Italy.

[2] **Olguin, G.** and Bollen, M.H.J. "The Method of Fault Position for Stochastic Prediction of Voltage Sags: A Case Study", Proceedings of 7th International Conference on Probabilistic Methods Applied to Power Systems, PMAPS 2002, Vol. 2, pp. 557-562, September 22-26, Naples, Italy.

[3] **Olguin, G.** and Bollen, M.H.J. "Stochastic Assessment of Unbalanced Voltage Dips in Large Transmission Systems" Power Tech Conference Proceedings, 2003, IEEE Bologna, Vol.4, 23-26 June 2003.

[4] **Olguin, G.** and Bollen, M.H.J. "Optimal Dips Monitoring Program for Characterization of Transmission System", Power Engineering Society General Meeting, 2003, IEEE, Vol.4, 13-17 July 2003 pp. 2484-2490.

[5] **Olguin, G.**, Vuinovich, F., Bollen, M.H.J. "An Optimal Monitoring Program for Obtaining Voltage Sag System Indices" IEEE Transaction on Power Systems, manuscript number TPWRS-00257-2004.R1, in print.

[6] **Olguin, G.** Leborgne, R. Coelho, J. "Ensuring Electromagnetic Compatibility by Analytic Study of Voltage Dips Caused by Faults". Proceedings of IEEE Induscon Conference 2004, October 12-15, Joinville, Brazil.

[7] **Olguin, G.**, Bollen M., Karlsson D. "Voltage Sag Estimation in Power Systems via Optimal Monitoring and Stochastic Assessment", submitted to IEEE Transactions on Power Systems, manuscript number TPWRS-00181-2005.

[8] **Olguin, G.**, Karlsson, D. Leborgne, R. "Stochastic Assessment of Voltage Sags (Dips): The Method of Fault Positions versus a Monte Carlo Simulation Approach". To appear in Conference Proceedings of IEEE St. Petersburg Power Tech 2005, 27-30 June 2005, St. Petersburg, Russia.

[9] **Olguin, G**. "An Optimal Trade-off between Monitoring and Simulation for Voltage Dips Characterization of Transmission System". Submitted to IEEE PES Transmission and Distribution Conference and Exhibition, August 14-18 2005, Dalian, China.

[10] **Olguin, G.**, Aedo, M., Arias, M., Ortiz, A. "A Monte Carlo Approach to the Method of Fault Positions for Stochastic Assessment of Voltage Dips (Sags)". Submitted to IEEE PES Transmission and Distribution Conference and Exhibition, August 14-18 2005, Dalian, China.

The author has also participated in the following publications not fully addressed in this dissertation.

[11] Bollen, M. H. J., **Olguin, G.**, Martins, M. "Voltage Dips at the Terminals of Wind Power Installations". Proceedings of Nordic Wind Power Conference, NWPC 2004, Gothenburg, Sweden March 2004.
[12] Di Perna, C., **Olguin, G.**, Verde, P., Bollen, M.H.J. "On Probabilistic System Indices for Voltage Dips". Proceedings of International Conference on Probabilistic Methods Applied to Power Systems, 2004, 12-16 Sept. 2004 Pages: 796-800.
[13] Leborgne, R., **Olguin, G.**, Bollen, M. H. J. "Sensitivity Analysis of Stochastic Assessment of Voltage Dips". Proceedings of International Conference on Power System Technology 2004, POWERCON 2004, November 21-24, Singapore.
[14] Leborgne, R., **Olguin, G.**, Bollen, M.H.J. "The Influence of PQ-Monitor Connection on Voltage Dip Measurements" Proceedings of 4th Mediterranean Conference on Power Generation, Transmission and Distribution 2004, MedPwer 2004, November 14-17, Lemesos, Cyprus.
[15] Leborgne, R., Karlsson, D., **Olguin, G.** Analysis of Voltage Sag Phasor Dynamic". To appear in Conference Proceedings of IEEE St. Petersburg Power Tech 2005, 27-30 June 2005, St. Petersburg, Russia.

The author of this dissertation has also participated in the preparation of the following CIGRE report to be released by December 2005.

[16] CIGRE TF C4.1.02 J. A. Martinez-Velasco (Convenor) "Voltage Dips Evaluation and Predictions Tools"

1.10 Dissertation Outline

The dissertation is organised in ten chapters. Chapter 1 has introduced the general background of the work. The rest of the dissertation is organised as follows.

Chapter 2: Modelling and Tools
The aim of this chapter is to present the tools that are needed to develop the stochastic assessment of voltage dips via the method of fault positions. It presents a discussion regarding the stochastic nature

of voltage dips and the meaning of fault rate in power systems. Basic concepts of stochastic processes are also discussed. The impedance matrix of a power system is studied. The focus is on how to build the impedance matrix and on the meaning of its elements. The chapter also presents the symmetrical component technique for short-circuit calculations.

Chapter 3: Magnitude and Classification of Voltage Dips
This chapter derives equations for calculating the magnitude of dips caused by faults in meshed systems. A classification of dips is presented. The characteristic voltage for different type of dips is introduced. Equations for unbalanced dip magnitude are derived. Phasor diagrams are used to illustrate the dip types. The effect of transformers on the type of dip is discussed and the equations that take into account this effect are derived.

Chapter 4: Propagation and Counting of Voltage Dips in Power Systems
This chapter introduces the method of fault positions for stochastic assessment of voltage dips in large transmission systems. A hypothetical transmission system is used to introduce the method. The area affected by a fault is graphically described. Similarly, the exposed or area where the occurrence of faults leads to severe dips at a given observation bus is described on the one-line diagram of the network.

Chapter 5: Method of Fault Positions: Simulations and Results
Results of the stochastic assessment of voltage dips via the method of fault positions are presented. An existing large transmission system is used to illustrate the method. Results are presented by using tables and graphs. The exposed and affected areas are determined for some selected buses.

Chapter 6: Optimal Monitoring Programs
This chapter introduces an integer optimisation model in order to determine the optimal locations for a limited number of monitors. The monitor reach area is introduced to describe the area that can be monitored from the meter position. A number of cases are solved for different monitor thresholds. System indices are calculated based on a limited number of monitors optimally located.

Chapter 7: Analytic Approach to the Method of Fault Positions
This chapter presents an analytic approach to the method of fault positions. The aim of the approach is to solve the issue of finding the right number of fault positions. The analytic method is based on the algebraic description of the residual voltage at an arbitrary observation when a moving fault node is considered at any line.

Chapter 8: Comparing Stochastic Assessment and Measurements
Chapter 8 shows that the results from the method of fault positions are for long-term and that comparisons with actual measurements require adjustments. Fault scenarios are arbitrary created to simulate the outcome of a monitoring program, and results are compared against the prediction via the method of fault positions. A Monte Carlo approach to the method of fault positions is implemented to better describe the potential outcome of a monitoring program.

Chapter 9: Voltage Dip (Sag) Estimation
This chapter presents a method to estimate the dip performance at buses not being monitored. Finding fault positions likely to cause the residual voltages seen at some buses through power quality meters (limited monitoring program) and performing stochastic assessment around triggered monitors, the results of monitoring are extended to non-monitored buses. The algorithms for practical implementation are presented and tested in a 87-bus test system showing the applicability of the proposed method.

Chapter 10: Conclusions and Future Work
The chapter presents conclusions derived from this work. Several research issues are identified and proposed for future work.

1.11 Main Contributions of this Work

This dissertation reports the research work developed by the author during the past four years. It introduces the causes of voltage dips and their effects on sensitive loads. It provides a basic review of fault analysis in power systems to better understand the method of fault positions for stochastic assessment of voltage dips. The main contributions of the work can be summarised as follows:

1. It derivates the equations needed to calculate the complex residual voltage during the occurrence of faults in a power system. It models the effect of power transformers on the dip

type and presents clear algorithms to perform stochastic assessment of voltage dips via the method of fault positions.

2. It presents applications of the method of fault positions to an existing power system. It investigates the contribution of symmetrical and unsymmetrical faults to the total number of dips seen at an observation bus.
3. It proposes an analytic approach to the method of fault positions that overcomes the issue of the appropriate number of fault positions.
4. It discuses the drawbacks of the method of fault positions, in particular it raises the fact that the method cannot be used to predict the dip performance during a particular year. It proposes an alternative approach via Monte Carlo simulation that provides the complete spectrum of possible outcomes.
5. It proposes a method for optimal monitoring programs that makes it possible to obtain voltage dips indices to characterise the complete network with a minimum number of monitors.
6. It introduces a method for voltage dip estimation that extends results from limited monitoring to buses not being monitored.

The dissertation is self-contained and provides complementary references to issues not fully addressed in this work.

2 Modelling and Tools

This chapter presents the modelling chosen for the stochastic assessment of voltage dips. The stochastic nature of voltage dips and the meaning of the fault rate of transmission lines and buses are discussed. The bus impedance matrix is presented as a suitable modelling of the network for dip simulation. The well-known impedance-building algorithm is presented and discussed. Symmetrical and unsymmetrical faults are described and their equations are used to qualitatively describe the during-fault voltages.

2.1 System Modelling

The first step in the analysis of a system-disturbance interaction is the development of a suitable mathematical model to represent the reality. A suitable mathematical model is a compromise between the mathematical difficulty attached to the equations describing the system-disturbance interaction and the accuracy desired in the result. Voltage dips can be studied from different perspectives and the model used to describe the disturbance needs to satisfy the study objectives. Depending on the objective of the study the modelling must be able to give a reasonable representation of the reality.

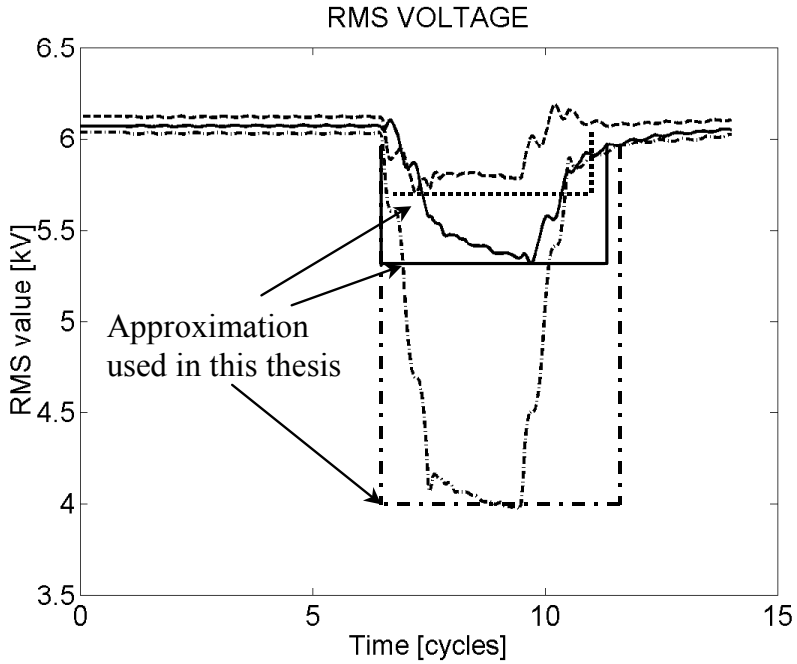

Figure 2.1: Sliding-window rms voltage versus time, for the three phases.

The objective of this work is the development of techniques for obtaining statistics on the magnitude of fault-originated sags. For that objective, a modelling based on phasors is considered suitable. It should be noted that the use of phasors restricts our model to the context of steady state alternating linear systems. The modelling used

in this dissertation is intended to give us the residual voltage during the fault and not the evolution as function of time. Figure 2.1 shows a three-phase unbalanced voltage dip in an 11 kV distribution network and the approximation considered in this dissertation. Depending on the fault type the shape of the rms voltage evolution will show different behaviours. A detailed discussion about this issue is contained in (Styvaktakis, 2002).

To introduce the basic ideas, consider a radial distribution feeder supplied from a busbar that also supplies a sensitive load. Suppose that we are interested in finding the residual voltage at the bus feeding the sensitive load during a fault at some point along the feeder. Assuming a no load condition, the voltage during the fault can be calculated by means of the voltage divider model shown in Figure 2.2.

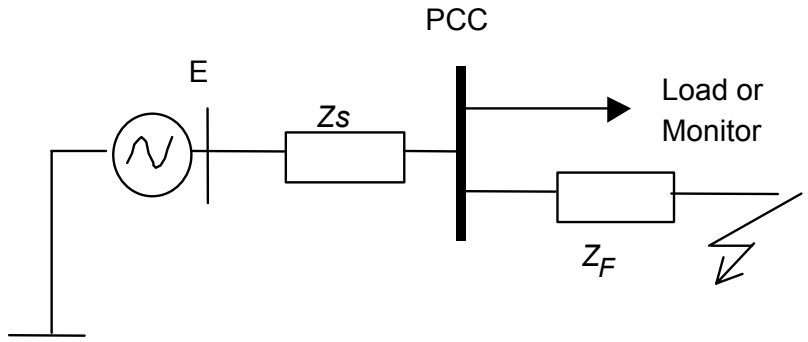

Figure 2.2: Voltage divider for dip magnitude calculation

In Figure 2.2 PCC is the point of common coupling between the load current and the fault current. It is the point where the magnitude of the dip needs to be estimated. Z_S is the source impedance and Z_F is the impedance between the PCC and the fault point. If the voltage behind the source impedance is assumed 1 p.u., then the voltage during the fault at the PCC is given by 2.1.

$$\bar{V}_{dip} = \frac{\bar{Z}_F}{\bar{Z}_F + \bar{Z}_S} \text{(p.u.)} \tag{2.1}$$

Equation (2.1) is suitable to analyse radial systems and is the basis of the method of critical distances discussed in section 2.3. For more complicated networks as meshed transmission systems, matrix calculation is more appropriate. In that case, the impedance matrix is used to represent the system. The admittance matrix could also be used to describe the system. However, the computational effort involved in the during-fault voltage calculation is larger when using the admittance matrix than when using the impedance matrix

(Anderson, 1973). In this work, the impedance matrix is used to model the system.

Faults in power systems can be symmetrical and unsymmetrical leading to balanced and unbalanced dips, respectively. For symmetrical faults only the positive sequence network is required to analyse the during-fault voltage. However the majority of the faults are single-phase-to-ground faults requiring the use of symmetrical components in the analysis.

As stated above, the main objective of this work is the development of techniques for obtaining statistics on magnitude of fault-originated voltage dips. The proposed modelling allows determining the magnitude of the dip for a given fault, however nothing has been said about the frequency of the event. For the stochastic assessment of dips one is interested in the expected number of events and their characteristics. To take into account this, the likelihood of the fault needs to be considered. The most important reliability data required for this is the fault rate, given in terms of a mean value of faults per year for each power system component.

Summarising the modelling chosen can be described by:

- The system is supposed to be composed of lines, power transformers, generation machines and buses.
- The system is balanced before the occurrence of the disturbance. This allows the independence of component sequences.
- The sequence impedance matrices are used to model the power system.
- Unsymmetrical faults are modelled by symmetrical components.
- The likelihood of faults is represented by the fault rate.

The coming sections present a review of the theoretical background. The material presented here is easily available in most textbooks on power systems. The discussion focuses on the application of these theories to the stochastic assessment of voltage dips.

2.2 The Stochastic Nature of Voltage Dips

For the purpose of this dissertation, a voltage dip is caused by a fault. Here it is worth noting the difference between failure and fault. Failure is the termination of the ability of an item to perform its required function whereas faults are short circuits caused by dielectric breakdown of the insulation system. A failure does not need to be fault, but a fault usually leads to a failure.

Faults can be categorised as self-clearing, temporary, and permanent. A self-clearing fault extinguishes itself without any external intervention. A temporary fault is a short circuit that will clear after the faulted component (typically an overhead line) is de-energized and reenergized. A permanent fault is a short circuit that will persist until repaired by human intervention (Brown, 2002).

Faults can be observed at the customer's premises as long interruptions, short interruptions, dips and swells. Swells are a temporary increase in the rms voltage. Outages occur when permanent faults take place in the direct path feeding the customer. Short interruptions are the result of temporary faults cleared by the successful operation of a breaker or recloser. Dips and swells occur during faults on the system that are not in the direct path supplying the load. Faults are of a stochastic nature and so are the dips caused by these faults.

Several random factors are involved in the analysis of voltage dips. An extensive list is presented in (Faired, 2002).

- Fault type. Three-phase faults are more severe than single-phase faults, but the latter are much more frequent.
- Fault location. Faults originated in transmission systems cause dips that can be seen tens of kilometres away. Faults at radial distribution systems are more frequent but have a localer effect.
- Fault initiation angle or point on wave. This uncertainty has an important effect on the ability of some equipment to tolerate the dip (ride-through). It affects the transient behaviour of the fault current, but it does not have much relevance for the counting of events.
- Fault impedance. Bolted or solid faults cause more severe dips than impedance faults. In transmission systems, however the fault resistance plays a minor role.
- Fault clearing time. A voltage dip lasts for the time the short-circuit current is allowed to flow throughout the system. Protection devices allow different settings causing dips of different duration. Line protection in transmission grids is usually implemented by using distance protection. If the fault is located in the first zone then the fault duration is typically less than 100 ms, however if the faulted node is in the second zone, then a longer duration (about 400 ms) can be expected. Duration is not study in this work.
- Reclosing time. It is common practice to set one or two reclosing attempts in radial distribution feeder protections. This practice is

known as fuse saving and has an important impact on the frequency of dips originating at distribution levels. Reclosing can also be found in transmission lines. Some utilities implement only one attempt to clear the fault by means of single or three poles reclosing whereas others use more than one attempt.

- Fault duration. The duration of a dip caused by a self-cleared fault depends on the fault itself and not on the protection setting. Most faults in transmission and distribution systems are single-phase-to-ground and self-clearing faults. They may occur due to lightning and over-voltages created by switching and other phenomena.
- Power system modifications. The impedance between the point of observation and the fault point affects the residual voltage during a fault. However the system is not static and changes that affect this impedance are continuous. A new line can be built, a transformer can be taken out of the system or a new power station can be put into operation.
- Severe weather. The occurrence of faults and hence of dips is notoriously higher during severe weather, which can take many forms as wind, rain, ice, snow, lightning, etc.

The previous list of random factors is not complete but is sufficient to illustrate the stochastic nature of voltage dips. Having in mind that dips are of a stochastic nature, our description of the disturbance-system interaction needs to be probabilistic. The main two factors to be considered in this probabilistic approach are the fault rate and the fault position. The following section gives a discussion about the fault rate.

2.2.1 Fault Rate and Stochastic Models

Reliability of power systems is a well-developed area of power system knowledge (Billinton, 1983). In order to estimate the reliability performance, the analysed power system has to be represented by stochastic components. A stochastic component is a component-model with two or more states. The transition from the present state is selected randomly from the possible next states.

The basic variable in reliability evaluation is the duration for which a component stays in the same state. This is a stochastic quantity because its precise value is unknown. However, the mean duration value of staying in each state can be used to give the average performance of the system. For the purpose of this dissertation, two states of a power system component can be identified: operative and

faulted state. During the faulted state, the component is submitted to reparation and so this state is known as repair state. Figure 2.3 shows a two-state model and their transitions.

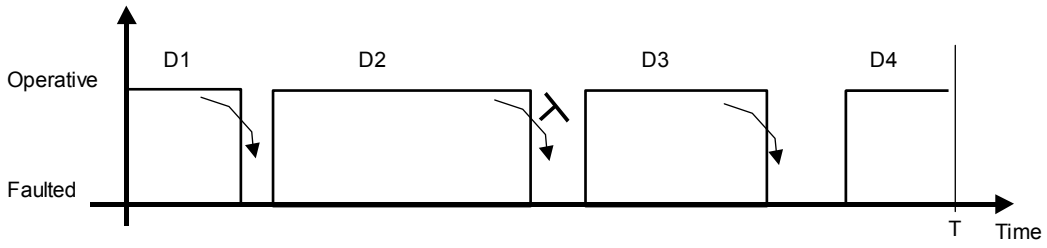

Figure 2.3: Single component system: Mean time diagram.

The diagram presented in Figure 2.3 may represent the behaviour of a transmission line or a bus of a transmission system. In that case, D_i is the time the line is in operation without a fault being present. The average value of D_i (within the cycle time T) is called mean time to fault. In this work, the interest is in the expected number of faults that may lead to a dip and for that purpose the transition rate between the operative and faulted state is useful. This transition rate is called fault rate λ and is the rate at which faults occur in a healthy component. Numerically, it is given by the reciprocal of the mean time to fault.
When the cycle time T is much longer than the mean time to fault, the fault rate is numerically similar to the frequency of encountering a system state. Power system components have a high availability, meaning that the time in the operative state is much longer than the time in the faulted state. In this case the frequency of encountering a state and the fault rate have approximately the same value.
In practical terms the fault rate is calculated by examining the historical performance in terms of faults occurring on a component of the system. The average number of faults during a period of some years, is used as an indicator of the fault rate.

2.3 Method of Critical Distance

Bollen (1999) proposed the method of critical distances as a fast assessment method for voltage dips in distribution systems. The method uses the simple voltage divider model shown in Figure 2.2 to estimate voltage dips due to short circuit faults in distribution feeders. Despite the fact that the method is based on simplifications as no load and a unique feeder, it facilitates the understanding of key concepts related to the matter of this work. A brief review of it is presented here.

In equation (2.1) Z_F is a function of the fault point whereas Z_S is a function of the point of common coupling, PCC. This means that for a given PCC the source impedance Z_S is fixed whereas the feeder impedance to the fault Z_F depends upon the location of the fault along the feeder. Equation (2.1) shows that the residual voltage becomes lesser for faults electrically closer to the PCC.

A critical residual voltage V_{crit} that depends upon the sensitivity of the load is used to estimate the expected number of trips due to voltage dips. It is assumed that the load will certainly trip if the residual voltage goes below V_{crit}. To find out the number of dips with residual voltage below than V_{crit} we write (2.1) for V_{crit} and get:

$$\bar{V}_{crit} = \frac{\bar{Z}_{Fcrit}}{\bar{Z}_{Fcrit} + \bar{Z}_S} \tag{2.2}$$

In (2.2) we have replaced V_{dip} by V_{crit} and Z_F by Z_{Fcrit} to emphasize that there is a point on the feeder (critical point) where the impedance to the PCC is the critical impedance Z_{Fcrit}. Faults on the critical point will cause residual voltages equal to the critical voltage, faults between the PCC and the critical point will cause dips with less residual voltage.

The critical distance is defined as the length of line exposed to faults that may lead to tripping of sensitive loads. To find the critical distance we express Z_{Fcrit} in terms of the length of the feeder measured from the PCC to the fault point. In addition, we introduce the following approximation: the X/R ratios of source and feeder impedances are equal. This assumption may not be valid for different voltages levels and will be corrected latter.

Thus, we find an approximate expression for the critical distance.

$$L_{crit} = \frac{Z_S}{z_F} \cdot \frac{V_{crit}}{(1 - V_{crit})} \tag{2.3}$$

where z_F is the feeder impedance per unit of length (km) and V_{crit} is the critical voltage in p.u.

The frequency of occurrence is calculated by using the long-term average fault rate. If the fault rate of the feeder is λ faults per km-year, then the expected number of trips due to voltage sags $Fsag_{crit}$ can be calculated by multiplying L_{crit} by λ.

$$Fsag_{crit} = \frac{Z_S}{z_F} \cdot \frac{V_{crit}}{(1 - V_{crit})} \cdot \lambda \tag{2.4}$$

Equation (2.4) does not give the total number of sags expected at PCC but only the critical ones, those that will cause equipment trips.

To fully describe the PCC in terms of voltage sags it is necessary to segment the residual voltage range and estimate the frequency in each range. Equation (2.4) can also be used for that. We make V_{crit} variable and plot *Fsag* versus residual voltage. Figure 2.4 shows that relation in qualitative terms and corresponds to the cumulative frequency of residual voltages (dips) up to a given magnitude.
From Figure 2.3 it is clear that in radial systems the expected number of less severe sags (0.8 < Vsag < 0.95) is much higher than the number of severe ones.

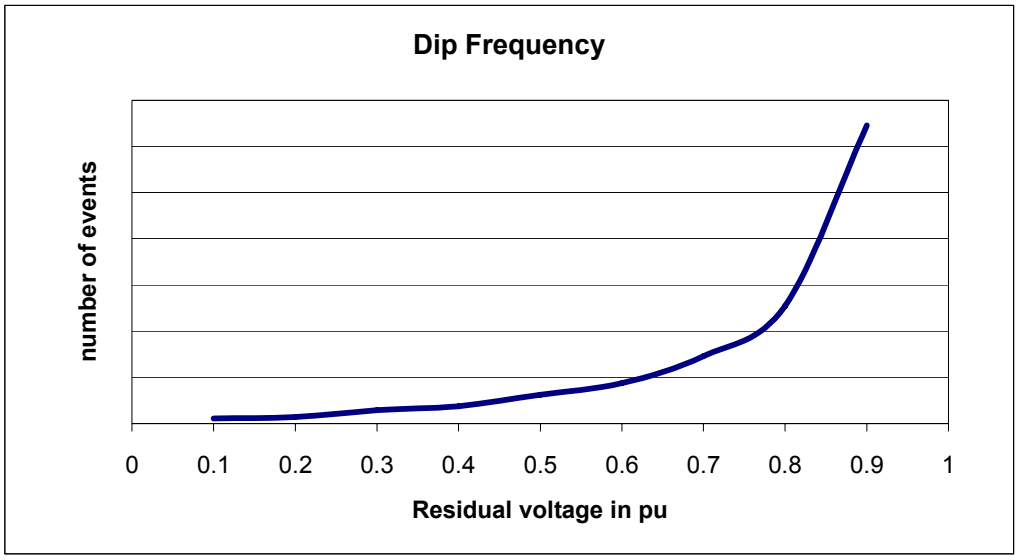

Figure 2.4: Relative voltage dip frequency

2.3.1 Phase-Angle Jump and More Accurate Expressions

Along with the depression of the magnitude of the voltage, a fault also leads to a change in the voltage phase angle. Phase-angle jumps affect the angle at which thyristors are fired and are therefore of serious concern for some equipment. Under the no load assumption, the phase-angle jump ϕ is found from (2.1) by taking the argument of V_{dip}.

$$\phi = \arg(\bar{Z}_F) - \arg(\bar{Z}_F + \bar{Z}_S) \tag{2.5}$$

The phase-angle jump is equal to the angle between the feeder impedance Z_F and the total impedance up to the fault point $Z_S + Z_F$. This is shown in Figure 2.5, where α is the "impedance angle" between Z_S and Z_F. In mathematical terms:

$$\alpha = \arctan\left(\frac{X_F}{R_F}\right) - \arctan\left(\frac{X_S}{R_S}\right) \tag{2.6}$$

where X and R are the reactance and resistance of feeder (F) and source (S) impedances.

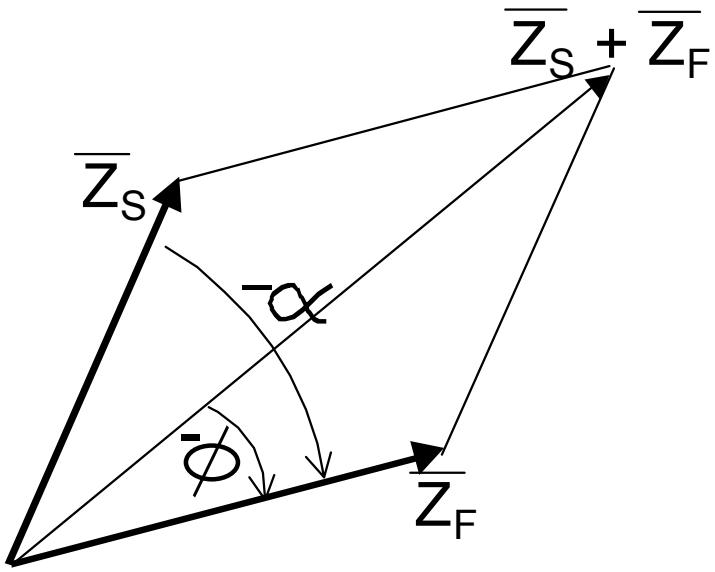

Figure 2.5. Phasor diagram with complex impedances

In order to get an expression of the phase-angle jump as function of the distance the cosine rule can be used twice in the lower triangle of Figure 2.5 to give:

$$\left|\overline{Z_S}+\overline{Z_F}\right|^2 = \left|\overline{Z_S}\right|^2 + \left|\overline{Z_F}\right|^2 - 2\left|\overline{Z_S}\right|\left|\overline{Z_F}\right|\cos(180-\alpha) \tag{2.7}$$

and:

$$\left|\overline{Z_S}\right|^2 = \left|\overline{Z_S}+\overline{Z_F}\right|^2 + \left|\overline{Z_F}\right|^2 - 2\left|\overline{Z_S}+\overline{Z_F}\right|\left|\overline{Z_F}\right|\cos(\phi) \tag{2.8}$$

Inserting (2.7) into (2.8) gives an expression for the phase-angle jump as a function of the distance *L*.

$$\cos(\phi) = \frac{\rho + \cos\alpha}{\sqrt{1+\rho^2+2\rho\cos\alpha}} \tag{2.9}$$

where ρ is a measure of the electrical distance to the fault (2.10) and α the impedance angle (2.6).

$$\rho = \left|\frac{L\cdot\overline{z_F}}{\overline{Z_S}}\right| \tag{2.10}$$

Accurate expressions for the residual voltage and the critical distance can be derived by considering that the X/R ratios of source and feeder impedance may be different. We now derive such expressions. Taking the modulus of both sides of (2.1) we get (2.11), where the

feeder impedance is expressed in terms of the per-unit of length impedance z_F.

$$V_{dip} = \frac{\left| L \cdot \bar{z}_F \right|}{\left| L \cdot \bar{z}_F + \bar{Z}_S \right|} \tag{2.11}$$

With (2.7) and some algebraic manipulations, the following expression for the residual voltage can be written:

$$V_{dip} = \frac{\rho}{(1+\rho)} \cdot \frac{1}{\sqrt{1 - \frac{2\rho(1-\cos\alpha)}{(1+\rho)^2}}} \tag{2.12}$$

The first factor in the right hand-side of (2.12) gives de dip magnitude when the difference in X/R ratio is neglected (i.e. α=0), the same expression as (2.1). The second factor takes into account the difference in X/R ratio through a value α greater than zero. For α small, the dip magnitude can be calculated with the approximate expression (2.1) without introducing a significant error.

To obtain a more accurate expression for the critical distance related to the critical voltage we need to solve ρ from (2.12) and then L from (2.10). Equation (2.12) can be written as a second order polynomial expression in ρ.

$$\rho^2\left(V^2 - 1\right) + 2\rho V^2 \cos\alpha + V^2 = 0 \tag{2.13}$$

Taking the positive solution of (2.13) and solving for L_{crit} the critical distance for a given critical voltage can be found.

$$L_{crit} = \frac{V_{crit} \cdot Z_S}{(1 - V_{crit}) \cdot z_F} \cdot \left\{ \frac{V_{crit}\cos\alpha + \sqrt{1 - {V_{crit}}^2 \sin^2\alpha}}{V_{crit} + 1} \right\} \tag{2.14}$$

Note that the expression (2.3), derived assuming equal X/R ratios, differs from (2.14) only in a factor k, defined by:

$$k = \frac{V_{crit}\cos\alpha + \sqrt{1 - {V_{crit}}^2 \sin^2\alpha}}{V_{crit} + 1} \tag{2.15}$$

The more this k factor deviates from one, the larger the error made by using the simplified expression (2.3). The simplified expression (2.3) overestimates the critical distance, but the error is small, with the exception of systems with very large phase-angle jumps.

2.4 The Impedance Matrix

This dissertation focuses on dips caused by short-circuit faults. An electrical network under short-circuit fault conditions can be considered as a network supplied by generators with a single load connected at the faulted bus. The pre-fault load currents can usually be ignored since they are small compared to the fault current. Usually they are considered by means of the superposition theorem if needed.
It was recognised very early that if the bus impedance matrix **Z**, with its reference bus chosen as the common bus behind the generator reactance is available, the complete fault analysis of the network can be readily obtained with a small amount of additional computation (Brown, 1985).
The use of the impedance matrix provides a convenient means for calculating fault currents and voltages. The main advantage of this method is that once the bus impedance matrix is formed the elements of this matrix can be used directly to calculate the currents and voltages associated with various types of faults. In this section key concepts regarding the impedance matrix are discussed.

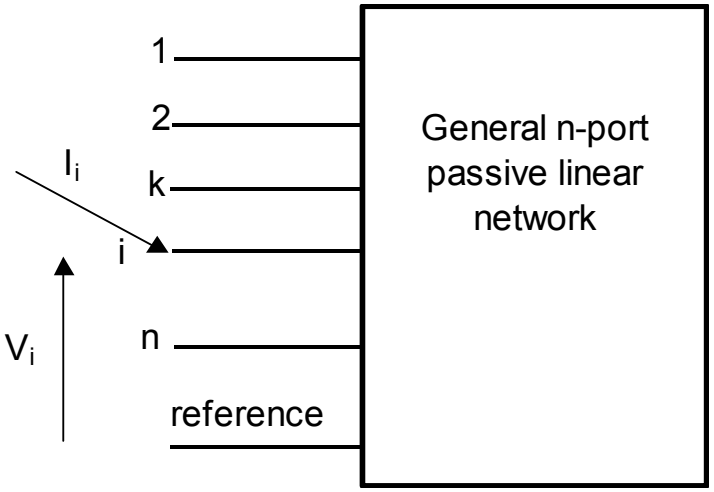

Figure 2.6: A general n-port network.

Consider the general n-port passive linear network of Figure 2.6. Equation (2.16) expresses the network-node voltages.

$$\begin{aligned}
\overline{v}_1 &= \overline{z}_{11}\cdot\overline{i}_1 + \overline{z}_{12}\cdot\overline{i}_2 + \ldots\ldots\overline{z}_{1n}\cdot\overline{i}_n \\
&\vdots \\
\overline{v}_k &= \overline{z}_{k1}\cdot\overline{i}_1 + \overline{z}_{k2}\cdot\overline{i}_2 + \ldots\ldots\overline{z}_{kn}\cdot\overline{i}_n \\
&\vdots \\
\overline{v}_n &= \overline{z}_{n1}\cdot\overline{i}_1 + \overline{z}_{n2}\cdot\overline{i}_2 + \ldots\ldots\overline{z}_{nn}\cdot\overline{i}_n
\end{aligned} \qquad (2.16)$$

It should be noted that (2.16) is valid for the voltages and currents as indicated in Figure 2.6. In other words node currents entering into the network and voltages are measured with respect to the reference node. Also note that we are dealing with complex variables. Equation (2.16) can be written in matrix notation.

$$\mathbf{V} = \mathbf{Z} \cdot \mathbf{I} \tag{2.17}$$

where **Z** is the bus impedance matrix of the network.

The impedance matrix contains, in its diagonal, the driving point impedance of every node with respect to the reference node. The driving point impedance of a node is the Thevenin's equivalent impedance seen into the network from that node. Hence the diagonal elements of the impedance matrix allow determining the short-circuit current of every potential fault at buses of the system.

The off-diagonal elements of the impedance matrix are the transfer impedances between each bus of the system and every other bus with respect to the reference node. Both the driving point impedance and the transfer impedance can be calculated from (2.16) making the relevant current equal to 1 p.u. and the rest equal to zero. For instance, (2.18) would give a general entry (*k,j*) of **Z**.

$$\overline{z_{kj}} = \left.\frac{\overline{v_k}}{\overline{i_j}}\right|_{\substack{i_1=i_2.....=i_n=0 \\ i_j \neq 0}} \tag{2.18}$$

From (2.18) it can be seen that the transfer impedance gives the voltage at bus *k* when a unity current is injected at node *j*. Hence the transfer impedance allows us to find the during-fault voltages due to the fault currents.

In contrast to the admittance matrix, which is a sparse matrix, the positive-sequence impedance matrix is a full matrix for a connected network. It contains zeros only when the system is subdivided into independent parts. Such sub-networks arise in the zero-sequence networks of the system because of the delta-connected transformer windings or other discontinuity in the zero-sequence network. For a connected network all elements of the impedance matrix are non-zero. However the matrix is diagonal dominant. Diagonal dominance of the impedance matrix **Z**, mathematically resulting from diagonal dominance of the admittance matrix **Y**, insures that the transfer impedances are smaller in magnitude than their diagonal counterparts in the same row and column. In turn, the causative diagonal dominance of the admittance matrix **Y** is assured by the nature of our practical power networks usually involving series impedance

corresponding to lines but little shunt capacitance. One could in theory obviate diagonal dominance by increasing shunt capacitance, but this does not occur in practice. The relevance of the transfer impedance z_{kj} is that it can be seen as a measure of the electrical closeness between the buses involved (k,j). Electrical closeness is a measure of the effects of a disturbance. The smaller in magnitude the transfer impedance, the less the impact a change at bus k has on the voltage at bus j. Machine reactances play a major role in the impedance matrix. Since the Thevenin impedances effectively become shunt or Norton admittances at the buses, they have a relevant effect on the complete matrix. In fact, a change in any network impedance will in general affect every term of the impedance matrix.
Equation (2.18) suggests that a general entry (k,j) of **Z** can be calculated by injecting a unity current at j and determining the voltage at node k, when all other currents are zero. Although conceptually correct, this is not a suitable way to determine **Z** for a big network. The well-known **Z** building algorithm is presented in the next section for being a useful way to build the matrix and modifications of it.

2.4.1 Bus Impedance Matrix Building Algorithm

The bus impedance matrix can be built element by element by using three algorithms, which represent three potential additions or modifications to the network (Brown, 1985 and Stevenson, 1982):

a) Addition of a branch impedance from the reference node to a new bus.
b) Addition of a radial branch impedance from an existing node to a new bus.
c) Addition of a link impedance between two existing nodes.

The building process of the impedance matrix needs to be started with a branch connected to the reference node. The first branch connected to the reference node results in a 1 by 1 impedance matrix formed by the added impedance.
The addition of an impedance ξ from a new bus p to the reference node does not affect the elements of the already built impedance matrix. As the new node p is directly connected to the reference through the impedance ξ a current injected into the new node p will produce no voltage on any other bus. The voltage at the new node p will not be affected by any current injected in nodes other than p. All off-diagonal elements of the new row and column, needed to consider

the new node, are therefore zero (2.19a). The injection of an unity current in p will cause a voltage equal to ξ at node p. Hence the driving point impedance is equal to the added impedance (2.19b).

$$\overline{z_{ip}} = \overline{z_{ip}} = 0, i \neq p \tag{2.19a}$$

$$\overline{z_{pp}} = \xi \tag{2.19b}$$

Once the first impedance connected to the reference node has been assembled into the impedance matrix additional branches can be added.

The addition of a radial branch between an already assembled node k and a new node q through an impedance ξ increases the dimension of the impedance matrix. A new row and column need to be added to $\mathbf{Z}$ to consider node q. Off-diagonal elements of row and column q can be found realising that a current injected into node q produces voltages on all other buses of the system that are identical to the voltages that would be produced if the current was injected into node k. Hence the transfer impedances of the new node are the same as the transfer impedances of the node at which it is connected (2.20a). The driving point impedance can be found by realising that an injected current into node q produces a voltage at that node that is equal to the voltage at node k plus the voltage drop in the added impedance ξ connecting q and k. Hence the diagonal element in row and column q is given by driving point impedance of node k plus the impedance of the branch being added (2.20b).

$$\overline{z_{qi}} = \overline{z_{iq}} = \overline{z_{ik}}, i \neq q \tag{2.20a}$$

$$\overline{z_{qq}} = \overline{z_{kk}} + \xi \tag{2.20b}$$

The third modification considers adding a link between two existing nodes j and k by means of an impedance ξ. In this case no new node is created in the original impedance matrix (old) but all its elements need to be recalculated due to the current flowing through the added impedance ξ between nodes j and k. The current between j and k can be expressed in terms of the added link impedance and nodal voltages, which are functions of the nodal currents. This creates a new equation that needs to be eliminated by a Kron reduction. Equations (2.21) show the new impedance matrix.

$$\mathbf{Z}^{\mathbf{new}} = \mathbf{Z}^{\mathbf{old}} - \frac{1}{C} \cdot \mathbf{M} \tag{2.21a}$$

$$C = \overline{z_{jj}} + \overline{z_{kk}} + \xi - 2\overline{z_{jk}} \tag{2.21b}$$

$$\mathbf{M}=\begin{bmatrix} \underline{z}_{1j}-\underline{z}_{1k} \\ \underline{z}_{kj}-\underline{z}_{kk} \\ \underline{z}_{ij}-\underline{z}_{ik} \\ \underline{z}_{jj}-\underline{z}_{jk} \end{bmatrix} \times \begin{bmatrix} \underline{z}_{j1}-\underline{z}_{k1} \\ \underline{z}_{jk}-\underline{z}_{kk} \\ \underline{z}_{ji}-\underline{z}_{ki} \\ \underline{z}_{jj}-\underline{z}_{kj} \end{bmatrix}^{T} \tag{2.21c}$$

The impedance matrix algorithm is a useful way to model modifications of the original system. For instance, the effect of a new parallel line in the magnitude of the expected dip can easily be taken into account by means of the last modification.

2.5 Symmetrical Components and Fault Calculation

Power systems are usually analysed assuming symmetrical and balanced operation. Under this condition, the system and its behaviour can be studied using a single-phase model of the network. When the network itself, the sources, or the loads are not symmetrical and balanced, the single-phase representation is not enough and three-phase models are needed.

The method of symmetrical components provides a means of extending the single-phase analysis for symmetrical systems subject to unbalanced load conditions or faults (Anderson, 1973).

Symmetrical components theory allows analysing an unbalanced set of voltages and currents by means of two symmetrical three-phase systems having opposite phase sequences (positive and negative) plus a third set of three identical vectors having zero phase displacement (zero sequence). The technique requires describing the system by means of its sequence networks: positive, negative and zero. Each sequence network represents the behaviour of the system to that sequence source: voltage or current. Sequence networks are built by means of sequence impedances that represent the element response to each sequence voltage. When a voltage of a given sequence is applied to a device (line, transformer, motor, etc.) a current of the same sequence flows. The device may be characterised as having a definite impedance to this sequence. Special names have been given to these impedances: positive-sequence impedance, negative-sequence impedance, and zero-sequence impedance (Wagner and Evans, 1933).

In this work the technique is used to calculate short-circuit currents and the voltages during the fault. For symmetrical faults only the positive-sequence impedance matrix is needed. For non-symmetrical faults the three sequence networks are needed.

Equation (2.22) gives the basic transformation for currents, where the superscript *z*, *p*, and *n* identify zero, positive and negative sequence currents and *a* is the Fortescue transformer *a*-operator, given by (2.22b). The same equation is valid for voltage transformation.

$$\begin{vmatrix} i^z \\ i^p \\ i^n \end{vmatrix} = \frac{1}{3} \cdot \begin{vmatrix} 1 & 1 & 1 \\ 1 & a & a^2 \\ 1 & a^2 & a \end{vmatrix} \begin{vmatrix} i^a \\ i^b \\ i^c \end{vmatrix} \tag{2.22a}$$

$$a = e^{j\frac{2\pi}{3}} \tag{2.22b}$$

From (2.22) it can be seen that any symmetrical component variable - current or voltage- is completely determined by its phase components and the other way around. This means that at the observation bus an unbalanced dip can be described by three phase voltages or by three sequences voltages.

2.5.1 Sequence Impedances

The impedance encountered by the sequence currents depends on the type of power system equipment: generator, line, transformer, etc. Sequence impedances are needed for component modelling and analysis. In this work, it is assumed that three types of components form the system: transmission lines, power generators and power transformers.

The impedance of symmetrical non-rotating apparatus is the same for both positive and negative sequences. Hence the positive and negative sequence series-impedances and shunt-capacitance of transposed lines are equal. The zero-sequence impedance of a transmission line is of different character from either positive or negative-sequence impedance because it involves the impedance to currents that are in phase in the three conductors, which necessitates a return path either in a neutral or ground wire (Wagner and Evans, 1933). The zero-sequence impedance of overhead lines depends on the presence of ground wires, tower footing resistance, and grounding and it is between two and six times the positive sequence impedance.

The positive and negative-sequence impedances of a transformer are equal to its leakage impedance. As the transformer is a symmetrical static apparatus, the sequence impedances do not change with the phase sequence of the applied balanced voltages. The zero sequence impedance can, however, vary from an open circuit to a low value depending on the transformer winding connection, method of neutral grounding and the core construction (Das, 2002). If there is no path

for the zero-sequence current the corresponding zero-sequence impedance is infinite. Delta and ungrounded wye windings present infinite impedance to zero-sequence current. An impedance in a neutral wire or ground connection is zero-sequence impedance, but its value needs to be multiplied by three in the zero sequence model to obtain the equivalent value for phase to neutral.

For a synchronous machine three different reactance values are specified (Wagner and Evans, 1933). In positive sequence, X_d'' indicates the subtransient reactance, X_d' the transient reactance and X_d the synchronous reactance. These direct axis values are necessary for calculating the short-circuit current at different times after the fault occurs. The positive sequence synchronous reactance, X_d, is the value that is commonly used for problems involving steady state calculations of machine performance.

Manufacturers specify negative and zero-sequence impedances for synchronous machines on the basis of test results.

The negative-sequence impedance is measured with the machine driven at rated speed and the field windings short-circuited. A balanced negative-sequence voltage is applied and the measurements are made. The negative-sequence reactance is usually approximated to one halve of the direct plus the quadrature axis subtransient reactances. An explanation of this averaging is that the reactance per phase measured varies with the position of the rotor.

The zero-sequence impedance is measured by driving the machine at rated speed, field windings short-circuited, all three phases in series and a single-phase voltage applied to circulate a single-phase current. The zero-sequence reactance of generators is low. In general it is much smaller than the positive and negative-sequence reactance.

A practical approximation for short-circuit studies is to take the zero-sequence reactance of synchronous machines in the range of:

$0.15X_d'' < X^z < 0.6X_d''$ (Anderson, 1973).

2.5.2 Sequence Networks and their Impedance Matrix

If the system is assumed to be symmetrical up to the point of fault, where an unsymmetrical fault occurs, then the three sequence components are independent of each other. Independence of symmetrical components is usually assumed in short circuit studies. The relation that must be satisfied to obtain symmetry of the network is that for every set of self or mutual impedances, the values for each phase must be equal. In transmission lines this is obtained by transposition of phase conductors.

Assuming sequence independence, three single-phase sequence-network diagrams are required for individual consideration: one for positive, one for negative and one for zero-sequence. These sequence diagrams are single-phase models of the power system and the impedance matrix can be used to model them.
For a power system consisting of lines, transformers and generators, the negative-sequence network is a duplicate of the positive-sequence with two exceptions: the negative-sequence network does not contain a source and the negative-sequence reactance of the generator may be different from the positive one. The positive-sequence impedance matrix Z^p is structurally equal to the negative one Z^n, but numerically different. This numerical difference is small and can be neglected.
The zero-sequence network (and its impedance matrix) is in general quite different from positive and negative ones. It has no voltage source, it has discontinuities due to transformer winding connections and the impedance values are different from positive ones.

2.5.3 Fault Current Calculation

Once the sequence networks have been built the calculation of the fault currents can be performed. Fault currents are calculated in the sequence component domain and transformed back to phase values.
The sequence networks are interconnected in the point of unbalance to describe the border conditions imposed by the fault to the phase quantities. These border conditions are derived from the three-phase diagram corresponding to the fault under consideration. Four short-circuit faults are considered in this work. It should be noted that equations consider complex variables, however a simplified notation is adopted.
The superscripts *z*, *p* and *n* over the variables indicate the zero, positive, and negative sequence components.

Three-phase fault.
Since the three-phase fault is symmetrical the negative-sequence and zero-sequence currents are zero. Only the positive-sequence network, which is the normal balanced diagram for a symmetrical system, and its impedance matrix are needed to determine the fault current. The fault current, *i*, is equal to the positive-sequence current. The impedance looking into the network from the faulted bus *f* is given by diagonal element z_{ff} of the positive-sequence impedance matrix. The pre-fault voltage is of positive-sequence and is equal to the pre-fault

voltage at the faulted bus. Hence, (2.23) gives the short circuit current and Figure 2.7a shows the sequence network connection.

$$i = i^{p} = \frac{v^{a}_{pref(f)}}{z^{p}_{ff}} \tag{2.23}$$

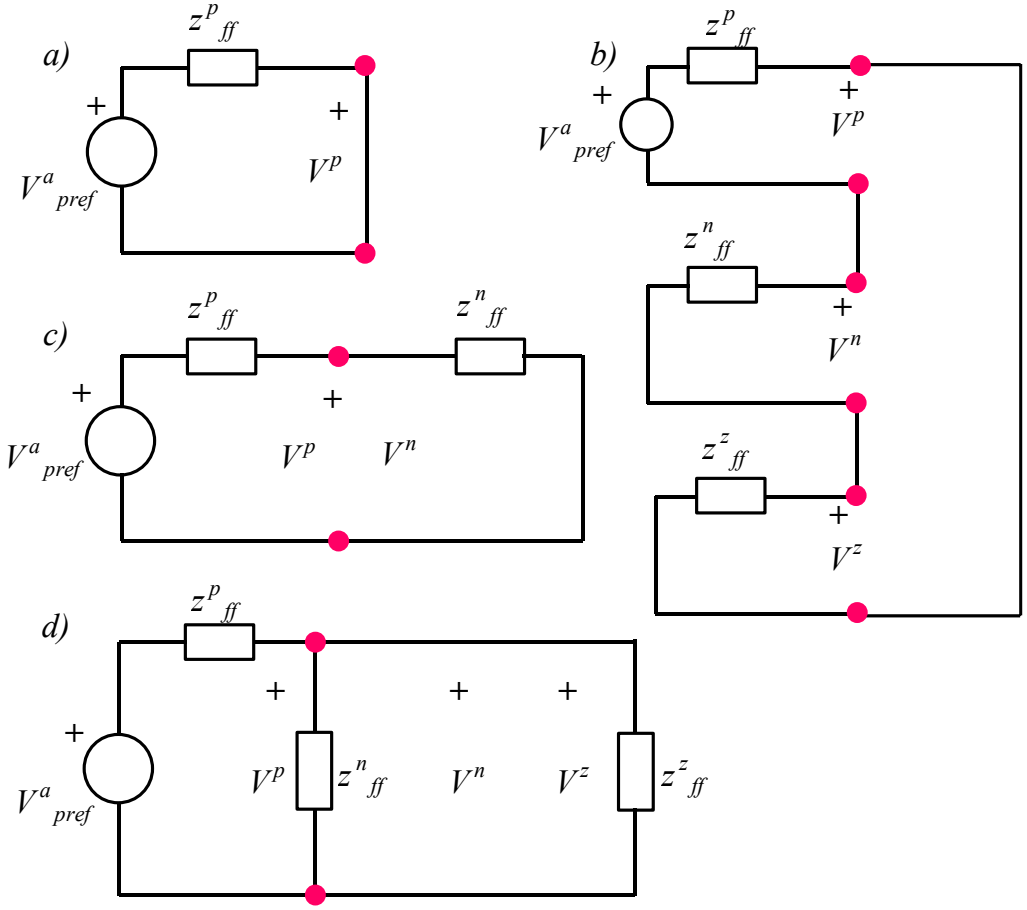

Figure 2.7:Sequence-networks diagrams for calculation of short-circuit fault. a) Three-phase fault; b) Single-phase-to-ground fault; c) Phase-to-phase fault; d) Two-phase-to-ground fault.

Single phase-to-ground fault (phase a)

A single phase-*a* to ground fault implies the relations described by (2.24) for phase voltages and phase currents at the fault point. Note that the pre-fault currents are neglected.

$$i^{b} = i^{c} = 0 \tag{2.24a}$$

$$v^{a} = 0 \tag{2.24b}$$

Applying the sequence transformation (2.22) to voltages and currents in (2.24) it can be shown that the sequence networks need to be connected in series (Figure 2.7b) to satisfy these conditions in the domain of symmetrical components. The addition of the sequence voltages is equal to v^{a}, the faulted-phase voltage, and hence zero. The sequence currents are the same and equal to the reciprocal of the

summation of the impedances seen from the fault point of each sequence network. Thus (2.25) gives the sequence currents and fault current.

$$i^z = i^p = i^n = \frac{v^a_{pref}}{z^z_{ff} + z^p_{ff} + z^n_{ff}} \tag{2.25a}$$

$$i^a = \frac{3 \cdot v^a_{pref}}{z^z_{ff} + z^p_{ff} + z^n_{ff}} \tag{2.25b}$$

Phase-to-phase fault(phases b and c)

Equations (2.26) describe the border conditions for a phase-to-phase fault.

$$i^a = 0 \tag{2.26a}$$

$$i^b = -i^c$$

$$v^b = v^c \tag{2.26b}$$

By applying the transformation to sequence components the connection between the sequence networks can be found. The zero-sequence current is zero because the fault does not provide a path for the zero-sequence current to flow. Thus the zero-sequence network does not intervene in the analysis. The summation of the sequence currents is equal to i^a which is zero for this fault. Hence the negative-sequence current is equal to the positive-sequence current but it has opposite direction. The positive and negative-sequence networks need to be connected in parallel to satisfy the fault conditions. Equation (2.27) shows the sequence and fault currents. Figure 2.7c shows the sequence networks connection.

$$i^z = 0; \quad i^p = i^n = \frac{v^a_{pref}}{z^p_{ff} + z^n_{ff}} \tag{2.27a}$$

$$i^b = -i^c = -j \cdot \sqrt{3} \cdot \frac{v^a_{pref}}{z^p_{ff} + z^n_{ff}} \tag{2.27b}$$

Two-phase-to-ground fault (phases b and c)

A two-phase-to-ground fault is similar to a phase-to-phase fault, but in this case there exists a path for the zero-sequence current to flow. The fault can be described in phase domain by (2.28).

$$i^a = 0 \tag{2.28a}$$

$$v^b = v^c = 0 \tag{2.28b}$$

The application of the transformation indicates how the sequence networks need to be connected. The summation of the three sequence

currents is equal to i^a, which is zero. From (2.28b) it follows that the three sequence voltages are equal indicating the parallel connection of the sequence networks. Equations (2.29) show the sequence and fault currents. Figure 2.7d shows the connection of the sequence networks.

$$i^p = \frac{v^a_{pref}}{z^p_{ff} + \dfrac{z^z_{ff} \cdot z^n_{ff}}{z^z_{ff} + z^n_{ff}}} \tag{2.29a}$$

$$i^z = -i^p \cdot \frac{z^n_{ff}}{z^n_{ff} + z^z_{ff}} \tag{2.29b}$$

$$i^n = -i^p \cdot \frac{z^z_{ff}}{z^n_{ff} + z^z_{ff}} \tag{2.29c}$$

$$i^b = \frac{v^a_{pref}}{z^p_{ff} + \dfrac{z^z_{ff} \cdot z^n_{ff}}{z^z_{ff} + z^n_{ff}}} \cdot \left(\frac{-z^n_{ff}}{z^z_{ff} + z^n_{ff}} + a^2 + \frac{-a \cdot z^z_{ff}}{z^z_{ff} + z^n_{ff}} \right) \tag{2.29d}$$

$$i^c = \frac{v^a_{pref}}{z^p_{ff} + \dfrac{z^z_{ff} \cdot z^n_{ff}}{z^z_{ff} + z^n_{ff}}} \cdot \left(\frac{-z^n_{ff}}{z^z_{ff} + z^n_{ff}} + a + \frac{-a^2 \cdot z^z_{ff}}{z^z_{ff} + z^n_{ff}} \right) \tag{2.29e}$$

2.5.4 Neutral System Grounding

Power systems are said to be solidly grounded if the neutral of transformers or generators are connected directly to ground; impedance grounded if an impedance (resistor or reactor) is connected between the neutral and ground, and ungrounded if there is no intentional connection to ground. Grounding practices have an important effect on the fault currents.

When considering earth or ground faults (single-phase-to-ground and two-phase-to-ground faults) it has so far been considered that the network was solidly grounded, meaning that the transformer neutral point is directly connected to ground. Equations developed in the previous section are valid for solidly grounded systems but they are easily extensible to impedance grounded systems adding the triple value of the grounding impedance in the zero sequence network (Wagner and Evans, 1933). They can also be extended to ungrounded systems. For that purpose, it is worth noting that although called ungrounded, this type of system is in reality coupled to ground through the distributed capacitance of its phase conductors. Hence the

distributed line capacitance should appear in the positive, negative and zero sequence networks (Lakervi, 1989).
Different policies for grounding the neutral of a system affect the system behaviour. In particular grounding affects the maximum levels of earth fault currents and the overvoltages. When earth fault current and overvoltages are of concern a classification of systems into grounded or ungrounded, without any further restrictions, is unsatisfactory because it takes into account only the impedance between the neutral point and the ground, instead of the total effective zero-sequence impedance which includes line and apparatus impedance as well as that of the grounding impedance. In fact, the zero-sequence impedance of a solidly-grounded system may actually be higher than that of a system grounded through a neutral impedance of low value. A more accurate classification is based on the ratios of zero and positive-sequence impedances and is known as the degree of grounding, low values of this ratio corresponding to solidly-grounded systems and high values to ungrounded systems.
An effectively-grounded system will have a ratio:
$X^z/X^p \leq 3$ and $R^z/X^p \leq 1$.
The magnitude of the ground fault current as compared to three-phase fault current can also be used to determine the degree of grounding. The higher the ground fault current in relation to the three-phase fault current the greater the degree of grounding (IEEE Std 142, 1991). Effectively-grounded systems will have a line-to-ground fault current at least 60% of the three-phase fault current.
In general maximum values of fault currents are obtained for low values of X^z and X^n. However this is not the case for the zero-sequence resistance R^z. The effect of adding zero-sequence resistance to a system having no resistance is, first, to increase the line current in a two-phase-to-ground fault; subsequent increase in zero-sequence resistance reduces line currents as well as ground currents.

2.5.5 During Fault Voltages: a Qualitative Discussion

The equations in the preceding section provide sequence and fault currents for four different faults. During-fault voltages can be derived from the sequence currents and network impedances. During-fault voltages are voltage dips and their expressions will be derived in the next chapter. Here a qualitative discussion is presented based on Figure 2.8 in which a transmission line is fed by two ideal generators. The resistive part of impedances is neglected.

Under a balanced condition only positive-sequence currents and voltages are present in every point of the network. Under an unbalanced load or fault there may exist the three sequence voltages and currents. On an ungrounded system (three-phase three-wire), there is no intentional path for the zero-sequence current to flow, but the distributed capacitance of lines may provide a high-impedance path for the zero-sequence current to flow. However the zero-sequence current in a ungrounded system is usually neglected.

The phase voltages at any point of the network can be calculated by determining its sequence-component voltages. During a fault the change in voltages at a given bus can be expressed as in (2.30).

Depending on the type of fault, voltage changes of negative and zero-sequence may be present. A positive-sequence voltage change will always be present.

$$\begin{vmatrix} \Delta v^a \\ \Delta v^b \\ \Delta v^c \end{vmatrix} = \begin{vmatrix} 1 & 1 & 1 \\ 1 & a^2 & a \\ 1 & a & a^2 \end{vmatrix} \begin{vmatrix} \Delta v^z \\ \Delta v^p \\ \Delta v^n \end{vmatrix} \tag{2.30}$$

During a solid three-phase fault only positive-sequence current flows through the network. The sudden increase in the current causes a depression in the bus voltages, which are of the same sequence as the currents that cause them. Thus for a three-phase fault the depression in the rms voltage contains only a positive sequence. The voltage at the fault point becomes zero but does not change in the ideal sources until the regulators act to change the generator fields. By this time the fault should be cleared by the protective relays. Thus the voltage profile is as shown in Figure 2.8a.

During a single-phase-to-ground fault, positive and negative-sequence currents flow through the network and cause voltage drops that correspond to the sequence currents. A zero-sequence current flows only if there is a path for the current to flow to a ground or neutral point. The changes in the voltage at a remote bus will be of positive and negative-sequence voltage. Voltage changes of zero-sequence may exist or not depending on the existence of a zero-sequence path (zero-sequence transfer impedance greater than zero) from the fault point to the bus of observation. At the fault point, the voltage in the faulted phase (symmetrical phase) becomes zero and is equal to the summation of the three sequence voltages. The pre-fault voltage only contains a positive-sequence component. Hence during the fault at the observation bus the positive-sequence voltage is of opposite sign compared to the negative and zero-sequence. Figure

2.8b presents the voltage profile when the zero-sequence impedance is slightly larger than the positive one.

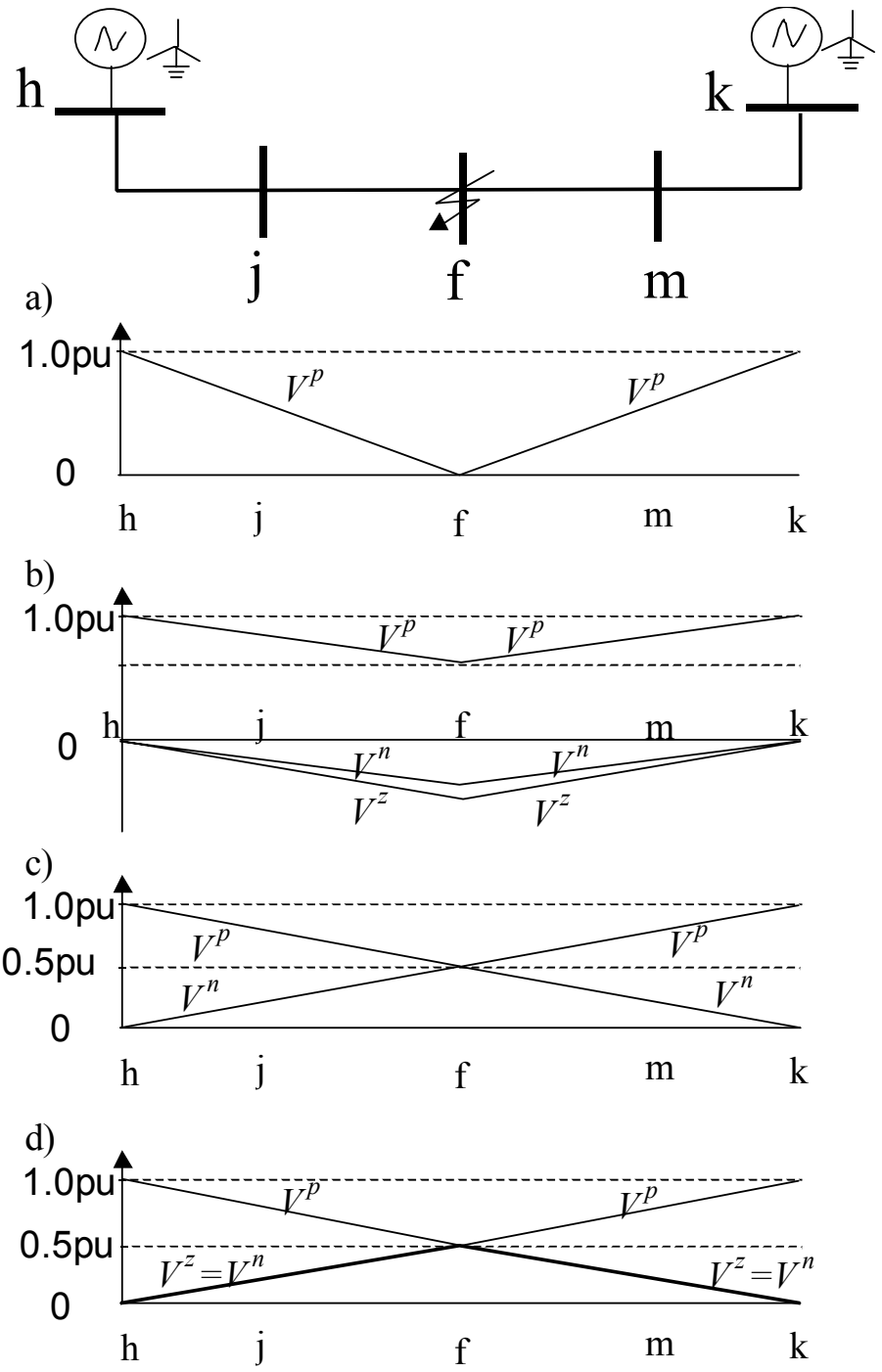

Figure 2.8: Sequence phase-a voltage profiles during faults: a) three-phase fault; b) single-phase-to-ground fault; c) phase-to-phase fault; d) two-phase-to-ground fault.

The phase-to-phase fault does not provide a path for the zero-sequence current to flow. The symmetrical phase voltage (healthy phase *a*) is equal to the addition of positive and negative-sequence voltages, which are equal at the fault point. The flow of positive and

negative-sequence current causes voltage-changes of the corresponding sequence. Figure 2.8c shows the sequence voltage profile for $Z^p = Z^n$.

Positive, negative and zero-sequence current can flow when a two-phase-to-ground fault occurs. The three sequence currents are present at the faulted point. The negative and zero-sequence voltages are equal at the fault point. Figure 2.8d shows the voltage profile.

The fundamental concept illustrated in Figure 2.8 is that negative and zero-sequence voltages are maximum at the fault point and minimum at the sources. Zero-sequence voltage is zero at the generators and at the grounded neutral. Negative-sequence voltage is zero at the generators. Positive-sequence voltage is greatest at the generators and minimum at the fault point (Blackburn, 1998).

3 Magnitude and Classification of Voltage Dips

In this chapter, equations for determining the voltage dip magnitude due to symmetrical and unsymmetrical faults are derived. The characteristic voltage and positive-negative factor are presented. Voltage dip classification is presented. Equations to take into account the effect of power transformers on the residual voltage are derived.

3.1 Voltage Dip Magnitude and Classification

The residual voltage during the fault gives the magnitude of a voltage dip. Depending on the type of fault that causes the dip the voltage during the event may be equal or different in the three phases. According to the symmetrical-component classification (Bollen, 2003) three dip types can be recognised: A, C and D.

Three-phase faults cause dips called type A. They are balanced dips meaning that the phase voltages during the fault are equal in the three phases. For this kind of dips only one complex vector is needed to characterise the magnitude and phase angle of the dip.

An unsymmetrical fault may cause dips type C or D. Phasor diagrams corresponding to these dips will be presented in Section 3.3 where the magnitude of unbalanced voltage dips is derived.

Dips type D are dips with the main drop in one phase. To identify the sagged phase a subscript is added, hence D_a would be a dip with the main drop in phase *a*.

Dips type C are dips with a main drop between two phases. A subscript identifies the less sagged phase. Hence C_a would be a dip with the main drop between phase *b* and *c*.

Dips C and D are unbalanced dips meaning that the retained phase voltages during the fault are different in each one of the phases. Thus, it is not possible to characterise the dip with a single magnitude and the three different voltage magnitudes need to be calculated. An alternative approach has been proposed by Zhang (1999) that is based on symmetrical components and the assumption that the positive sequence impedance is equal to the negative-sequence impedance. Additionally the zero sequence voltage is treated as a separate characteristic. The method will be examined at the end of this chapter, but first the general equations for voltages during the fault will be derived for symmetrical and unsymmetrical faults. For the

latter ones the effect of transformer winding connections will be considered in Section 3.5.

3.2 Balanced Voltage Dip Magnitude

Three-phase faults cause balanced dips, type A. Consider a network with $N+1$ nodes (N buses plus a reference node) and its impedance matrix $\mathbf{Z}$. The reference node is named zero and is chosen to be the common generator node. According to the superposition theorem the voltage at node k during a three-phase fault at node f is given by (3.1a).

$$v_{kf} = v_{pref(k)} + \Delta v_{kf} \tag{3.1a}$$

The voltage during the fault is the pre-fault voltage at the observation bus plus the change in the voltage due to the fault. In (3.1a) $v_{pref(k)}$ is the pre-fault voltage at node k and Δv_{kf} is the voltage-change at node k due to the fault at node f. It should be noted that we are dealing with complex variables of the type $a+jb$, however the bar over the variables has been omitted to simplify the notation.

Equation (3.1a) can be interpreted as matrix relation (3.1b) in which case v_{kf} is the (k,f) element of a matrix named here "dip matrix" $\mathbf{V_{dfv}}$. The dip matrix contains all the during-fault voltages. For example row k of $\mathbf{V_{dfv}}$ contains the residual voltages at that node when faults occur at nodes 1,2,..k,..N, while the column f of $\mathbf{V_{dfv}}$ contains the residual voltage at nodes 1,2,..k,..N for a fault at node f. $\mathbf{V_{pref}}$ is the pre-fault voltage matrix and because the pre-fault voltage at node k is the same for a fault at any node, the pre-fault voltage matrix is conformed by N equal columns. $\mathbf{\Delta V}$ is a matrix containing the changes in voltage due to faults everywhere. This matrix-based approach is useful for computational implementation of the stochastic assessment.

$$\mathbf{V_{dfv}} = \mathbf{V_{pref}} + \mathbf{\Delta V} \tag{3.1b}$$

The voltage changes Δv_{kf} can be calculated by means of the impedance matrix. As stated in Chapter2, the impedance matrix, $\mathbf{Z}$, contains the driving-point impedances z_{ff} and the transfer impedances z_{kf} between each bus of the system and every other bus with respect to the reference bus.

During a three-phase short-circuit at node f, the current "injected" into the node f is given by (3.2), where $v_{pref(f)}$ is the pre-fault voltage at the faulted bus f, z_{ff} is the impedance seen looking into the network at the faulted node f, and the minus sign is due to the direction of the

current. Only positive sequence values are needed to perform the calculations.

$$i_f = \frac{-v_{pref(f)}}{z_{ff}} \tag{3.2}$$

Once the "injected" current, due to the fault at node *f*, is known the change in voltage at any bus *k* can be calculated using the transfer impedance z_{kf} between bus *k* and node *f*. The transfer impedance is the voltage that exists on bus *k*, with respect to the reference, when bus *f* is driven by an "injection" current of unity. Then (3.3a) gives the change in voltage due to the current expressed by (3.2). The matrix version for this equation is given in (3.3b), where **inv(diagZ)** is the inverse of the matrix containing the diagonal elements of the impedance matrix, the asterisk (*) denotes element-element multiplication and the *T* over $\mathbf{V_{pref}}$ indicates transposition of the pre-fault voltage matrix.

$$\Delta v_{kf} = -z_{kf} \cdot \frac{v_{pref(f)}}{z_{ff}} \tag{3.3a}$$

$$\mathbf{\Delta V} = -\mathbf{Z} \cdot \mathbf{inv(diagZ)} * \mathbf{V}_{\mathbf{pref}}^{\mathbf{T}} \tag{3.3b}$$

It should be noted that $\mathbf{\Delta V}$ is a non-symmetric matrix, i.e. $\Delta v_{kf} \neq \Delta v_{fk}$ because $z_{ff} \neq z_{kk}$.

The dips for a three-phase fault are found applying (3.1), this is adding to (3.3) the pre-fault voltage as shown in (3.4).

$$v_{kf} = v_{pref(k)} - z_{kf} \cdot \frac{v_{pref(f)}}{z_{ff}} \tag{3.4}$$

Equation (3.4) can be simplified by neglecting the load, which allows taking the pre-fault voltages equal to 1 p.u. This may appear an unacceptable approximation here, but as we will use the expression for stochastic prediction of the magnitude of voltages during the fault, the approximation is allowed. On the other hand, as the pre-fault voltages are unknown (depends on load, generator scheduling, transformer tap-changers and capacitor banks) we take the expected value (1p.u.) in the calculations.

Equation (3.4) shows that the voltage change at a bus *k* due to a three-phase fault at node *f* is given by the quotient between the transfer impedance and the driven point impedance at the fault node. The positive-sequence impedance matrix **Z** is a diagonal dominant full matrix for a connected network. This means that every bus in the network is exposed to dips due to faults everywhere in the network, however the magnitude of the voltage drop depends on the transfer

impedance between the observation bus and the faulted point. In general the transfer impedance decreases with the distance between the faulted point and load bus. Hence load points will not seriously be affected by faults located far away in the system.
The voltage change also depends on the driving impedance at the faulted bus. The driving impedance determines the weakness of the bus. The stronger the faulted bus the larger the voltage drop at another bus and vice versa.

3.2.1 Phase Angle Jump

Along with the depression of the voltage magnitude, a remote fault also leads to a variation in the phase angle of the voltage. This phase angle variation is known as phase-angle jump (Bollen, 1995) and is caused by the angular difference between the impedances involved in the dip calculation. From (3.4) it can be seen that for a no-load condition, the phase-angle jump is the angular difference between the transfer impedance and the driving impedance at the fault point. In other words a phase-angle jump occurs when the quotient z_{kf}/z_{ff} is not a real number. Equation (3.4) also shows that the angular difference between the pre-fault voltages play an important role in the phase angle jump. At transmission levels, this angular difference may be larger than the phase-angle jump due to the difference in impedances, particularly if the observation bus is heavily loaded and the fault occurs at a generation bus.

3.3 Unbalanced Voltage Dip Magnitudes

Unbalanced voltage dips are caused by unsymmetrical faults requiring the use of symmetrical components for their analysis. However the same principles and approach presented in Section 3.2 can be used to determine the during-fault voltages. The superposition theorem is valid allowing the use of (3.1) both in phase and symmetrical component domain.
Because of the independence of sequences in symmetrical systems, we can write (3.1) for each sequence network and determine the during-fault voltage for each of the sequence components. Before the fault, node voltages only contain a positive-sequence component, thus pre-fault voltage matrices of zero and negative sequences are zero.

$$\mathbf{V}_{\mathbf{dfv}}^{\mathbf{z}} = \mathbf{0} + \Delta\mathbf{V}^{\mathbf{z}} \tag{3.5a}$$

$$\mathbf{V}_{\mathbf{dfv}}^{\mathbf{p}} = \mathbf{V}_{\mathbf{pref}}^{\mathbf{p}} + \Delta\mathbf{V}^{\mathbf{p}} \tag{3.5b}$$

$$\mathbf{V}^{\mathbf{n}}_{\mathbf{dfv}} = \mathbf{0} + \Delta\mathbf{V}^{\mathbf{n}} \tag{3.5c}$$

Once the sequence during-fault voltages are determined, the phase voltages can be calculated applying the symmetrical components transformation. Thus (3.6) gives the phase voltages considering phase *a* as the symmetrical phase.

$$\mathbf{V}^{\mathbf{a}}_{\mathbf{dfv}} = \mathbf{V}^{\mathbf{z}}_{\mathbf{dfv}} + \mathbf{V}^{\mathbf{p}}_{\mathbf{dfv}} + \mathbf{V}^{\mathbf{n}}_{\mathbf{dfv}} \tag{3.6a}$$

$$\mathbf{V}^{\mathbf{b}}_{\mathbf{dfv}} = \mathbf{V}^{\mathbf{z}}_{\mathbf{dfv}} + a^2 \cdot \mathbf{V}^{\mathbf{p}}_{\mathbf{dfv}} + a \cdot \mathbf{V}^{\mathbf{n}}_{\mathbf{dfv}} \tag{3.6b}$$

$$\mathbf{V}^{\mathbf{c}}_{\mathbf{dfv}} = \mathbf{V}^{\mathbf{z}}_{\mathbf{dfv}} + a \cdot \mathbf{V}^{\mathbf{p}}_{\mathbf{dfv}} + a^2 \cdot \mathbf{V}^{\mathbf{n}}_{\mathbf{dfv}} \tag{3.6c}$$

Inserting (3.5) into (3.6) we can write (3.7)

$$\mathbf{V}^{\mathbf{a}}_{\mathbf{dfv}} = \mathbf{V}^{\mathbf{p}}_{\mathbf{pref}} + \Delta\mathbf{V}^{\mathbf{z}} + \Delta\mathbf{V}^{\mathbf{p}} + \Delta\mathbf{V}^{\mathbf{n}} \tag{3.7a}$$

$$\mathbf{V}^{\mathbf{b}}_{\mathbf{dfv}} = a^2 \cdot \mathbf{V}^{\mathbf{p}}_{\mathbf{pref}} + \Delta\mathbf{V}^{\mathbf{z}} + a^2 \cdot \Delta\mathbf{V}^{\mathbf{p}} + a \cdot \Delta\mathbf{V}^{\mathbf{n}} \tag{3.7b}$$

$$\mathbf{V}^{\mathbf{c}}_{\mathbf{dfv}} = a \cdot \mathbf{V}^{\mathbf{p}}_{\mathbf{pref}} + \Delta\mathbf{V}^{\mathbf{z}} + a \cdot \Delta\mathbf{V}^{\mathbf{p}} + a^2 \cdot \Delta\mathbf{V}^{\mathbf{n}} \tag{3.7c}$$

Equation (3.7) gives the residual phase voltages during the fault and is valid independent of the fault type. The only missing part is the change in voltage during the fault $\Delta\mathbf{V}$ for each sequence. The following sections derive these expressions. Equations will be derived for a general element (*k,f*) but matrix expressions can be derived from them. All the analysis is for phase *a* as the symmetrical or reference phase.

3.3.1 Voltage Changes caused by a Single-phase-to-ground Fault

A single-phase-to-ground fault causes unbalanced dips that will propagate through the system. As shown in Chapter 2, the short circuit current is found by connecting the sequence networks in series. The current flowing through the three sequence networks is the same. Thus (3.8) gives the injected current into the positive, negative and zero sequence networks.

$$i_f^p = \frac{-v^a_{pref(f)}}{z^p_{ff} + z^n_{ff} + z^z_{ff}};\;\; i_f^z = i_f^p = i_f^n \tag{3.8}$$

To find the changes in voltage we apply the meaning of the transfer impedance in each sequence network: the sequence voltage at node *k* due to a unity current injected at node *f* is given by the sequence transfer-impedance between *k* and *f*. The sequence voltage-changes at bus *k* due to the phase-to-ground fault at node *f* are given by (3.9).

$$\Delta v^p_{kf} = -z^p_{kf} \cdot \frac{v^a_{pref(f)}}{z^p_{ff} + z^n_{ff} + z^z_{ff}} \tag{3.9a}$$

$$\Delta v_{kf}^{n} = -z_{kf}^{n} \cdot \frac{v_{pref(f)}^{a}}{z_{ff}^{p} + z_{ff}^{n} + z_{ff}^{z}} \tag{3.9b}$$

$$\Delta v_{kf}^{z} = -z_{kf}^{z} \cdot \frac{v_{pref(f)}^{a}}{z_{ff}^{p} + z_{ff}^{n} + z_{ff}^{z}} \tag{3.9c}$$

The pre-fault voltage at the load point k, $v_{pref(k)}$, only contains a positive-sequence component and is equal to the pre-fault voltage in phase a. The during-fault sequence voltages at node k are given by (3.10).

$$v_{kf}^{p} = v_{pref(k)}^{a} - z_{kf}^{p} \cdot \frac{v_{pref(f)}^{a}}{z_{ff}^{p} + z_{ff}^{n} + z_{ff}^{z}} \tag{3.10a}$$

$$v_{kf}^{n} = -z_{kf}^{n} \cdot \frac{v_{pref(f)}^{a}}{z_{ff}^{p} + z_{ff}^{n} + z_{ff}^{z}} \tag{3.10b}$$

$$v_{kf}^{z} = -z_{kf}^{z} \cdot \frac{v_{pref(f)}^{a}}{z_{ff}^{p} + z_{ff}^{n} + z_{ff}^{z}} \tag{3.10c}$$

The residual phase-voltages are obtained by transforming back to phase components.

$$v_{kf}^{a} = v_{pref(k)}^{a} - (z_{kf}^{z} + z_{kf}^{p} + z_{kf}^{n}) \cdot \frac{v_{pref(f)}^{a}}{z_{ff}^{p} + z_{ff}^{n} + z_{ff}^{z}} \tag{3.11a}$$

$$v_{kf}^{b} = a^{2} \cdot v_{pref(k)}^{a} - (z_{kf}^{z} + a^{2} \cdot z_{kf}^{p} + a \cdot z_{kf}^{n}) \cdot \frac{v_{pref(f)}^{a}}{z_{ff}^{p} + z_{ff}^{n} + z_{ff}^{z}} \tag{3.11b}$$

$$v_{kf}^{c} = a \cdot v_{pref(k)}^{a} - (z_{kf}^{z} + a \cdot z_{kf}^{p} + a^{2} \cdot z_{kf}^{n}) \cdot \frac{v_{pref(f)}^{a}}{z_{ff}^{p} + z_{ff}^{n} + z_{ff}^{z}} \tag{3.11c}$$

From 3.10c it is clear that phase voltages at node k will not contain a zero sequence component if the transfer impedance z^{z}_{kf} is zero. This is particularly true when the load and the fault point are at different sides of a transformer with delta winding or when the user's device is connected in delta or ungrounded star.

Equations 3.11 give the residual phase-voltage for a general case. If the zero sequence voltage can be neglected (or if z^{z}_{kf} is zero) and the positive-sequence impedance-matrix is equal to the negative-sequence, (3.11) can be simplified as indicated in (3.12).

$$v_{kf}^{a} = v_{pref(k)}^{a} - z_{kf}^{p} \cdot \frac{v_{pref(f)}^{a}}{z_{ff}^{p} + \frac{z_{ff}^{z}}{2}} \tag{3.12a}$$

$$v_{kf}^{b} = a^{2} \cdot v_{pref(k)}^{a} + \frac{1}{2} \cdot z_{kf}^{p} \cdot \frac{v_{pref(f)}^{a}}{z_{ff}^{p} + \frac{z_{ff}^{z}}{2}} \tag{3.12b}$$

$$v_{kf}^{c} = a \cdot v_{pref(k)}^{a} + \frac{1}{2} \cdot z_{kf}^{p} \cdot \frac{v_{pref(f)}^{a}}{z_{ff}^{p} + \frac{z_{ff}^{z}}{2}} \tag{3.12c}$$

Note that (3.12) shows that the residual phase voltages at the observation point can be calculated using a balanced short circuit algorithm by adding a fault impedance equal to half of the value of the zero-sequence driving-point-impedance at the fault point. This means that a single-phase-to-ground fault is less severe than a three-phase fault in terms of the depression in the voltage seen at the load bus. Due to the zero-sequence impedance, the faulted phase shows a smaller drop compared to a dip originated by three-phase fault. Figure 3.1 shows a phasor diagram of this kind of dips. The non-faulted phases show the same magnitude and direction in their voltage change. These voltage changes are half of the value of the magnitude of the voltage change in the faulted phase. The voltage change in the non-faulted phases has the same direction to the pre-fault voltage of phase *a*. These expressions only hold when the zero sequence voltage can be neglected and the positive-sequence impedance is equal to the negative-sequence impedance.

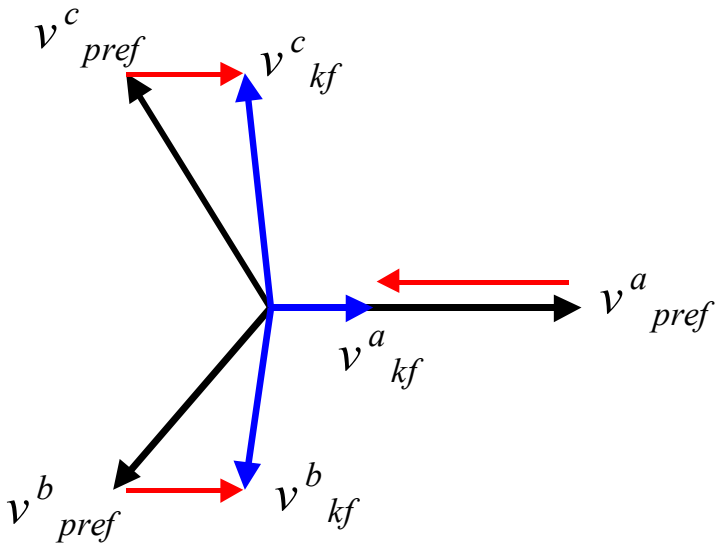

Figure 3.1: Phasor diagram of a single-phase-to-ground fault caused dip, for Z^p=Z^n and z^z_{kf} =0

The voltage dip shown in Figure 3.1 is a D_a dip. One could conclude that a single-phase-to-ground fault involving phase *a* causes a D_a dip,

however as we will see in Section 3.5, a transformer between the faulted point and the observation bus may change the character of three-phase unbalanced dips. What we can conclude is that a single-phase-to-ground fault is seen as a dip D as long as there is no transformer or phase shifting device between the observation bus and the fault point.

3.3.2 Voltage Changes caused by a Phase-to-phase Fault

For a phase-to-phase fault only the positive and the negative-sequence networks take part in the analysis. The zero sequence-current is zero and so is the zero-sequence voltage. As shown in Chapter 2, Figure 2.7c, the positive-sequence current at the fault location is equal in magnitude to the negative-sequence current, but in opposite direction. Equation (3.13) gives the injected currents in the sequence networks.

$$i_f^p = \frac{-v^a_{pref(f)}}{z^p_{ff} + z^n_{ff}} \;;\; i_f^p = -i_f^n \tag{3.13}$$

The change in positive- and negative-sequence voltage is given by (3.14). The zero-sequence voltage-change is zero.

$$\Delta v^p_{kf} = -z^p_{kf} \frac{v^a_{pref(f)}}{z^p_{ff} + z^n_{ff}} \tag{3.14a}$$

$$\Delta v^n_{kf} = z^n_{kf} \frac{v^a_{pref(f)}}{z^p_{ff} + z^n_{ff}} \tag{3.14b}$$

The residual phase-voltages are obtained by adding the pre-fault voltage to (3.14a) and transforming back to phase components.

$$v^a_{kf} = v^a_{pref(k)} + (z^n_{kf} - z^p_{kf}) \cdot \frac{v^a_{pref(f)}}{z^p_{ff} + z^n_{ff}} \tag{3.15a}$$

$$v^b_{kf} = a^2 \cdot v^a_{pref(k)} + (-a^2 \cdot z^p_{kf} + a \cdot z^n_{kf}) \cdot \frac{v^a_{pref(f)}}{z^p_{ff} + z^n_{ff}} \tag{3.15b}$$

$$v^c_{kf} = a \cdot v^a_{pref(k)} + (-a \cdot z^p_{kf} + a^2 \cdot z^n_{kf}) \cdot \frac{v^a_{pref(f)}}{z^p_{ff} + z^n_{ff}} \tag{3.15c}$$

If the positive-sequence impedance matrix is equal to the negative-sequence impedance matrix, (3.15) takes the form indicated in (3.16).

$$v^a_{kf} = v^a_{pref(k)} \tag{3.16a}$$

$$v_{kf}^{b} = a^{2} \cdot v_{pref(k)}^{a} + j \cdot \sqrt{3} \cdot z_{kf}^{p} \cdot \frac{v_{pref(f)}^{a}}{2 \cdot z_{ff}^{p}} \tag{3.16b}$$

$$v_{kf}^{c} = a \cdot v_{pref(k)}^{a} - j \cdot \sqrt{3} \cdot z_{kf}^{p} \cdot \frac{v_{pref(f)}^{a}}{2 \cdot z_{ff}^{p}} \tag{3.16c}$$

Figure 3.2 shows the phasor diagram for a dip caused by a phase-to-phase fault when the positive-sequence impedance is equal to the negative-sequence. The non-faulted phase does not see any change in the voltage. The change in the voltages of the faulted phases is equal in magnitude but opposite in direction. In the faulted phases, the voltages drop along the direction of pre-fault line-to-line voltage between the faulted phases. This kind of dip is called type C. Hence a phase-to-phase fault is seen as a dip C as long as there is no transformer or phase shifting device between the observation bus and the fault point.

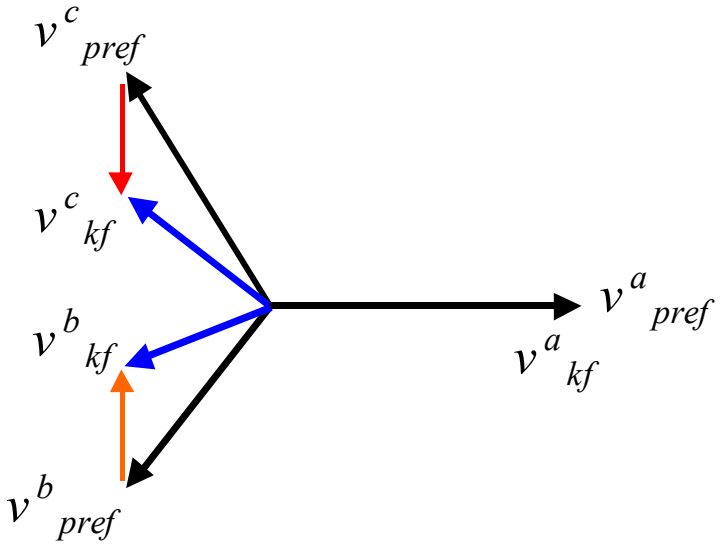

Figure 3.2: Phasor diagram of a phase-to-phase fault caused dip, for Z^p=Z^n

3.3.3 Voltage Changes caused by a Two-phase-to-ground Fault

The sequence networks need to be connected in parallel to derive the fault current in a two-phase-to-ground fault. The three sequence currents are different. Equation (3.17) gives the injected currents in each one of the sequence networks.

$$i_{f}^{p} = \frac{-v_{pref(f)}^{a}}{z_{ff}^{p} + \frac{z_{ff}^{z} \cdot z_{ff}^{n}}{z_{ff}^{z} + z_{ff}^{n}}} = \frac{-v_{pref(f)}^{a} \cdot (z_{ff}^{z} + z_{ff}^{n})}{z_{ff}^{p} \cdot z_{ff}^{z} + z_{ff}^{n} \cdot z_{ff}^{p} + z_{ff}^{z} \cdot z_{ff}^{n}} \tag{3.17a}$$

$$i_f^n = \frac{z_{ff}^z}{z_{ff}^p \cdot z_{ff}^z + z_{ff}^n \cdot z_{ff}^p + z_{ff}^z \cdot z_{ff}^n} \cdot v_{pref(f)}^a \tag{3.17b}$$

$$i_f^z = \frac{z_{ff}^n}{z_{ff}^p \cdot z_{ff}^z + z_{ff}^n \cdot z_{ff}^p + z_{ff}^z \cdot z_{ff}^n} \cdot v_{pref(f)}^a \tag{3.17c}$$

Once the currents injected into each sequence network are known the changes in nodal voltages can be determined by means of the transfer impedances in the corresponding sequence. The only sequence voltage present before the fault is the positive-sequence voltage and is equal to the pre-fault voltage at phase *a*. Thus (3.18) gives the during-fault sequence voltages.

$$v_{kf}^z = z_{kf}^z \cdot \frac{z_{ff}^n}{z_{ff}^p \cdot z_{ff}^z + z_{ff}^n \cdot z_{ff}^p + z_{ff}^z \cdot z_{ff}^n} \cdot v_{pref(f)}^a \tag{3.18a}$$

$$v_{kf}^p = v_{pref(k)}^a + z_{kf}^p \cdot \frac{-(z_{ff}^z + z_{ff}^n)}{z_{ff}^p \cdot z_{ff}^z + z_{ff}^n \cdot z_{ff}^p + z_{ff}^z \cdot z_{ff}^n} \cdot v_{pref(f)}^a \tag{3.18b}$$

$$v_{kf}^n = z_{kf}^n \cdot \frac{z_{ff}^z}{z_{ff}^p \cdot z_{ff}^z + z_{ff}^n \cdot z_{ff}^p + z_{ff}^z \cdot z_{ff}^n} \cdot v_{pref(f)}^a \tag{3.18c}$$

Finally the retained phase voltages are found by applying the symmetrical component transformation.

$$v_{kf}^a = v_{pref(k)}^a + \frac{v_{pref(f)}^a \cdot \left\{(z_{kf}^n - z_{kf}^p) \cdot z_{ff}^z + (z_{kf}^z - z_{kf}^p) \cdot z_{ff}^n\right\}}{z_{ff}^p \cdot z_{ff}^z + z_{ff}^n \cdot z_{ff}^p + z_{ff}^z \cdot z_{ff}^n} \tag{3.19a}$$

$$v_{kf}^b = a^2 \cdot v_{pref(k)}^a + \frac{v_{pref(f)}^a \cdot \left\{(a \cdot z_{kf}^n - a^2 \cdot z_{kf}^p) \cdot z_{ff}^z + (z_{kf}^z - a^2 \cdot z_{kf}^p) \cdot z_{ff}^n\right\}}{z_{ff}^p \cdot z_{ff}^z + z_{ff}^n \cdot z_{ff}^p + z_{ff}^z \cdot z_{ff}^n} \tag{3.19b}$$

$$v_{kf}^c = a \cdot v_{pref(k)}^a + \frac{v_{pref(f)}^a \cdot \left\{(a^2 \cdot z_{kf}^n - a \cdot z_{kf}^p) \cdot z_{ff}^z + (z_{kf}^z - a \cdot z_{kf}^p) \cdot z_{ff}^n\right\}}{z_{ff}^p \cdot z_{ff}^z + z_{ff}^n \cdot z_{ff}^p + z_{ff}^z \cdot z_{ff}^n} \tag{3.19c}$$

From (3.19) it can be seen that two effects govern the change in the voltage of the non-faulted phase *a*: 1) the difference between the transfer impedances of positive and negative sequence, and 2) the difference between the transfer impedances of positive and zero sequence. For both effects the non-faulted phase drops when the positive-sequence impedance increases. At transmission levels the positive and negative-sequence impedances are similar and the zero-sequence impedance is usually larger than the positive one, so we expect a rise in the non-faulted phase-voltage.

3.4 The Characteristic Voltage and Positive-Negative Factor

The set of three sequence-component voltages fully determines the three-phase voltages everywhere in the network. For the symmetrical phase (phase *a* in our analysis) the phase-voltage is given by the addition of zero, positive and negative-sequence voltages. For the non-symmetrical phases a rotation of the negative and positive sequence components are needed before adding these components to the zero sequence. This is shown in equation (3.7).

Sequence voltages are a function of the sequence impedances and their connections in the sequence networks. The three sequence networks are needed to determine the three sequence voltages. However, under the assumption of equal positive and negative sequence impedance the number of variables is reduced to two. This is what the two-component method does (Anderson, 1973). The method takes the positive sequence impedance equal to the negative one and defines two new positive sequence variables: the sum and subtraction of the positive and negative sequence voltages (and currents). By this change in variables the number of networks needed to perform the calculations is reduced from three to two, since both the sum and subtraction of positive and negative-sequences are defined as variables of the positive-sequence network. Hence a new transformation matrix is defined as indicated in (3.20).

$$\begin{vmatrix} V^a \\ V^b \\ V^c \end{vmatrix} = \begin{vmatrix} 1 & 1 & 0 \\ 1 & -1/2 & -j\sqrt{3}/2 \\ 1 & -1/2 & -j\sqrt{3}/2 \end{vmatrix} \begin{vmatrix} V^z \\ V^\Sigma \\ V^\Delta \end{vmatrix}; \qquad \begin{aligned} V^\Sigma &= V^p + V^n \\ V^\Delta &= V^p - V^n \end{aligned} \tag{3.20}$$

In (3.20) V^Σ and V^Δ are a new set of sequence variables associated with the positive-sequence network and called sigma and delta respectively.

The equality between positive and negative-sequence impedance does not mean equality between positive and negative-sequence voltages, but reduces the number of relevant variables needed to characterise the three phase voltages and thus the dip. This idea was used by Zhang (1999) to define a single characteristic to describe the magnitude of a three-phase unbalanced dip: the characteristic voltage, V_{kf}. The characteristic voltage and positive-negative factor, F_{kf}, was introduced in (Zhang, 1999) as a characterisation methodology of three-phase unbalanced dips.

The method is based on the assumption that the positive-sequence impedance is equal to the negative-sequence one. The zero-sequence voltage is treated as a separate characteristic and is sometimes neglected. This is particularly valid if the observation bus k and the fault point f are located at different sides of a delta or ungrounded wye winding. Under these considerations unbalanced voltage dips can, mainly, be characterised by one vector: the characteristic voltage. The additional vector, positive-negative factor, is introduced to take into account the fact that positive and negative sequence impedances might not be equal. The positive-negative factor also quantifies the effect of motor load on dips and the difference between dips due to phase-to-phase and due to two-phase-to-ground faults. For single-phase-to-ground and phase-to-phase faults the positive-negative factor is equal to the pre-fault voltage at the observation bus if the equality between positive and negative-sequence impedances applies.
In order to derive equations for the new transformation one needs to analyse the fault type, its boundary conditions and apply the new transformation equation (3.20) in the same way as we did when deriving the during fault voltages. However, it is possible to get the same results by calculating sigma and delta quantities from the expressions for the positive and negative-sequence voltages and introducing the equality between positive and negative-sequence impedances.

Three-phase fault
A three-phase fault causes a balanced dip, type A. There is neither negative nor zero-sequence voltage. The dip is fully characterised by its phase-residual voltage, which is of positive-sequence. For this dip the characteristic voltage can be defined both as the sum, sigma, or subtraction, delta, of positive and negative-sequence voltages. Equation (3.4) shows the residual voltage that is the same for positive sequence. This is also the characteristic voltage for a balanced dip.

Single-phase fault
A single-phase-to-ground fault causes unbalanced dips D with residual sequence voltages as shown in (3.10). For this dip type, the characteristic voltage is defined as sigma, whereas the positive-negative factor is defined as delta. From (3.10) taking the sum and subtraction of positive and negative-sequence voltages and considering positive-sequence impedances equal to negative ones, we get (3.21):

$$V_{kf} = v^{a}_{pref(k)} - z^{p}_{kf} \cdot \frac{v^{a}_{pref(f)}}{z^{p}_{ff} + \frac{z^{z}_{ff}}{2}} \tag{3.21a}$$

$$F_{kf} = v^{a}_{pref(k)} \tag{3.21b}$$

Note that the characteristic voltage V_{kf} is exactly the retained voltage in the faulted phase (3.12a) and the positive-negative factor F_{kf} is the pre-fault voltage at the observation bus k.

Phase-to-phase fault

This fault is fully determined by the during-fault positive- and negative-sequence voltages. The changes in sequence voltages due to a phase-to-phase fault are given in (3.14). The fault generates dips type C. For this kind of dip the characteristic voltage is defined as the residual positive-sequence voltage minus the residual negative-sequence voltage, i.e. delta. The positive-negative factor is defined as sigma.

$$V_{kf} = v^{a}_{pref(k)} - z^{p}_{kf} \cdot \frac{v^{a}_{pref(f)}}{z^{p}_{ff}} \tag{3.22a}$$

$$F_{kf} = v^{a}_{pref(k)} \tag{3.22b}$$

$$V^{b-c}_{kf} = v^{b-c}_{pref(k)} - z^{p}_{kf} \cdot \frac{v^{b-c}_{pref(f)}}{z^{p}_{ff}} \tag{3.22c}$$

Again the positive-negative factor F_{kf} is the pre-fault voltage at the observation bus k. The characteristic voltage V_{kf} is the same as for a three-phase fault. From (3.16) it can be seen that the characteristic voltage is also equal to the magnitude of the phase-to-phase during-fault voltage between the faulted phases divided by √3. In other words (3.22a) can be read as the during-fault voltage between faulted phases, as indicated in (3.22c).

Two-phase-to-ground fault

For this fault the characteristic voltage is defined in the same way as for phase-to-phase fault. The difference of positive and negative-sequence voltages is the characteristic voltage and the positive-negative factor is given by the sum of them. Equation (3.18) shows the residual voltage in sequence components. From (3.18) and the additional assumption that the pre-fault voltage at the load point is equal to the pre-fault voltage at the faulted bus, it can be shown that (3.23) gives the characteristic voltage and the positive-negative factor.

$$V_{kf} = v^{a}_{pref(f)} - z^{p}_{kf} \cdot \frac{v^{a}_{pref(f)}}{z^{p}_{ff}} \tag{3.23a}$$

$$F_{kf} = v^{a}_{pref(f)} - \frac{z^{p}_{kf}}{z^{p}_{ff} + 2 \cdot z^{z}_{ff}} v^{a}_{pref(f)} \tag{3.23b}$$

Again the resulting characteristic voltage is equal to the characteristic voltage for a three-phase fault. The positive-negative factor is less than the pre-fault voltage. It is interesting to note that for two-phase-to-ground faults in a high-impedance-grounded system the positive–negative factor is close to the pre-fault voltage. In other words, phase-to-phase and two-phase-to-ground faults result in the same dips in a high-impedance-grounded system.

3.5 Effect of Power Transformers on the Dip Type

In the previous section equations for calculating the residual voltages during the fault have been developed. Four different fault types were considered: three-phase fault, single-phase-to-ground fault, two-phase fault and two-phase-to-ground fault. Those equations are general and consider the pre-fault voltages at the faulted and load bus but do not consider the effect of power transformers. Power transformers affect the phase voltages. Two effects can be identified: re-labelling of phases at the secondary of the transformer and phase shift due to winding connection.

The effect introduced by re-labelling can be considered by changing the symmetrical component in the corresponding equation. The only effect here is a changing in variables. The dip does not change its type.

Depending on the winding connections of the transformer the retained voltages seen at the secondary side due to an unsymmetrical fault at the primary side may be modified. This means that the dip type may change when going through the transformer.

A delta or ungrounded wye winding removes the zero-sequence voltage component. This zero-sequence blocking is taken into account by modelling the zero-sequence impedance of the transformer. Positive and negative-sequences (voltages and currents) pass through the transformer, and in the sequence networks, the impedance is the same independently of the winding connections. In case of delta-wye transformers, a phase shift is introduced by the winding connections of the transformer that need to be considered to calculate the correct during fault voltages. Such a phase shift is seen in practice as a transformation between fault types. In other words a

phase-to-phase fault at one side of the transformer is seen as a phase-to-ground fault at the other and this effect has not been modelled yet in our equations.

Delta-wye connections are discussed, as these are the most commonly used. For transformers manufactured according to the ANSI/IEEE standard (ANSI/IEEE, 1988), the low voltage side, whether in wye or delta, has a phase shift of 30^o lagging with respect to the high voltage side phase-to-neutral voltage vector. These phase displacements are applicable to positive-sequence voltages. Hence in passing through the transformer from the fault side to the observation side, the positive-sequence phase voltages of the corresponding phase are shifted 30^o in one direction, and the negative-sequence quantities are shifted in the other direction. These phase shifts can be incorporated into the dip equations to consider the effect of transformers. However, from the point of view of dip characterisation what is important is the complex during-fault voltage with respect to the pre-event voltage at the same bus, see (3.1a). At the observation point the pre-fault phase voltage is of positive-sequence and is the reference for the dip at that point. Hence the positive-sequence voltage does not need to be shifted, but the negative one needs to be shifted $\pm 60^o$ to take into account the effect of the transformer.

To clarify, consider an IEEE standard power transformer between two sectors of a transmission system, as shown in Figure 3.3.

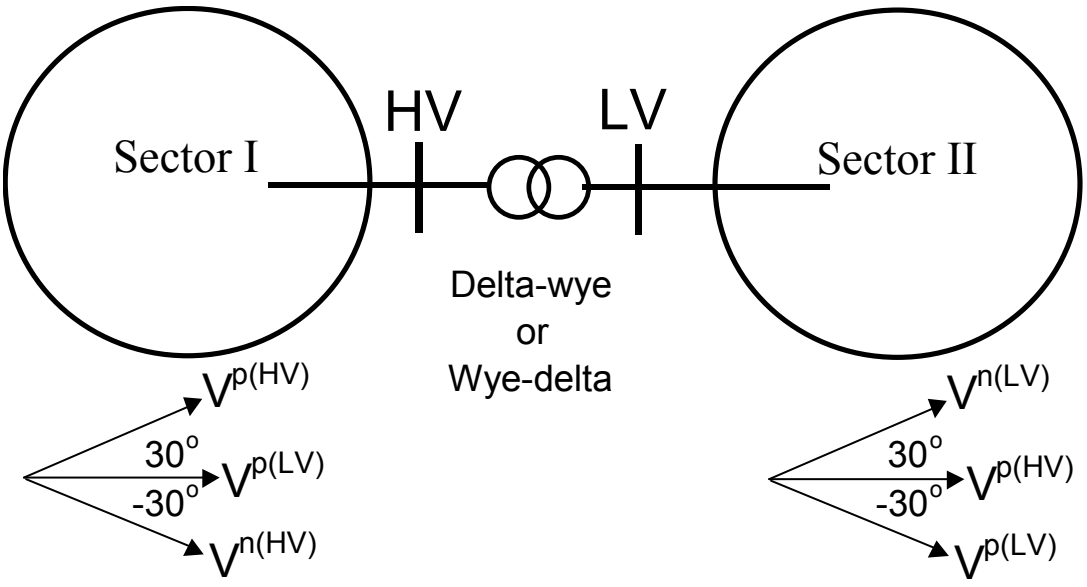

Figure 3.3: A Delta-wye power transformer between two sectors of a transmission system

Sector I is the high voltage sector while sector II is the low voltage sector. According to (ANSI/IEEE, 1988) the positive-sequence phase

to neutral voltage at sector II has a phase shift of -30° with respect to the positive-sequence phase to neutral voltage of sector I. In terms of dips, this phase shift is seen as a ±60° phase shift in the negative sequence with respect to the positive sequence voltage of the same sector. The direction of the rotation, the sign, depends on the observation bus, the reference, and on the fault point, the origin of the event.

For unbalanced dips originated at the HV sector and observed at the LV sector the rotation in the negative sequence is +60°.

For unbalanced dips originated at the LV sector and observed at the HV sector a -60° shift needs to be considered in the negative sequence.

The phase angle shift introduced by the transformer in the negative sequence can be written in terms of the Fortescue *a*-transformer operator.

$$+60^{o} = -a^{2} \tag{3.24a}$$

$$-60^{o} = -a \tag{3.24b}$$

Now consider a phase-to-phase fault involving phase *b* and *c* in the HV sector. The dip caused by this fault is seen at the HV sector as a C_a dip and it was described in Section 3.3.2. In the HV sector, there is no need for shifting the negative-sequence because the fault point and the observation bus are located at the same sector. The same fault causes a dip at the LV, but in this case a phase shift of +60° is introduced into the negative-sequence as shown in (3.25). Equation (3.25) has been derived shifting the negative sequence of equation (3.15).

$$v^{a}_{kf(LV-HV)} = v^{a}_{pref(k)} + (-a^{2} \cdot z^{n}_{kf} - z^{p}_{kf}) \cdot \frac{v^{a}_{pref(f)}}{z^{p}_{ff} + z^{n}_{ff}} \tag{3.25a}$$

$$v^{b}_{kf(LV-HV)} = a^{2} \cdot v^{a}_{pref(k)} + (-a^{2} \cdot z^{p}_{kf} - a^{3} \cdot z^{n}_{kf}) \cdot \frac{v^{a}_{pref(f)}}{z^{p}_{ff} + z^{n}_{ff}} \tag{3.25b}$$

$$v^{c}_{kf(LV-HV)} = a \cdot v^{a}_{pref(k)} + (-a \cdot z^{p}_{kf} - a^{4} \cdot z^{n}_{kf}) \cdot \frac{v^{a}_{pref(f)}}{z^{p}_{ff} + z^{n}_{ff}} \tag{3.25c}$$

Using basic relations of the Fortescue *a*-operator, (3.25) can be written as shown in (3.26).

$$v^{a}_{kf(LV-HV)} = a^{2} \cdot a \cdot v^{a}_{pref(k)} + (-a \cdot z^{n}_{kf} - a^{2} z^{p}_{kf}) \cdot \frac{a \cdot v^{a}_{pref(f)}}{z^{p}_{ff} + z^{n}_{ff}} \tag{3.26a}$$

$$v^{b}_{kf(LV-HV)} = a \cdot a \cdot v^{a}_{pref(k)} + (-a \cdot z^{p}_{kf} - a^{2} \cdot z^{n}_{kf}) \cdot \frac{a \cdot v^{a}_{pref(f)}}{z^{p}_{ff} + z^{n}_{ff}} \quad (3.26b)$$

$$v^{c}_{kf(LV-HV)} = a \cdot v^{a}_{pref(k)} + (-z^{p}_{kf} - z^{n}_{kf}) \cdot \frac{a \cdot v^{a}_{pref(f)}}{z^{p}_{ff} + z^{n}_{ff}} \quad (3.26c)$$

Expressing the $v_{pref(k)}$ of phase *c* in terms of phase *a*, we can write (3.27).

$$v^{a}_{kf(LV-HV)} = a^{2} \cdot v^{c}_{pref(k)} - (a \cdot z^{n}_{kf} + a^{2} z^{p}_{kf}) \cdot \frac{v^{c}_{pref(f)}}{z^{p}_{ff} + z^{n}_{ff}} \quad (3.27a)$$

$$v^{b}_{kf(LV-HV)} = a \cdot v^{c}_{pref(k)} - (a \cdot z^{p}_{kf} + a^{2} \cdot z^{n}_{kf}) \cdot \frac{v^{c}_{pref(f)}}{z^{p}_{ff} + z^{n}_{ff}} \quad (3.27b)$$

$$v^{c}_{kf(LV-HV)} = v^{c}_{pref(k)} - (z^{p}_{kf} + z^{n}_{kf}) \cdot \frac{v^{c}_{pref(f)}}{z^{p}_{ff} + z^{n}_{ff}} \quad (3.27c)$$

Comparing (3.27) with (3.11) we conclude that the C_a dip is seen at the other side (low voltage) of the transformer as a D_c dip the only difference being the zero-sequence component. The similarity can be made clearer taking the positive and negative-sequence impedances equal and neglecting the zero-sequence component. In this case we get (3.28) which we compare with (3.12).

$$v^{a}_{kf(LV-HV)} = a^{2} \cdot v^{c}_{pref(k)} + \frac{1}{2} \cdot z^{p}_{kf} \cdot \frac{v^{c}_{pref(f)}}{z^{p}_{ff}} \quad (3.28a)$$

$$v^{b}_{kf(LV-HV)} = a \cdot v^{c}_{pref(k)} + \frac{1}{2} \cdot z^{p}_{kf} \cdot \frac{v^{c}_{pref(f)}}{z^{p}_{ff}} \quad (3.28b)$$

$$v^{c}_{kf(LV-HV)} = v^{c}_{pref(k)} - z^{p}_{kf} \cdot \frac{v^{c}_{pref(f)}}{z^{p}_{ff}} \quad (3.28c)$$

The same phasor diagram of Figure 3.1 is applicable with phase *c* as the symmetrical phase.

Note that the previous analysis shows that a C_a dip at the HV sector is seen as a D_c dip at the LV, but also that a D_c dip at the LV sector is seen as a C_a dip at the HV sector. A similar analysis shows that a D_a dip at the LV sector is seen as a dip C_b at the HV sector. Although the previous analysis allows identifying the phases involved in the dip type, in practice the phases involved depend on the re-labelling of phases. Hence what can be concluded is that delta-wye transformers change the dip type from D to C and the other way around. This means that the total number of dips type D seen at one sector are

caused by single-phase faults at the same sector plus the ones caused by phase-to-phase and two-phase-to-ground faults at the other sector.

4 Propagation and Counting of Voltage Dips in Power Systems

This chapter introduces the method of fault positions for stochastic assessment of dips. It also describes graphical ways to present the effect of a fault on the system and the area where faults cause severe dips on a given load: affected area and exposed respectively. A hypothetical system is used to illustrate the ideas.

4.1 Prediction and Propagation of Voltage Dips

Voltage dips associated with faults have many predictable characteristics. In this work, magnitude and frequency of the dip are of main concern. It was shown in Chapter 3 that predicting the magnitude of the dips requires a model of the network and the application of short circuit techniques in order to calculate during-fault voltages at buses of the system. The rms voltage depression caused by a fault propagates through the network and is seen as a dip at remote observation buses.

Predicting dip characteristics a sensitive load will see during several years of operation requires a probabilistic approach. It is impossible to predict exactly where each fault will occur, but it is reasonable to assume that many faults will occur throughout the network. Faults might occur on buses or lines leading to different dip magnitudes. Faults on lines are more frequent than faults on buses.

The voltage seen at a remote bus k due to a fault at node f can be expressed by the general equation (3.1b) presented in Chapter 3. For a three-phase fault the dip-matrix is given by (4.1) where $\mathbf{Z}$ is the impedance matrix, $\mathbf{V_{pref}}$ is the pre-fault voltage matrix and **inv(diagZ)** is the matrix formed by the inverse of the diagonal elements of the impedance matrix.

$$\mathbf{V_{dfv}} = \mathbf{V_{pref}} - \mathbf{Z} \cdot \mathbf{inv(diagZ)} * \mathbf{V_{pref}^{T}} \qquad (4.1a)$$

If the pre-fault load can be neglected, then voltages before the fault can be considered 1 p.u. Under this assumption, (4.1a) can be written as (4.1b) where **ones** is a matrix full of ones and such that its dimension is equal to the dimension of $\mathbf{Z}$. As explained in Chapter 3, this approximation is allowed because we use the expressions for stochastic prediction.

$$\mathbf{V_{dfv}} = \mathbf{ones} - \mathbf{Z} \cdot \mathbf{inv(diagZ)} * \mathbf{ones} \qquad (4.1b)$$

The square N by N matrix $\mathbf{V_{dfv}}$ contains the dips observed at each bus of the network caused by a fault at each one of the buses. The during fault voltage at a general bus j when a fault occurs at that bus is contained in the diagonal of $\mathbf{V_{dfv}}$ and is zero for a solid three-phase fault. Off-diagonal elements of $\mathbf{V_{dfv}}$ are the residual voltages at a general bus k caused by a fault at a general position f. Hence, column f contains the residual voltages at buses $1,2\ldots f,\ldots N$ during the fault at node f. This means that the effect, in terms of dips, of a fault at a given bus of the system is contained in columns of the dip matrix. This information can be graphically presented on the one-line diagram of the power system and it is called affected area. The following section presents this concept in details.
The dip matrix can also be read by rows. A given row k identifies that bus in the system and the potential dips to which the load connected at this bus is exposed due to faults in the system. This information can also be presented in a graphical way on the one-line diagram and is called exposed area. Section 4.1.2 presents this idea.

4.1.1 Affected Area

Consider the hypothetical power system of Figure 4.1 and its impedance matrix. The power system contains 19 buses plus the reference node that is chosen to be the common generator node.

$$\mathbf{V_{dfv}} = \begin{bmatrix} 0 & 1-\frac{z_{1,2}}{z_{2,2}} & .. & 1-\frac{z_{1,8}}{z_{8,8}} & .. & 1-\frac{z_{1,11}}{z_{11,11}} & .. & 1-\frac{z_{1,19}}{z_{19,19}} \\ 1-\frac{z_{2,1}}{z_{1,1}} & 0 & .. & 1-\frac{z_{2,8}}{z_{8,8}} & .. & 1-\frac{z_{2,11}}{z_{11,11}} & .. & 1-\frac{z_{2,19}}{z_{19,19}} \\ : & : & 0 & : & : & : & : & : \\ 1-\frac{z_{8,1}}{z_{1,1}} & 1-\frac{z_{8,2}}{z_{2,2}} & .. & 0 & .. & 1-\frac{z_{8,11}}{z_{11,11}} & .. & 1-\frac{z_{8,19}}{z_{19,19}} \\ : & : & : & : & 0 & : & : & : \\ 1-\frac{z_{11,1}}{z_{1,1}} & 1-\frac{z_{11,2}}{z_{2,2}} & .. & 1-\frac{z_{11,8}}{z_{8,8}} & .. & 0 & .. & 1-\frac{z_{11,19}}{z_{19,19}} \\ : & : & .. & : & .. & : & 0 & : \\ 1-\frac{z_{19,1}}{z_{1,1}} & 1-\frac{z_{19,2}}{z_{2,2}} & .. & 1-\frac{z_{19,8}}{z_{8,8}} & .. & 1-\frac{z_{19,11}}{z_{11,11}} & .. & 0 \end{bmatrix} \quad (4.2)$$

Applying (4.1b) we get the during fault voltages for the 19 buses due to faults at each one of the 19 buses. Equation (4.2) shows the

resulting dip matrix. It can be seen that column 11 of the dip matrix contains the during fault voltages at each one of the 19 buses when a three-phase fault occurs at bus 11. Column 11 of the dip matrix contains the information to identify the area of the network affected by a fault at bus 11 and is called affected area.

Affected area is the region of the network where the residual voltage during a fault at a given point is less than a threshold value.

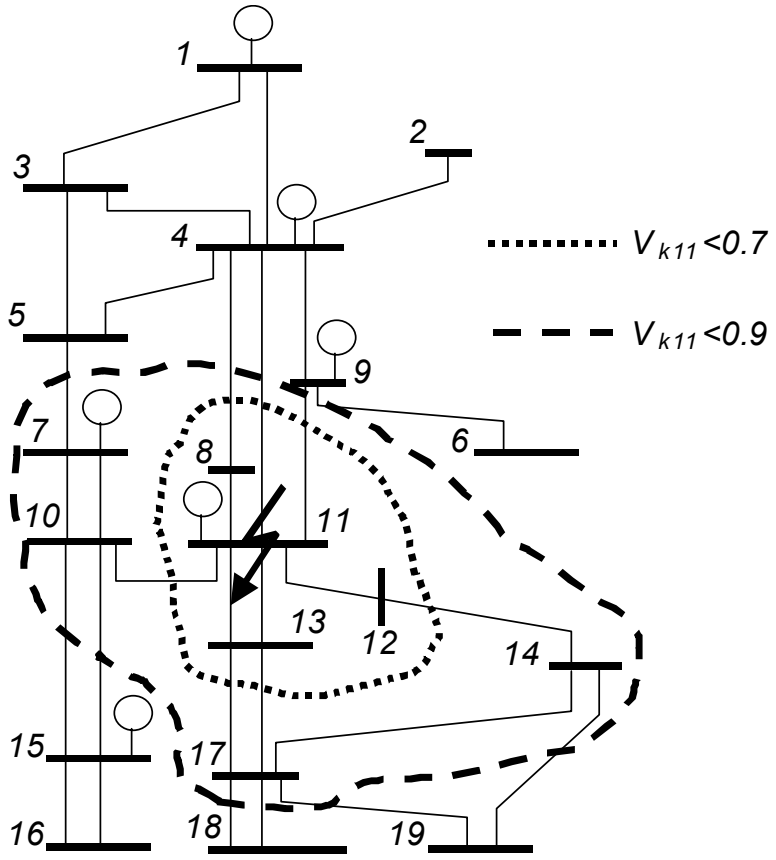

Figure 4.1: Affected areas for a three-phase fault at node 11

In Figure 4.1 two affected areas are presented for a three-phase fault at node 11. The larger one encloses the load buses presenting less residual voltage than 0.9 p.u. Similarly, the smaller affected area contains the load buses that will see a residual voltage less than 0.7 p.u. during the occurrence of a fault at bus 11.

The affected area presented in Figure 4.1 has been built considering potential three-phase faults at buses of the system and only the original impedance matrix of positive-sequence of the system has been used. Faults on lines are more frequent than fault at buses of the system, but the latter cause in general more severe dips. In practice, symmetrical and unsymmetrical faults should be analysed and both faults along the lines and at buses of the system should be considered.

4.1.2 Exposed Area

The exposed area or area of vulnerability is contained in the rows of the voltage-dip matrix and can be graphically presented on the one-line diagram.
Exposed area is the region of the network that encloses nodes and line segments where the occurrence of faults will lead to dips more severe than a given value at the observation bus.
Figure 4.2 presents the exposed area of bus 8.

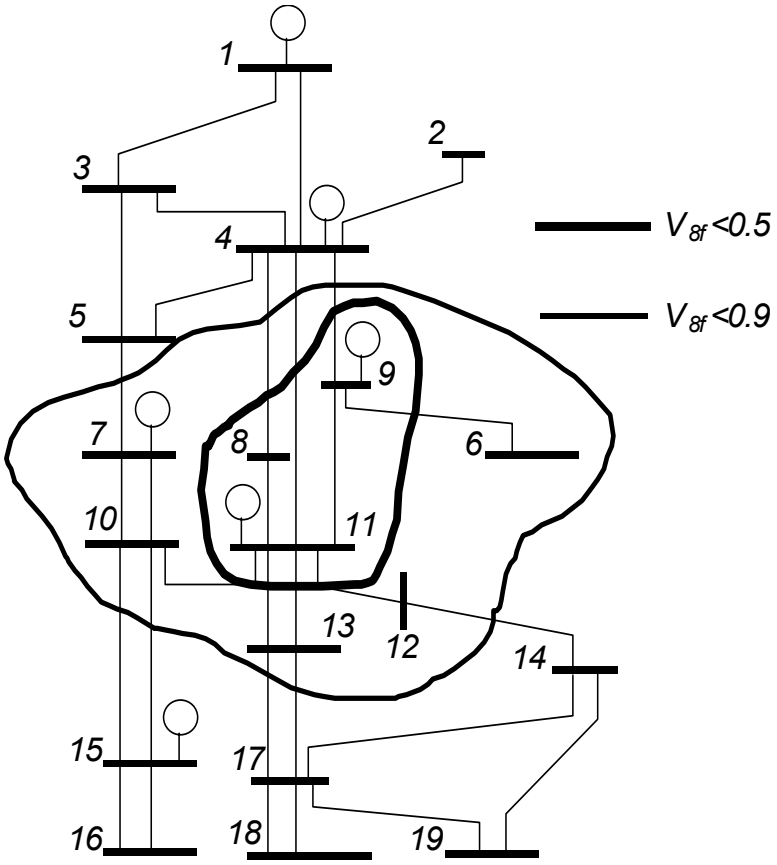

Figure 4.2: Exposed area of bus 8 for three-phase faults

The 0.5 p.u. exposed area of bus 8 contains buses 8, 9 and 11 and lines connecting them indicating that faults at these buses and lines will cause less residual voltage than 0.5 p.u. at bus 8. Similarly, the 0.9 p.u. exposed area of bus 8 contains all the buses and line segments where faults will cause less residual voltage than 0.9 p.u.
Figure 4.2 suggests that the exposed area is the closed region of the network containing buses and the lines connecting them. However, this is not necessarily the case because faults on the lines might cause dips less severe than the threshold that defines the exposed area. In

other words, part of the line may be actually outside the exposed area, meaning that faults in this part of the line will lead to dips less severe than the magnitude under consideration. To clarify, suppose that bus 6 is fed through a relatively long double circuit line from bus 9. In such a case, faults on any of the lines occurring far from the buses 6 or 9 will be seen as shallow voltage dips at bus 6. However, faults near bus 6 or bus 9 will be seen as severe dips at bus 6. The exposed area for bus 6 (severe dips) would be formed by bus 6, segments of the lines connecting this bus, bus 9 and segments of the lines connecting bus 9. The central part of the lines between buses 9 and 6 might be outside of the exposed area.

The exposed area shown in Figure 4.2 has been built using the original bus impedance matrix of the system, however a more precise description of the exposed areas needs to take into account that faults occur on lines. In order to simulate faults on lines additional fictitious nodes are needed along the lines. Those fictitious nodes are called fault positions. The more fault positions are used to calculate the exposed areas the more precise is the description of these areas and the better the stochastic assessment, but also the larger the computational effort needed to perform the calculation.

Consider the 0.5 p.u. exposed area corresponding to bus 8 in Figure 4.2. The contour that defines the border of this area crosses the line between bus 9 and bus 4. In other words, a fault at bus 4 causes a residual voltage at bus 8 above 0.5 p.u. whereas a fault at bus 9 leads to a residual voltage below 0.5 p.u. at bus 8. To better define the contour, the residual voltage at bus 8 should be determined for faults at different locations on the line between bus 9 and bus 4. In addition, fault positions should be also considered along the other lines connecting bus 8. This will result in a new dip matrix $\mathbf{V}_{\mathbf{dfv}}$ with the same number of rows (physical buses), but with a lager number of columns representing the number of possible fault positions.

Unsymmetrical faults can also be considered to define the exposed area of a sensitive load. Positive, negative and zero-sequence impedance matrices are needed to perform the calculations. Load connection and the transformer between the load and the transmission system need to be taken into account to determine the critical voltage to be considered in the exposed area. This will be illustrated in the next chapter.

It should be noted that the exposed area of a bus *k* is also the area that can be monitored by a power quality meter installed at bus *k*, for the same voltage threshold. For example, if a power quality meter were

installed at bus 8 and the voltage threshold to start recording were adjusted to 0.5 p.u., then the meter would be able to see events within the 0.5 p.u. exposed area of bus 8. When referring to power quality meters the exposed area will be called Monitor Reach Area. In Chapter 6, the monitor area will be used to model an optimisation problem to find the optimal locations for monitors so that the performance of the network in terms of dips can be assessed with a minimum number of monitors.

4.2 Counting Voltage Dips

The residual voltage is usually used to classify the total number of dips experienced by a given load. In order to distinguish between severe dips and shallow ones a classification of these in terms of magnitude is useful.

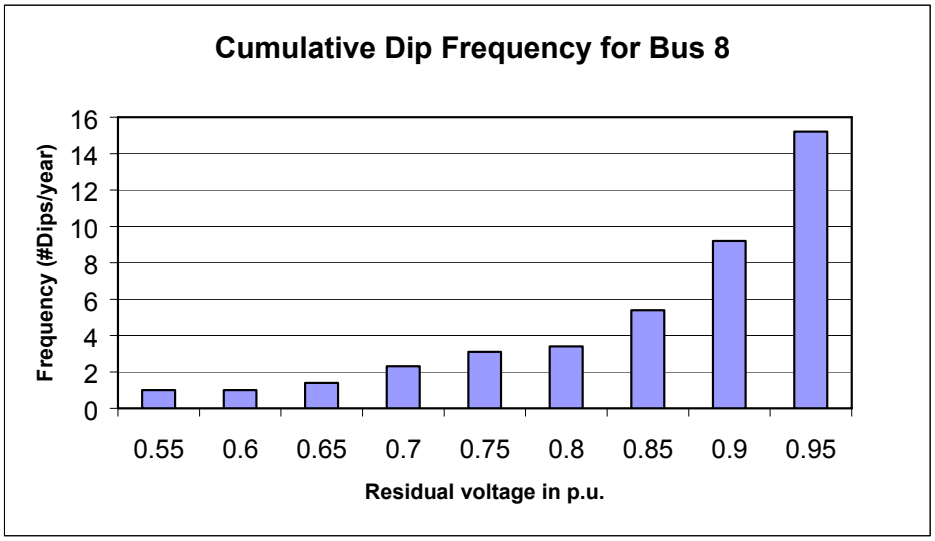

Figure 4.3: Cumulative annual frequency of dips at bus 8

From the point of view of a sensitive load, what matters is the total number of dips with residual voltage less than a given value, because all these events will expose the load to a potential outage. A suitable way to present this information is the cumulative histogram of dips in which the number of events with residual voltage up to a given magnitude is presented. Figure 4.3 shows a hypothetical histogram for bus 8 of the system shown in Figure 4.2. In this example, bus 8 is subject to three dips with a residual voltage lower than 0.75 p.u. It should be noted that that the dip threshold is a load-specific characteristic. Typically, values between 0.85 and 0.95 of the nominal voltage have been used for this threshold (IEC 61000-2-8, 2002).

How often a particular voltage dip occurs at a given location depends on several factors, the number of faults occurring in the "electrical neighbourhood" being the most important one. This "electrical neighbourhood" has already been identified as the exposed area. Other factors, which do affect the magnitude of the dips and hence their distribution along the magnitude axis of Figure 4.3, can be identified as system configuration, generation scheduling, number of lines connecting the load bus, etc.

Predicting dip frequency requires an accurate model of the network and reliability data for all the components. The magnitude of a dip caused by a fault at a bus *f* of the system can be determined using the equations presented in Chapter 3. How often one of those dips occurs at a given bus *k* depends on the reliability of the bus *f*, or more precisely on the fault rate of the fault position *f*. If the fault rate of the fault position *f* is λ_f the particular dip caused by this fault will be seen λ_f times per year. The exposed area of Figure 4.2 shows that bus *k* will see dips caused by faults inside this area. The expected number of faults inside the exposed area is given by the sum of the fault rates of the fault positions contained in the exposed area. Therefore, the frequency of dips can be calculated from the dip matrix and the fault rate corresponding to the fault positions.

Consider the system presented in Figure 4.1 and its impedance matrix. Suppose the sequence impedance matrices have been built considering a number of fault positions on buses as well as along lines. This means that the impedance matrices for the zero, negative and positive-sequence impedance are available. From them, the dip-matrices for symmetrical and unsymmetrical faults can be calculated. Unsymmetrical faults cause unbalanced dips which need three voltage dip-matrices, each one for each phase voltage. If we take the lowest phase voltage to characterise the dip magnitude, then four dip-matrices characterise the four dips caused by faults: three-phase, single-phase-to-ground, two-phase and two-phase-to-ground fault caused dips. We will call these matrices $\mathbf{V_{dfv3p}}$, $\mathbf{V_{dfv1p}}$, $\mathbf{V_{dfv2p}}$ and $\mathbf{V_{dfv2pg}}$ respectively. The final step is to combine these dip matrices with the fault rates of the fault positions to get a stochastic prediction of the dip frequencies.

The dip-matrices contain more nodes than the physical buses because they include several fault positions on lines. Nodes corresponding to physical buses of the system have a fault rate given by the actual fault rate of the bus. Fault positions on lines have a fault rate that is a fraction of the actual line fault rate. If more than one fault position is

considered on the line, the actual fault rate needs to be divided by the number of fault positions in order to calculate the frequency of the resulting dips. If only one fault position is considered on a given line, then the actual fault rate is taken.

Once the fault rate for all fault positions is determined, the expected number of dips and their characteristics can be determined by combining the dip-matrices and the fault rates. Let $\boldsymbol{\lambda}$ be the vector containing the corresponding fault rate of each one of the *Fp* fault positions.

$$\boldsymbol{\lambda} = \left(\lambda_1 \ldots. \quad \lambda_k \quad \ldots \quad \lambda_N \ldots. \quad \lambda_f \quad .. \quad \lambda_{Fp}\right) \tag{4.3}$$

Each fault will cause a drop in voltage that will be seen at all buses. However, only part of these fault-caused events will be counted as dips at load buses (v_{kf} < dip threshold). A large part of these events will result in retained voltages above the dip threshold. The number of total fault-caused events is the same for all buses, however the resulting during-fault voltages are different which result in different cumulative histograms. Hence, vector $\boldsymbol{\lambda}$ contains the annual rate of events (voltage drops) caused by faults. To illustrate this, consider an arbitrary observation bus *k* and the residual voltages caused by faults in the system. Table 4.1 shows row *k* (transposed) of the dip matrix and vector $\boldsymbol{\lambda}$.

Table 4.1:An arbitrary row (k) of the dip matrix (transposed) and the fault rates corresponding to all fault positions

Residual voltage (dip) at bus *k* (v_{kf})	Rate of occurrence ($\boldsymbol{\lambda}$)
v_{k1}	λ_1
v_{k2}	λ_2
…	…
v_{kN}	λ_N
…	…
v_{kFp}	λ_{Fp}

To build the cumulative histogram, the residual voltages contained in Table 4.1 need to be grouped according to the dip magnitude of interest. For example, if we take the bins magnitude shown in Figure 4.3 then Table 4.2 would be the data table for building the cumulative histogram.

Note that the second column of Table 4.2 contains the summation of the fault rates corresponding to fault positions where the occurrence of a fault cause a residual voltage less than or equal to the value indicated in the first column.
Finally, in order to take into account the different fault types, the procedure described needs to be performed for each one of the dip-matrices and the resulting frequencies combined according to the probability distribution of fault types.

Table 4.2: Cumulative dip frequency at a general bus k:

Dip Magnitude bins (p.u.)	Frequency (events/year)
0.55	$\sum_i \lambda_i : v_{ki} \leq 0.55$
0.6	$\sum_i \lambda_i : v_{ki} \leq 0.6$
0.65	$\sum_i \lambda_i : v_{ki} \leq 0.65$
:	:
0.9	$\sum_i \lambda_i : v_{ki} \leq 0.9$
0.95	$\sum_i \lambda_i : v_{ki} \leq 0.95$

In Chapter 5 results of simulations performed using this method are presented.

5 Method of Fault Positions: Simulations and Results

The method of fault positions is implemented and simulations are performed in order to obtain a stochastic assessment of voltage dips. An existing large transmission system is used to illustrate the method. Balanced and unbalanced dips are simulated, and the effect of power transformers on the dip type is taken into account.

5.1 Description of the System

The test system used in this work is a simplified model of the National Interconnected System of Colombia (230 kV and 500 kV) at December 1999.

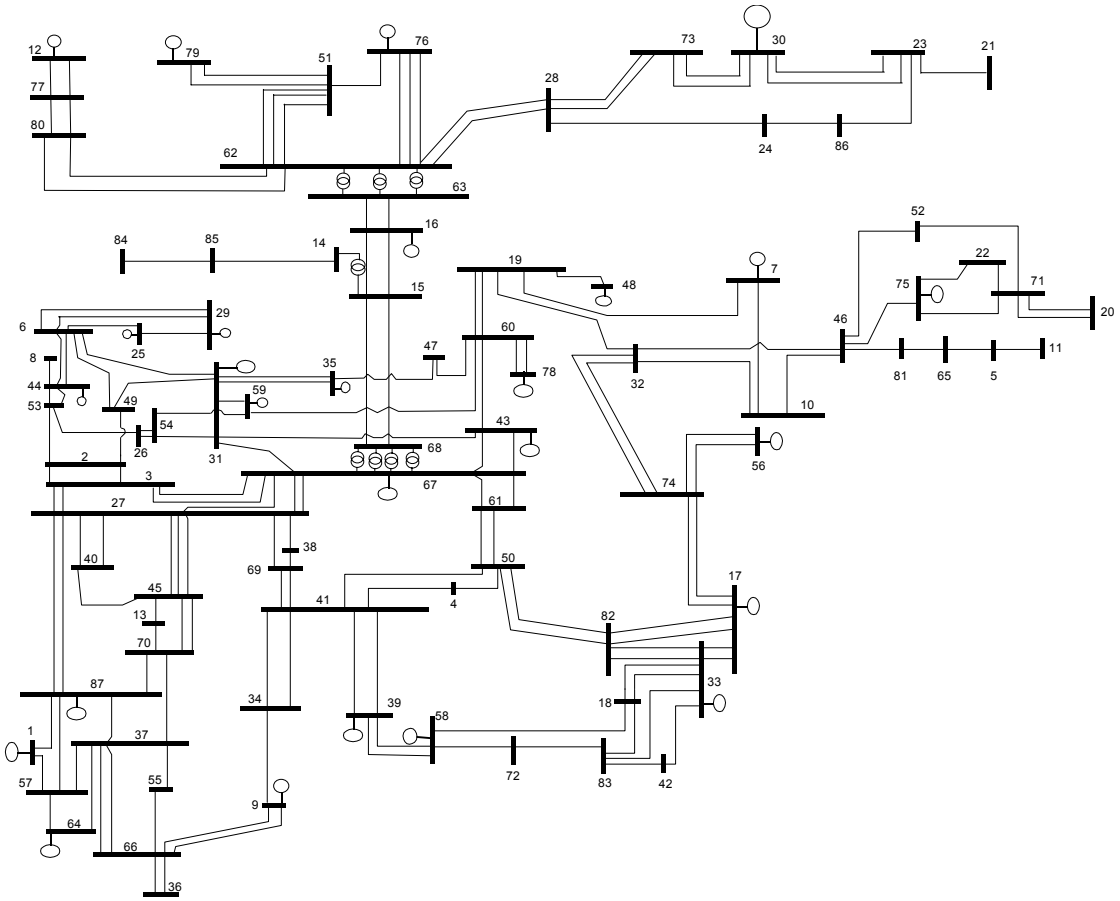

Figure 5.1: National Interconnected System of Colombia, simplified model

A real system is used to apply the methodologies proposed, however the results cannot be applied to this system because some assumptions were necessary to complete the study. The system has 87 buses and 164 lines with a total length of 11651 km. It consists of two 230 kV

grids connected by a double-circuit 500 kV line. Buses 15, 16, 63 and 68 form part of the 500 kV system. Data for the study has been obtained from the *Informe de Operación* at the web site of ISA (ISA, 2002).
Line impedances of positive and zero-sequence are provided in the operational report and are reproduced in Appendix A.
To calculate the impedance of generation buses, the maximum short circuit level at some buses was used. It was assumed that generators machines were connected to the transmission network through delta-wye transformers with the high voltage side solidly grounded (IEEE C57.116-1989). The resistive component of the generator impedance was neglected.
Power transformers (500/230 kV) were modelled as delta-wye, solidly grounded. This is not the actual case, but it allows the study of the effect of delta-wye transformers on the type of voltage dips.

5.2 Balanced Dips

Simulations were performed in order to obtain the stochastic assessment of balanced dips and their magnitude. The positive-sequence impedance matrix was used to model the system. Line capacitance was neglected for these balanced dip simulations. Three-phase faults were simulated all over the system and the residual voltages caused by them saved in the dip-matrix. The fault rate for lines is 0.0134 faults per year-km and is the same for the 164 lines. The fault rate for buses is 0.08 faults per bus-year and is the same for the 87 buses. In order to investigate the effect of the generation scheduling on the expected number of dips, a second simulation was performed considering a lower short circuit level.
Four simulations were performed where the residual during-fault voltage was calculated at each bus due to the occurrence of faults everywhere in the network. The cumulative frequency was determined for each bus.

- Base case: This simulation considers 87 fault-positions each one coinciding with a bus position. Faults at lines were represented by the fault position at the nearest bus. The fault rate for each fault position was calculated taking the quotient between the expected total number of faults (buses and lines) and the number of fault positions -87 in this case-. This is a rough estimation but it helps to identify the boundaries of dip frequencies. No provision was made for different number of lines connected to a bus and for different line lengths.

- Case 1: This simulation considers 251 fault positions with 87 at buses and 164 at lines. Fault positions on lines were chosen in the middle of each line. Fault rates were assigned at each fault-position corresponding to the type of fault (bus or line). The fault rate for faults on lines was determined from the quotient between the expected annual number of faults on lines and the number of fault positions on lines. No provision was made for different line lengths.
- Case 2: This simulation considers 781 fault positions with 87 faults at buses and 694 faults at lines. Lines were divided so that each line segment was no longer than 15 km. Fault rates were assigned corresponding to the type of fault. The fault rate for line faults was determined in the same form as in case 1. In this case the number of fault-positions per line was dependent on the line length.
- Case 3: This simulation is the same as case 2, but the short circuit level was reduced to investigate the effect of generator scheduling in the network performance in terms of sags.

5.2.1 Balanced During-Fault Voltages

The magnitude of residual voltage at each bus and for each fault position was calculated and saved in the dip matrix, see Table 5.1.

Table 5.1: Residual Voltages (Dips) due to Three-Phase Faults

SUBSTATIONS > ---------- FAULT POSITIONS	1	6	17	24	29	37	41	55	59	87
6	0.99	0.00	1.00	1.00	0.63	0.98	0.99	0.98	0.88	0.97
17	1.00	1.00	0.00	1.00	1.00	0.99	0.83	0.99	1.00	0.99
24	1.00	1.00	1.00	0.00	1.00	1.00	1.00	1.00	1.00	1.00
29	0.99	0.61	1.00	1.00	0.00	0.99	0.99	0.99	0.94	0.99
37	0.79	0.99	1.00	1.00	0.99	0.00	0.98	0.14	0.99	0.61
41	0.98	0.98	0.82	1.00	0.99	0.95	0.00	0.95	0.99	0.95
55	0.92	0.99	1.00	1.00	1.00	0.63	0.99	0.00	1.00	0.84
59	0.99	0.87	1.00	1.00	0.93	0.99	0.99	0.99	0.00	0.98
87	0.63	0.97	0.99	1.00	0.98	0.30	0.95	0.35	0.98	0.00
50% Line 27_87	0.95	0.99	1.00	1.00	0.99	0.90	0.98	0.91	0.99	0.87
50% Line 57_87	0.74	0.99	0.99	1.00	0.99	0.48	0.97	0.53	0.99	0.50
50% Line 39_41	0.98	0.98	0.83	1.00	0.99	0.96	0.10	0.96	0.99	0.95
50% Line 37_57	0.77	0.99	1.00	1.00	0.99	0.28	0.98	0.37	0.99	0.65
50% Line 37_55	0.88	0.99	1.00	1.00	1.00	0.46	0.99	0.08	1.00	0.78
50% Line 24_86	1.00	1.00	1.00	0.35	1.00	1.00	1.00	1.00	1.00	1.00

Table 5.1 shows the residual voltages at some selected observation buses (1, 6, 17, 24, 29, 37, 41, 55, 59, 87) for faults at lines and buses. Faults in substations are in the top part of the Table 5.1 whereas faults in the middle of some lines are in the bottom part of the table.
Table 5.1 is a part of the voltage-dip matrix presented Chapter 4 and it has been transposed to present the results in a more suitable manner. From the table it is easy to note that substations near to the fault experience severe dips, i.e. less residual voltage. Consider substation 87 and its residual voltages in the last column of Table 5.1. When a fault occurs at bus 6 (far from 87), the voltage at 87 only drops 3% with respect to the pre-fault voltage. However, when the fault occurs at bus 37 the voltage drops 49% with respect to the pre-fault voltage. Also faults on the lines connecting substation 87 cause severe dips at this bus.

5.2.2 Area Affected by a Symmetrical Fault

As explained in Chapter 4, the relation between electrical distance and magnitude of the dip can be graphically visualized by using the affected and exposed areas.

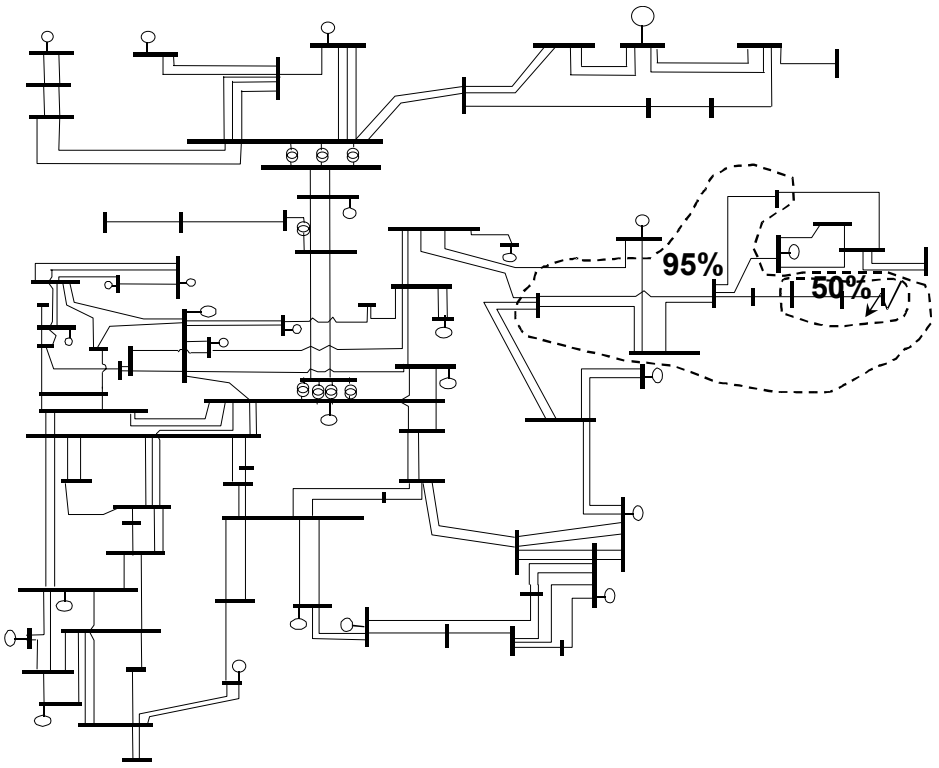

Figure 5.2: Affected area due to a three-phase fault at bus 11, Canolimon

Figure 5.2 shows the residual voltage at different buses of the power system during the occurrence of a three-phase fault at bus 11

(Canolimon), which is one of the weakest buses in the system. The contours enclose the substations with during-fault voltages lower than 50% and 95%.

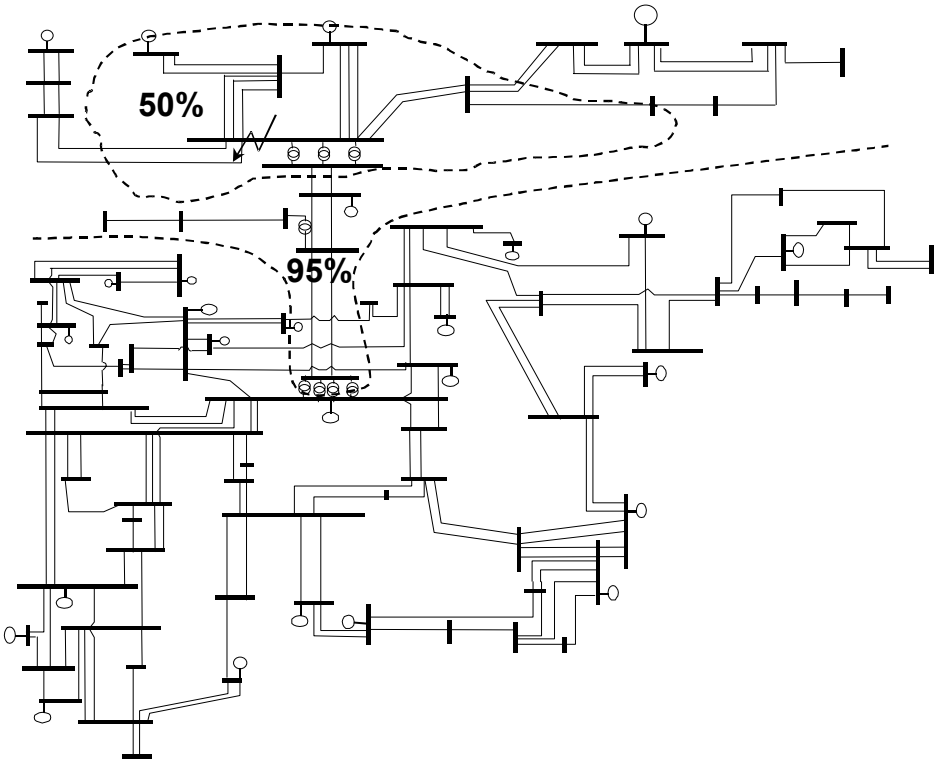

Figure 5.3: Affected area due to a three-phase fault at bus 62, Sabanalarga230

Figures 5.3 and 5.4 show the affected area for a fault at bus 62 (Sabanalarga230) and 67 (Sancarlos230) respectively. It is clear that faults at those buses affect a larger area of the system.
Figure 5.4 shows that more than half of the buses of the power system experience dips more severe than 95% when a fault occurs at bus 67, Sancarlos230. Consequently, such a fault has the potential to cause dip-related equipment tripping for a large number of customers. Bus 67 is one of the strongest buses of the system.
In general, the size of the affected areas depends on the short circuit level at the fault point, which depends on the generator scheduling. The stronger the bus (higher short circuit level) the stronger the influence of a short-circuit fault on the system and the larger the affected area.
The affected area, then, is the region of the network that will be exposed to dips more severe than a given value of residual voltage during the occurrence of a fault at a given point of the network.

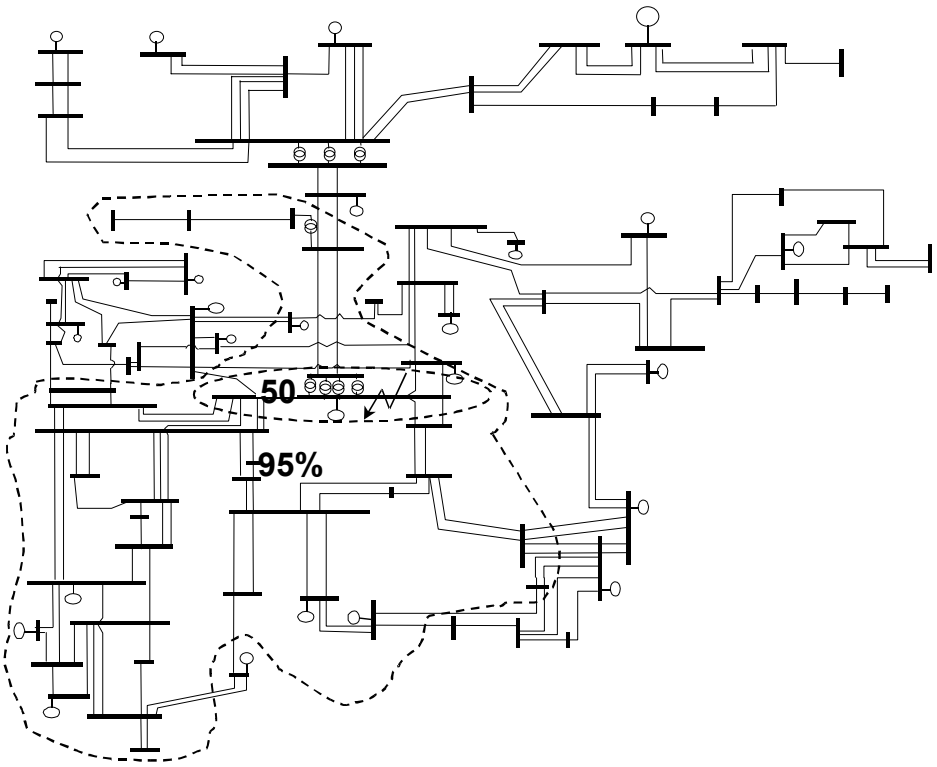

Figure 5.4: Affected are due to a three-phase fault at bus 67, Sancarlos230

5.2.3 Exposed Area of a Load Bus due to Symmetrical Faults

The information in Table 5.1 can also be used to answer the question: how large is the area around a load bus in which faults lead to less residual voltage a given value? This area is called exposed area of the load bus, and it contains fault positions (buses and line segments) where the occurrence of faults causes dips more severe than a given value at the load bus. Figures 5.5 and 5.6 show the exposed areas for substations 28 (Fundacion) and 11 (Canolimon) respectively. It should be noted that part of the transmission lines connecting buses inside the exposed areas might be actually outside the exposed areas. This point is discussed further in Section 5.3.2 of this chapter.

In Figure 5.5 the 95% exposed area encloses all the buses and line segments where the occurrence of faults causes a residual voltage lower than 95% at the load bus 28, Fundacion. The same contour is shown for substation 11, Canolimon.

Comparing the exposed area of substations 11 and 28 it can be seen that the shape and size of the exposed areas are different. The short circuit level of buses and hence the scheduling of generators can again explain this. The exposed area of bus 11 (weak bus) seems to be larger. The reason of this may be that the available generation in this area is less than the generation in the area where substation 28 is located.

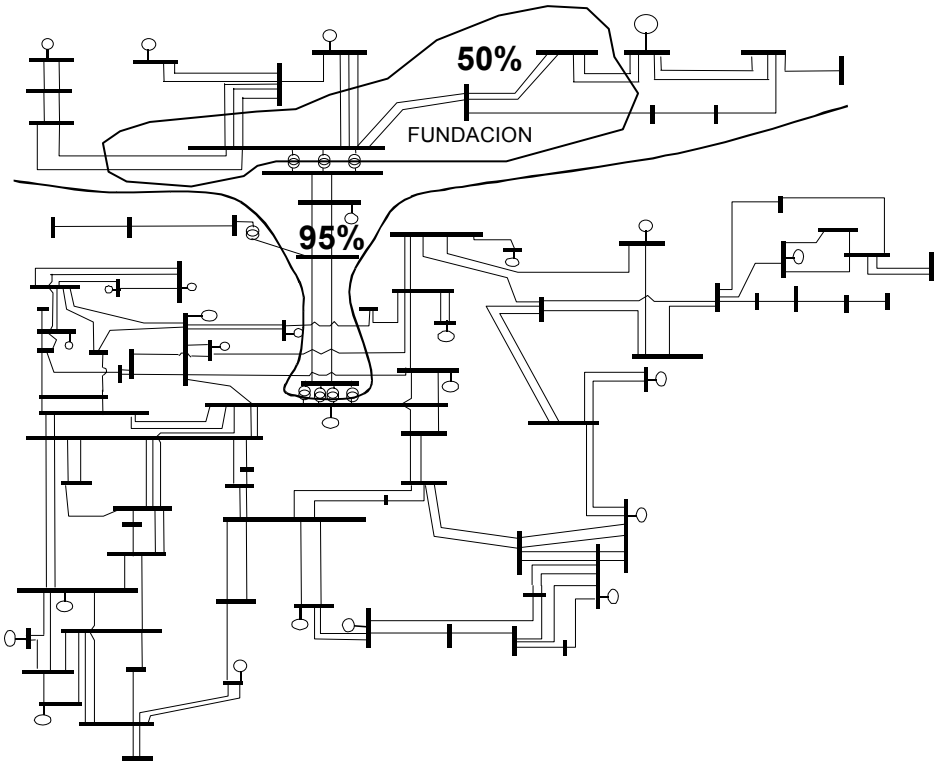

Figure 5.5: Exposed area (50% and 95%) for bus 28, Fundacion

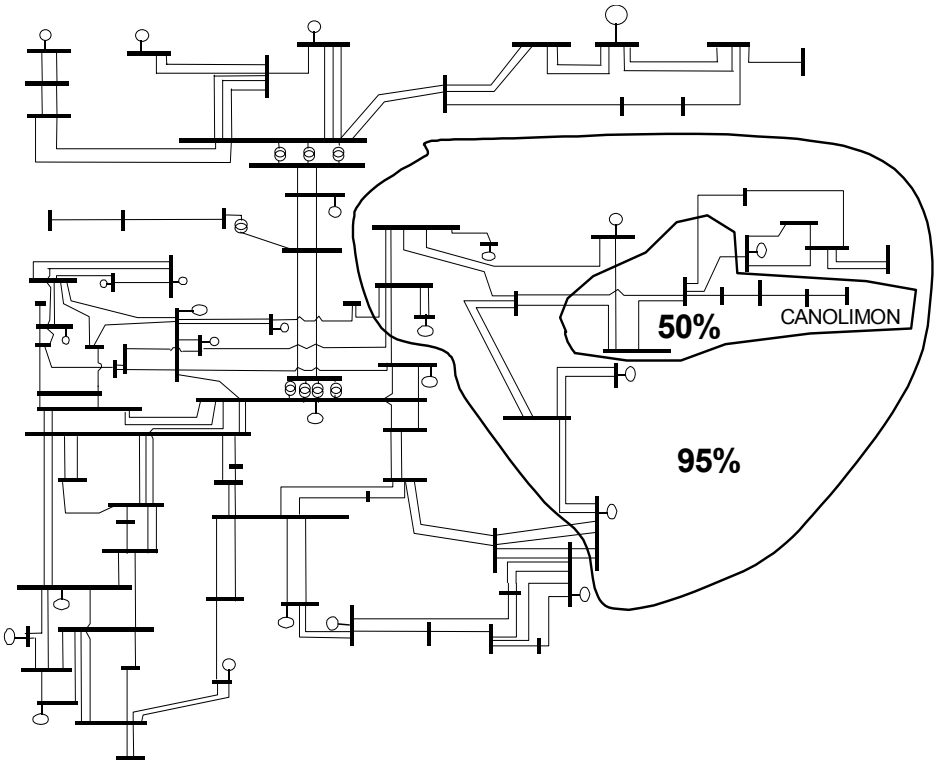

Figure 5.6: Exposed area (50% and 95%) for bus 11, Canolimon

5.2.4 Cumulative Balanced Dip Frequencies

The histogram of cumulative dip frequency answers the question: How often does a particular dip occur at a defined load point in the network?
The expected number of dips can be estimated by combining the information contained in Table 5.1 and the corresponding fault rate at each fault position. This analysis was performed for all cases: Base case only considers fault-positions at buses, Case 1 considers 251 fault positions with 87 at buses and 164 in the middle of each line, and Case 2 considers 781 fault positions with 87 faults at buses and 694 faults at lines.
The cumulative dip frequency for substations 11 (Canolimon) and 67 (Sancarlos230) is presented in Figure 5.7 and 5.8. It can be seen that the result of the assessment depends on the number of fault positions. The more the fault positions, the more accurate the estimation of long term expected number of dips. In the limit, an infinite number of fault positions would be necessary to get the continuous frequency function of dips at each bus. The rough estimation obtained by using the base case shows the same shape as the more elaborated cases 1 and 2. This confirms that the base case is a good starting point. The base case cannot be seen as an over estimation or an under estimation of the real expected number of dips.
Another observation from figures 5.7 and 5.8 is that the expected number of dips and their shape notably differs between buses with different short circuit levels. Based on Case 2, the weak bus 11 (Canolimon) presents about 20 dips per year whereas the strong bus 67 (Sancarlos230) presents 8 dips with residual voltage lower than 85%.
Engineers often resort to indices to quantify complex phenomena. This strategy is useful in reducing the complexity at little sacrifice of information. Instead of presenting the complete histogram, one could use a simpler index. Voltage dip performance is often quantified by using event-counting indices. A well-known index in this sense is the System Average RMS (variation) Frequency Index (SARFI-X) that indicates the number of events with a residual voltage less than X. The index could be calculated by using the number of customers affected by each event as weighing factor but as this information is usually not available, the index is just a counting of the events. The SARFI index for different residual voltages can be read directly from the cumulative histograms.

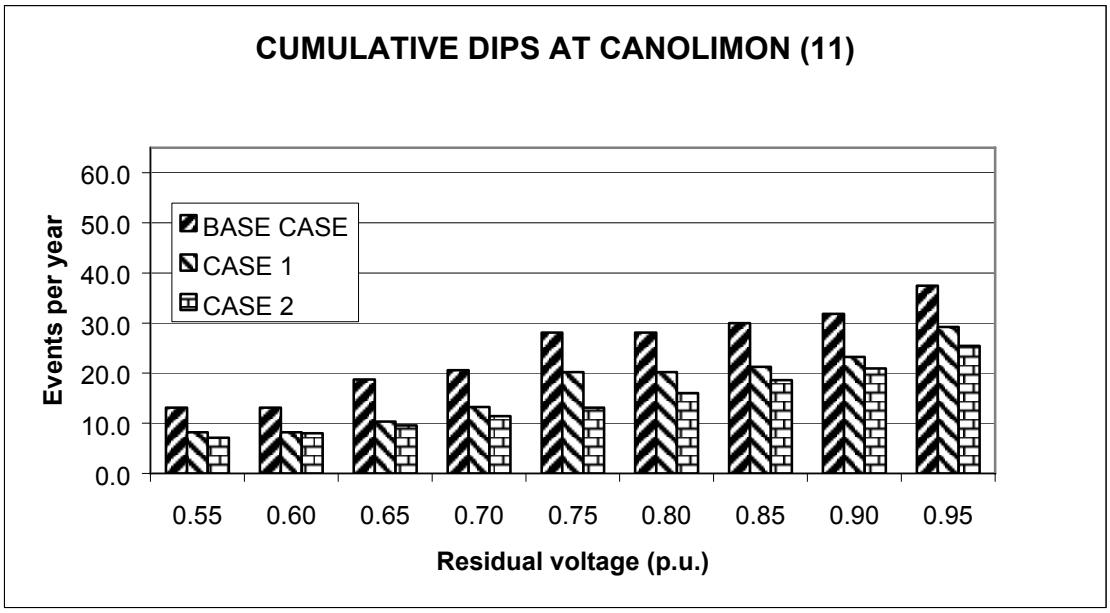

Figure 5.7: Cumulative dip frequency at bus 11, Canolimon for maximum generation

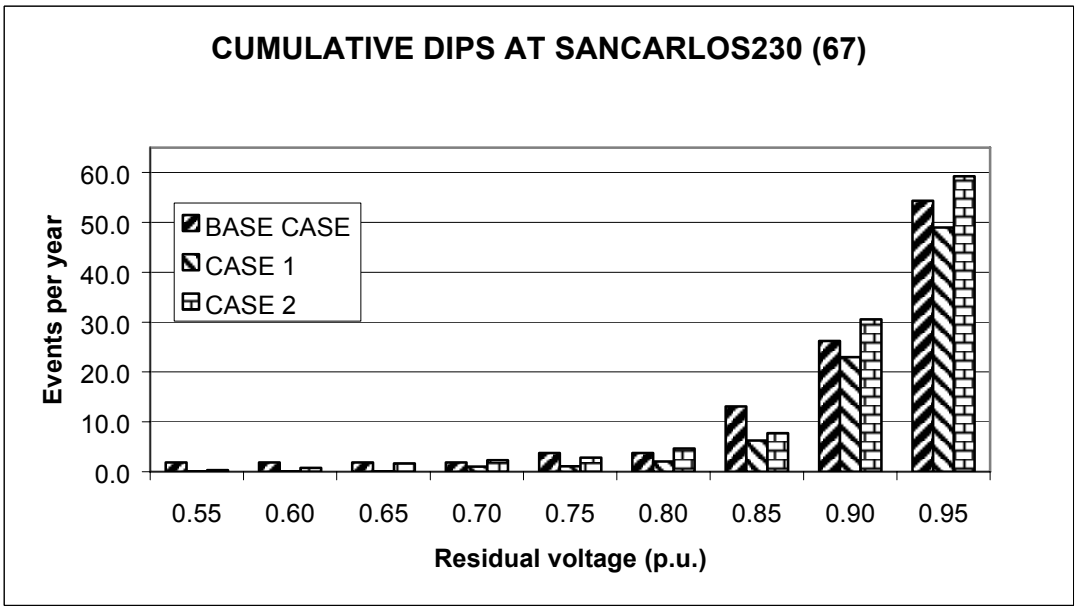

Figure 5.8: Cumulative dip frequency at bus 67, Sancarlos230 for maximum generation

5.2.5 Voltage Dip Maps

Another way to present the results of a voltage dip assessment is by means of voltage dip maps.

A voltage dip map is a graphical representation of the quality of voltage -in terms of dip frequency- around the system. In a dip map, lines enclose load points with similar cumulative dip frequency for a given value of residual voltage.

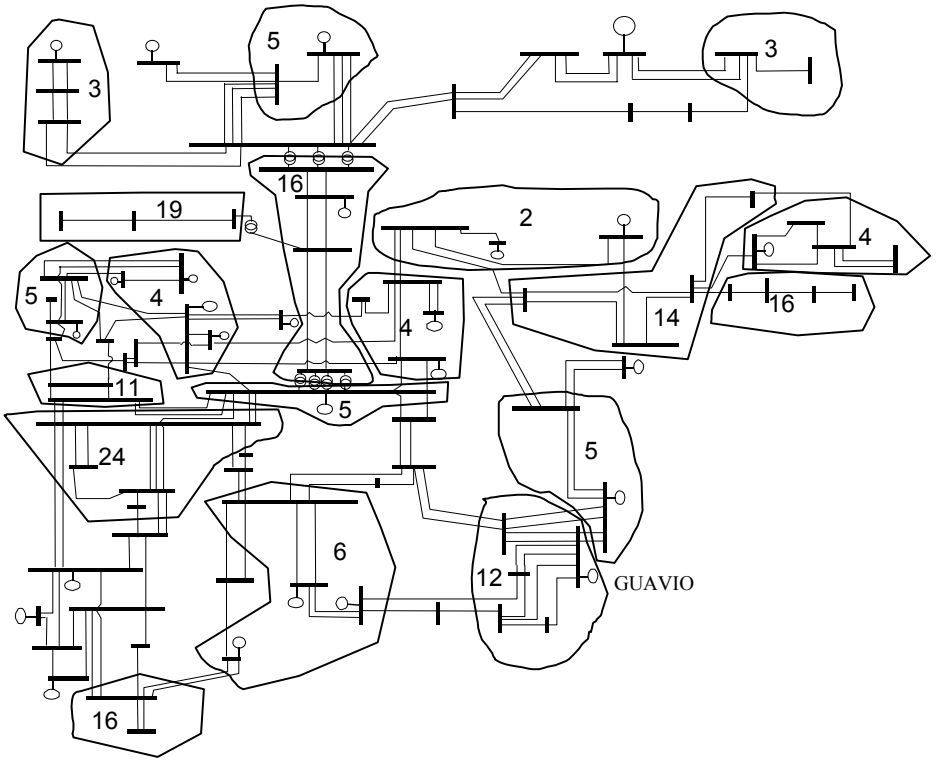

Figure 5.9: 80% Dip map; number of events with residual voltage less than 80% of pre-event voltage, for a maximum generation scheduling (case 2)

Figure 5.9 shows the 80% dip map based on case 2. The figure shows how many dips -with residual voltage less than 80% - each area of the network presents. There are buses with dip frequency up to 24 events per year, whereas other areas show a much better dip performance.
Generally, the dip frequency is lower near the generation substations, but the number of lines converging to a bus and their length affect this general rule. This could explain why bus 33 (Guavio) presents 12 events per year. Several lines are used to connect the power station with the rest of the system at that substation.

5.2.6 Influence of Generation

How does the generation scheduling affect the expected number of dips? In previous sections, this question was analysed from one point of view. It was observed that for a given generation scheduling, the dip frequencies vary around the network depending on the strength (short circuit level) of the buses. Stronger buses are less susceptible to remote faults. The resulting dips at these buses are mainly shallow dips whereas dips at weak buses are much more severe.
In this section, case 3 and case 2 are compared to explore the network performance when the generation is reduced. The impedances of generation buses are increased to model a lower generation level.

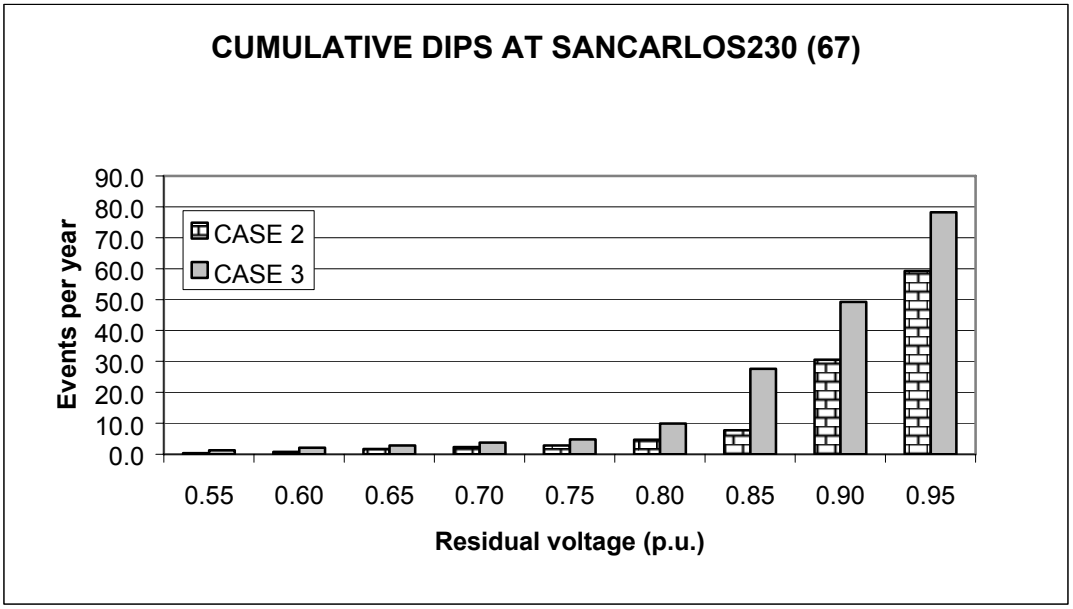

Figure 5.10: Cumulative dip frequency at bus 67, Sancarlos230, for two generation levels

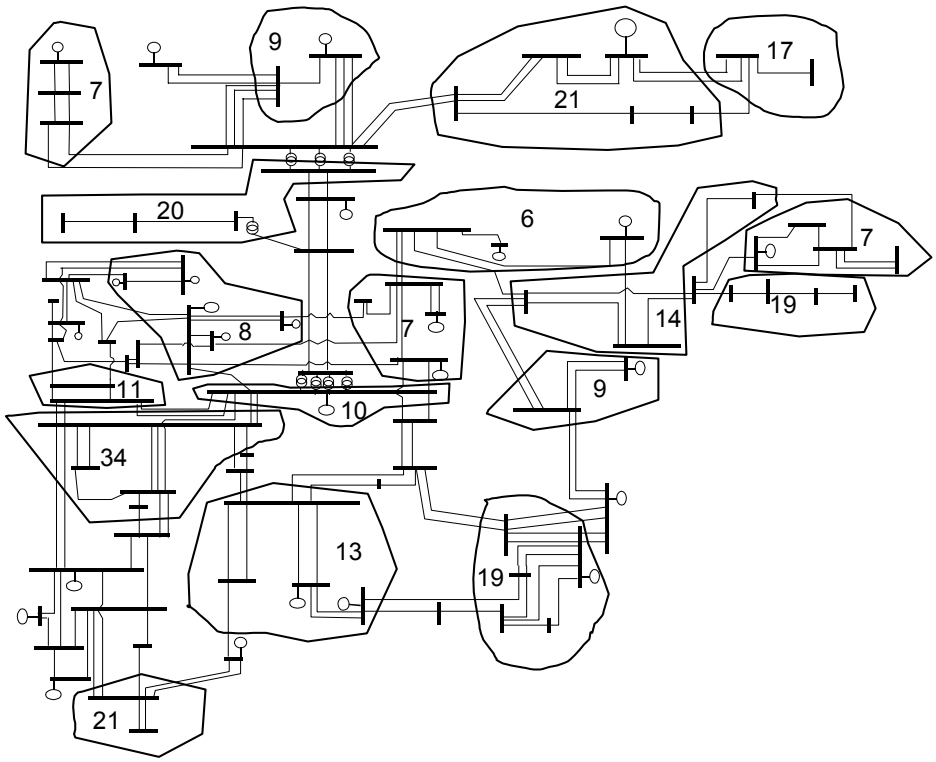

Figure 5.11: 80% dip map: Cumulative 80% dip frequency for a low generation scheduling (case3)

In our simulations, we have increased the generator impedance in the same proportion at each generation bus (in case 3) to model a lower generation level. This hypothetical situation does not represent a real case, but it illustrates the fact that a change in the generation

scheduling has an important impact on the residual voltages and therefore on the frequency of dips.
Figure 5.10 shows how the cumulative dip frequency at bus 67 (Sancarlos230) varies when a lower generation scheduling is used to estimate the expected performance of the network. Cases 2 and 3 have the same number of fault positions, the same fault rate, and the same configuration of the system. The total number of simulated events is the same, but its distribution in the residual voltage bins is different. It is clear that a weak system –case 3- presents a larger number of dips for every bin. The same conclusion can be derived from Figure 5.11 where the dip map for case 3 is shown. Comparing Figure 5.9 and 5.11 it is clear that the generation scheduling has a significant effect on the estimation of voltage dip frequencies.

5.2.7 System Statistics based on Balanced Dips

To characterize the system as a whole, dip indices are needed. One approach is to characterize the system by means of the average number of cumulative dip frequency for a given magnitude. This average number takes into account the spatial variation around the network. It is the average of the cumulative expected number of dips -in a given bin- of the all network buses. It could be interpreted as the expected performance of the average bus. Another approach is to describe the system performance by means of the 95 percentile. Again, the spatial variation of the performance is taken into account. In this case, the index can be interpreted as the number of dips that is not exceeded by 95% of the system buses. Table 5.2 shows system statistics for the four simulated cases. It should be noted that the indices are based only on balanced dips. In Section 5.3.4 system statistics are based on balanced and unbalanced dips.
From Table 5.2-A it can be seen that for dips more severe than 90%, the worst site is located in the area of node 27, substation Esmeralda. This is confirmed by Figure 9 and 11 where this area shows the highest dip frequency for dips of 80% or less residual voltage. In Table 5.2-B there is no clarity about the worst site for dips more severe than 70%, however we should expect the worst site near node 14, Cerromatoso230 substation, because Case 2 is our most elaborated simulation. This lack of clarity could be explained by the need of a non-homogeneous split of lines for fault position purpose. For some lines a 15 km long segmentation of the line implies a similar short circuit level along the line, for others this same 15 km

implies an important variation in short-circuit level. Hence, some dips are over or under-classified in terms of severity.

Table 5.2: System statistics based on balanced voltage dips

A.- Number of dips with residual voltage less than 0.9 p.u. (SARFI-0.9)						
Case	#F. posit.	# Events	Worst site		95^{th} %	Average
Base	87	2068	46.86	69 Sanfelipe	41.24	23.77
1	251	1787	40.87	27 Esmeralda	38.10	20.53
2	781	1556	44.65	40 Lahermosa	40.55	17.88
3	781	2221	57.21	69 Sanfelipe	51.61	25.53
B.- Number of dips with residual voltage less than 0.7 p.u. (SARFI-0.7)						
Case	#F. posit.	# Events	Worst site		95^{th} %	Average
Base	87	913	20.62	5 Banadia	20.06	10.49
1	251	623	15.87	28 Fundacion	13.21	7.16
2	781	540	18.86	14 Cerrom..230	15.70	6.21
3	781	734	18.86	14 Cerrom..230	16.55	8.44

5.3 Unbalanced Dips

The same system presented in the previous section was used to simulate unbalanced dips. Three unsymmetrical fault types were considered: phase-to-phase faults, two-phase-to-ground faults and single-phase faults. Three-phase faults are also included.

The system was modelled by means of the positive and zero sequence impedance matrices. The negative sequence impedance matrix was taken equal to the positive one. Lines were modelled as medium-length lines perfectly transposed. Lines' shunt parameters were considered. Independence of sequence components is assumed, meaning that the different sequences do not react upon each other. Transformers were modelled as delta-wye solidly grounded.

The simulations are based on case 2. They consider 781 fault positions with 87 faults at buses and 694 faults at lines. In order to count the number of dips occurring at the load positions, the following criterion was adopted: each fault-originating event, balanced or unbalanced, was counted as one single dip. The minimum phase-to-neutral voltage was used to characterize the resulting dip. Residual voltages were registered for all buses and for each simulated fault.

Three simulation cases were developed:

- Case A. This simulation only considers three-phase faults. The fault rate for lines is 0.0134 faults per year-km and is the same for the 164 lines. The fault rate for buses is 0.08 faults per bus-year and is the same for the 87 buses. This case is equal to

Case 2 in the previous section, however lines' capacitances are taken into account.

- Case B. Only single-phase-to-ground faults were simulated. Fault rates as in case A.
- Case C. Four kinds of shunt faults were simulated: single-phase-to-ground, phase-to-phase, two-phases-to-ground and three-phase fault. The distribution probability of fault type was assumed 80% single-phase-to-ground, 5% phase-to-phase, 10% two-phases-to-ground and 5% three-phase-fault. Fault rates as in Case A.

5.3.1 Exposed Area of a Load Bus due to Unsymmetrical Faults

The simulations give the residual voltages for all buses. To derive conclusions about the exposed area for symmetrical and unsymmetrical faults, both cases A and B are presented in Figure 5.12.

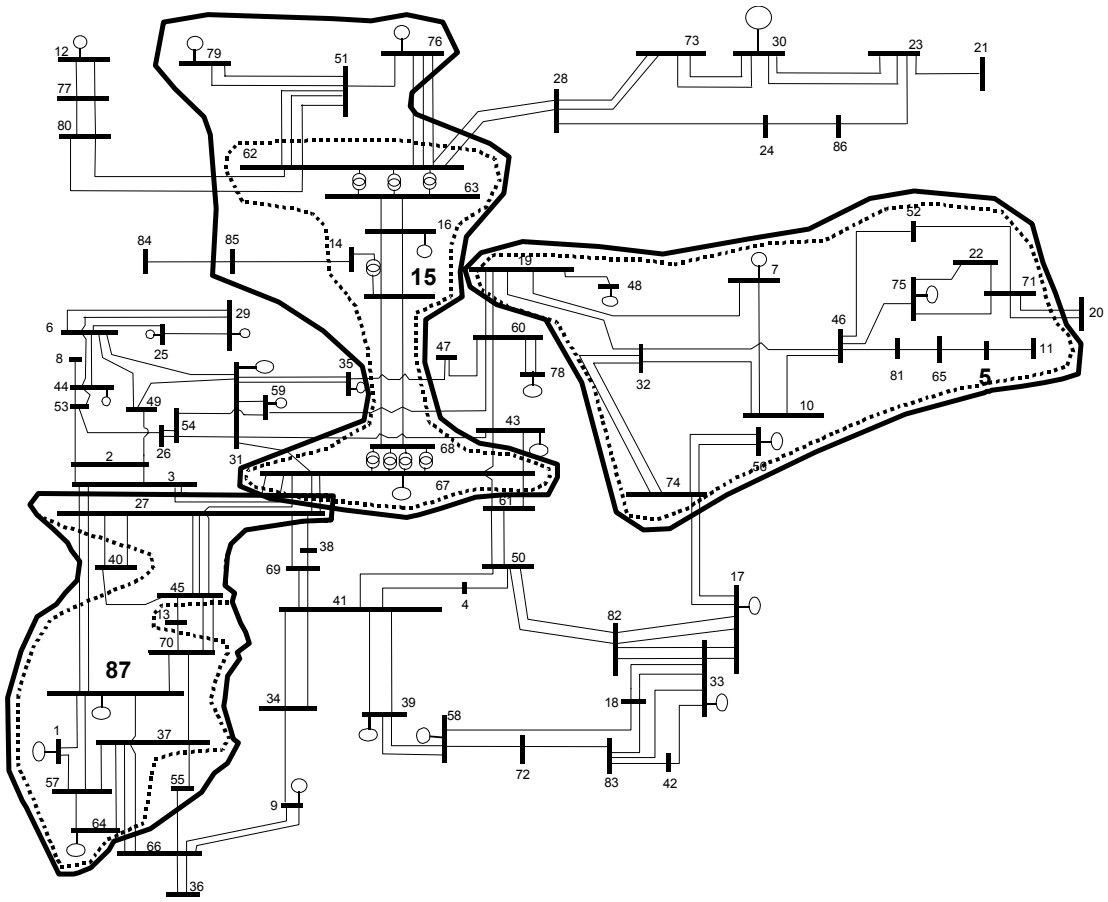

Figure 5.12: 85% Exposed Areas for buses 5 (Banadia), 15 (Cerromatoso500) and 87 (Yumbo). Dashed line for single-phase fault caused dips. Solid line for balanced dips.

Figure 5.12 presents the 85% exposed areas for buses 5 (Banadia), 15 (Cerromatoso500) and 87 (Yumbo). The lowest phase-to-ground voltage is used to characterize the magnitude of the event. Faults on buses or lines inside the areas would cause a remaining voltage in the worst phase lower than 85% at the indicated buses. The dashed line is used for the single-phase-to-ground fault exposed area, whereas the solid line is used for the three-phase fault exposed area.
The single-phase fault exposed areas for buses 5 (Banadia) and 87 (Yumbo) are almost coincident with the three-phase fault exposed area, however slightly smaller. The three-phase fault exposed area is larger than the single-phase fault exposed area but they do not differ too much when there is no power transformer inside the area. The shape of the exposed area changes drastically when it contains power transformers. This can be explained by the blocking of the zero-sequence component and the changing in the dip type caused by the winding connection of the transformers.
For an impedance-grounded system the single-phase fault exposed area would be significantly smaller than for three-phase faults.

5.3.2 A closer look at the Exposed Areas

The exposed areas presented in Figure 5.12 have been drawn as closed sets to simplify the drawing, however they might be isolated sets enclosing the part of the system in which a fault would cause a dip more severe than a given value. To illustrate this, consider the lines connecting bus 87 (Yumbo) and 27 (Esmeralda).
Figure 5.13 shows the residual voltage at bus 87 (Yumbo) when a moving fault is applied on the line connecting these buses. Single-phase-to-ground and three-phase faults are shown. It can be seen that for both fault types part of the line does not pertain to the 85% exposed area of bus 87 (Yumbo).
The term critical distance is used to describe the length of a line exposed to faults that lead to critical dips (Bollen, 1998b). Hence, for this line and three-phase faults, the critical 85%-distance would be approximately the first 40% of line plus the last 10% of it.
Figure 5.13 corresponds to a line connecting the observation bus. The data contained in the voltage-dip matrix also allows the description of the residual voltage caused by faults on lines not connecting the observation bus.

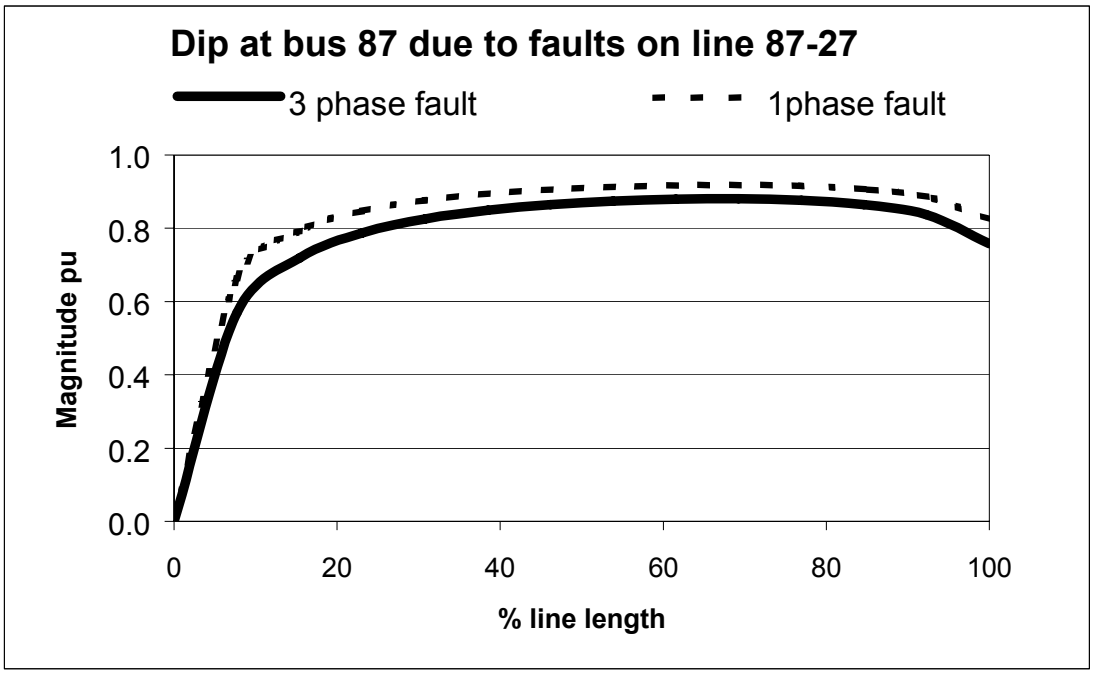

Figure 5.13: Residual voltage at bus 87 (Yumbo) caused by faults on line 87-27 (Yumbo-Esmeralda). Dashed line for single-phase faults, solid line for three-phase faults

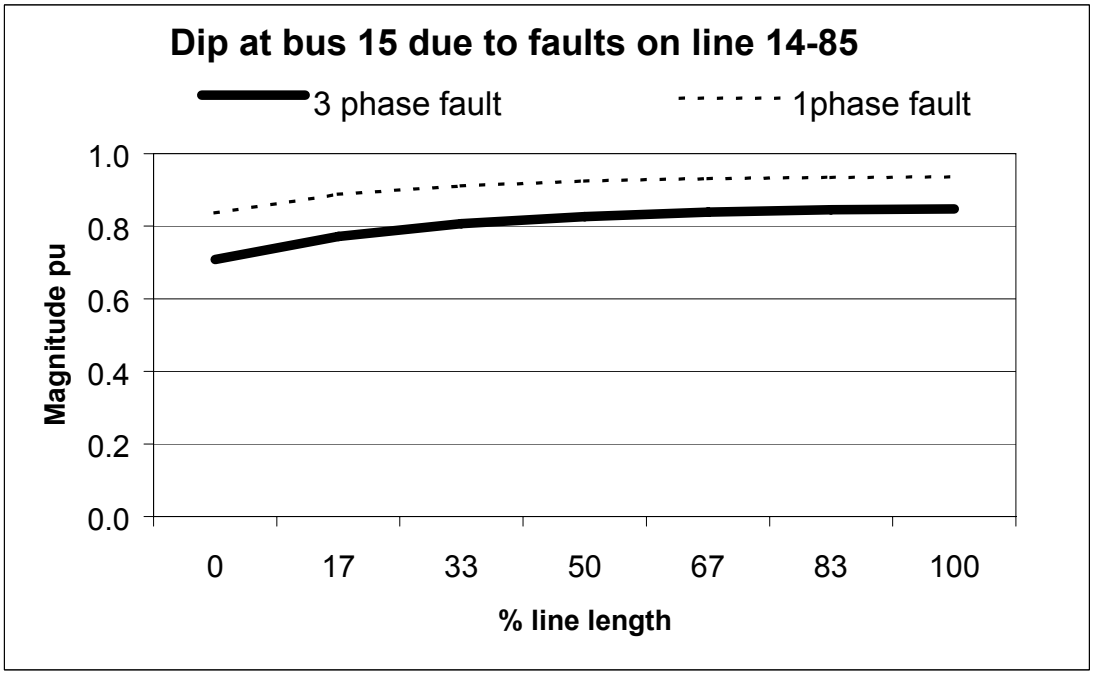

Figure 5.14: Residual voltage at bus15 (Cerromatoso500) during faults on line 76-62 (Tebsa-Sabanalarga230). Dashed line for single-phase faults, solid line for three-phase faults.

Consider the line connecting nodes 62 (Sabanlarga230) and 76 (Tebsa). According to the exposed areas shown in Figure 5.12, only part of this line is inside the 85% exposed area of bus 15 for single-

phase-to-ground faults. This is confirmed by Figure 5.14, which shows the resulting residual voltage for faults along line 76-62. Figure 5.14 also shows the effect of the zero-sequence blocking by the transformers. The voltage drop due to single-phase faults are only about half of the drops due to three-phase faults.
Both Figure 5.13 and 5.14 confirm the fact that single-phase faults are less severe than three-phases faults, in the sense that the worst phase shows a higher residual voltage than the dip due to a three-phase fault at the same position.

5.3.3 Contribution of Symmetrical Faults to Dip Frequency

The purpose of this section is to analyse the contribution of symmetrical faults to the total cumulative frequency. The complete list of results is given in Appendix B.

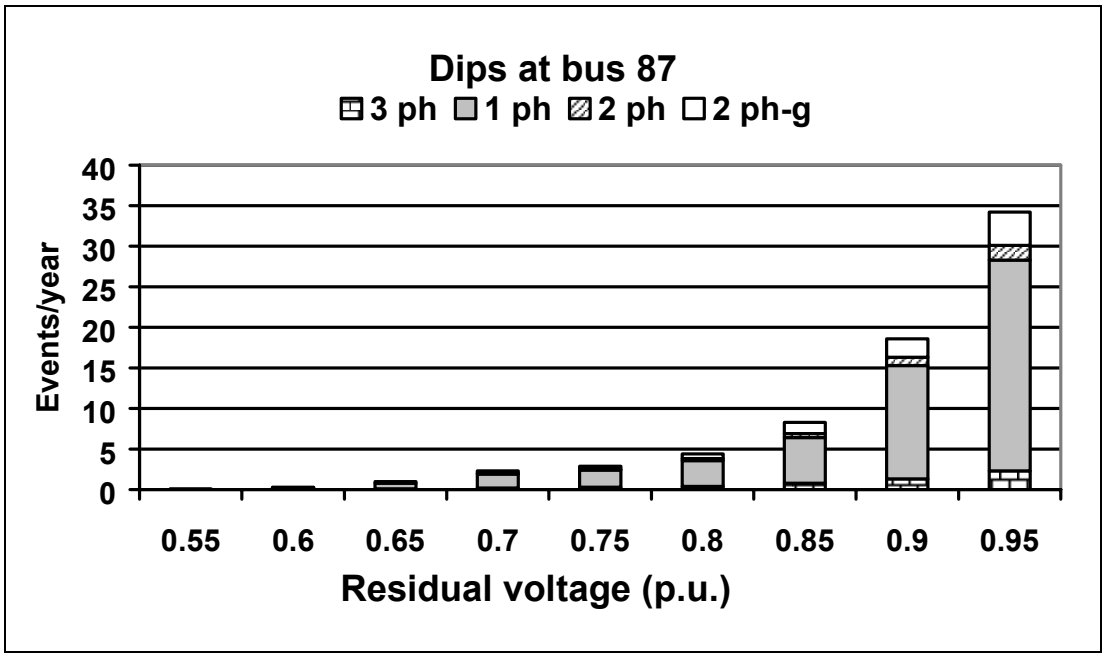

Figure 5.15 Cumulative dip frequency at bus 87 (Yumbo). Contribution of balanced and unbalanced dips are shown

Figures 5.15 to 5.17 show the cumulative number of dips at buses 87, 15 and 5 due to symmetrical and unsymmetrical faults. Symmetrical faults cause balanced dips whereas unsymmetrical faults cause unbalanced dips.
As it would be expected, the contribution of single-phase-to-ground faults is dominant. However, the contribution of the different type of faults does not exactly follow the probability distribution of fault types. The exposed area again can explain this. As the exposed area

for three-phase faults is larger than for any other type of fault, the resulting contribution of this fault type to the total frequency of dips is more than the 5% that could be expected.

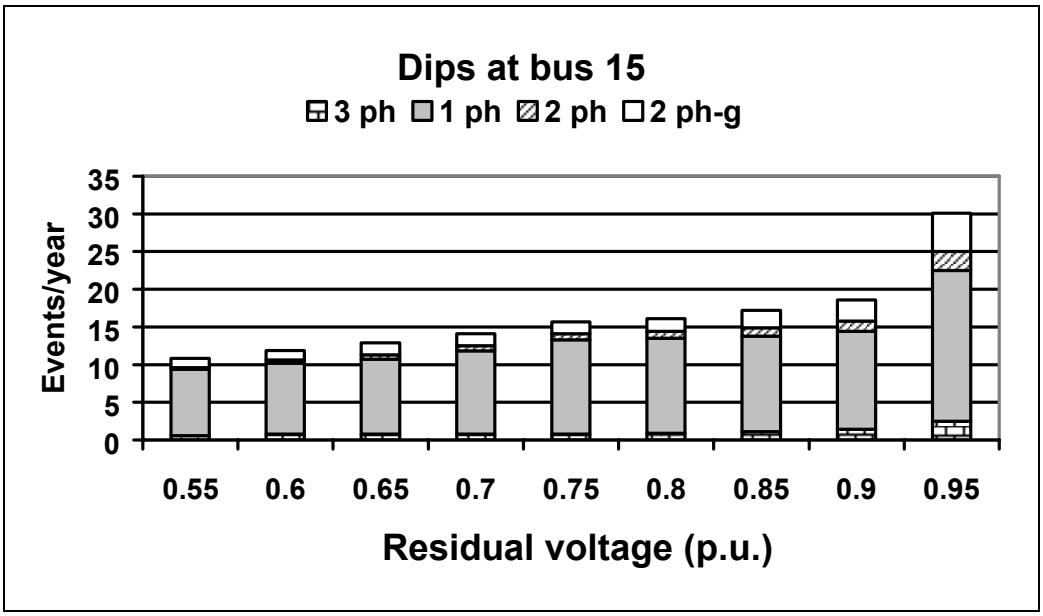

Figure 5.16 Cumulative balanced and unbalanced dip frequency at bus 15 (Cerromatoso500)

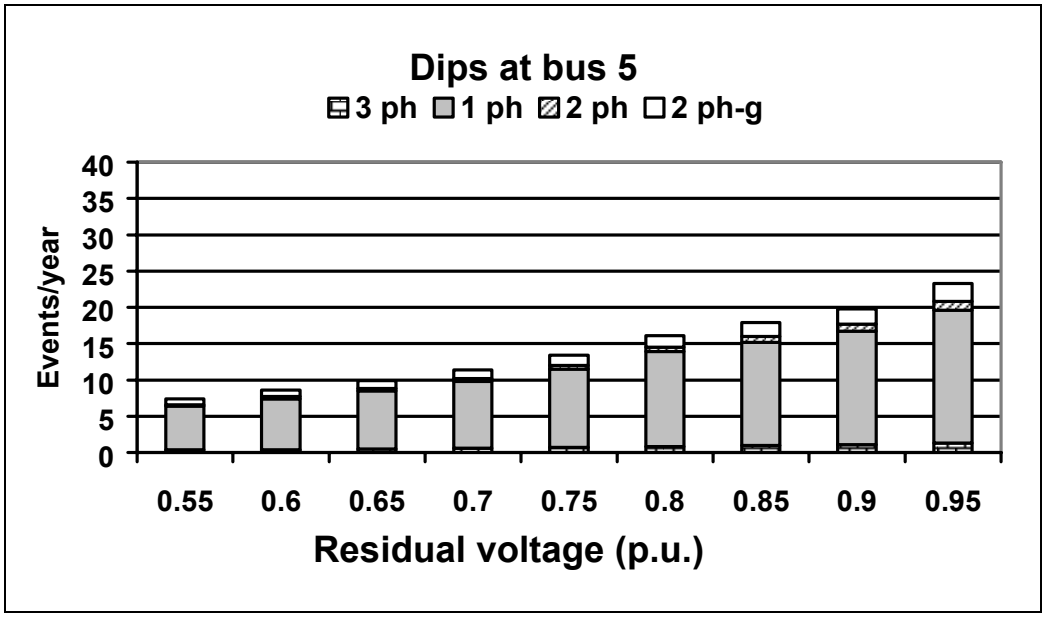

Figure 5.17 Cumulative balanced and unbalanced dip frequency at bus 5 (Banadia)

Table 5.3 shows that at bus 87 (Yumbo), three-phase faults contribute with almost 30% of the total number of dips more severe than 0.6 p.u. Several lines converge to that bus.

The simulations show that the probability distribution of the type of fault is a reasonable indicator of the contribution of dip types to the total number of dips only for buses radially fed. Table 5.4 shows the contribution of the different dips to the total number of dips at bus 5 (Banadia). Bus 5 is fed from the system by means of a single line. The contribution of the different type of dips follows the probability distribution of fault types.

Table 5.3: Cumulative Dip Frequency at Bus 87

Residual voltage v_{kf} p.u.	Cumulative Dip Frequency at Bus 87				
	3 ph	1 ph	2 ph	2 ph-g	Total
0.55	0.04	0.13	0.00	0.04	0.21
0.60	0.10	0.13	0.01	0.11	0.34
0.65	0.12	0.67	0.02	0.21	1.02
0.70	0.16	1.70	0.10	0.26	2.22
0.75	0.28	2.06	0.12	0.39	2.85
0.80	0.45	3.20	0.23	0.62	4.50
0.85	0.82	5.55	0.46	1.44	8.26
0.90	1.28	14.02	0.99	2.33	18.62

Table 5.4: Cumulative Dip Frequency at Bus 5

Residual voltage v_{kf} p.u.	Cumulative Dip Frequency at Bus 5				
	3 ph	1 ph	2 ph	2 ph-g	Total
0.55	0.39	6.03	0.25	0.78	7.4
0.60	0.45	6.99	0.29	0.90	8.6
0.65	0.54	8.02	0.33	1.07	10.0
0.70	0.60	9.16	0.41	1.19	11.4
0.75	0.68	10.79	0.54	1.36	13.4
0.80	0.83	13.08	0.64	1.64	16.2
0.85	0.98	14.16	0.82	1.91	17.9
0.90	1.07	15.60	1.00	2.09	19.8

5.3.4 System Statistics based on Balanced and Unbalanced Dips

System statistics have been already calculated in Section 5.2.7 using symmetrical faults and different number of faults positions.
In this section, system statistics are calculated using results of Case C, where balanced and unbalanced dips are considered. Table 5.5 presents system statistics. For comparison purposes Case 2 (balanced dips) from Table 5.2 is also included.

An interesting conclusion can be derived from Table 5.5. The stochastic assessment of dips overestimates event frequencies when only symmetrical faults are considered. The error seems more important for severe dips. An explanation for this overestimation is the fact that three-phase faults are more severe resulting in larger exposed areas for the load. In other words, the load is geographically more exposed to balanced dips than to unbalanced dips. Therefore, the stochastic assessment based only on symmetrical faults overestimates the frequency of events in comparison to one that considers symmetrical and unsymmetrical faults.

Table 5.5: System statistics based on balanced and unbalanced dips

A.- Number of dips with residual voltage less than 0.9 p.u. (SARFI-0.9)						
Case	#F.posit	# Events	Worst site		95^{th} %	Average
C	781	1333	43.30	27 Esmeralda	37.50	15.33
2	781	1556	44.65	40 Lahermosa	40.55	17.88
B.- Number of dips with residual voltage less than 0.7 p.u. (SARFI-0.7)						
Case	#F.posit	# Events	Worst site		95^{th} %	Average
C	781	415	14.11	36 Jamondino	11.94	4.83
2	781	540	18.86	14 Cerrom..230	15.70	6.21

6 Optimal Monitoring Programs

This chapter focuses on the optimisation of monitoring programs for voltage dip characterization of a transmission system. The optimal number of monitors and their location in the network are determined. The method is based on a re-formulation of the expressions for the voltage during a fault obtained by using the node impedance matrix.

6.1 Characterization of Dip Performance by Monitoring

In Chapter 1, it was shown that monitoring presents some limitations when used to characterize individual sites of a power system. However, these limitations are not so important when the purpose of the monitoring program is the characterization of the system as a whole. Monitoring is needed to calibrate the results of a stochastic assessment of voltage dips (Sikes, 2000; Carvalho et al. 2002a,b). In the stochastic assessment, a historical behaviour of the network is used to predict the expected number of faults on lines and buses and the consequent dips. This stochastic assessment can be adjusted by taking into account the real number of dip-events in some selected buses. To be useful the monitoring program must be representative and cover the whole system. At least, four questions need to be answered:

- How many power quality meters (monitors) need to be installed to cover the system?
- Where should the monitors be installed in order to cover the whole system?
- What voltage threshold should be set?
- How long should the monitoring program be? (Koval, 1990)

This chapter addresses the first three questions. Chapter 10 will recall this monitoring program to develop a method to extend monitoring results to non-monitored buses.

6.2 Optimal Monitor Location

In order to find an optimal monitoring program, the following two premises are considered.

1) A minimum number of monitors should be used to describe the system performance in terms of dips
2) No essential information concerning the performance of load buses in terms of dips should be missed

Premise 2 can be interpreted as a constraint of premise 1: minimizing the number of monitors subject to the coverage of the entire network. In the coming sections this optimisation problem will be formulated and solved.

The number of dips recorded at a site during a given monitoring time depends upon the critical threshold setting of the power quality monitor (Koval, 1990). The threshold level is the voltage p in p.u. at which the power quality meter starts recording. If the threshold is set too low (say 0.6 p.u.), then the monitor will not capture an important number of disturbances. On the other extreme, if the p threshold is set too high (0.95 p.u. or higher), then the number of dips recorded could be excessive and even exceed the storage capability of the monitor.

This increase or decrease in the number of events captured by the meter can be explained from the growth of the exposed area (of the meter) with increasing sensitivity of the monitor. The monitor reach area is defined as the area of the network that can be observed from a given monitor position. The monitor reach area of a monitor installed at a bus k is exactly the exposed area of that bus for the same voltage threshold.

The ability of the power quality meter to trigger on a remote fault is determined by the voltage threshold setting p. The monitor reach area is greater for larger (residual) voltage thresholds than for small ones. In theory, one monitor would be able to capture all events in the network for p equal to 1 p.u. And, only solid faults occurring at the monitor position would be seen for a threshold p equal to 0 p.u. An algorithm to mathematically describe the monitor reach area is presented in the next section.

6.3 Monitor Reach Area

The part of the network that can be observed by a monitor installed at node k can be regarded as the area containing node k and its electrical neighbourhood. The size of this area depends mainly upon the voltage threshold setting of the monitor p and it is called p-Monitor Reach Area for node k.

p-Monitor Reach Area of bus k: Area of the transmission network for which the monitor at bus k is able to capture voltage drops that result in a residual voltage less than or equal to p p.u.

Mathematically speaking, the p-monitor reach area of node k can be described by a set of indices pointing to fault positions (buses and line

segments) where faults lead to a residual voltage less than p p.u. at bus k. Then,

$MRA_{k(p)}$: is the set containing the indices of the fault positions within the p-monitor reach area of node k.

As for the exposed area, the monitor reach areas can be easily determined from the rows of the voltage-dip matrix. A given bus i will be part of the monitor reach area of a bus k if the voltage at bus k during a fault at bus i is lower than or equal to p p.u. Using the voltage dip-matrix $\mathbf{V}_{dfv}$, the $MRA_{k(p)}$ can be determined as indicated in (6.1).

$$MRA_{k(p)} = \{k, i\}; i = 1....Fp : v_{ki} \le p \; \forall k \tag{6.1}$$

In (6.1) Fp is the total number of fault positions and v_{ki} is the (k,i) entry of the dip-matrix. Equation (6.1) allows describing all potential monitor reach areas and for any voltage threshold setting of the monitor. This description, however, is not suitable for implementing an optimisation problem.

An alternative way to describe the monitor reach areas of all potential monitor positions is to use a binary matrix the size of which is equal to N by Fp. For a given voltage threshold setting p the monitor reach areas can be described through a N by Fp binary matrix in which a 1 in entry (i,j) indicates that bus j belongs to the monitor reach area of bus i. Equation (6.2) shows this matrix, where v_{ij} is the (i,j) entry of the dip-matrix.

$$\mathbf{MRA}_p = mra_{ij} = \begin{cases} 1, & if\ v_{ij} \le p \\ 0, & if\ v_{ij} > p \end{cases}, \forall i, j \tag{6.2}$$

Once the monitor-reach areas for all possible locations are determined, the optimisation problem can be formulated.

6.4 Optimisation Problem

Consider a binary-decision-variable-vector (row) $\mathbf{X}$ of length N indicating the need for a monitor at bus i. Elements of $\mathbf{X}$ are x_i as indicated in (6.3). Call this vector "monitor positions vector". A given value of the monitor positions vector indicates where to install the monitors.

$$x_i = \begin{cases} 1 \text{ if a monitor is needed at bus } i \\ 0 \text{ otherwise} \end{cases}, \forall i \tag{6.3}$$

Note that the product of a particular value of the monitor positions vector $\mathbf{X}$ by a particular column j of the $\mathbf{MRA}_p$ matrix indicates the number of monitor reach areas that contain the fault position j. In

order to satisfy premise 2, we want this product to be greater than or equal to 1 for each fault position. In other words, we want each fault position to be in at least one monitor reach area so that at least one monitor triggers on every fault. Let **b** be a vector containing ones. Then the optimisation problem can be formulated as indicated in (6.4).

$$\begin{aligned} &\min(\sum_{1}^{N} x_i) \\ &\text{Subject to :} \\ &\sum_{i=1}^{N} x_i \cdot mra_{ij} \geq b_j;\ \ j = 1,2...Fp \\ &x_i \text{ binary} \end{aligned} \tag{6.4}$$

where mra_{ij} is the (i,j) entry of the $\mathbf{MRA}_p$, N is the number of potential monitor positions (actual buses of the power system), and b_j is the j-th entry of right hand side vector **b.**

The problem described by (6.4) is an integer programming optimisation problem. A number of algorithms, including total enumeration, have been proposed for solving this sort of problem. Total enumeration is discarded because is impracticable even for a small number of discrete variables. The Branch and Bound algorithm is used in almost all optimisation packages (OTC, 2003) because it is an efficient way to deal with this kind of problem (Rardin, 2000). The Branch and Bound search will be used to solve (6.4) for a large transmission network.

6.5 Application

The same system presented in Chapter 5 has been used to test the methodology.

The maximum generation level was used to optimise the monitoring program because the size of the monitor reach areas increases when the generation level is decreased. The minimum generation level leads to less monitors but it does not guarantee that the complete network is covered during the maximum generation. For simplicity, only three-phase faults at actual buses of the network are used to model the monitor reach areas. In Chapter 10, however, single-phase-to-ground faults and 781 fault positions at buses and lines are used to model the monitor reach areas.

The monitor reach area matrix $\mathbf{MRA}_p$ for different choices of p was built and the optimisation problem solved by using the Branch and Bound algorithm. The following cases were considered.

- Case A1: voltage threshold p of monitors equal to 0.9 p.u. Initial value of all x_i=1.
- Case A2: voltage threshold p of monitors equal to 0.9 p.u. Initial value of all x_i=1. Two monitor positions are chosen a priori fixing x_{42} and x_{60} to 1.
- Case B1: voltage threshold p of monitor equal to 0.85 p.u. Initial x_i=1.
- B2: voltage threshold p of monitor equal to 0.85 p.u. Initial value for all x_i=0.
- Cases C1 and C2 consider p equal to 0.8 p.u.
- Cases D1 and D2 consider p equal to 0.75 p.u.

In Table 6.1 results for all the cases are presented. All the solutions presented satisfy the constraints: the chosen monitor positions are able to cover the whole system and the number of monitors is the minimum possible.

Table 6.1: Optimal Monitor Locations

		Monitors			
Case	***p (p.u.)***	***Initial***	***Final***	***Pre-Opt***	***Optimal monitor positions (buses)***
A1	0.9	87	8	-	2,4,28,33,36,78,81,85
A2	0.9	87	8	42,60	2,24,42,50,60,66,81,85
B1	0.85	87	12	-	4,5,12,13,14,18,24,26,36,41,47,75
B2	0.85	0	12	-	12,18,41,53,61,66,69,75,78,81,85,86
C1	0.8	87	14	-	25,27,34,54,55,61,66,75,78,80,81,83, 85,86
C2	0.8	0	14	-	13,24,25,34,54,57,61,66,75,77,78,81, 83,85
D1	0.75	87	15	-	6,14,24,34,37,40,52,54,61,66,78,80,8 1,83,86
D2	0.75	0	15	-	5,8,21,26,34,40,51,52,57,61,66,78,80, 83,85

From Table 6.1 it is clear that the number of monitors needed to cover the whole system increases with the decrease of the monitor threshold.

It is also clear that the optimisation problem has multiple solutions: in cases A1 and A2, the minimum number of monitors required to cover the entire network is eight but the location of the meters is different.

The same can be stated for cases B, C and D. Two different solutions are presented for each one of the cases.
Table 6.2 presents $MRA_{k(0.9)}$ sets for the optimal monitor locations in cases A1 and A2. Table 6.3 presents $MRA_{k(0.7)}$ sets for the optimal locations in case C1.

Table 6.2: Monitor Reach Areas for Optimal Locations Cases A1 and A2

0.9 p.u. Monitor Reach Areas for Optimal Locations Cases A1 and A2												
Mra 2	***Mra 4***	***Mra 24***	***Mra 28***	***Mra 33***	***Mra 36***	***Mra 42***	***Mra 50***	***Mra 60***	***Mra 66***	***Mra 78***	***Mra 81***	***Mra 85***
2	4	12	12	4	1	4	4	7	1	19	5	2
3	17	15	15	17	9	17	17	19	9	31	7	3
6	18	16	16	18	27	18	18	31	27	35	10	14
8	33	21	21	33	36	33	33	35	36	43	11	15
13	34	23	23	39	37	39	34	43	37	47	19	16
15	39	24	24	41	45	41	39	47	45	48	20	31
25	41	28	28	42	55	42	41	48	55	59	22	51
26	50	30	30	50	57	50	50	59	57	60	32	62
27	58	51	51	58	64	58	58	60	64	78	46	63
29	61	62	62	72	66	72	61	78	66		48	67
31	67	63	63	82	70	82	67		70		52	68
35	69	73	73	83	87	83	69		87		56	76
38	72	76	76				72				65	79
40	82	77	77				82				71	84
44	83	79	79				83				74	85
45		80	80								75	
49		86	86								81	
53												
54												
59												
67												
68												
70												
87												

Comparing Table 6.2 and Table 6.3 it can be seen that the monitor reach area corresponding to a threshold of 0.9 p.u. is larger than the one corresponding to a threshold of 0.7 p.u.
Figure 6.1 graphically presents the result for case A1.

Table 6.3: Monitor Reach Areas for Optimal Locations, Case C1

0.8 Monitor reach area for case C1													
Mra 25	***Mra 27***	***Mra 34***	***Mra 54***	***Mra 55***	***Mra 61***	***Mra 66***	***Mra 75***	***Mra 78***	***Mra 80***	***Mra 81***	***Mra 83***	***Mra 85***	***Mra 86***
6	2	4	2	1	4	9	20	47	12	5	4	14	21
8	3	33	3	37	33	36	22	60	62	7	17	15	23
25	13	34	6	45	39	37	71	78	63	10	18	16	24
29	27	39	26	55	41	55	75		76	11	33	62	28
44	37	41	31	57	43	57			77	19	39	63	30
	38	50	35	64	50	66			80	22	41	67	51
	40	58	44	66	58	70				32	42	68	62
	41	82	49	70	61	87				46	50	84	63
	45		53	87	67					48	58	85	73
	67		54		68					52	72		76
	68		59		82					56	82		79
	69									65	83		86
	70									71			
	87									74			
										75			
										81			

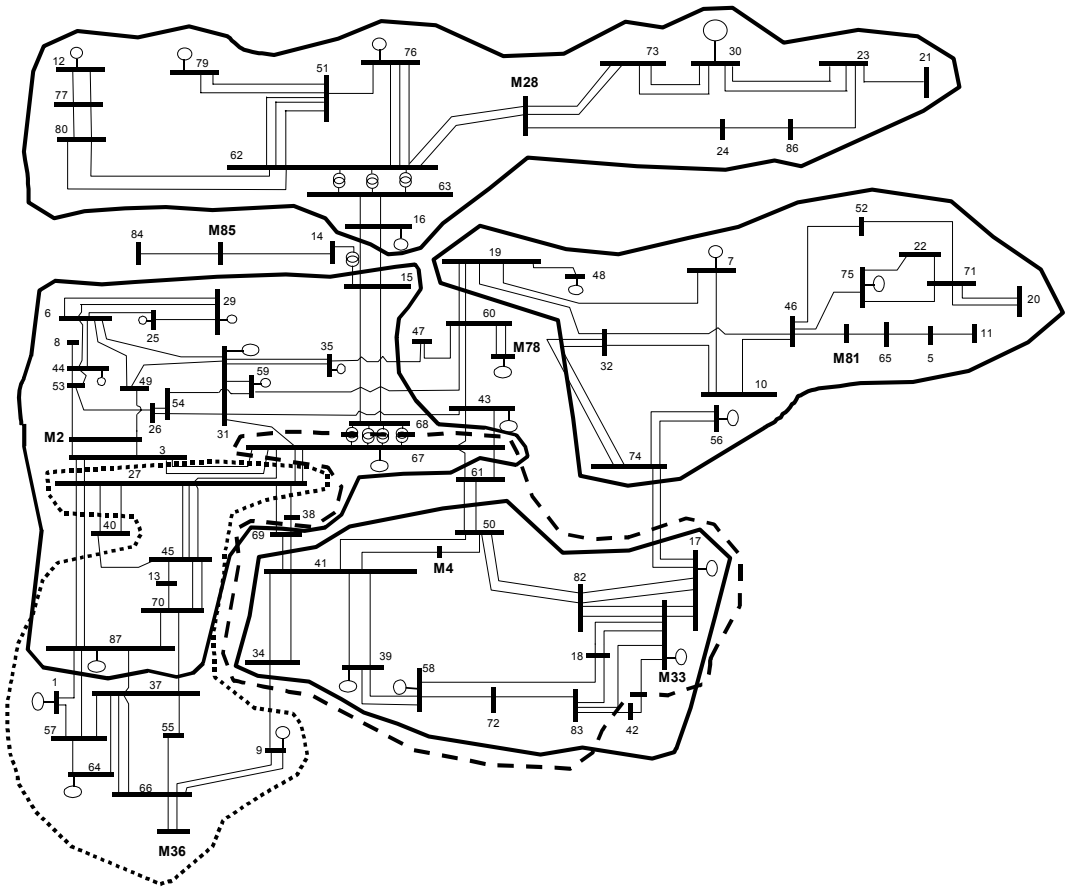

Figure 6.1: Optimal Monitors Locations, Case A1

In Figure 6.1, only six monitors reach areas are explicitly presented to avoid confusion due to the number of sets. Monitors M_{28}, M_{81}, M_4, M_2 and M_{36} cover most of the system. M_{85} is needed to cover buses 84, 85 and 14. M_{78} for monitoring of buses 43, 47, 60 and 78 and M_{33} is needed just to cover bus 42.

6.6 Redundancy

In Figure 6.1, it can be seen that there are several fault positions (buses in this case) being observed from more than one monitor position. This can also be observed in Table 6.2. In other words, there is redundancy. From the point of view of system characterization based on average SARFI-X, redundancy should be minimized in order to avoid counting events more than once. Reducing the monitor reach areas of some monitors can decrease redundancy. In Figure 6.1, the redundancy between M_4 and M_{33} can be reduced by eliminating M_{33} and installing a monitor at bus 42. In order to decrease the redundancy between M_{42} and M_{33}, dips above a certain value should not be considered for the purpose of system characterization. This is equivalent to reduce the monitor reach area of M_{42}.

Redundancy should be minimized when the purpose of the monitoring program is the characterization of the average performance in network. However, when the purpose of the monitoring program is to determine the causes of the events, redundancy provides useful information. In this sense, the optimisation problem formulated allows modelling different levels of redundancy. For instance making b_i equal to 2 on the right hand side of the constraints we make sure that the resulting number of monitors and their positions will be so that every bus is observed by at least two monitors. This approach will be used in Chapter 10 to develop a method to estimate the residual voltages at non-monitored buses.

6.7 System Statistic From Limited Number of Monitors

It is not possible to monitor each bus of a large transmission system. Selection of suitable buses to monitor must be made optimally in order to minimise the number of monitors and to get a reasonable description of the system performance. In the previous section, an algorithm has been proposed for designing an optimal monitoring program. The main purpose of this program is the description of the system in terms of voltage dips with a limited number of monitors.

The proposed method is based on the monitor reach area, which is function of the bus impedance matrix. The fault rate has not been taken into account for the formulation of the algorithm.
Once the results of the monitoring program are available, system indices can be calculated. The indices to be calculated are the same as computed in Chapter 5 using the stochastic assessment of dips. In Chapter 5, system statistics were computed using the dip performance of 87 buses. In this section, the system statistics are calculated with a limited number of monitors placed according to the optimisation algorithm. Ideally, we should use measurements at the selected buses to calculate the indices and compare them with the system statistics based on a full monitoring program. In absence of actual measurements, results from the stochastic assessment are considered the real performance of the system.
Table 6.4 shows system statistic based on cases A1, A2, D1, and D2. For comparison purposes system indices based on a full monitoring program (case 2 from Table 5.2) are also presented.

Table 6.4: System statistic based on limited number of monitors

A.- Number of dips more severe than 0.9 p.u. SARFI-0.9						
Case	#F. posit.	# Events	Worst site		95^{th} %	Average
2	781	1556	44.6	40 Lahermosa	40.55	17.88
A1	8 monit.	150	24.1	2 Anconsur	23.36	18.75
A2	8 monit.	151	24.1	2 Anconsur	23.16	18.91
B.- Number of dips more severe than 0.7 p.u. SARFI-0.7						
Case	#F. posit.	# Events	Worst site		95^{th} %	Average
2	781	540	18.86	14 Cerrom..230	15.70	6.21
D1	15 monit.	103	13.8	66 Sanberna..no	12.96	6.91
D2	15 monit.	88	13.8	66 Sanberna..no	12.10	5.80

From Table 6.4 it can be seen that the optimal positions allow identifying the system average performance. However, the 95 percentile is not well identified. The 95 percentile obtained for case 2 is based on the performance of the 87 buses and hence the worst case is explicitly identified. Identifying the worst site needs more than the algorithm developed because the expected number of faults, the fault rate, has an important effect on the number of dips seen at a given bus. One option to get the 95 percentile would be to choose, a priori, the position of one monitor at the worst site. However, this option is based on the availability of the stochastic assessment of dips.

7 Analytic Approach to the Method of Fault Positions

This chapter presents an alternative analytic approach to perform voltage dip stochastic assessment. The method is based on the algebraic description of the residual voltage at an observation bus when a moving fault node is considered at any line.

7.1 Introduction

The method of fault positions as introduced in Chapter 4 and 5 is a powerful tool for stochastic assessment of voltage dip performance that can be used in planning, as well as in operation activities to decide about alternative system investments or topologies of the network. The result of the method based on long-term fault-rates is the long-term average prediction of the network performance, and comparison against measurements during a particular year needs adjustment and judging (Carvalho et al., 2002a; Sikes, 2000). One drawback of the method of fault positions is the lack of clarity in the appropriate number of fault positions to be considered. As shown in Chapter 5, the result of the assessment depends on the number of fault positions used in the simulations. More fault positions produce a more accurate assessment. In the limit situation, an infinite number of faults should be simulated in the system to obtain the continuous frequency function of events, something that would be impossible with the approach presented in Chapter 4 and 5.

In this chapter, an analytic approach to the method of fault positions is presented. The method is similar to the approach introduced by Lim et al. (Lim, Y. S., 2002), where the probability density function of voltage-dips caused by faults across the network is determined. The residual voltage at a given bus is expressed as a function of the position of a moving fault node providing a deterministic relation between two stochastic variables: 1) fault position and 2) residual voltage. Although powerful, the method is hard to understand and difficult to implement. The method proposed here focuses on the cumulative frequency of events with residual voltage up to a given value. From the point of view of a sensitive load, what matters is the number of dips with a residual voltage less than a given value. Moreover, this approach facilitates the understanding of the method and the computational implementation. We begin by deriving the

equation for the residual voltage at a general bus *m* during a fault at a moving node *f*.

7.2 Residual Voltage Caused by a Moving Fault Node

In this section, we derive the equations for the residual voltage at a general observation bus *m* when a moving fault node *p* travels along a general line connecting nodes *k* and *j* (Han, 1982).

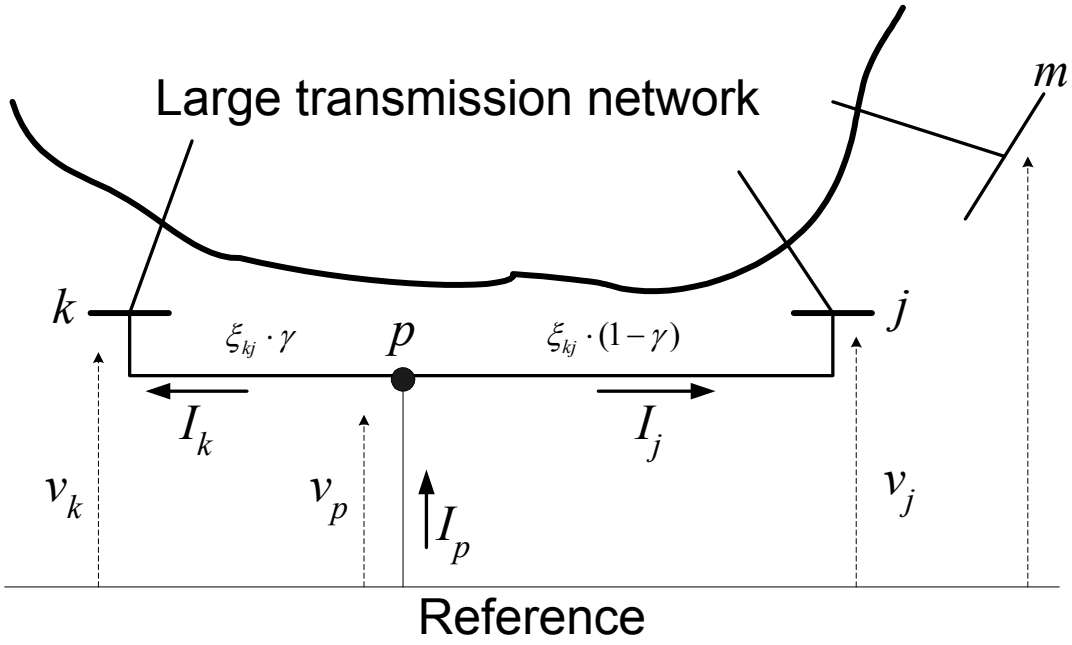

Figure 7.1: A moving fault node travels from bus k to bus j

Consider Figure 7.1 where a general line connecting buses *k* and *j* is shown. The series line impedance is ξ_{kj} p.u. Node voltages are measured with respect to the reference node. A node *p* travels from bus *k* to bus *j* and in the figure is at a distance γ in per unit of the line length measured from bus *k*.

The following equations can easily be derived. The current flowing from *p* and being injected at bus *k* is shown in (7.1). Similarly, the current from *p* to *j* is given by (7.2). Applying Kirschoff's current laws to node *p* we get (7.3).

$$I_k = \frac{v_p - v_k}{\gamma \cdot \xi_{kj}} \tag{7.1}$$

$$I_j = \frac{v_p - v_j}{(1-\gamma) \cdot \xi_{kj}} \tag{7.2}$$

$$I_p = I_k + I_j \tag{7.3}$$

Summing (7.1) and (7.2) and solving for v_p we get an expression (7.4) relating node voltages, the current I_p (the fault current), the series impedance of the line, and the distance to the fault from bus *k*.

$$v_p = I_p \cdot \gamma \cdot (1-\gamma) \cdot \xi_{kj} + \gamma \cdot v_j + (1-\gamma) \cdot v_k \tag{7.4}$$

Equation (7.4) is a general relation of: 1) the node voltage at an arbitrary node *p*, 2) the current injected at that node and, 3) the bus voltages at the extremes of the line.

Recall equation (2.16) relating network-node voltages and injected currents. Recall also that the transfer impedance (z_{mp}= z_{pm}) can be interpreted as the voltage that appears at node *p* when a current 1 p.u. is injected at node *m* and all other injected currents are zero. Suppose that a current I_m of value 1 p.u. is injected at node *m* and all other currents are zero. In particular make I_p=0 in (7.4). Then the voltages at all buses will equal the transfer impedances between *m* and the corresponding bus. Mathematically:

$$\text{if } I_m = 1\,\text{p.u.} \wedge I_i = 0 \,\forall\, i \neq m \Rightarrow v_i = z_{mi} \tag{7.5}$$

Therefore, (7.4) can be written:

$$z_{mp} = z_{mj} \cdot \gamma + z_{mk} \cdot (1-\gamma) = (z_{mj} - z_{mk}) \cdot \gamma + z_{mk} \tag{7.6}$$

Equation (7.6) shows that the transfer impedance between the observation bus *m* and the moving node *p* is a linear function of the distance γ to the fault. For a given line connecting buses *k* and *j*, the transfer impedance between the observation bus *m* and bus *k* (or *j*) is constant. Both transfer impedances z_{mk} and z_{mj} are available in the impedance matrix **Z**. Therefore, only the distance to the fault (γ in per unit) is needed to evaluate the transfer impedance z_{mp} between the observation bus and any fault position along the line.

Recall now that the driving point impedance of a node *p* (Thevenin impedance) can be interpreted as the voltage that appears at node *p* when a current 1 p.u. is injected at that node, and all other currents are zero. If I_p=1 p.u. is the unique current being injected then, the bus voltage at *p* equals the Thevenin impedance seen into the network from *p* and the other bus voltages equal the transfer impedances between *p* and the corresponding bus. Mathematically:

$$\text{if } I_p = 1\,\text{p.u.} \wedge I_i = 0 \,\forall\, i \neq p \Rightarrow v_i = z_{pi} \tag{7.7}$$

Then (7.4) results:

$$z_{pp} = \gamma \cdot (1-\gamma) \cdot \xi_{kj} + z_{pj} \cdot \gamma + z_{pk} \cdot (1-\gamma) \tag{7.8}$$

Using (7.6) to express the transfer impedances z_{pj} and z_{pk} and inserting these expressions into (7.8), we get (7.9).

$$z_{pp} = (z_{kk} + z_{jj} - 2z_{kj} - \xi_{kj}) \cdot \gamma^2 + (2z_{kj} - 2z_{kk} + \xi_{kj}) \cdot \gamma + z_{kk} \tag{7.9}$$

Equation (7.9) shows that the driving point impedance at node *p* is a quadratic function of the distance to the fault. It also shows that the elements of the impedance matrix together with the series impedance of the faulted line can be used to determine the driving point impedance at the faulted node *p*.
In Chapter 3, it is shown that the residual voltage during a fault can be calculated by using (3.4). If the pre-fault voltages are assumed 1 p.u., then (3.4) can be simplified as shown in (7.10).

$$v_{mp} = 1 - \frac{z_{mp}}{z_{pp}} \tag{7.10}$$

Replacing the impedances by their expressions in (7.6) and (7.9) an analytic expression for the residual voltage is determined.

$$v_{mp} = 1 - \frac{(z_{mj} - z_{mk}) \cdot \gamma + z_{mk}}{(z_{kk} + z_{jj} - 2z_{kj} - \xi_{kj}) \cdot \gamma^2 + (2z_{kj} - 2z_{kk} + \xi_{kj}) \cdot \gamma + z_{kk}} \tag{7.11a}$$

$$v_{mp} = 1 - \frac{M_{kj} \cdot \gamma + N_{kj}}{A_{kj} \cdot \gamma^2 + B_{kj} \cdot \gamma + C_{kj}} \tag{7.11b}$$

Equation (7.11a) is a complex variable expression resulting in magnitude and angle of the residual voltage. In this work, only magnitude is addressed. Equation (7.11b) facilitates computer implementation.
In order to apply (7.11) the observation bus *m*, the faulted line, and the distance to the fault are needed, buses *k* and *j* are fixed once the faulted line is chosen.

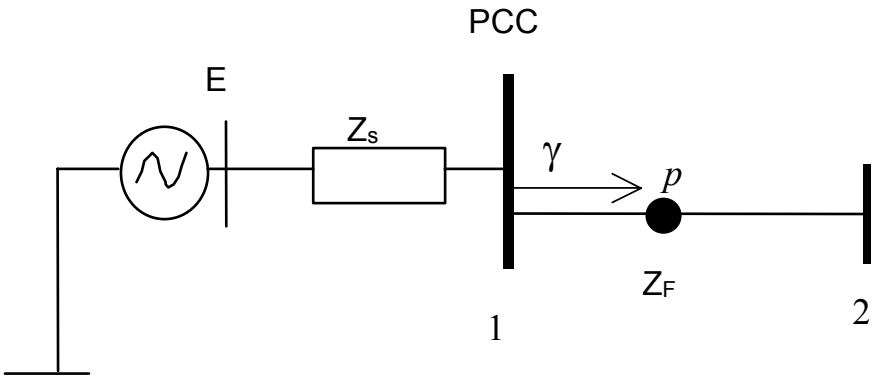

Figure 7.2: Voltage divider for dip magnitude calculation

To illustrate the applicability of (7.11) consider Figure 7.2. In order to determine the bus impedance matrix the PCC is given node label 1

and the far end of the feeder is labelled 2. The impedance matrix can easily be determined resulting in (7.12).

$$\mathbf{Z} = \begin{bmatrix} Z_S & Z_S \\ Z_S & Z_S + Z_F \end{bmatrix} \tag{7.12a}$$

$$z_{11} = z_{12} = z_{21} = Z_S \tag{7.12b}$$

$$z_{22} = Z_S + Z_F$$

To calculate the residual voltage at PCC for a fault at node p (7.11) is used with m=k=1 and j=2 to obtain (7.13a) which is the well-known voltage divider model. Replacing γ by its expression in terms of the length of the line we get (7.13b) which can also be written in terms of the impedance of the feeder in per unit of length of the feeder as shown in (7.13c).

$$v_{1p} = 1 - \frac{Z_S}{Z_F \cdot \gamma + Z_S} = \frac{Z_F \cdot \gamma}{Z_F \cdot \gamma + Z_S} \tag{7.13a}$$

$$v_{1p} = \frac{Z_F \cdot \dfrac{L_{1p}}{L_{12}}}{Z_F \cdot \dfrac{L_{1p}}{L_{12}} + Z_S} \tag{7.13b}$$

$$v_{1p} = \frac{z_F \cdot L_{1p}}{z_F \cdot L_{1p} + Z_S} \tag{7.13c}$$

7.3 Expected Number of Voltage Dips

Equation (7.11) is a deterministic function relating two stochastic variables: 1) the fault position γ and 2) the residual voltage v_{mp}. Let $\phi_{kj}(\gamma)$ be the deterministic function so that (7.11) can be written as shown in (7.14).

$$v_{mp} = \phi_{kj}(\gamma) \tag{7.14}$$

A sensitive load will most likely trip whenever the voltage at terminal of the load is less than a given critical voltage. Then, what matters is the expected number of dips with a residual voltage less than the critical voltage because all these events expose the load to a potential trip. In other words, the cumulative frequency of dips up to a given residual voltage is the most suitable way to characterise the dip performance at a particular site of the network.

Let F_v be the cumulative frequency function (cff) of residual voltages and let F_γ be the cff of faults expressed as a function of the fault position γ. Then, our problem is to express F_v in terms of F_γ.

Probability principles (Suhir, 1997; Kinney, 1997) show that for a monotonically increasing function the problem is rather simple. The cumulative frequency function is given by (7.15) where ϕ^{-1} is the inverse function ϕ, this is $\gamma=\phi^{-1}(v)$.

$$F_v(v) = F_\gamma\left(\phi_{kj}^{-1}(v)\right) \tag{7.15}$$

For example, consider the residual voltage at bus 1 of Figure 7.2, which increases with increasing distance to the fault node. In that case ϕ is given by the expression of the voltage divider (7.13) and $\gamma=\phi^{-1}(v)$ results:

$$\phi(\gamma) = v_{1p} = \frac{Z_F \cdot \gamma}{Z_F \cdot \gamma + Z_S} \Rightarrow \phi^{-1}(v) = \gamma = \frac{Z_S}{Z_F} \cdot \left(\frac{v_{1p}}{1 - v_{1p}}\right) \tag{7.16}$$

If faults are distributed uniformly along the line, then the cff of faults F_γ is given by (7.17) where N is the total number of faults affecting the feeder per year.

$$F_\gamma(\gamma) = N \cdot \gamma \tag{7.17}$$

Applying (7.15) we obtain (7.18a) which in terms of the constant fault rate λ of the feeder can be written as (7.18b) resulting in the method of critical distance discussed in Chapter 2.

$$F_v(v) = N \cdot \frac{Z_S}{Z_F} \cdot \left(\frac{v_{1p}}{1 - v_{1p}}\right) \tag{7.18a}$$

$$F_v(v) = L_{12} \cdot \lambda \cdot \frac{Z_S}{Z_F} \cdot \left(\frac{v_{1p}}{1 - v_{1p}}\right) = \frac{Z_S}{z_F} \cdot \left(\frac{v_{1p}}{1 - v_{1p}}\right) \cdot \lambda \tag{7.18b}$$

In general, however, the function ϕ_{kj} shown in (7.11) is neither monotonically increasing nor monotonically decreasing in the range of γ, the distance to the fault node in p.u. ($0 \le \gamma \le 1$). In particular $\phi_{kj}(\gamma)$-v = 0 results in a concave quadratic equation in γ meaning that two solutions for γ can be obtained for a given value of residual voltage. For such a ϕ function, the cff must be calculated using (7.19), where $\phi_{kj}^{-1}(v)^+$ and $\phi_{kj}^{-1}(v)^-$ denote the two inverse functions obtained from ϕ and $F_\gamma(1)$ is the total number of faults expected to occur along the line being analysed. Care must be taken in order to make sure that the solutions $\gamma_1=\phi_{kj}^{-1}(v)^+$ and $\gamma_2=\phi_{kj}^{-1}(v)^-$ are feasible, i.e. both contained in the range of γ [0 1].

$$F_v(v) = F_\gamma(1) + F_\gamma\left(\phi_{kj}^{-1}(v)^-\right) - F_\gamma\left(\phi_{kj}^{-1}(v)^+\right) \tag{7.19}$$

If faults are uniformly distributed along the line, (7.20) gives the cff of dips at an arbitrary observation bus *m* caused by three-phase faults

on a general line connecting buses k and j. In (7.20) N_{kj} is the total number of faults expected to occur on line k-j.

$$F_v(v) = N_{kj}(1 + \phi_{kj}^{-1}(v)^- - \phi_{kj}^{-1}(v)^+) \tag{7.20}$$

Equation (7.19) gives the cff of dips at a given bus m for faults on a general line connecting buses k and j. In order to fully describe the expected performance of bus m, faults at all lines need to be considered. The complete cff is then obtained by summing cff corresponding to relevant lines as shown in (7.21) where *nLi* is the total number of lines in the system.

$$F_v^m(v) = \sum_{line=1}^{nLi} F_v(v) \tag{7.21}$$

7.3.1 Algorithm and Details of Computer Implementation

Suppose that the impedance matrix **Z** and the data in Table 7.1 are available. Consider columns of Table 7.1 vectors containing the corresponding data.

Table 7.1: Data for analytic approach to the method of fault positions

Line index	From (k)	To (j)	Series ξ_{kj}	Length L_{kj}	Fault rate λ_{kj}
1	3	4	ξ_{34}	L_{34}	λ_{34}
2					
:					
nLi					

The following algorithm would perform stochastic assessment of voltage dip performance at a particular bus m.

Calculate A, B, C for each line (7.11b)
For bus=m
For index=1:nLi (for each line), evaluate (7.20)
Complete cff by summing all F_v (7.21)

Note that the evaluation of the constants A, B, and C is straightforward from Table 7.1 and the impedance matrix **Z**.

For index=1:nLi
k=From(index)
j=To(index)

$$A(index) = z(k,k) + z(j,j) - 2z(k,j) - \xi(index)$$
$$B(index) = 2z(k,j) - 2z(k,k) + \xi(index)$$
$$C(index) = z(k,k)$$

This allows calculating the driving point impedance at any position along line *k-j*.

7.3.2 Unsymmetrical Faults

Voltage dips caused by unsymmetrical faults can also be analysed by the method introduced above. Equation (7.11) is valid in the sequence domain. The residual-sequence voltages can be expressed as functions of the fault position γ. Positive, negative and zero sequence impedances need to be considered making the equation cumbersome. Moreover, the effect of power transformers between the observation bus and the fault point need to be modelled. The resulting cff for different types of faults are combined according to the probability of occurrence to obtain the total cff.

7.3.3 Simulation Results

The proposed method has been applied to the test network introduced in Chapter 5. In this section, simulation results are presented.
Only symmetrical faults are used here to illustrate the method. Charging of lines is considered, which makes the results presented here slightly different to those in Chapter 5. The difference is however small. The lumped-circuit model of a line requires shunt capacitance at the extremes of the line and therefore all the elements of the impedance matrix change.
Figure 7.3 shows the stochastic assessment of voltage dips at some buses by using the analytic approach. Assessed buses correspond to these included in the optimal monitoring program presented in Chapter 6. As seen in Figure 7.3, the results are presented as a continuous-cumulative frequency-function allowing a better description of the expected performance of buses.
Figure 7.4 shows the stochastic assessment of dips at buses 11 (weak bus) and 67 (strong bus). The graph includes the results obtained from the application of the method of fault positions using 781 fault positions (bus11_2a and bus67_2a) as well as the results obtained by applying the proposed method. Small differences can be seen between the assessments. The proposed method is equivalent to the most

elaborated simulation (781 fault positions) confirming the applicability of the method.

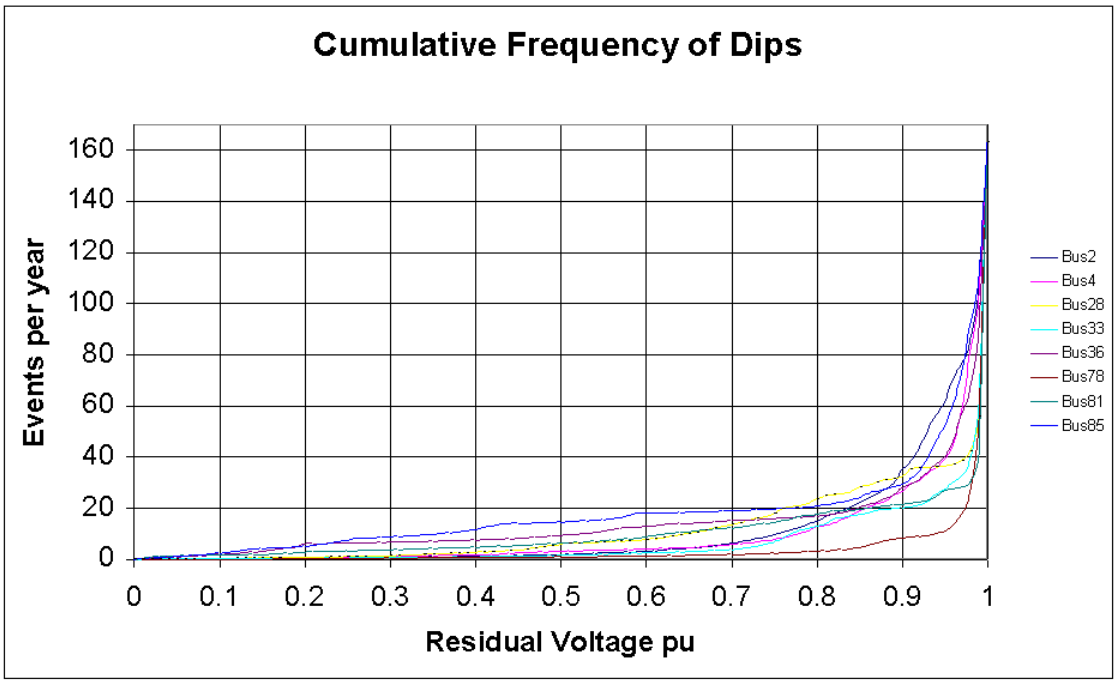

Figure 7.3: Cumulative frequency of voltage dips for selected buses

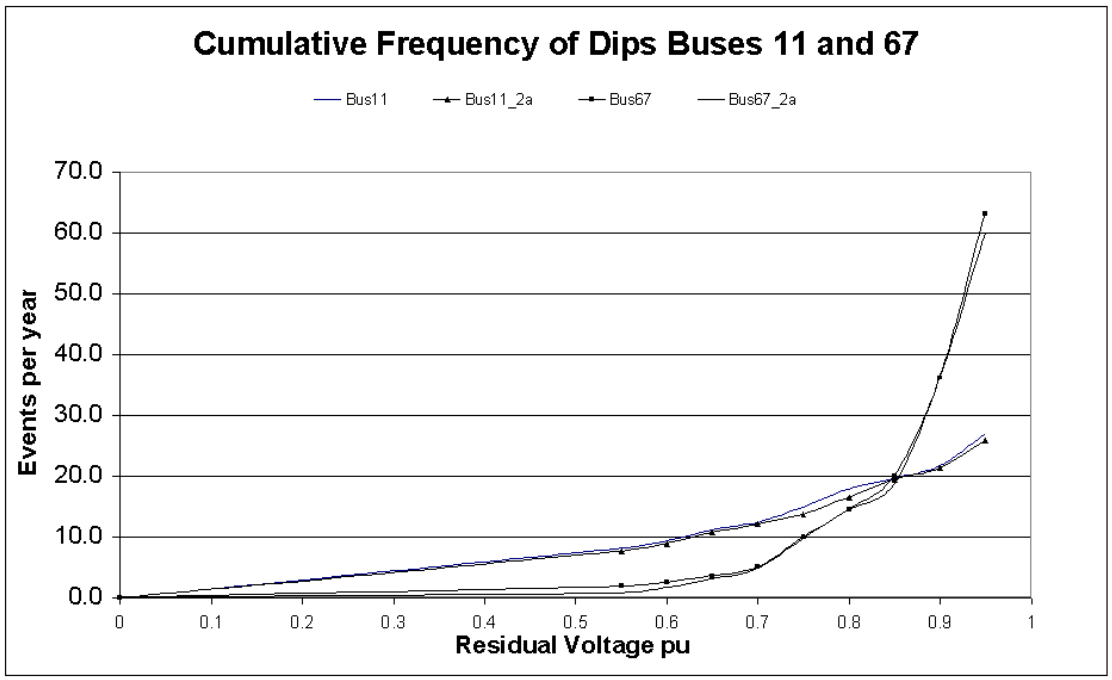

Figure 7.4: Cumulative frequency of dips at buses 11 and 67

An interesting application of the method is the direct evaluation of SARFI-X index. The SARFI-X index is the number of events with residual voltage less than X. It can easily be calculated from (7.21) replacing the corresponding residual voltage. Alternately the SARFI-

X can be read from the cumulative frequency function. For example, the resulting SARFI-0.7 and SARFI-0.9 at bus 67 and bus 11 are shown in Table 7.2.

Table 7.2: SARFI-0.9 for buses 11 and 67

	Bus 11	Bus 67
SARFI-0.9	21.7	36.2
SARFI-0.7	12.5	5.1

System indices can also be determined by using the proposed approach. In Chapter 5, system indices (SARFI-0.7 and SARFI-0.9) were presented in tabular form (Table 5.2). With the proposed approach, it is easy to build the average cumulative frequency for the desired system index.

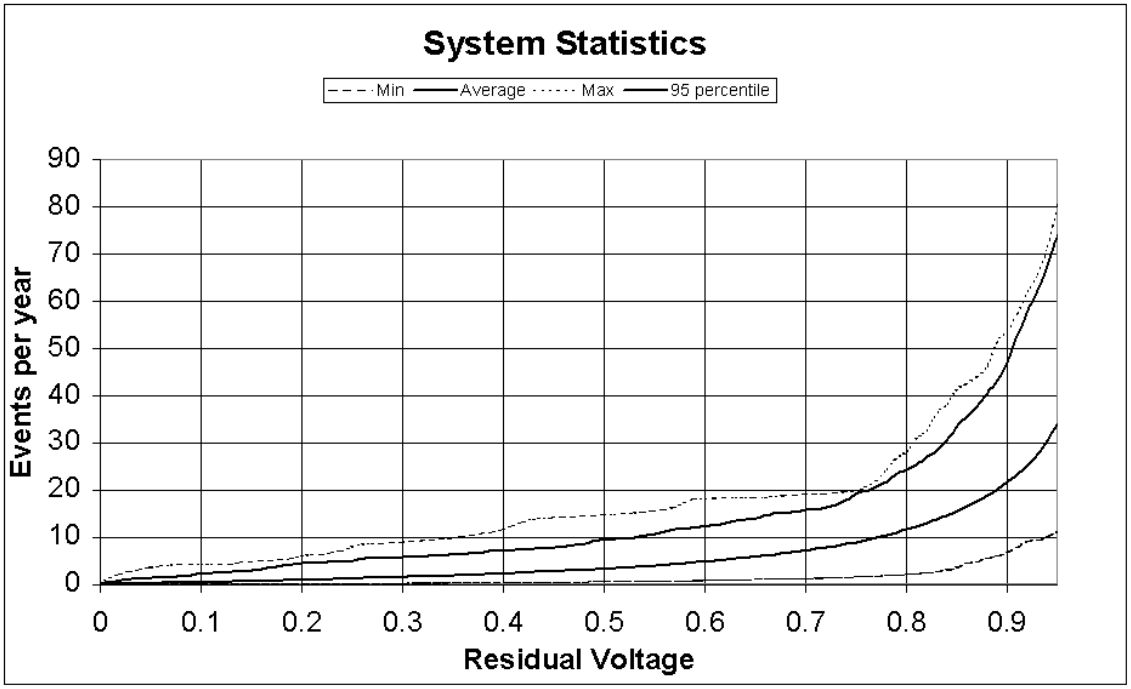

Figure 7.5: System statistics calculated using the analytic approach

Figure 7.5 shows system statistics. The cumulative frequency function of dips corresponding to any bus will fall between the minimum and maximum curve shown in Figure 7.5. Statistics are derived from site performance within the corresponding residual voltage range. The performance of a hypothetical average bus could be represented by the average curve. The worst site could be represented by the 95 percentile.

8 Comparing Stochastic Assessment and Measurements

In this chapter, a discussion regarding the comparison between measurements and stochastic assessment is presented. Fault scenarios are created and pseudo-measurements are obtained in order to compare stochastic assessment against measurements. The chapter shows that the method of fault positions cannot be used to predict the network performance during a particular year, unless correcting factors are used to adjust the assessment. A Monte Carlo simulation approach is suggested to better describe the expected dip performance. It is shown that whereas the method of fault positions gives long-term mean values, the Monte Carlo approach provides the complete distribution function of the SARFI-X index.

8.1 Introduction

In this dissertation, it has been shown that the method of fault positions is a powerful tool for assessing the expected dip performance of a network. Chapter 7 has proposed an analytic approach to overcome the problem of finding the right number of fault positions. An expression for the continuous-cumulative frequency-function of voltage dips is derived which leads to a more precise description of the expected performance of the network. System and site indices, in terms of residual voltage and frequency of occurrence (SARFI-X), can easily be evaluated by reading the corresponding values in the cumulative frequency function.

The simulation is certainly improved by considering the continuous-cumulative function, however it is very unlikely that the assessment predicts exactly the performance during a particular year. The method of fault positions as presented so far predicts long-term mean values and not the particular performance during a given year. In this sense, it is important to realize that the method relies on average values to determine long-term expected performance. Average fault rates and average mix of fault types calculated over a number of years are used to implement the method. Therefore, the result of the method of fault positions is a long-term average prediction of the annual performance. Moreover, the topology of the network and the generation schedule is usually considered unique.

This chapter illustrates the variability of dip performance from year-to-year. It also contrasts pseudo-monitoring results against the assessment based on the method of fault positions. This is particularly

important when the method of fault positions is used to answer sensitive customers' concerns about the expected number of dips and their characteristics.
In Section 8.2, the approach to randomness is rather informal. Arbitrary selected scenarios of faults are used to calculate the annual dip performance. In Section 8.3, Monte Carlo simulation approach is used to further illustrate the variability in annual dip performance. The method is also suggested to improve the assessment of the dip performance.

8.2 Creating Faults Scenarios

In order to compare the dip performance predicted by the method of fault positions against actual measurements, simulations are used to create pseudo-monitoring results corresponding to different fault scenarios.
Scenario technique is a well-known technique in management, economics and engineering. The use of the scenario technique derives from the need for strategies that play well across several possible futures. It arises from the impossibility of knowing precisely how the future will be, and that a good decision or strategy to adopt is one that plays well across several possible futures (scenarios). To find that good strategy, scenarios are created such that each scenario diverges from the others (Kees van der Heijden, 1997). Usually, names like pessimist, optimist and most likely are given to scenarios.
In our case, scenarios are specially constructed stories about the number of faults per year, the fault type distribution, and the fault location, each one modelling a distinct future network performance.
The approach to randomness in number of faults, fault positions and fault type is rather informal. Fault scenarios are chosen, to some extent, arbitrary.
In creating fault scenarios for the 87-bus system, the following aspects are taken into consideration:

1. The system contains 11651 km of line. On average, the fault rate equals 0.0134 faults/km-year.
2. The system contains 87 buses and the average fault rate at buses equals 0.08 faults/year.
3. On average, the type of faults distributes: 80% single-phase-to-ground (SLG), 5% phase-to-phase (LL), 10% two-phase-to-ground (LLG) and 5% three-phase (LLL).

It should be noted that the information given above is very limited to build scenarios. Nothing is said with respect to variability of the

number of faults per year. Obviously, some lines fail more than others and from year to year, the number of faults must be different. The fault type contribution is also given as a constant distribution, but it surely varies from line to line and from year to year. Therefore, a lot of engineering judgment and experience with the network is required to create fault scenarios.

Five scenarios are created based on an arbitrary basis. A unique topology of the network and a single generation schedule is used here to create scenarios, in practice however at least the minimum and maximum generation should be used.

The point 1 mentioned earlier, indicates that we may expect about 156 line faults per year. This number will most likely be different for a particular year, but the long-term annual-average should tend to 156 faults. Point 2 indicates that about 7 bus faults may occur in the system per year. Again, this number may be larger or smaller but the long-term average tends to 7 faults at buses per year. Point 3 indicates that the total number of faults (163 per year) may be distributed as follows 130 single-phase-to-ground faults (SLG), 8 phase-to-phase faults (LL), 16 two-phase-to-ground faults (LLG) and 9 three-phase faults (LLL).

From the previous simple analysis, the fault scenarios presented in Table 8.1 are created. Note that scenarios, though arbitrary created, keep the characteristics described in points 1, 2 and 3.

Table 8.1: Fault scenarios

Scenario	# faults	SLG	LL	LLG	LLL	Notes
Sc1	163	130	8	16	9	Faults at every line.
Sc2	120	114	0	6	0	Faults at the longest lines
Sc3	180	126	16	20	18	Randomly chosen
Sc4	183	160	1	19	3	Sector North mostly affected
Sc5	169	120	15	19	15	Sector South mostly affected
Average	163	130	8	16	9	

Scenario Sc1 consists of the long-term average number of faults (163). Faults are simulated at every line no matter the length of it. This may be unrealistic but it helps to see an unlikely scenario. Since

there are 164 lines, one line (the shortest) does not fail. At the shortest lines (less than 10 km), faults are simulated at the connecting buses.
Scenario Sc2 considers 120 faults simulated at the 120 longest lines. No fault is simulated at buses.
Scenario Sc3 considers 180 faults randomly chosen over the network, but no fault is simulated at buses.
Scenario Sc4 considers 183 faults. The North sector (upper part of the network) is mostly affected.
Scenario Sc5 considers 169 faults. The South sector is mostly affected.

8.2.1 Simulation Results

Figures 8.1 to 8.4 summarise the results of the simulations. All figures present the number of dips with residual voltage up to a given magnitude. The SARFI-X index can be directly read from the histograms.

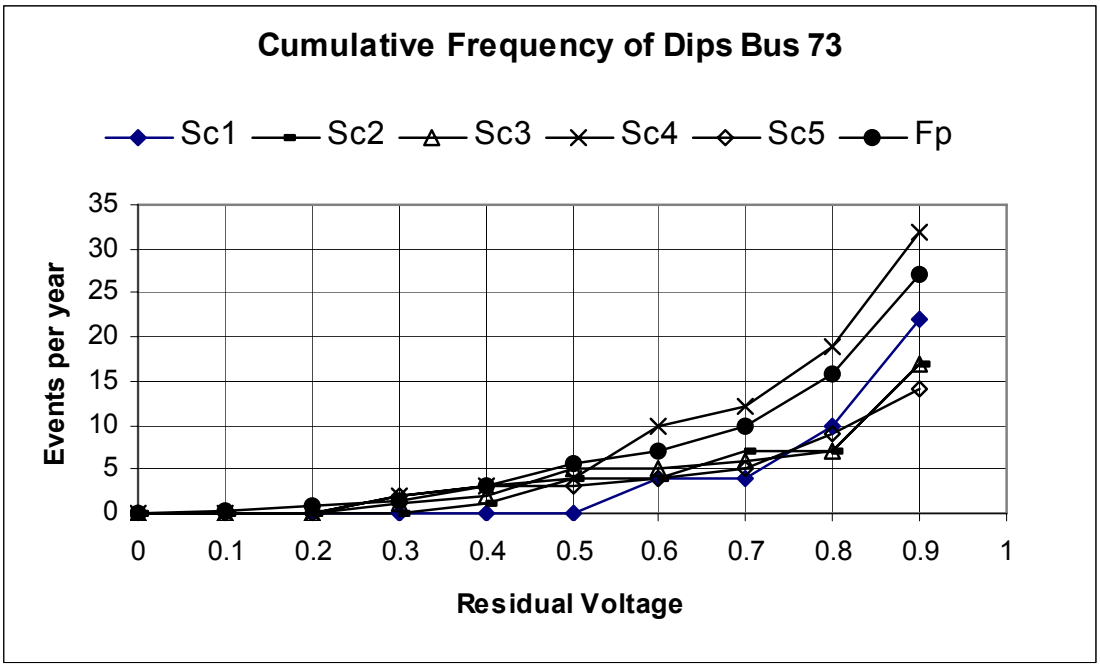

Figure 8.1: Cumulative dip frequency at bus 73 via method of fault positions and scenarios

Figure 8.1 shows the performance of bus 73 in the Sector North of the network, evaluated from the five scenarios (Sc). Results from the method of fault positions (Fp) are also shown. From the figure, it can be seen that the different scenarios lead to different performances. Due to the scale used to plot the data, it may seem that the difference is only important for shallow or less severe dips, however, a careful

examination of the data shows that important differences can also appear for severe dips. Table 8.2 shows the data corresponding to figure 8.1. An important difference can be seen between the method of fault positions and the pseudo measured performance. For example, the method of fault positions predicts seven events with residual voltage less than 0.6 p.u. whereas Sc4 gives ten events and Sc5 four events in the same range. Note also that a correction in the number of faults is not enough to adjust the assessment based on the method of fault positions. Scenario Sc5 considers a number of faults (169) similar to the number of expected faults in the method of fault positions (163.1), however the resulting difference between the assessments is important.

Table 8.2: Cumulative number of dips at bus 73

	Residual Voltage									
Bus 73	0	0.1	0.2	0.3	0.4	0.5	0.6	0.7	0.8	0.9
Sc1	0	0	0	0	0	0	4	4	10	22
Sc2	0	0	0	0	1	4	4	7	7	17
Sc3	0	0	0	1	2	5	5	6	7	17
Sc4	0	0	0	2	3	4	10	12	19	32
Sc5	0	0	0	2	3	3	4	5	9	14
Fp	0.0	0.4	0.8	1.5	3.2	5.8	7.0	9.8	15.9	27.1

An additional example is presented in Figure 8.2 and Table 8.3. This time, the assessment corresponds to bus 83 located in the Sector South of the network.

Again, it is easy to observe, graphically from Figure 8.2 and in detail by reading Table 8.3 that the assessment via the method of fault positions differs from the particular performance of a given scenario. For example, Scenario Sc2 considers 120 faults and the SARFI-0.7 is 6 events at bus 83. The scenario Sc3 considers 180 faults randomly spread and the resulting SARFI-0.7 is 5. The prediction based on the method of fault positions for the same index is 10.4 events. Again, a simple scaling of the number of faults would not be enough to adjust the method of fault positions to the actual performance. Even for scenarios that consider the same number of faults and fault type contribution as the method of fault positions, the difference may be important for a particular residual voltage magnitude.

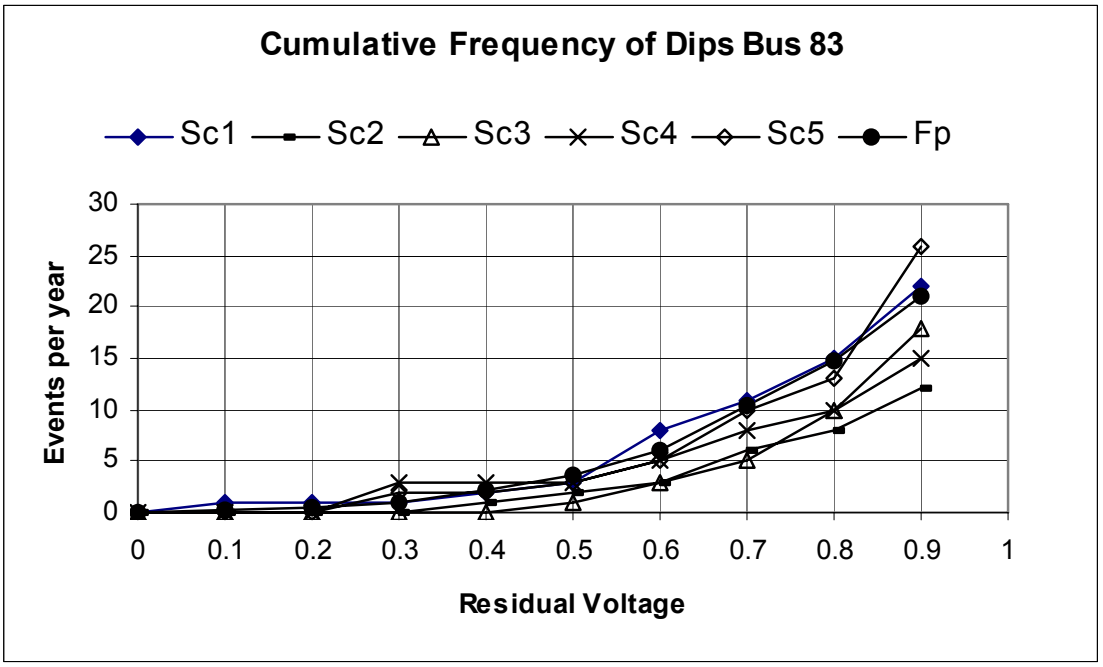

Figure 8.2: Cumulative dip frequency at bus 83 via method of fault positions and scenarios

Table 8.3: Cumulative number of dips at bus 83

	Residual Voltage									
Bus 83	0	0.1	0.2	0.3	0.4	0.5	0.6	0.7	0.8	0.9
Sc1	0	1	1	1	2	3	8	11	15	22
Sc2	0	0	0	0	1	2	3	6	8	12
Sc3	0	0	0	0	0	1	3	5	10	18
Sc4	0	0	0	3	3	3	5	8	10	15
Sc5	0	0	0	2	2	3	5	10	13	26
Fp	0.0	0.3	0.6	1.0	2.1	3.6	6.1	10.4	14.8	21.1

Not only actual site performance will differ from the stochastic assessment via the method of fault positions, but also the predicted system indices. Figure 8.3 shows the system performance based on the average number of dips within each magnitude range. Similarly, Figure 8.4 shows the 95 percentile of the number of events within each magnitude bin, for the five scenarios and for the prediction via the method of fault positions. Note that the system performance corresponding to every scenario is better than the prediction via the method of fault positions. The average number of events per bus and year is overestimated by the method of fault positions with respect to the measured performance. This can be explained from the fact that in the scenarios, faults are simulated in the middle of lines whereas in

the method of faults positions faults are simulated every 15 km of line.

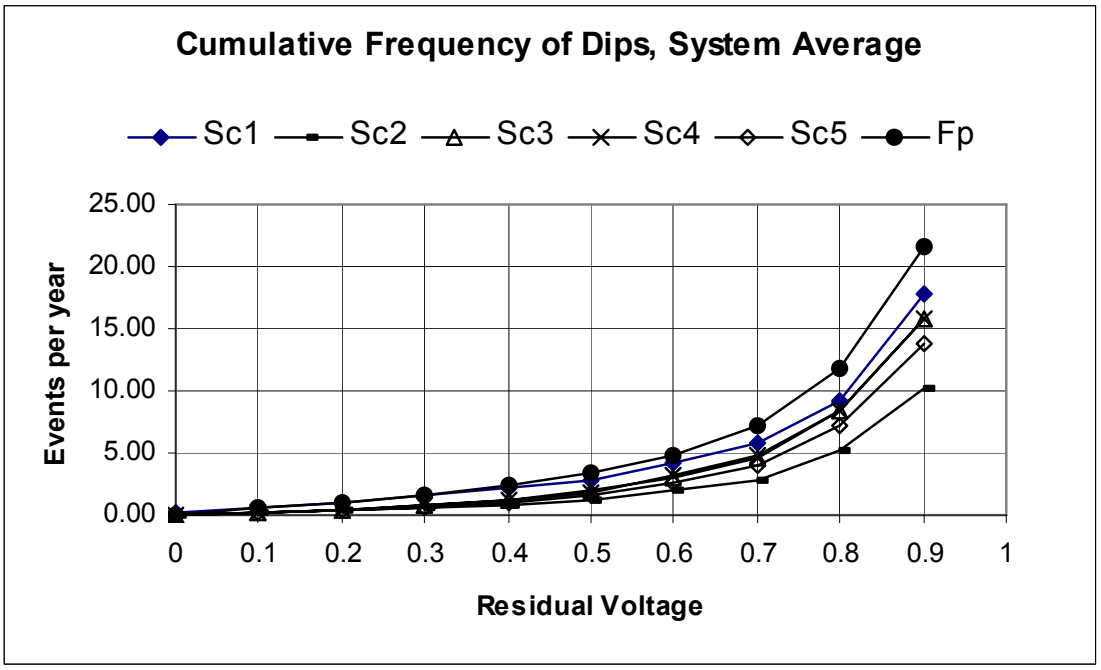

Figure 8.3: Average cumulative frequency of dips

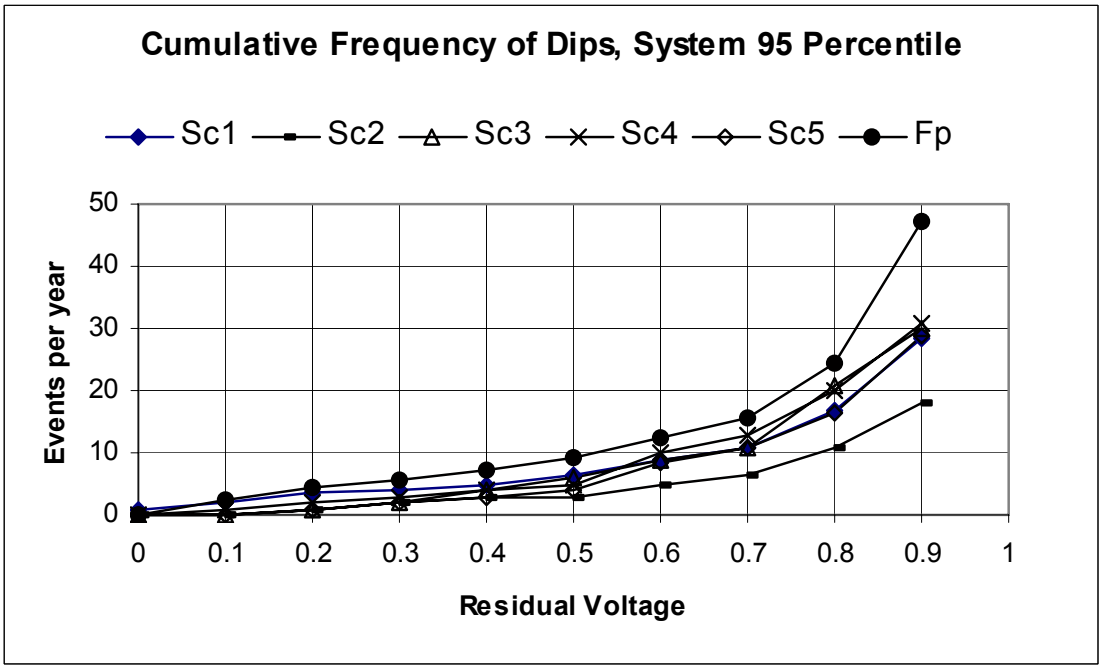

Figure 8.4: Cumulative frequency of 95 percentile dips

In conclusion, the method of fault positions based on average fault rate predicts long-term average performance. Therefore, comparisons against actual performance require some sort of adjustment. Such adjustment may include the number of faults, the contribution of fault

types, the generation scheduling, and/or the number of fault positions per line. In Chapter 9, a method for Voltage Dip Estimation that allows this adjustment is proposed. To stress the need for such adjustment, the next section presents a Monte Carlo simulation approach to the method of fault positions for stochastic assessment of voltage dips.

8.3 A Monte Carlo Simulation Approach

It has been reported (Sikes, 2000) that divergences are found when the prediction based on the method of fault positions is compared against actual measurements. The method of fault positions gives only long-term average or mean values. Mean values are extremely useful indices of the system performance against which the sensitivity of equipment can be compared. However, mean values do not provide any information about the variability of the index. On the other hand the frequency distribution of the index provides the complete spectrum of possible outcomes from which mean values can easily be calculated. It also provides important information on significant outcomes that although they occur very infrequently can have serious negative effects on the sensitive load.

In order to obtain the distribution function of the SARFI-X index a Monte Carlo simulation approach is used in this section. The main idea of the Monte Carlo approach is the creation of simulated data taking into account as much uncertainty as possible. In other words, a fictitious long-term historical behaviour is created so that the variability of several factors can be taken into account.

Monte Carlo simulation is a powerful numerical method for exploring and solving mathematically formulated problems by modelling random variables. In general, it provides approximate solutions to a problem by performing statistical sampling experiments on a computer. For this reason it is also known as the method of statistical testing. Since Monte Carlo simulation provides approximate solutions, the error is never zero but it reduces with an increasing number of simulations. In simple words, a computer program that carries out a single random test is developed (the assessment of one single scenario). The test is repeated a number of times, each test being independent from the others, and the results of all the conducted tests are then averaged (Suhir, 1997).

The key factor in Monte Carlo simulation is the use of random numbers (pseudo random strictly speaking) to model the behaviour of stochastic variables (Ross, 1996). Instead of using just the average

value to model uncertain variables, the complete distribution function is used to describe their behaviour. This of course requires more information regarding the historical performance of the system.

8.3.1 Algorithm

The algorithm implemented can be summarised as follows.
1.- Set an observation bus.
2.- Set a simulation time in years.
3.- For each element (line or bus) generate a random number and convert it into time-to-fault according to the probability distribution function of the time-to-fault of the element. Calculate the cumulative time.
4.- For each fault at lines, generate a random number and convert it into fault position according to the probability distribution function of this parameter.
5.- For each fault, generate a random number and convert it into fault type (SLG, LL, LLG, LLL) according to the probability distribution function of the fault type.
6.- Calculate the residual voltage at the bus of interest caused by the resulting fault by using the analytic approach of Chapter 7.
7.- If cumulative time is less than the simulation time, go to 3.
8.- Output results.

Simulation parameters:
The simulation parameters are only illustrative and others can easily be implemented.

- The mean-time-to-fault is taken as the reciprocal of the fault rate (0.0134 faults/year-km). For example, a 100 km long line has a mean-time-to-fault of 0.74 years. This parameter is assumed normally distributed with a mean value given by the above calculation and a standard deviation equal to 30% of the mean value.
- The fault position is assumed uniformly distributed along each line.
- The fault type distribution is assumed: 80% single-phase-to-ground (SLG), 5% phase-to-phase (LL), 10% phase-to-phase-to-ground (LLG), and 5% three-phase faults (LLL).

8.3.2 Simulation results

The amount of data generated by Monte Carlo simulation is huge. Only a very small sample of the results is presented here. On the other hand, simulation results are not intended to be analysed individually or by scenario but in batch so that general patterns can be detected.

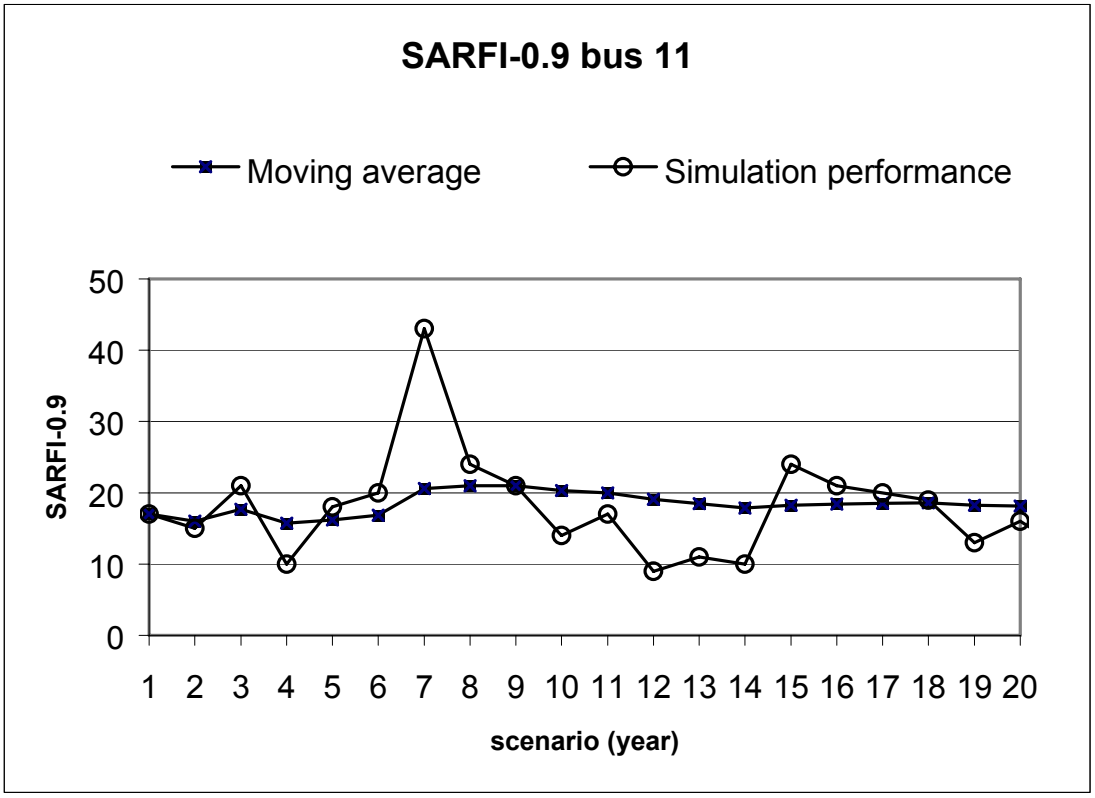

Figure 8.5: SARFI-0.9 for bus 11 based on 20 Monte Carlo simulations

Figure 8.5 shows a characteristic behaviour of Monte Carlo simulations. The system average rms variation frequency index at bus 11 estimated via Monte Carlo simulation is shown. The SARFI-0.9 resulting for each simulation (annual scenario) and the average SARFI-0.9 calculated over the cumulative number of simulations are shown. Although the SARFI-0.9 corresponding to each scenario is volatile, the average is rather stable. After some initial oscillations, the average SARFI-0.9 at bus 11 seems to converge to a value about 19. This of course depends on the variability of the random parameters. In particular, we have taken a rather small standard deviation for the mean-time-to-fault (30%). A larger standard deviation will require more simulations to show convergence to a given value.

The outcomes of the Monte Carlo approach are average values calculated over different sample sizes. Therefore, the outcome of the

Monte Carlo method distributes normally and the error in the estimate can be calculated building a confidence interval for the actual mean value (Bollen, 1999).
In order to evaluate how accurate the last average value (19.2) in Figure 8.5 is, the sample standard deviation *s* is used to build a confidence interval for the expected SARFI-0.9. The standard deviation *s* corresponding to the *n*=20 simulations in Figure 8.5 is about 1.6 from which the 95% confidence interval results:

$$\text{SARFI-0.9} \in \left[\overline{X} - \frac{2.08 \cdot s}{\sqrt{n}}, \overline{X} + \frac{2.08 \cdot s}{\sqrt{n}} \right] \tag{8.1a}$$

$$\text{SARFI-0.9} \in [18.5, 19.9] \tag{8.1b}$$

where $\overline{X}$ is the average SARFI-0.9 calculated over the 20 previous values and 2.08 is the critical value corresponding to a 95% of confidence of the standard *t*-distributed variable.
Equation 8.1 shows that the error can be reduced by increasing the number of simulations.
Table 8.4 shows the SARFI-0.9, SARFI-0.7 and SARFI-0.6 at buses 11 and 67 obtained via the method of fault positions and 1000 Monte Carlo simulations. Symmetrical and unsymmetrical faults are considered. Note that more severe events (SARFI-06) require more Monte Carlo simulations to be described with accuracy. Table 8.4 validates the Monte Carlo approach but does not illustrate the advantage with respect to the method of fault positions.

Table 8.4: SARFI at buses 11 and 67 via fault positions and Monte Carlo simulation.

	Fault positions from Appendix B		Monte Carlo 1000 simulations	
	Bus 11	Bus 67	Bus 11	Bus 67
SARFI-0.9	19.8	19.2	20.6	21.5
SARFI-0.7	11.6	2.3	12.3	2.4
SARFI-0.6	8.8	0.4	9.1	1.4

In order to illustrate the advantage of the Monte Carlo approach, suppose that a sensitive customer wants to evaluate the need for expensive mitigation devices and has required the stochastic assessment at two buses of the systems, as shown in Table 8.4. The information regarding the SARFI-X contained in Table 8.4 will certainly help to evaluate such a need, however the absence of a variability indicator may lead to wrong decisions.

Figure 8.6 shows the frequency distribution and cumulative frequency of 1000 Monte Carlo simulations for the SARFI-0.7 of bus 11. The average SARFI-0.7 is about 12 events per year meaning that we may expect 12 events per year with a residual voltage less than 0.7 p.u. This histogram, however, provides more information. It can be seen that in 50 % of the cases the SARFI-0.7 exceeds the average value 12. More severe but less probable scenarios can easily be evaluated. For example, in more than 20% of the cases the SARFI-0.7 is larger than 16 events meaning that more than 16 dips with residual voltage less than 0.7 p.u. may be observed at the load. If the sensitive customer is planning the industrial plant for a lifetime of 30 years, then the sensitive load may be exposed to a SARFI-0.7 greater than 16 for 6.6 years. To a customer looking into a long-term business, such information is relevant and therefore it should be provided in order to minimize the customer damage costs caused by voltage dips.

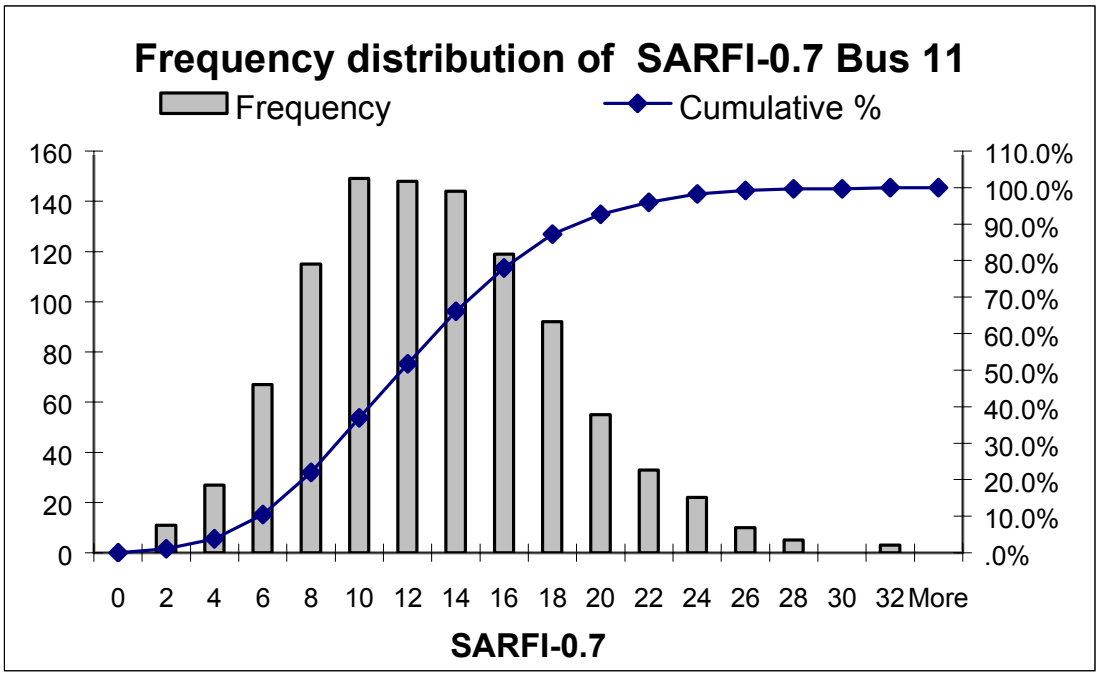

Figure 8.6: Expected frequency of SARFI-0.7 at bus 11

9 Voltage Dip (Sag) Estimation

This chapter presents a method to estimate the dip performance at buses not being monitored. By finding fault positions likely to cause the residual voltages seen at some buses through power quality meters (limited monitoring program) and performing stochastic assessment around triggered monitors, the dip performance at non-monitored buses can be estimated. The chapter extends the application of the optimal monitoring program. The algorithms for practical implementation are presented and tested in our 87-bus test system showing the applicability of the proposed method.

9.1 Introduction

Chapter 1 shows that voltage dips must be treated as a compatibility problem between sensitive loads and power supply. Such an approach requires a suitable description of the sensitivity or vulnerability of the load to voltage dips. It also requires a description of the performance of the network in terms of the expected number of events and their characteristics. In general, the performance of the network is described by means of a two-dimensional description of the event: 1) minimum residual voltage during the event and 2) time during which the rms voltage stays below the voltage threshold. The performance of the network is described using tables or histograms where the number of events up to a given magnitude is presented. Duration has not been considered in this work but it may be as relevant as magnitude. The information needed to complete such tables or histograms can be obtained either from stochastic assessment of voltage dips or power quality monitoring programs.

The method of fault positions for stochastic assessment of voltage dips has been used in this work to assess the dip performance of an existing network. It is shown that, if long-term average fault rates are used to model the likelihood of faults, the results of the method of fault positions cannot be compared against monitoring results of a particular year, unless adjustments are introduced in the predicted results. Since such adjustments are only possible once the information regarding uncertain variables is available, the method of fault positions can only be applied for long-term assessment.

Monitoring of power supply is well accepted by engineers as a means of profiling power quality. However it is expensive, it requires long metering periods, and a large number of meters when the aim is to characterize an entire transmission system. Ideally, a full monitoring

program should be used to characterize the performance of an entire system, i.e. every load bus should be monitored. Such a monitoring program is not economically justifiable and only a limited set of buses can be chosen for a monitoring program. This has led to the optimal monitoring program proposed in Chapter 6. The monitoring program searches for the minimum number of monitor positions that guarantee observability of the entire network. In this chapter, results from the optimal monitoring program are extended to buses not being monitored. This issue is presented here as voltage dip (or sag) estimation method (VSE), a technique that allows assigning voltage dips and their frequency of occurrence to buses not being monitored.

9.2 Voltage Dip Estimation: Conceptualisation

Voltage dip or sag estimation (VSE) is a method that makes it possible to estimate the rate of occurrence of voltage dips as well as the magnitude of them at non-monitored buses. The estimation is based on deterministic and stochastic data: 1) the triggering of at least one power quality meter, 2) the magnitude of the residual voltages seen at the triggered monitors, and 3) the rate of occurrence of faults likely to be the cause of the dip seen at the triggered monitors. Therefore, VSE is based on a limited monitoring program.

Voltage sag estimation does not aim at finding the exact fault position that causes the residual voltages seen at triggered power quality meters, but a good estimation of the voltage dip at buses not being monitored. Since tables and histograms usually present the performance of the network in discrete bins for the residual voltages, some error in the estimation can be accepted.

Not all buses of a transmission system can be equipped with power quality meters or monitors, therefore the estimation must rely on an incomplete set of simultaneous voltage dip measurements and the rate of occurrence of potential fault positions to find good candidates for the actual fault position.

Voltage dip estimation differs from the traditional state estimation as applied in transmission systems, where more measurements than state variables are available. Such a state estimation method calculates state variables (voltage magnitude and angle) at every bus of the system by minimizing the error between the mathematical solutions of load flow equations and the redundant set of measurements (Abur, 2004).

9.3 Monitoring for Voltage Dip Estimation

In order to perform voltage dip estimation, a monitoring program must be designed so that at least one of the following objectives can be accomplished:

1. The monitoring program should allow the estimation of one unique residual voltage per fault event at each non-monitored bus. This is a magnitude estimation of the voltage dip on an event per event basis.
2. The monitoring program should allow an approximate calculation of the number of dips within given bins of residual voltage at buses not being monitored. This is an estimation of frequency of occurrence based on a long monitoring period.

Note that the second objective can be obtained from the first one. Objective 1 is more demanding because it requires estimating the resulting residual voltage at each non-monitored bus by using information from some monitors. It seems reasonable that in order to improve the estimation of the residual voltage at a non-monitored bus, more monitors should provide information. Objective 2 aims at finding the number of dip events within given magnitude bins. Such bins are discrete ranges and hence an error in the estimation of the magnitude can be accepted.

Both objectives require information from power quality meters. Such information is given in terms of residual voltage, duration, time of occurrence, and simultaneity of meters' triggering. Both objectives need a monitoring program that guarantees that the set of meters sees any potential fault, i.e. a monitoring program that covers the entire network. A minimum monitoring program that makes sure that every potential fault is seen by at least b monitors can be designed by solving the optimisation problem introduced in Chapter 6 and repeated here for convenience.

$$
\begin{aligned}
&Min(x_1 + x_2 + ...x_n) \\
&S.t.: \\
&mra_{11} \cdot x_1 + mra_{21} \cdot x_2 + ...mra_{n1} \cdot x_n \geq b_1 \\
&mra_{12} \cdot x_1 + mra_{22} \cdot x_2 + ...mra_{n2} \cdot x_n \geq b_2 \\
&: \\
&mra_{1Fp} \cdot x_1 + mra_{2Fp} \cdot x_2 + ...mra_{nFp} \cdot x_n \geq b_{Fp}
\end{aligned}
\tag{9.1}
$$

Equation (9.1) describes the integer optimisation problem that guarantees that a given number of power quality meters trigger on every fault. Recall that mra_{kj} is the (k,j) entry of the monitor reach

area matrix that describes the area of the network seen by each power quality meter. Recall also that x_i is i-th element of the binary decision variable **X**. Vector **b** defines the level of redundancy of the monitoring program. A particular value of b_i indicates that a fault at the fault position i will trigger at least b_i monitors. The level of redundancy of the monitoring program is the minimum number of monitors that is guaranteed to trigger on the occurrence of any fault.

$$\text{Level of Redundancy} = \min(b_i) \forall \, \text{i} = 1,...Fp \tag{9.2}$$

A minimum monitoring program is a monitoring program that makes sure that every fault triggers at least one monitor. In other words, a minimum monitoring program is the particular arrangement of monitors described by **X** that solves (9.1) for b_i=1. Such a monitor program for our test system is presented in Chapter 6, however only three-phase faults at buses of the system are used to determine the monitor reach areas. In this chapter, single-phase-to-ground faults are used to design monitoring programs of different levels of redundancy, which are then used to perform VSE. In absence of actual measurements, simulated ones are used to contrast results from the VSE against pseudo-measurements.

9.4 Magnitude Approach to Voltage Dip Estimation

VSE can be performed on an event per event basis to estimate one and only one residual voltage per fault at each non-monitored bus. For this purpose, two or more power quality meters should trigger on every fault, i.e. the level of redundancy of the monitoring program should be larger than one. The multiple triggering of monitors (redundancy) allows the VSE method to find good candidates for the actual fault position, which in turns makes it possible to calculate residual voltages at non-monitored buses. Depending on the level of redundancy of the monitoring program, this procedure may lead to several fault positions, and therefore to different residual voltages to be assigned to non-monitored buses for each fault. A probabilistic approach is suggested to estimate one residual voltage per fault. The residual voltage is estimated by the weighted average residual voltage, calculated by taking the relative rate of occurrence of probable fault positions as weighting factors. Section 9.6 presents the mathematical formulation.

9.5 Frequency Approach to Voltage Dip Estimation

The method for VSE can also be applied on a long-period monitoring basis, one year or longer. The aim of the frequency approach is to estimate the number of dips within given ranges of magnitude after a long-period monitoring program. At least, a minimum monitoring program should be used to perform frequency voltage dip estimation. In addition to the information given by the triggering of at least one meter, the fault rate of each most probable fault position is used to assign a per-unit rate of occurrence to each resulting dip. Instead of calculating one residual voltage at each non-monitored bus, the frequency approach adjusts the stochastic assessment around monitored buses by considering all most probable residual voltages and their per-unit rate of occurrence. The VSE will select fault positions conforming to the information of triggered (and non triggered) monitors and following the rate of occurrence of potential fault positions. The magnitude approach estimates a unique residual voltage per fault at every non-monitored bus, whereas the frequency approach assigns all probable residual voltages to each non-monitored bus according to the corrected fault rate of potential fault positions.

9.6 Mathematical Formulation and Algorithm for Voltage Dip Estimation

The VSE method presented here is mathematically formulated by using the concept of "monitor reach area" (MRA), presented in Chapter 6 and a key part of the optimisation problem in (9.1).

In Chapter 3, it was shown that given a system configuration and generation level, the residual voltage is largely determined by the fault location (which determines the z_{mp} and z_{pp}). If the values of residual voltages are known in advance, potential fault positions can be determined based on the measured residual voltage at a certain number of buses (Galijasevic, 2002).

To illustrate this, consider the hypothetical network diagram shown in Figure 9.1 where the 0.9 p.u. and 0.5 p.u. monitor reach area of bus 8 are shown. Inside the $MRA_{8(0.9)}$ eight buses (B1, B2, B3, B4, B5, B6, B7 and M8) and six particular fault positions (fp1, fp2, fp3, fp4, fp5 and fp6) are depicted. Each fault position represents a limited length of line, and hence a fraction of the fault rate is assigned to each fault position. Note that in practice the monitor reach area is not a circle but any polygonal figure. It may even be the union of disjoint sets.

This however does not affect the mathematical formulation presented below.

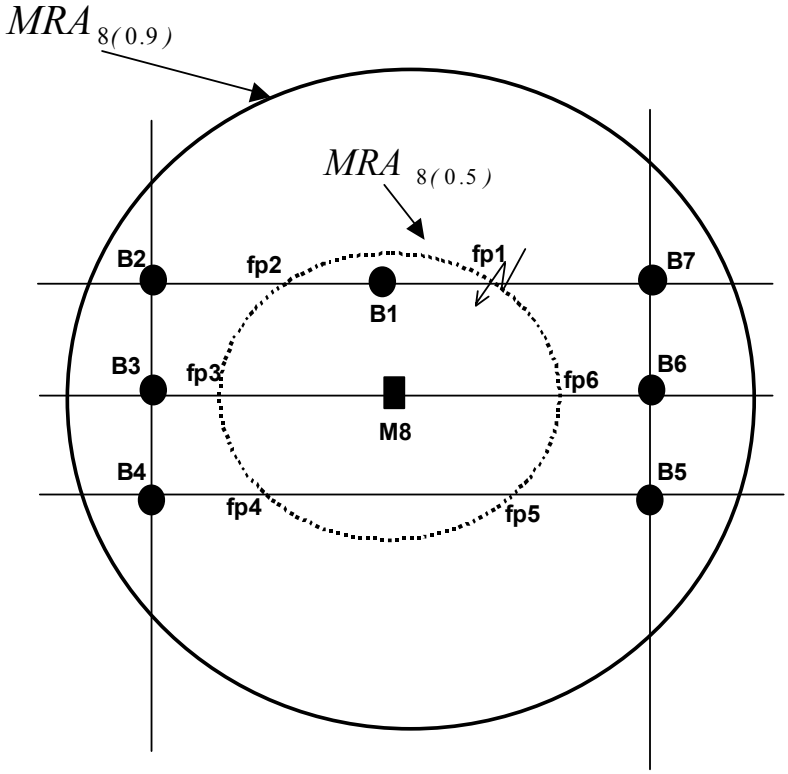

Figure 9.1: A simplified diagram of a part of a transmission network. It shows eight buses (B1, B2, B3, B4, B5, B6, B7 *and* M8) *and six potential fault positions* (fp1, fp2, fp3, fp4, fp5 *and* fp6) *likely to cause the residual voltage 0.5 p. u. seen at* M8.

Suppose that a fault at an unknown position triggers monitor M8 and that a residual voltage 0.5 p.u. (± error) is recorded. From this limited information, a number of potential fault positions can be found (fp1, fp2, fp3, fp4, fp5, and fp6). Let PFP be the set of potential fault positions. Then, PFP is formed by the indices corresponding to fault positions in the areas of the network where faults will result in a residual voltage similar to 0.5 p.u. at bus 8. Elements of PFP can be identified by looking at the monitor-reach-area set of bus 8 and selecting the fault positions that result in a residual voltage similar to the value recorded by M8. Mathematically:

$$\text{fpi} \in \text{PFP} \Leftrightarrow \begin{cases} \text{fpi} \in MRA_{8(0.9)} \\ v_{8\,\text{fpi}} = 0.5 \pm \zeta \end{cases}, \forall \ \text{i} \tag{9.3}$$

where fpi is the i-th fault position, $MRA_{8(0.9)}$ is the monitor-reach-area set of bus 8, v_{8fpi} is the residual voltage at bus 8 during a fault at the fault position i, and ζ is a tolerance factor that takes into account

uncertainties and errors, namely measurements, fault impedance, system configuration, etc.
The information given by only one monitor does not allow finding the exact fault position, however a unique residual voltage at each non-monitored bus can stochastically be estimated.

9.6.1 Magnitude Voltage Dip Estimation

In the magnitude or event per event approach, only one residual voltage is assigned at each non-monitored bus per fault. The proposal is to calculate a weighed average residual voltage, the average calculated from all potential residual voltages, using the per-unit fault rate of potential fault positions as weighing factors. For example, (9.4) gives the unique residual voltage to be assigned to a general bus k of the hypothetical network in Figure 9.1.

$$v_{k*} = \frac{1}{\sum_1^6 \lambda_{fpi}} \sum_{i=1}^{6} \lambda_{fpi} \cdot v_{k\ fpi} \tag{9.4}$$

where v_{k*} is the estimated residual voltage at bus k caused by a fault at an unknown fault position *, λ_{fpi} is the long-term fault rate of fault position i, and v_{kfpi} is the residual voltage at bus k caused by a fault at position i.
Note that the application of (9.4) to bus M8 results in $v_{8*} = 0.5$ p.u., the value recorded at bus 8.

9.6.2 Frequency Voltage Dip Estimation

In the frequency approach, we do not demand one residual voltage per fault but an adjustment of the method of fault position around triggered monitors, which in turn results in the correction of the assessment of non-monitored buses. All potential fault positions and their per-unit fault-rate are used to adjust the stochastic assessment via the method of fault positions. This is particularly true if the estimation is performed after a long monitoring period (one year at least). In that case, the residual voltage at bus 8 ($0.5\pm\zeta$) will have been observed a number of times, allowing the selection of fault positions from the PFP set according to the pattern of fault occurrence. For example, if the residual voltage $0.5\pm\zeta$ have been seen 12 times during the monitoring program and the six potential fault positions are equally likely, then every fault position should be selected 2 times to calculate residual voltage at non-monitored buses. It is however unlikely to end up with an integer number of dips at

non-monitored buses, but this is just the result of the adjustment of the estimation based on the method of fault positions.
Table 9.1 shows the six residual voltages and their rate of occurrence at bus 2 for the hypothetical case illustrated in Figure 9.1. The summation over the relative rate of occurrence equals one. The residual voltages are different because some fault positions are near bus 2 whereas others are far from it. In order to build the cumulative histogram of dips, the residual voltages in Table 9.1 need to be grouped according to some selected magnitude ranges, in the way described in Chapter 4. Note that the application of such a procedure to bus M8 will result in one event with residual voltage 0.5 p.u., the value recorded at that bus.

Table 9.1: VSE for bus 2, frequency approach

VSE frequency approach for bus 2	
Residual Voltage	Rate of occurrence
$v_{2\,fp1}$	$\lambda_{fp1} \Big/ \sum_{i=1}^{6} \lambda_{fpi}$
$v_{2\,fp2}$	$\lambda_{fp2} \Big/ \sum_{i=1}^{6} \lambda_{fpi}$
$v_{2\,fp3}$	$\lambda_{fp3} \Big/ \sum_{i=1}^{6} \lambda_{fpi}$
$v_{2\,fp4}$	$\lambda_{fp4} \Big/ \sum_{i=1}^{6} \lambda_{fpi}$
$v_{2\,fp5}$	$\lambda_{fp5} \Big/ \sum_{i=1}^{6} \lambda_{fpi}$
$v_{2\,fp6}$	$\lambda_{fp6} \Big/ \sum_{i=1}^{6} \lambda_{fpi}$

9.6.3 Using Redundancy to Improve the Estimation

A minimum monitoring program is one that guarantees that every fault is seen at least by one power quality meter. However, some faults may trigger two or more meters. In such a case, the number of potential fault positions can be reduced by intersecting the monitor-reach-area sets of triggered monitors, improving the estimation of residual voltages. This improvement in the estimation can also be achieved by increasing the level of redundancy of the monitoring program, i.e. designing a monitoring program that solves (9.1) for b_i greater than one.

An example of overlapping monitor reach areas is shown in Figure 9.2, where an extended view of Figure 9.1 is presented. An additional power quality meter at bus 11 is shown. The same fault (at an unknown position) triggers both monitors M8 and M11 with residual voltages 0.5 p.u. and 0.7 p.u. respectively. Counting on the information given by M11 the number of probable fault positions can be reduced. The set of potential fault positions can now be found from (9.5).

$$\text{fpi} \in \text{PFP} \Leftrightarrow \begin{cases} \text{fpi} \in \left\{ MRA_{8(0.9)} \cap MRA_{11(0.9)} \right\} \\ v_{8\text{fpi}} = 0.5 \pm \zeta \wedge v_{11\text{fpi}} = 0.7 \pm \zeta \end{cases}, \forall \text{ i} \qquad (9.5)$$

Two fault positions, fp1 and fp6, would be elements of PFP if (9.5) were applied to our hypothetical example. A higher level of redundancy can be treated in a similar way reducing the number of elements in PFP.

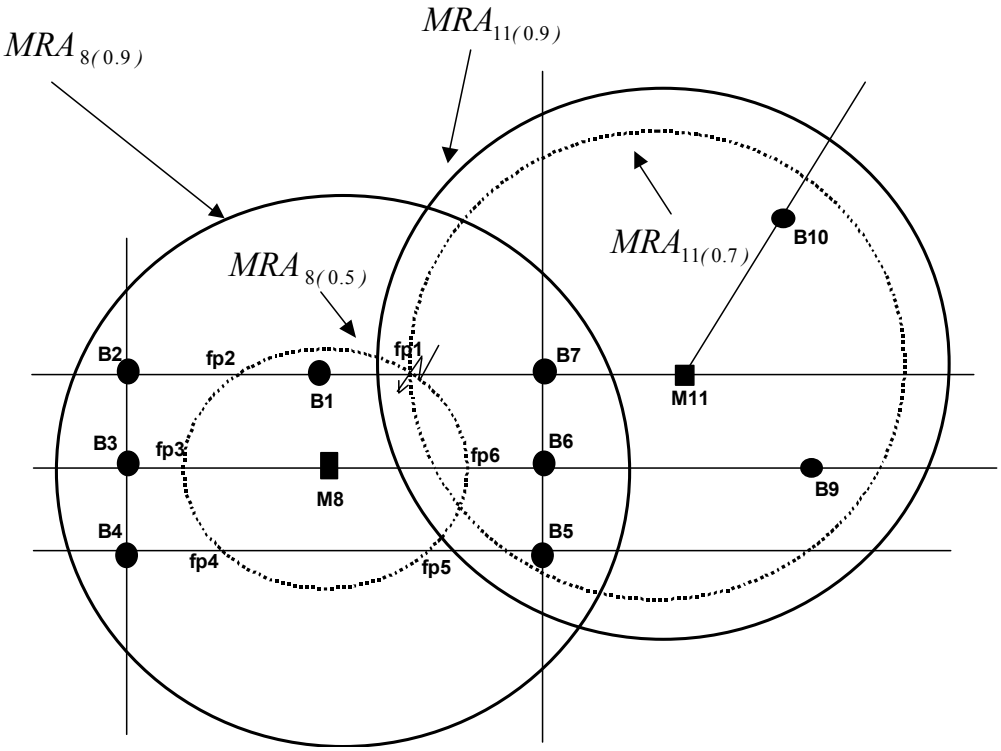

Figure 9.2: A simplified diagram of part of a transmission network. It shows eleven buses (B1, B2, B3, B4, B5, B6, B7, M8, B9, B10 *and* M11) *and six fault positions* (fp1, fp2, fp3, fp4, fp5 *and* fp6)*. Monitor reach areas corresponding to monitors installed at bus 8 and 11 are shown. Fault positions inside the intersection of* MRA_8 *and* MRA_{11} *are more likely to be the cause of the dips monitored at buses 8 and 11.*

9.6.4 Using Information from Non-triggered Monitors to Improve the Estimation

Non-triggered monitors can also provide useful information regarding the location of potential faults. If a monitor has not triggered then the fault must have occurred outside the monitor reach area of the non-triggered monitor.

The set of potential fault positions PFP is formed of fault positions in the intersection of monitor reach areas of triggered meters. However, some of these fault positions may be part of the monitor reach area of a non-triggered meter and therefore can be excluded from the PFP set improving the estimation of residual voltages.

Let NTM be the set of indices pointing to non-triggered monitor. Let MPFP be the set of most probable fault positions, a subset of PFP that excludes fault positions that would trigger meters in NTM. Then:

$$\text{fpi} \in \text{MPFP} \Leftrightarrow \begin{cases} \text{fpi} \in \text{PFP} \\ v_{k\text{fpi}} > 0.9 \pm \zeta \end{cases}, \forall\, \text{i} \wedge \forall\, \text{k} \in \text{NTM} \tag{9.6}$$

Equation (9.6) says that elements of MPFP are those fault positions in PFP for which the residual voltage at non-triggered monitors is larger than the voltage threshold of non-triggered meters, 0.9 p.u. in this case.

In practice, several fault positions will satisfy the conditions to remain in the set MPFP because all the uncertainties, and because lines can be divided into an infinite number of segments. Therefore, the approaches introduced above have to be used to calculate residual voltages and frequency of occurrence. In other words, equation (9.4) should be applied to elements in MPFP to perform magnitude VSE and Table 9.1 to perform frequency VSE.

9.6.5 Algorithm for Voltage Dip Estimation VSE

Once the results from the monitoring program are available, the following algorithm can be used to perform VSE.

1) Create the set of potential fault positions PFP, i.e. find the intersection of MRA of triggered monitors, and select fault positions that lead to a similar residual voltages at triggered monitors, see (9.5).

2) Find the set of most probable fault positions MPFP, i.e. exclude from the set PFP fault positions that would trigger non-triggered meters, see (9.6).

3) Magnitude VSE: calculate one residual voltage per fault for each non-monitored bus. In other words, calculate the weighted average

residual voltage using the per-unit fault rate of most probable fault positions. See (9.4).
4) Frequency VSE: calculate all residual voltages corresponding to the most probable fault positions MPFP and the corresponding per-unit fault rate. See Table 9.1.
5) Calculate site statistics and system statistics.

9.7 VSE: Simulations and Results

The test network introduced in Chapter 5 is used to implement the voltage dip estimation methods: magnitude VSE and frequency VSE.

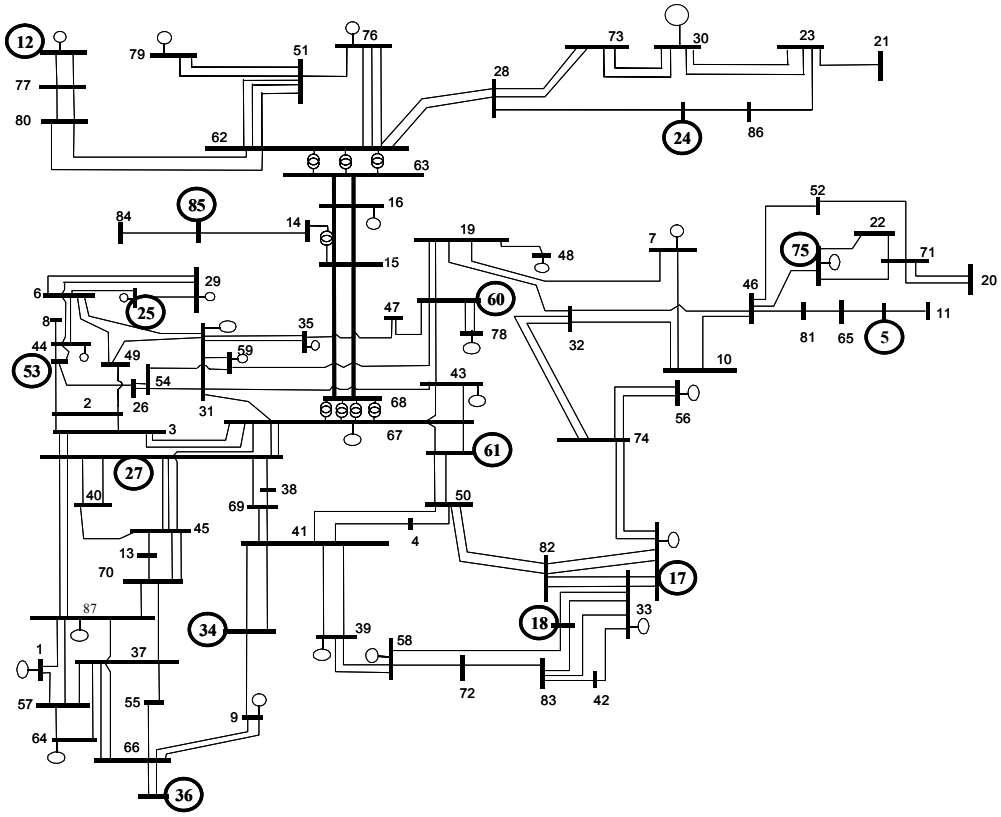

Figure 9.3: A reduced model of the National Interconnected System of Colombia at 230 and 500 kV. A minimum monitoring program is also shown. Monitored buses are shown encircled.

Figure 9.3 shows the test system and a minimum-monitoring program. Encircled buses are meter locations obtained by solving the optimisation problem (9.1). The MRA matrix is built using 781 single-phase-to-ground fault positions, 81 at buses and 694 at lines. Fault positions along lines are located in such a way that two adjacent fault positions are no further apart than 15 km. In order to obtain a minimum-monitoring program the level of redundancy **b** is set to 1. This minimum-monitoring program is referred to as MP1, it requires

14 meters and guarantees that any single-phase-to-ground fault triggers at least one monitor.
An additional monitoring program is designed by incrementing the level of redundancy **b** to 2. This monitoring program is referred to as MP2. MP2 is a monitoring program that requires 33 meters and guarantees that any fault triggers at least two meters. The following buses are monitored in MP2: 9-11-14-17-18-20-21-22-23-26-27-29-34-36-38-41-43-44-46-48-50-54-55-56-60-61-62-63-67-72-77-78-85.

9.7.1 Monitoring results

The purpose of this chapter is the development of a method for voltage dip estimation, VSE. Basic algorithms have been presented in previous sections. In order to test the proposed method, the monitoring programs described above MP1, MP2 should be implemented and one-year measurement results should be used to run the algorithm. In absence of actual measurements, simulated ones are used to test the methods. This, on the other hand, allows comparing estimated results with pseudo measured ones. Randomly chosen faults (single-phase-to-ground) are simulated on lines and buses, and the residual voltages at every bus are saved for comparison against the values obtained using the VSE methods. Residual voltages calculated by traditional short circuit theory are referred to as full monitoring results, whereas residual voltages estimated by using the proposed VSE are referred to as VSE on MP1 (or MP2) values.

9.7.2 Magnitude VSE

Figure 9.4 shows the residual voltage at each bus of the system when a single-phase-to-ground fault occurs at bus 81, which is located near the monitored bus 5, in a rather weak area of the network. VSE on MP1 refers to residual voltages estimated by using the proposed magnitude approach. Full monitoring refers to pseudo-measured residual voltages.
The minimum-monitoring program (MP1 with 14 monitors) has been used to estimate residual voltages at each one of the 73 non-monitored buses, as shown in Figure 9.4. MP1 is a monitoring program that ensures that any single-phase-to-ground fault triggers at least one meter. The fault at bus 81 only triggers the meter at bus 5, and this is the minimum information that can be obtained from the monitoring program MP1. Therefore, the fault at bus 81 can be seen as the worst case for magnitude estimation based on MP1. Figure 9.4

shows that the occurrence of a dip, i.e. the occurrence of a residual voltage less than 0.9 is well identified by the magnitude estimation. However, some dips are overestimated in terms of magnitude severity.

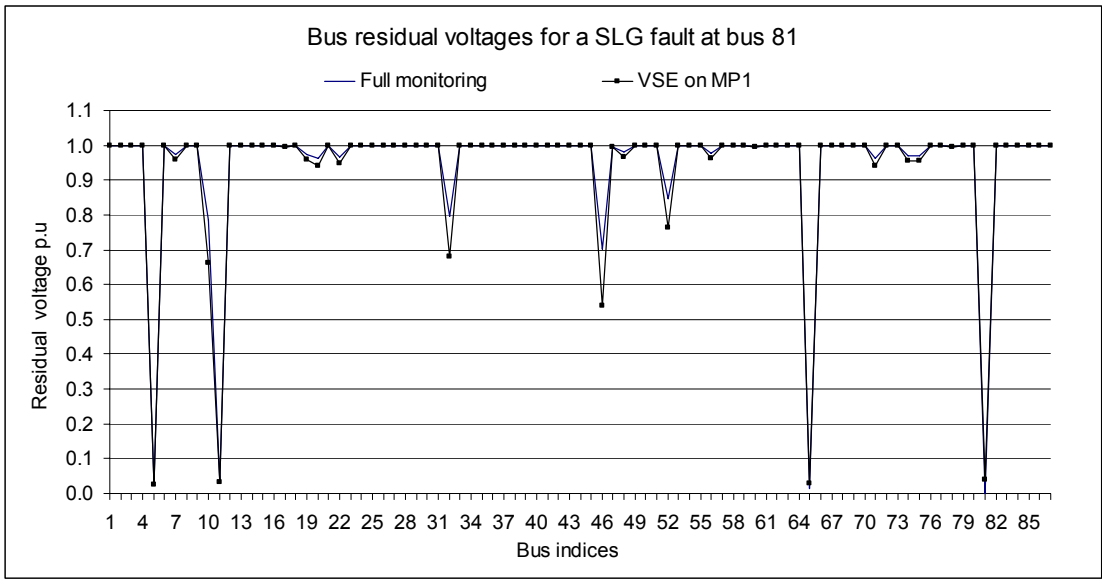

Figure 9.4: Residual voltages at all buses caused by a fault at bus 81. "VSE on MP1" refers to values estimated via magnitude VSE using 14 monitors located according to MP1. "Full monitoring" refers to values obtained via conventional short-circuit theory.

MP1 is a minimum-monitoring program, however some faults trigger more than one meter. The multiple triggering of monitors provides useful information to select the most probable fault positions, and to improve the estimation of residual voltages, as the following example illustrates.

Figure 9.5 shows pseudo measured and estimated dips caused by a fault at bus 67, one of the strongest buses. MP1 is used to monitor the network. Four meters are triggered by the fault, providing information to estimate the residual voltages. The estimation is so good that estimated voltages cannot be distinguished from measured ones. Figure 9.5 shows the best case for MP1 in the sense that information from four monitors is used to find the most probable fault position.

Figures 9.4 and 9.5 show two extreme cases for the performance of the magnitude estimation method. It can be presumed that the method will also perform reasonably well for any other fault at a bus of the system. However, faults at buses are less probable than faults at lines. The next example tests the proposed algorithm for a fault at a particular line.

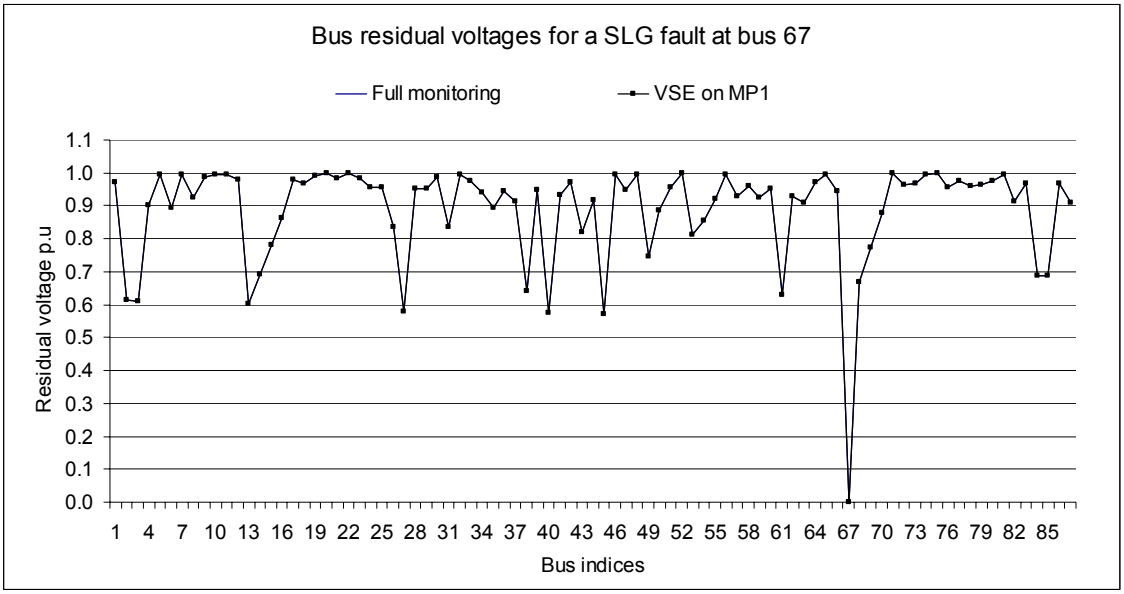

Figure 9.5: Residual voltages at all buses of the test system during a single-phase-to-ground fault at bus 67.

Figure 9.6 shows the measured and estimated residual voltages at buses of the system during a single-phase-to-ground fault on the line connecting buses 61 and 67. This is a much less severe fault than the previous case and only four buses would be exposed to a residual voltage less than 0.9 p.u., but only one would provide information through a power quality meter (bus 61). The estimation is again good enough for statistical purposes.

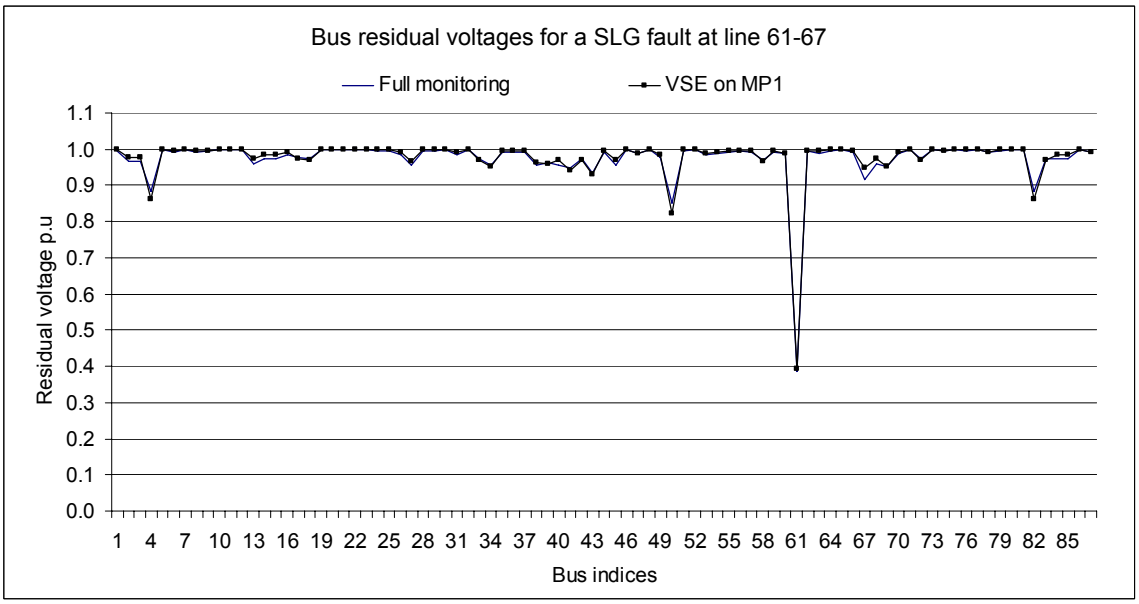

Figure 9.6: Residual voltages at all buses of the test system during a single-phase-to-ground fault at the line between buses 61 and 67

9.7.3 Frequency VSE

The frequency estimation approach provides long-term statistics and not per fault analysis. Given a fault, the frequency estimation method gives several residual voltages to be assigned to each non-monitored bus. Therefore, the results of such an approach cannot be presented as in the case of magnitude estimation where only one residual voltage is calculated per fault. It is however, illustrative to see the residual voltages and rate of occurrence calculated for one particular event. Let us consider the fault at bus 81 and the monitoring program MP1 again.
Table 9.2 shows the residual voltages at two particular buses (10 and 46) during a single-phase-to-ground fault at bus 81. It also shows the measured residual voltage (in bold font) and the per-unit rate of occurrence for each potential fault position. Note that the summation over the rate of occurrence is one.

Table 9.2:Frequency VSE at buses 10 and 46, based on MP1for a SLG at bus 81

Residual voltages in p.u.		λ p.u.
Bus 46	Bus 10	
0.7017	**0.7856**	
0.040	0.294	0.063
0.842	0.887	0.178
0.080	0.305	0.063
0.705	0.788	0.092
0.704	0.787	0.092
0.700	0.784	0.164
0.703	0.786	0.092
0.702	0.786	0.164
0.702	0.786	0.092
Sum		1.0

The magnitude VSE method uses the values of residual voltages shown in Table 9.2 and their rate of occurrence to calculate one and only one weighed average value using equation (9.4). Frequency VSE takes into account all the potential values to derive long-term statistics.

The pseudo-measured residual voltages at buses 10 and 46 caused by the fault at bus 81 are shown in the first data row of Table 9.2 in bold font. It can be seen that most of the calculated values are similar to the pseudo measured ones.
Values in Table 9.2 need to be grouped in magnitude bins to build the cumulative frequency histogram. Table 9.3 shows the same data of Table 9.2 but now grouped according to the magnitude bins. Figure 9.7 shows the expected cumulative number of dips at buses 10 and 46 caused by a fault at bus 81.

Table 9.3: Cumulative frequency of dips at buses 10 and 46, based on MP1 for a SLG fault at bus 81

Cumulative frequency		Residual Voltage bins
Bus 46	Bus 10	
0.127	0.000	0.1
0.127	0.000	0.2
0.127	0.063	0.3
0.127	0.127	0.4
0.127	0.127	0.5
0.127	0.127	0.6
0.290	0.127	0.7
0.822	0.822	0.8
1	1	0.9
1	1	1

Looking at Figure 9.7 one may get the impression that a number of different events have been seen at buses 10 and 46 for a unique fault at bus 81. However, this is only the result of the adjustment of the method of fault positions. Figure 9.7 shows that the number of dips with residual voltage less than 0.9 is one showing that this is only one fault that is stochastically treated in order to handle the uncertainty regarding the actual fault position.
The frequency VSE has been applied to a single event to illustrate the method. However, the main objective of VSE is the statistical description of dip performance of buses not being monitored after a long monitoring period. As it will be illustrated in the next section, both the magnitude and frequency VSE can be used to accomplish that task.

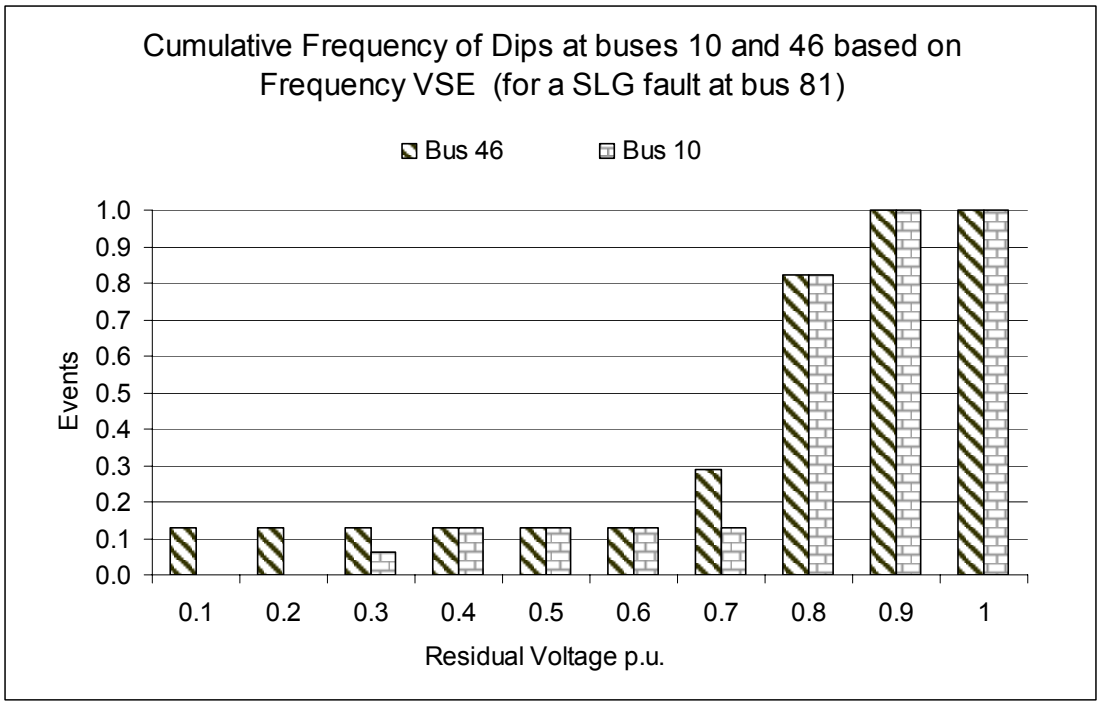

Figure 9.7: Frequency VSE at buses 10 and 46 for a SLG fault at bus 81, based on MP1

9.7.4 Site and System Statistics

If a full monitoring program was run over a long period, we would be able to describe the performance of every bus using the cumulative histograms of number of dips (site statistics). We would also be able to calculate system statistics based on the performance of all the buses. Also duration, phase angle jump and other dip's characteristics would be available for statistics. However, full monitoring programs are unfeasible because of costs and only a limited set of buses can be monitored. The optimal monitoring program proposed in Chapter 6 allows minimising the number of monitors, subject to the coverage of the entire network. Results from the monitoring program can then be used to perform magnitude VSE and frequency VSE allowing the extension of meter results to non-monitored buses. Different levels of redundancy can be demanded from the monitoring programs to improve the estimated residual voltages.

In this section, we compare statistics from a hypothetical full monitoring program against the results from magnitude and frequency estimation based on MP1 and MP2. One hundred and eighty (180) single-phase-to-ground faults are randomly spread over the network to simulate an arbitrary year. Residual voltages are determined by using traditional short circuit calculation for all buses, and site and system statistics derived from such data. These residual voltages are

referred to as monitored results. Residual voltages are also calculated via magnitude VSE and frequency VSE, and statistics are derived for monitored and non-monitored buses.
We begin contrasting the monitored performance versus the estimated performance at bus 5. Bus 5 is part of the monitoring program MP1 and hence there is no need to perform estimation at this bus, however this analysis illustrates the effect of the type of estimation on the statistics.

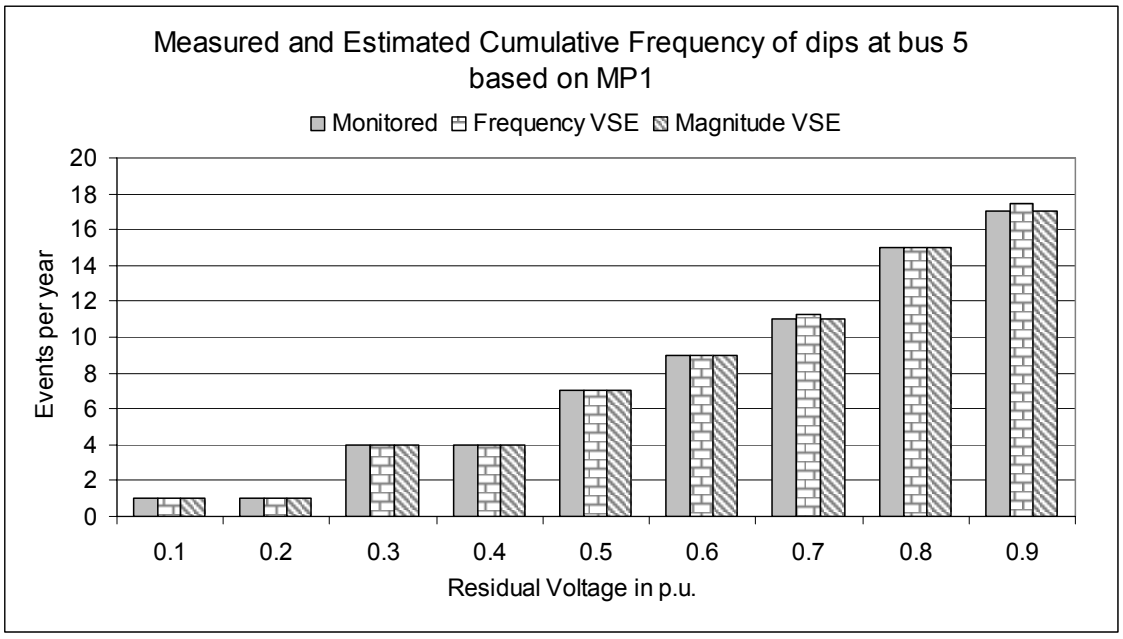

Figure 9.8 Site statistics at the monitored bus 5 from monitoring, frequency VSE and magnitude VSE.

Figure 9.8 shows dip statistics at the monitored bus 5, obtained via monitoring program MP1, frequency VSE and magnitude VSE. The minimum monitoring program MP1 is used to perform the estimation. Both magnitude and frequency VSE work well at bus 5. Note that magnitude estimation gives an integer number of dips whereas frequency estimation may give a real number. Since this is a monitored bus, the magnitude estimation matches exactly with the monitoring results, but this will unlikely happen in the case of a non-monitored bus.
The discrepancy between estimation and measurement depends on the bins chosen to collect events. Frequency estimation seems to slightly overestimate the number of dips with residual voltage less than 0.9 p.u., but such overestimation comes from a more severe bin. The overestimation appears first within the 0 to 0.7 p.u. bin, is then corrected in 0 to 0.8 p.u. and appears again in the 0 to 0.9 p.u. The

small discrepancy between frequency estimation and measurement is caused by the adjustment of the method of fault positions around the monitored bus 5 and it would be smaller for a longer monitoring program. This adjustment does not have any impact on the estimated performance of the monitored bus 5, but it does help to stochastically estimate the statistics at non-monitored buses which otherwise would not be assessed.

Figure 9.9 shows dip statistics at bus 32, a bus not included in MP1. The estimation works reasonably well for both approaches although not as well as for a monitored bus. Since this is a non-monitored bus, the magnitude estimation does not match the measurements. Frequency estimation underestimates the number of more severe events but predicts well the shallow dips.

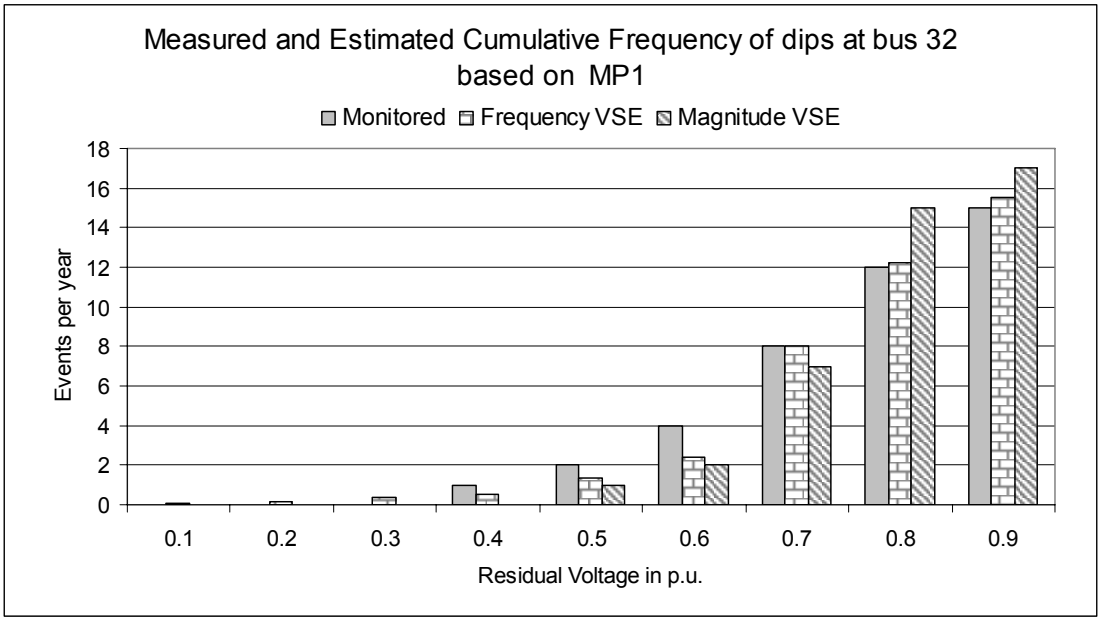

Figure 9.9: Site statistics at the non-monitored bus 32 from pseudo monitoring, frequency VSE and magnitude VSE.

It is worth highlighting that only 14 meters are being used to profile the dip performance of the 87-bus network. If the cost of the monitoring program were proportional to the number of monitoring points the monitoring program for VSE would cost about 16% of the cost of a full monitoring program and the results are still comparable. This may justify the small errors between estimation and measurements.

Another example is presented in Figure 9.10 where one of the strongest buses of the system is assessed. Both estimation methods give a good estimation of events with residual voltage less than 0.8

p.u., but seem to fail in finding the number of events in the 0.8 to 0.9 p.u. bin.

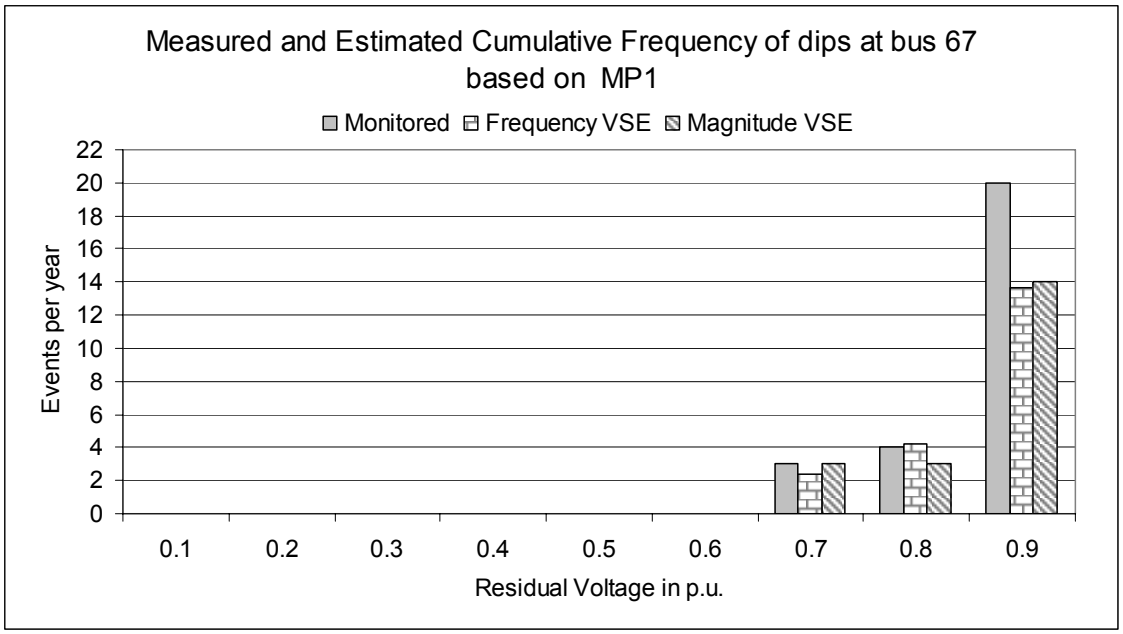

Figure 9.10: Site statistics at bus 67 from pseudo monitoring, frequency VSE and magnitude VSE

The rather large discrepancy between estimation and measurement of shallow dips can be explained as follows: Bus 67 is a strong bus and hence most of the dips seen at bus 67 are shallow dips caused by faults far from this bus. On the other hand, the chances that a fault that causes a shallow dip at bus 67 triggers more than one monitor are rather low, because the monitoring program is solved to minimize the number of meters with a voltage threshold set at 0.9 p.u. Moreover, the 0.9 p.u. monitor reach area of a meter at bus 67 is large which means that several potential fault positions will be part of the set of MPFP.

System statistics are important for regulatory purposes. System statistics are calculated in Chapter 5 using the performance of the entire system obtained via the stochastic assessment. In Chapter 6, system indices, SARFI-X, are calculated based on the optimal monitoring program. Here, system statistics will be calculated based on frequency and magnitude estimation.

Figure 9.11 shows the average performance of the system. Monitored and estimated performances are shown. Both estimation approaches succeed in describing the average system performance. The discrepancies between actual performance and estimation that appear

at site level (Figure 9.9 and 9.10) seem to compensate each other, resulting in good estimation of system indices.

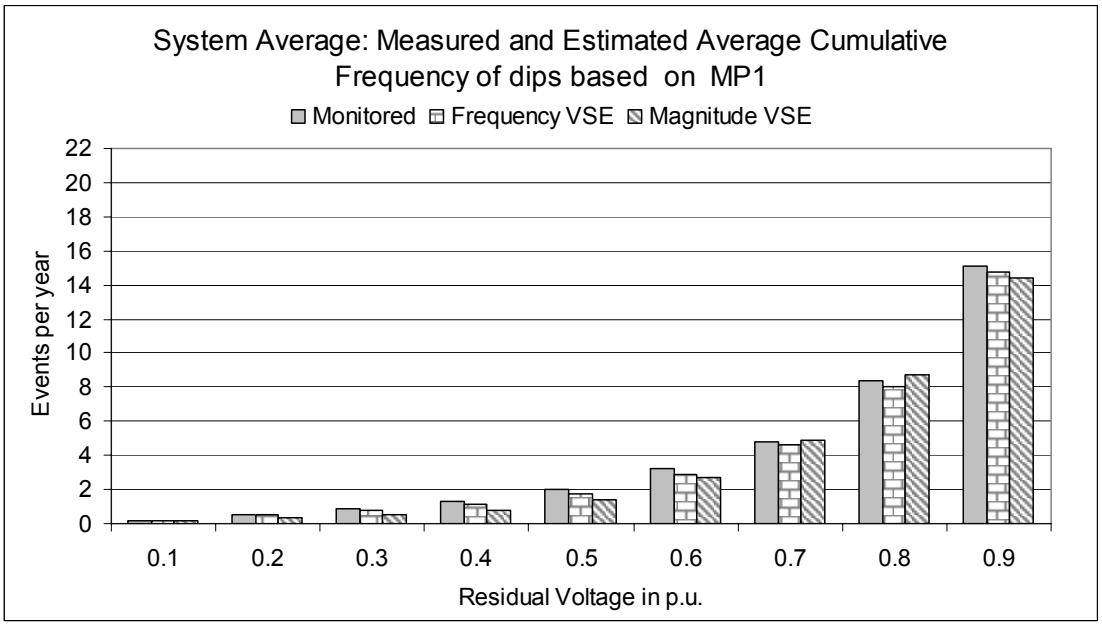

Figure 9.11: System statistics in terms of average performance, from pseudo monitoring, frequency VSE and magnitude VSE

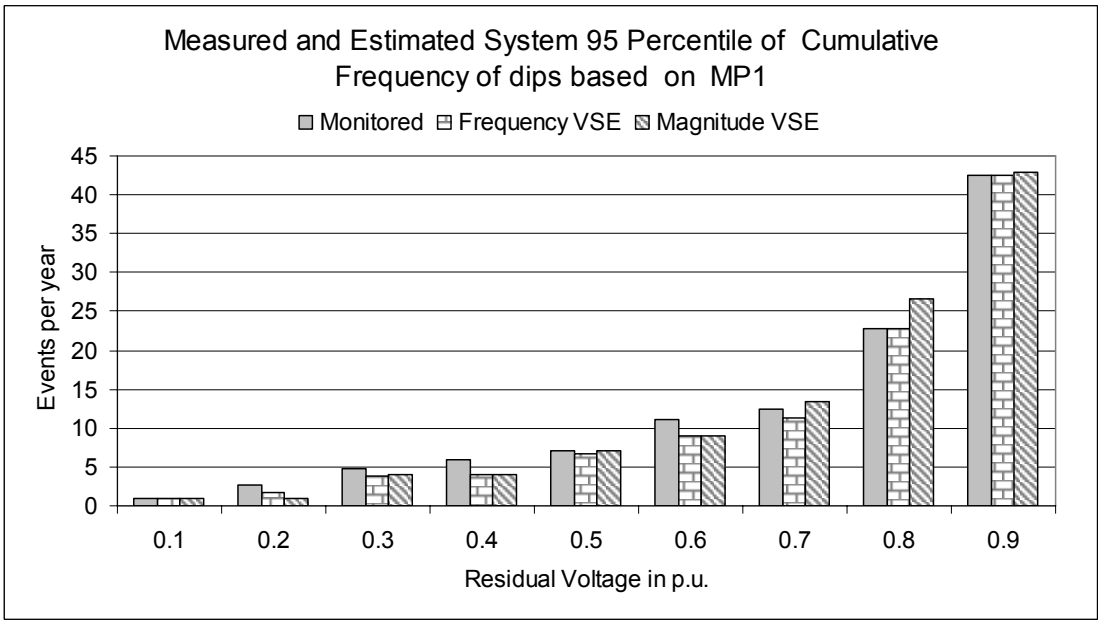

Figure 9.12: System statistics in terms of 95 percentile among buses, from pseudo monitoring, frequency VSE and magnitude VSE

Figure 9.12 shows the 95 percentile of buses performance. The 95 percentile is also well identified by both estimation methods, although small discrepancies are clear for some particular dip magnitudes.
The frequency VSE seems more accurate in predicting system statistics for both severe and shallow dips.

The minimum-monitoring program MP1 of 14 monitors has been used to describe the performance of the 87-bus system. In some cases, a better estimate of performance at non-monitored buses may be demanded. In order to improve the estimate we could decide to run a monitoring program with a level of redundancy equal to 2, meaning that every fault will trip at least two meters.
The monitoring program MP2 ensures that every single-phase-to-ground fault triggers at least two monitors. It considers 33 monitors at buses 9-11-14-17-18-20-21-22-23-26-27-29-34-36-38-41-43-44-46-48-50-54-55-56-60-61-62-63-67-72-77-78-85.
Figure 9.13 shows results of voltage dip estimation at the non-monitored bus 15. Magnitude and frequency estimation based on MP1 and MP2, together with the measured performance are shown. Both estimation methods based on MP2 match exactly the measured performance for dips with residual voltage above 0.7 p.u. In other words, the SARFI-0.7, SARFI-0.8 and SARFI-0.9 can be estimated with good accuracy. The estimate of the most severe dips is also improved by using MP2.

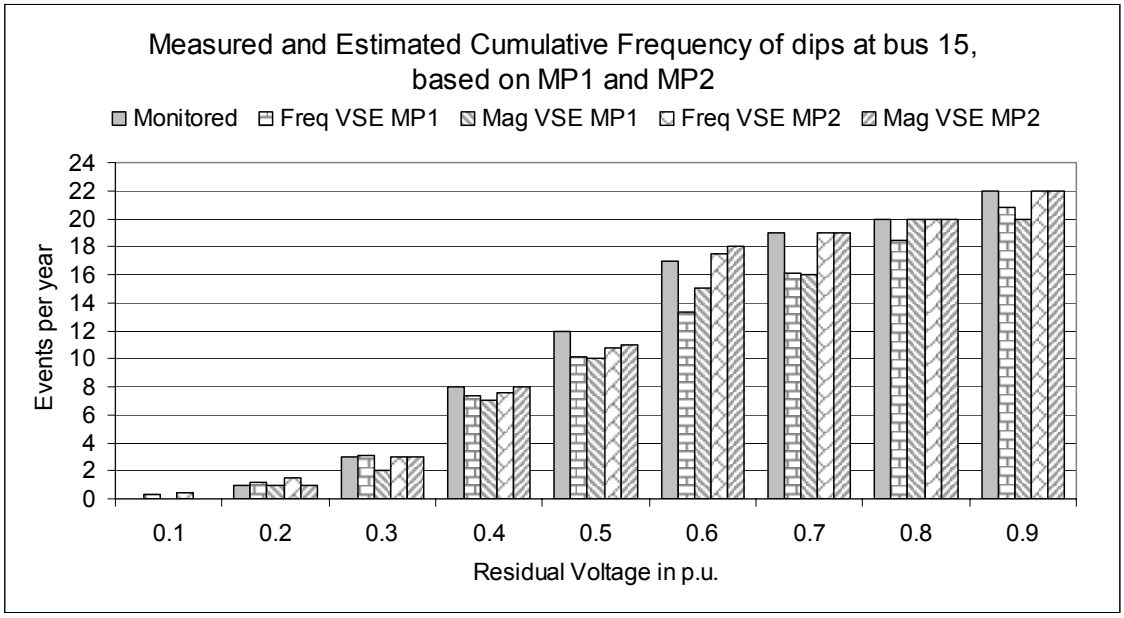

Figure 9.13: Site statistics at bus 15 from pseudo monitoring, frequency VSE and magnitude VSE

A final example is presented in Figure 9.14 that shows the performance of bus 32 calculated via magnitude and frequency VSE based on MP2. As in the previous case, the less severe dips are estimated with surprising accuracy.
It should be noted that MP2 is a monitoring program designed to guarantee that every fault is seen by at least two monitors. It may

however not be necessary to guarantee that every potential fault triggers two monitors, but just some of them. In such a case, some monitors can be added to MP1 to improve the estimate of buses of interest.

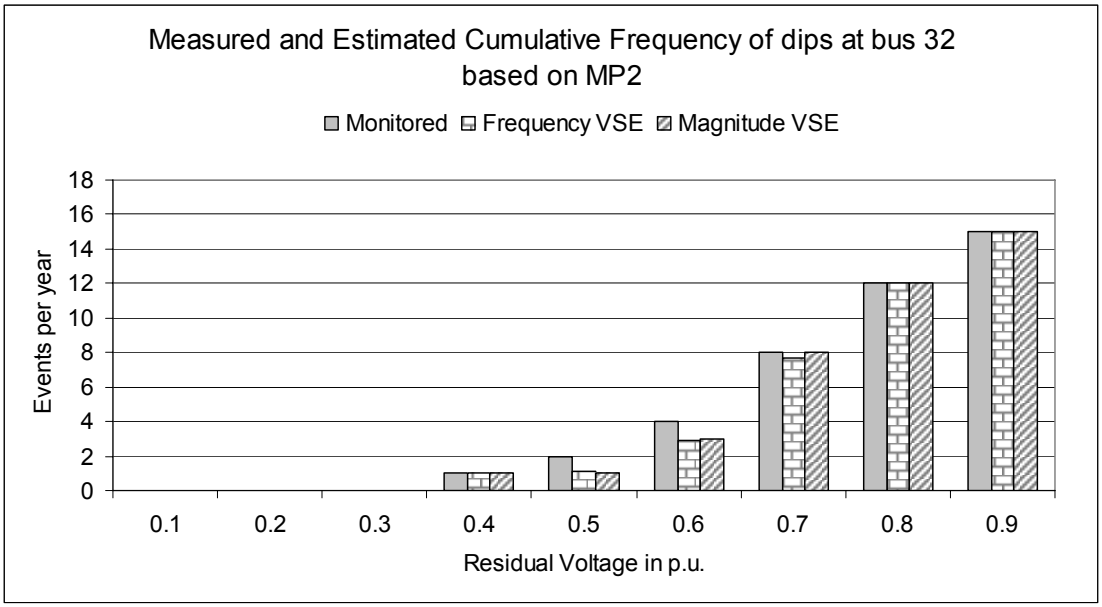

Figure 9.14: Site statistics at bus 32 from pseudo monitoring, frequency VSE and magnitude VSE

9.7.5 Additional uncertainties

The method for voltage dip estimation presented above has handled one of the uncertainties that a dip generation process presents, fault position. Only single-phase-to-ground faults, one network topology and a single generation schedule have been considered. In practice, however, faults may be other than single-phase-to-ground faults. They may include a fault impedance, and may occur during different generation schedules or different topologies of the network leading to different values of residual voltages. All these uncertainties can be handled in a similar way. This will certainly increase the computational effort and memory requirement but the estimates will still be good enough for statistics. For example if different fault types are to be considered, then the potential fault positions set PFP will not only include single-phase-to-ground faults but also three-phase, phase-to-phase and two-phase-to-ground faults likely to be the cause of the residual voltage, recorded at the triggered monitors. Since the residual voltage caused by a three-phase fault is notoriously different than the one caused by an unsymmetrical fault, the intersection of monitor reach areas of triggered monitors will discard some fault

types. Elements of the most probable fault positions set MPFP will then be two-dimensional elements containing information about fault positions and fault type of each potential fault. The corresponding per-unit rate of occurrence will have to be calculated from the fault rate of lines and fault type distribution. Moreover, not only one phase voltage should be used, but the three phase voltages together to determine the most probable fault positions.

Different generating scheduling can also be stochastically treated, for which purpose the participation of each potential generation level should be described by its probability. Suppose that a number of levels of generation and four types of faults are considered. Then the MPFP set will contain three-dimensional elements each one indicating fault position, generation level and fault type of the probable fault position. Again, the fault rate of each one of these most probable fault positions will have to be calculated from the participation of each fault position, generation level and fault type.

10 Conclusions and Future Work

This chapter presents the main conclusions derived from the present work. The chapter begins with a summary of the dissertation. Future work is also discussed.

10.1 Summary

Voltage dips or sags are short duration reductions in rms voltage. The main cause of voltage dips is the occurrence of remote faults in transmission and distribution systems. Many sensitive loads cannot discriminate between momentary interruptions and dips, and therefore a single voltage dip may stop an entire industrial plant. Sensitive loads may include process control equipment, contactors, motors, and power drives.

Voltage dips, as other power quality issues, need to be treated as a compatibility problem between the sensitive device and the supply. This compatibility approach needs the characterisation of the disturbance level present in the network and the description of the immunity of the device. Device immunity is usually described by means of a voltage tolerance curve like CBEMA or ITIC.

Characterisation of an individual dip event is done mainly by its magnitude and duration. The residual voltage during the event gives the magnitude of the dip. Other characteristics can be recognised, as phase angle jump and point on wave.

Gathering the events that occur at a given bus of a system during a period, usually one year, allows the characterisation of an individual site. Characterisation of individual sites is needed in order to decide about mitigation methods. Usually a table containing magnitudes and durations of dips is used for site description.

Characterisation of the system performance is achieved by deriving some statistics of individual site events. Typical statistics are the average and 95 percentile of dips for a given magnitude. System characterisation is needed for objective performance indicators in the deregulated electricity markets.

Statistics on dips and their characteristics can be obtained by monitoring power supply. This solution is time demanding and costly. There are also some drawbacks in using monitoring for dip characterisation, especially for individual sites. Monitoring for individual site characterisation requires a very long monitoring period and the results cannot be directly applied to other sites.

When used for characterisation of system performance, several monitors need to be installed, ideally one at each load bus. When only a limited number of monitors is available an optimal selection of locations needs to be made in order to get the best description of the system performance.

An alternative to monitoring, for dip characterisation, is stochastic assessment of voltage dips. Stochastic assessment of dips does not exclude monitoring because measurements are needed to calibrate the stochastic methods.

In this dissertation, the method of fault positions is implemented and simulations are performed in a large transmission system. The bus impedance matrix is used to describe the system. The impedance matrix is built considering actual buses as well as fictitious nodes along lines to simulate faults. Symmetrical and unsymmetrical faults are simulated in the system and the resulting residual voltages are stored in a matrix called dip-matrix. The dip-matrix contains the residual voltages at each existing bus caused by faults everywhere in the system. When dealing with unsymmetrical faults the lowest residual phase-to-ground voltage is chosen to characterise the magnitude of the dip.

The dip-matrix is combined with the fault rate of each fault position to obtain the stochastic assessment of voltage dips. It is shown that the generation level has an important effect on the result of the method. Since generator machine impedances become shunt parameters at the buses, they definitely affect the impedance matrix and therefore the residual voltages during faults in the system. The effect of the number of fault positions on the assessment is also studied. It is shown that an increase in the number of fault positions improves the assessment. An analytic approach to the method of fault positions is proposed solving the problem of choosing the suitable number of fault positions. The cumulative frequency of dips is described as a continuous function of the residual voltage. The results are compared with the traditional approach to validate the new method.

The method of fault positions is a powerful tool for planning and operational activities. It is shown that the method of fault position gives long-term expected results. Since the method uses long-term average fault rates to model the likelihood of faults, results are for such a temporal frame and comparison with the performance of a particular year needs adjustments.

Comparisons with pseudo monitoring results (actual performance of a network) are illustrated by arbitrary created scenarios and Monte Carlo simulation. A Monte Carlo simulation approach to the method of fault position is implemented to explore the variability of the outcome of the process. The Monte Carlo approach provides richer results because it not only provides the average value of a particular index, but also the variability of the index. This variability can be relevant to sensitive customers. Whereas the method of fault positions provides only long-term average values, the Monte Carlo approach describes the complete spectrum of possible outcomes allowing the customer to evaluate events that, although less probable, may have catastrophic effects on the sensitive load.

Monitoring is well understood and most engineers rely on it to evaluate the performance of the network. However, it is expensive and when used to characterise the performance of an entire network a large number of power quality meters need to be used. Ideally all buses should be monitored and for a long period. Such a full monitoring program is not economically feasible and only a limited number of buses must be selected to perform monitoring. A method to select buses to be monitored is proposed in this work. An optimal monitoring program, capable of extracting system performance through system indices, is implemented and tested, showing the applicability of the method.

Stochastic assessment, on the other hand, is still not well understood and there is some degree of unwillingness to apply it to profile the performance of a network. The misunderstanding of the method and the apparent discrepancies of measurements and stochastic assessment contribute to this reluctance. A method to combine measurements and stochastic assessment is proposed in this work. The method is named Voltage Dip/Sag Estimation because it allows the extension of monitored performance to non-monitored buses. The optimal monitoring program is used to design a monitoring program that guarantees that every fault is seen by a number of power quality meters. Two stochastic approaches are proposed to calculate the residual voltage at non-monitored buses. The magnitude approach determines one residual voltage per fault by averaging all most probable residual voltages. The frequency approach assigns a per-unit frequency of occurrence to each residual voltage and uses all these residual voltages for long-term statistics at non-monitored buses. This results in the adjustment of the method of fault positions of non-monitored buses. Both methods are implemented and applied to the

test system showing the applicability of the methods. It is shown that the complete performance of the network can be reasonably well described by a minimum-monitoring program. If a higher level of accuracy is needed, a monitoring program with a higher level of redundancy can be used.

10.2 Conclusions

Conclusions derived from the work presented in this dissertation are presented.

Regarding the method of fault positions
The stochastic assessment of voltage dips provides useful information regarding the expected performance of a system. As a simulation method, it allows different alternative topologies to be considered and hence it is a powerful tool for planning activities. It is important to realise that the results obtained from the method are long-term expected results. It is unlikely that the real performance of the system exactly matches the result of the stochastic assessment because several random factors are involved in the dip generation process. The fault rate is a long-term average obtained from historic behaviour of the system and so it is the stochastic assessment of dips that can be obtained by using it. In this sense, the accuracy of the method is given by the accuracy of the random factors involved in the calculations such as fault rate, most probable system configuration, and generation scheduling among others. The number of fault positions along lines is also an important parameter, because the magnitude of the dip depends on the position of the fault. In the limit situation an infinite number of faults should be simulated in order to obtain the frequency function of the magnitude of dips at each bus. The analytic method presented in Chapter 7 addresses this issue. However, as the dips are usually classified in a discrete scale of the magnitude, some fault positions per line are acceptable. Such a number should be a function of the line length. Another important factor is the generation scheduling. The generation level does not affect the fault frequency, but the sensitivity of the system in terms of the effect of a fault on the system.

Regarding balanced and unbalanced dips
The residual voltage during a fault is equal to the pre-fault voltage at the observation bus plus the voltage change caused by the occurrence of the fault. Three-phase dips can be described by their phase voltages

or their symmetrical components. In this work, it has been assumed that before the fault only positive-sequence voltage is present in the system. The occurrence of a symmetrical fault causes dips type A and induces changes in the positive-sequence voltage. Unsymmetrical faults cause dips type C and D for which the voltage-change may contain zero-sequence components. Positive and negative-sequences are always present in unbalanced dips.

Regarding the effect of power transformer on dip type
Power transformers modify dips. Delta-wye grounded transformers have been considered in this dissertation. For these transformers the zero-sequence is blocked and an angular shift is introduced in the phase voltages. Because of the angular-shift in phase-voltages, the dip type changes when going through the transformer. A dip type C is seen as a dip type D and vice versa. In terms of modelling, the during-fault voltage equations need to incorporate a $\pm 60^{o}$ rotation in the negative-sequence voltage. Positive-sequence does not need to be shifted because the positive-sequence pre-event voltage at the observation bus is used as the reference of the dip.

Regarding propagation of dips in power systems
Voltage dips propagate through the system. Depending on the dip type the propagation is more or less severe. Dips type A are caused by three-phase faults and propagate far from the fault point. Since this type of dip only contains positive-sequence, it can propagate through power transformers without large changes. Unbalanced dips C and D also propagate through the system. Propagation of unbalanced dips is, in general, less severe due to the existence of negative and zero-sequence impedances. In particular, dips caused by single-phase-to-ground faults propagate much less than balanced dips. In terms of area of susceptibility, the exposed area for symmetrical faults is always larger than the corresponding exposed area for unsymmetrical faults. Impedance grounded systems show exposed areas for unsymmetrical fault that are much smaller than for symmetrical faults.

Regarding the performance of buses in terms of dips
In this work, the performance of a bus in terms of dips is described by a frequency histogram. Dip magnitude is classified in several bins and the number of dip occurrences in each dip bin is counted. How many dips a given bus of a transmission system may suffer during a year is

a function of several factors, the number of faults occurring in the exposed area of the bus being the most important one. How the total number of dips distributes over the magnitude bins depends on the strength of the bus. The distribution of dips over the bins modifies the shape of the histograms. Weak buses are more exposed to severe dips than strong buses where dips are mainly shallow dips.

Regarding contribution of symmetrical faults to total dip frequency
Symmetrical faults are much less frequent than unsymmetrical faults. Usually the distribution probability of faults is around 80%, 10%, 5% and 5% for single-phase-to-ground, two-phase-to-ground, phase-to-phase and three-phase faults respectively. According to these numbers, it would be expected that the fraction of balanced dips is at most 5%. However, it is shown in this work that balanced dips contribute to the total number of dips with more than the fraction of symmetrical faults. This larger contribution is the result of the exposed area for symmetrical faults, which is larger than for unsymmetrical faults. The contribution of balanced dips becomes even more important for severe dips. Buses that are radially fed by long lines present a dip contribution that follows the fault type probability.

Regarding system statistics
System statistics are needed for system performance characterisation. Usually, the average number of dips and the 95 percentile in a given dip bin is used to quantify the system performance. System statistics are calculated in this work using the stochastic assessment of dips. It is found that when only balanced dips are used to perform the stochastic assessment, the event frequency is overestimated. This overestimation would be even larger if the system under consideration is impedance grounded.

Regarding optimal dips monitoring programs
Monitoring is needed to calibrate the stochastic assessment. In order to be useful, the monitoring program must be such that the performance of the system can be described with reasonable certainty. Because monitors are expensive, a minimum number of monitors should be used to perform the measurements. However, the amount of monitors should be such that no essential information is missed. A model to solve this problem has been introduced in this dissertation. An integer optimisation problem that minimises the number of

monitors subject to the coverage of the whole system is proposed. Optimal locations are found for different monitor thresholds. Subsequently, system indices are calculated based on this limited number of monitors. The average system performance is well described by the limited number of monitors. The 95 percentile however can only be identified if the worst site is included in the monitoring program.

Regarding the Monte Carlo approach to the method of fault positions
The method of fault positions is an effective way to profile the long-term expected performance of a network in terms of dips. However, it fails in describing the variability of the actual performance from year to year. The Monte Carlo approach provides richer results because it not only gives data enough to calculate the long-term average performance, but it also provides insight into scenarios of low probability that may have catastrophic effects on sensitive loads.

Regarding voltage dip estimation
A method to estimate the dip performance at non-monitored buses is presented. The method combines the measurement results from an optimal monitoring program with the assessment obtained using the method of fault positions. Two approaches are illustrated and both succeed in estimating the dip performance at non-monitored buses. The estimation can be significantly improved by adding meters so that the level of redundancy of the monitoring program ensures that every fault triggers at least two meters.

10.3 Future Work

This dissertation shows the potential of the stochastic assessment of voltage dips. The methodology is to some extent a simple technique. It is based on well-known theories such as power system modelling, short-circuit calculation, symmetrical components, reliability, and stochastic processes. The complexity of the method lies in the correct understanding of all these theories and their interrelation in order to implement a stochastic assessment of dips. Although known, the method is not well understood and practical applications in utilities are not common. The following research areas can be mentioned.

Application to real systems
The main idea is to apply the method to an existing transmission system in the same way as it has been done in this dissertation. An

important part of the research is the power system modelling. The gathering of accurate fault rates and consideration of symmetrical and unsymmetrical faults is also relevant. The effect of power transformers, phase shift transformers, HVDC links and series capacitive compensation of lines on the type of dips need to be modelled and measurements should be used to check the validity of the models. The work should describe the expected number of dips per bus, system indices, exposed areas, and dip-maps.

Including duration of dips
In this work, duration of dips has not been considered. At transmission level, the time to clear the fault is to some extent fixed. It only depends on the position of the fault along the line, i.e. first zone, second zone or third zone. It is, therefore, possible to include the clearing time of protection devices in order to obtain a more complete assessment of the dip performance. Probabilistic models of the performance of protection relays and fault current interruption devices can also be included to improve the assessment.

Dynamic behaviour of loads
Some loads affect the shape of the voltage dip. In this work, it has been assumed that dips are rectangular events that can be characterised by one magnitude and one duration value. This modelling corresponds to the basic assumption of an unloaded network. Actual dips may differ from this ideal model, especially due to the existence of motors in the load. Research is needed in order to obtain suitable load models that may be incorporated in the stochastic assessment of dips. A first approximation may include loads as constant impedances. A more elaborated model may include variable impedance loads. Time domain modelling of machines and other loads could also be used to study the dynamic behaviour of voltage dips. The behaviour of generation machines should also be modelled in order to improve the accuracy of the stochastic assessment.

Further development of the method for voltage dip estimation
The method for voltage dip estimation proposed in this work provides only the residual voltage. Presumably, the method can be improved to provide not only the magnitude of dips at non-monitored buses, but also other characteristics such as duration and type of dip at non-monitored buses. The duration of the dips seems to be the most achievable goal because the duration of a monitored dip will most

likely be a reasonable indicator of the duration of dips at non-monitored buses. The dip type seems also an achievable goal because registration of the three rms voltage signals makes it is possible to identify the dip type. How this dip will be seen at non-monitored buses requires a careful modelling of the power system elements between the monitored and non-monitored buses, particularly of power transformers.

References

Abur, A., Gómez-Expósito, A. (2004) "Power system state estimation: theory and implementation" New York: Marcel Dekker, cop. 2004.

Andersson, T., Nilsson D. (2002). "Test and Evaluation of Voltage Dip Immunity". Master research work, Department of Electric Power Engineering, Chalmers University of Technology, Gothenburg, Sweden.

Alves, M. and Fonseca, V (2001) "Voltage Sag Stochastic Estimate". IEEE Industrial Application Society, Proceedings of Annual Meeting, Chicago, USA, 2001.

Anderson, P. (1973) "Analysis of Faulted Power Systems". The Iowa State University Press. Ames, Iowa. First Edition 1973.

ANSI C57.21.10. (1988) "American National Standard For Transformers 230kV and Below 833/958 through 8333/10417 kVA, Single-Phase, and 750/862 through 60000/80000/100000 kVA, Three-Phase without Load Tap changing; and 3750/4687 through 60000/80000/100000 kVA with Load Tap Changing – Safety Requirements".

Bhattacharya, K., Bollen, M. and Daalder, J. (2001) "Operation of Restructured Power Systems". Kluwer's Power Electronics and Power Systems Series, Kluwer Academic Publishers.

Billinton, R. and Allan, R. (1983) "Reliability Evaluation of Engineering Systems: Concepts and Techniques". Pitman Publishing Inc. 1983.

Blackburn, J. Lewis. (1998) "Protective Relaying; Principles and Applications", Second Edition. Marcel Dekker Inc. Power Engineering Series, New York 1998.

Bollen, M.H.J. (1993 a). "Method for Reliability Analysis of Industrial Distribution Systems". IEE Proceedings C Generation, Transmission and Distribution, Volume: 140 Issue: 6, Nov. 1993. Page(s): 497 – 502.

Bollen, M.H.J. (1995). "Fast Assessment Methods for Voltage Sags in Distribution Systems". Thirtieth IEEE Industry Applications Conference, IAS, Annual Meeting 1995. Volume: 3, Page(s): 2282 - 2289 vol.3.

Bollen, M.H.J. (1996). "Voltage Sags: Effects, Mitigation and Prediction". Power Engineering Journal, June 1996. Page(s)129 – 135.

Bollen, M.H.J. (1998 a). "Additions to the Method of Critical Distances for Stochastic Assessment of Voltage Sags". Proceedings of IEEE Winter Meeting, New York 1998.

Bollen, M.H.J. (1998 b) "Method of Critical Distances for Stochastic Assessment of Voltage Sags". IEE Proceedings Generation, Transmission and Distribution, Volume: 145 Issue: 1, Jan. 1998. Page(s): 70 –76

Bollen, M.H.J. (1999). "Understating Power Quality Problems: Voltage Sags and Interruptions". IEEE Press series on power engineering, New York 1999.

Bollen, M.H.J. (2000). "Methods for Obtaining Voltage Dips Statistics". ELEKTRA project 3363. Project description. Electric Power Engineering Department, Chalmers University of Technology, September 2000

Bollen, M.H.J. and Zhang, L.D. (2003) "Different Methods for Classification of Three-phase Unbalanced Voltage Dips due to Faults". Electric Power Systems Research, V.66, No 1, July 2003, p59-69.

Bollen, M.H.J. Tayjasanant, T. Yalcinkaya, G. (1997). "Assessment of the Number of Voltage Sags Experienced by a Large Industrial Customer". IEEE Transactions on Industry Applications, Volume: 33 Issue: 6, Nov.-Dec. 1997 Page(s): 1465 –1471

Bollen, M.H.J., Massee, P. (1993 b). "Reliability Analysis Of Industrial Power Systems Taking Into Account Voltage Sags". Proceedings of Joint International Conference Athens Power Tech, 1993, Volume: 2 Page(s): 856 –860 Athens, Greece 1993.

Bollen, M.H.J., Qader, M.R., Allan, R.N. (1998 c). "Stochastical and Statistical Assessment of Voltage Dips". IEE Colloquium on Tools and Techniques for Dealing with Uncertainty (Digest No. 1998/200), 1998. Page(s): 5/1 -5/4.

Bollen, M.H.J.; Goossens, P.; Robert, A. (2004). "Assessment of voltage dips in HV-networks: deduction of complex voltages from the measured RMS voltages". IEEE Transactions on Power Delivery, Volume 19, Issue 2, April 2004, Page(s): 783 - 790

Brown, E.H. (1985). "Solution of Large Networks by Matrix Methods", Second Edition, Published by John Wiley Sons Inc. United Kingdom 1985.

Brown, R. (2002) "Electric Power Distribution Reliability". Marcel Dekker Inc, Power Engineering Series, New York 2002.

Carlsson, Fredrik (2003) "On Impacts and Ride-Through of Voltage Sags Exposing Line-Operated AC-Machines and Metal Processes" Doctoral Dissertation, Department of Electrical Engineering, Royal Institute of Technology, Sweden.

Carvalho J.M. et al. (2002 a). "Comparative Analysis between Measurements and Simulations of Voltage Sags". Proceedings of 10th International Conference of Harmonics and Quality of Power. October 2002, Rio de Janeiro Brazil.

Carvalho, J.M. et al (2002 b). "Analise Comparativa de Simulações e Medições de Afundamentos de Tensão". XIV Congresso Brasileiro de Automática, Natal RN Setembro 2002. In Portuguese.

Carvalho, J.M. et al (2002 c). “Softwares e Procedimentos para Simulação de Afundamentos de Tensão”. XIV Congresso Brasileiro de Automática, Natal RN, 2002. In Portuguese.

Conrad, L. Little, K. Grigg, C. (1991). “Predicting and Preventing Problems Associated with Remote Fault-clearing Voltage Dips”. IEEE Transactions on Industry Applications, Volume: 27 Issue: 1 Part: 1, Jan.-Feb. 1991 Page(s): 167 –172.

Das, J.C. (2002) “Power System Analysis; Short-circuit Load Flow and Harmonics”, Marcel Dekker Inc. Power Engineering Series, New York 2002.

Davenport, F. (1991). “Voltage Dips and Short Interruptions in Medium Voltage Public Electricity Supply” Systems”. Electricity Association, London. Group of Experts: F. W. T. Davenport (Chairman), D. Bose, U. Grape, M. Kasztler, J. N. Luttjehuizen, H. Seljeseth, M. Silvestri, D. J. Start, J-P Tete, J. Votsmeier, R. Tonon.

Dorr, D.S. (1992). “National Power Laboratory Power Quality Study Results Based on 600 Site-months”. Telecommunications Energy 14th International Conference, 1992. INTELEC '92. 1992 Page(s): 378 – 383.

Dorr, D.S. (1994) “Point of Utilization Power Quality Study Results”. Conference Record of the 1994 IEEE Industry Applications Society, Annual Meeting, 1994. Page(s): 2334 -2344 vol.3.

Dorr, D.S. et al (1996) M. “Interpreting Recent Power Quality Surveys to Define the Electrical Environment”. Conference Record of the 1996 IEEE Industry Applications Conference. Thirty-first IAS Annual Meeting. Page(s): 2251 -2258 vol.4.

Dugan, R., McGranaghan, F. and Wayne H. (1996) “Electrical Power Systems Quality”. McGraw-Hill New York, 1996.

Electricite de France (1992) “CREUTENSI: Software for Determination of Depth, Duration and Number of Voltage Dips (Sags) on Medium Voltage Networks”. 1992.

Faired, S.O. and Aboreshaid, S. (2002). “A Monte Carlo Technique for the Evaluation of Voltage Sags in Series Capacitor Compensated Radial Distribution Systems”, Proceedings of the 2002 Large Engineering Systems Conference on Power Engineering.

Fonseca, V. and Alves, M. (2002). “A Dedicated Software for Voltage Sag Stochastic Estimate”. International Conference on Harmonics and Quality of Power ICHQP 2002, Rio de Janeiro, Brazil 2002.

Galijasevic, Z., Abur, A. (2002) “Fault location using voltage measurements”. IEEE Transactions on Power Delivery, Vol 17, April 2002, Pages 441 – 445.

Gnativ, R. Milanovic, J.V. (2001). “Voltage Sag Propagation in Systems with Embedded Generation and Induction Motors”. Power Engineering Society, Summer Meeting 2001.

Han, Z. X. (1982) “Generalized Method of Analysis of Simultaneous Faults in Electric Power Systems”. IEEE Transactions on Power Apparatus and Systems, Vol. PAS-101, No 10, October 1982.

Heine, P., Lehtonen, M. and Lakervi, E. (2001). “Voltage Sag Analysis Taken into account in Distribution Network Design”. IEEE Power Tech Conference 2001. Porto, Portugal 2001.

Heydt, G. (1999). “Electric Power Quality”. Start in a Circle Publications, West LaFayette, Indiana 1991.

IEC 61000-2-1 (1990) “Electromagnetic Compatibility. Part 2: Environment. Section 1: Description of the environment – Electromagnetic environment for low –frequency conducted disturbances and signalling in public power supply systems”. International Electrotechnical Commission.

IEC 61000-2-8 (2002). “Electromagnetic Compatibility. Part 2-8: Environment – voltage dips and short interruptions on public electric power supply systems with statistical measurement results [draft, 22-02-2002]”. International Electrotechnical Commission.

IEEE Std 1346 (1998). “IEEE Recommended Practice for Evaluating Electric Power System Compatibility With Electronic Process Equipment”.

IEEE Std 142 (1991). “IEEE Recommended Practice for Grounding of Industrial and Commercial Power Systems; Green Book”. 1991.

IEEE Std 493 (1997). “Recommended Practice for the Design of Reliable Industrial and Commercial Power Systems; Gold Book”. 1997.

IEEE Std. 1100 (1999). “Recommended Practice for Powering and Grounding Electronic Equipment”. [Revision of IEEE Std 1100-1992].

IEEE C57.116 (1989). “IEEE Guide for Transformers Directly Connected to Generators”. IEEE C57.116-1989.

ISA, (2002) Interconexion Electrica S.A. (ISA), “Informe de Operacion 2002”. Available at http://www.isa.com.co/ publicaciones/InformeAnual/ azul/index.htm

Kees van der Heijden, (1997) “Scenarios, Strategies and the Strategy Process” Published by Nijenrode University Press, Breukelen, The Netherlands, January 1997. Available at February 2004 http://www.library.nijenrode.nl/library/publications/nijrep/1997-01/1997-01.html

Kinney, John J. (1997). “Probability: an introduction with statistical applications”. John Wiley & Sons, Inc, Canada 1997. ISBN 0-471-12210-6

Koval, D. (1990). “How Long Should Power System Disturbance Site Monitoring be to be Significant?” IEEE Transactions on Industry Applications, Vol. 26, No 4, July/August 1990.

Koval, D.O. and Hughes, B.M. (1996). “Frequency of Voltage Sags At Industrial and Commercial Sites in Canada”. Canadian Conference on Electrical and Computer Engineering, CCEC’96, Canada 1996.

Lakervi, E. and Holmes, E. (1989). "Electricity Distribution Network Design". IEE Power Engineering Series 9. Peter Peregrinus Ltda. England, 1989.

Lim, Y. S. and Strbac, G. (2002). "Analytical Approach to Probabilistic Prediction of Voltage Sags on Transmission Networks". IEE Proceedings Generation, Transmission and Distribution, Vol. 149, January 2002.

Martinez, J. and Martin-Arnedo J. (2002). "Voltage Sags Analysis Using an Electromagnetic Transient Program". IEEE Power Engineering Society Winter Meeting 2002, Vol. 2. Page(s): 1135-1140.

McGranaghan, M.; Mueller, D.; Samotyj, M. (1991). "Voltage Sags in Industrial Systems". Technical Conference on Industrial and Commercial Power Systems, 1991. Page(s): 18 –24.

Milanovic, J.V., Gnativ, R. and Chow, K.W.M. (2000). "The Influence of Loading Conditions and Network Topology on Voltage Sags". International Conference on Harmonics and Quality of Power 2000, Orlando Florida 2000.

Milanovic, J.V.; Myo Thu Aung; Gupta, C.P. (2005)"The influence of fault distribution on stochastic prediction of voltage sags". IEEE Transactions on Power Delivery, Vol.20, January 2005 Pages: 278-285.

Ortmeyer, T.H. and Hiyama, T. (1996 a). "Coordination of Time Overcurrent Devices with Voltage Sag Capability Curves". IEEE International Conference on Harmonics and Quality of Power ICHQP'96, Las Vegas, N.V. 1996.

Ortmeyer, T.H., Hiyama, T. and Salehfar, H. (1996 b). "Power Quality Effects of Distribution System Faults". Electric Power & Energy Systems, Vol. 18, No 5, page(s): 323 – 329, 1996.

OTC (2003) Optimization Technology Center, NEOS Guide, Optimization Tree. Available at http://www-fp.mcs.anl.gov/guide/optweb/ discrete/index

Pohjanheimo, P. and Lehtonen, E. (2002). "Equipment Sensitivity to Voltage Sags – Test Results for Contactors, Pcs and Gas Discharge Lamps". International Conference on Harmonics and Quality of Power, 2002. Rio de Janeiro, Brazil.

Pohjanheimo, Pasi (2003). "A Probabilistic Method for Comprehensive Voltage Sag Management in Power Distribution Systems". Dissertation for the degree of Doctor of Technology, Department of Electrical and Communications Engineering (Espoo, Finland), 2003, ISBN 951-22-6398-X

Qader, M.R.; Bollen, M.H.J.; Allan, R.N. (1999). "Stochastic Prediction of Voltage Sags in a Large Transmission System". IEEE Transactions on Industry Applications, Volume: 35 Issue: 1 Jan.-Feb. 1999 Page(s): 152 -162

Rardin, L. (2000). "Optimization in Operations Research". Prentice Hall International (UK) Limited, 2000.

Ross, Sheldom M. (1996) “Simulation; Statistical Modelling and Decision Science”. Academic Press.

Shih-An Yin, Chan-Nan Lu, E. Liu, Yu-Chang Huang, Chinug-Yi Huang (2001). “A Survey on High Tech Industry Power Quality Requirements”, in IEEE PES Transmission and Distribution Conference and Exposition, 2001.

Shih-An Yin; Rung-Fang Chang; Chan-Nan Lu (2003) “Reliability worth assessment of high-tech industry Power Systems”, IEEE Transactions on, Vol.18, Iss.1, Feb 2003 Pages: 359- 365

Sikes, D.L. (2000). “Comparison Between Power Quality Monitoring Results and Predicted Stochastic Assessment of Voltage Sags- “Real” Reliability for the Customer”. IEEE Transaction on Industry Applications, Vol. 36, No 2, March/April 2000.

Stevenson, W. (1982). “Elements of Power System Analysis”, Fourth Edition, McGraw-Hill Series in Electrical Engineering, McGraw-Hill Book Inc., 1982.

Stockman, K., D’hulster, K., Verhaege, K. (2003). “Ride-through of Adjustable Speed Drives During Voltage Dips”. To appear in Electric Power Systems Research.

Styvaktakis, E. (2002). “Automating Power Quality Analysis”, PhD thesis Department of Signal and Systems, Chalmers University of Technology. Gothenburg, Sweden 2002.

Suhir, Ephraim (1997). “Applied Probability for Engineers and Scientists”. McGraw-Hill 1997. ISBN 0-07-061860-7

Wacker, G.; Billinton, R. (1989). “Customer cost of electric service interruptions**”.** Proceedings of the IEEE, Vol.77, Iss.6, Jun 1989 Pages: 919-930

Wagner, C.F., Evans, R.D. (1933). “Symmetrical Components; As applied to the Analysis of Unbalanced Electrical Circuits”, First Edition, McGraw-Hill Book Inc., New York 1933.

Wagner, V.E., Andreshak, A.A., Staniak, J.P. (1990). “Power quality and factory automation”. IEEE Transactions on Industry Applications, Volume: 26 Issue: 4, July-Aug. 1990 Page(s): 620 –626

Zhang, L. (1999). “Three-phase Unbalance of Voltage Dips”, Licentiate Dissertation, Department of Electric Power Engineering, Chalmers University of Technology. Gothenburg, Sweden 1999.

Appendix A: System Data

From Bus	To Bus	Volt. (kV)	Length (km)	R1 Ω/km	X1 Ω/km	B1 Mho-km	R0 Ω/km	X0 Ω/km	B0 Mho-km
1	57	230	53.70	0.07	0.49	3.45	0.48	1.65	2.39
1	87	230	54.20	0.07	0.48	3.45	0.48	1.65	2.39
2	3	230	0.38	0.06	0.49	3.42	0.33	1.46	1.94
2	3	230	0.38	0.06	0.49	3.42	0.33	1.46	1.94
2	49	230	20.00	0.06	0.49	3.37	0.32	1.46	2.03
2	53	230	28.43	0.05	0.48	3.47	0.32	1.45	1.96
3	27	230	129.49	0.05	0.48	3.46	0.27	1.14	2.19
3	27	230	129.49	0.05	0.48	3.46	0.27	1.14	2.19
3	67	230	107.18	0.05	0.50	3.42	0.26	1.12	2.17
3	67	230	107.18	0.05	0.50	3.42	0.26	1.12	2.17
4	41	230	26.80	0.05	0.50	3.42	0.26	1.10	2.22
4	50	230	13.90	0.05	0.50	3.41	0.27	1.10	2.22
5	11	230	86.50	0.07	0.53	3.20	0.30	1.04	2.20
5	65	230	51.15	0.07	0.53	3.20	0.30	1.04	2.20
6	25	230	44.50	0.06	0.48	3.38	0.32	1.35	2.00
6	29	230	48.40	0.06	0.49	3.42	0.33	1.46	1.94
6	31	230	40.50	0.06	0.49	3.42	0.33	1.46	1.94
6	44	230	14.50	0.05	0.48	3.47	0.32	1.45	1.96
6	49	230	48.90	0.06	0.49	3.42	0.33	1.46	1.94
7	10	230	90.00	0.09	0.49	3.34	0.28	1.10	2.14
7	19	230	11.14	0.07	0.53	3.22	0.42	1.34	2.19
8	25	230	68.20	0.06	0.49	3.39	0.33	1.46	1.98
9	34	230	206.00	0.06	0.51	3.41	0.37	1.44	1.89
9	66	230	144.00	0.03	0.47	3.62	0.38	1.34	2.17
9	66	230	144.00	0.03	0.47	3.62	0.38	1.34	2.17
10	46	230	23.50	0.11	0.62	4.17	0.41	1.40	2.75
13	70	230	146.20	0.06	0.49	3.46	0.25	1.13	2.19
14	85	230	84.66	0.06	0.52	3.35	0.36	1.44	1.89
14	85	230	84.50	0.06	0.52	3.35	0.36	1.44	1.89
15	68	500	209.60	0.02	0.33	4.97	0.45	1.22	2.84
15	68	500	229.00	0.02	0.32	5.00	0.35	1.00	2.76
16	15	500	131.00	0.03	0.33	4.93	0.30	0.96	2.83
16	15	500	132.00	0.02	0.32	5.10	0.30	1.10	3.36
17	74	230	119.00	0.05	0.48	3.42	0.29	1.18	2.20
17	74	230	119.00	0.05	0.48	3.42	0.29	1.18	2.20
17	82	230	104.50	0.05	0.50	3.42	0.24	1.11	2.20
18	33	230	109.60	0.04	0.40	4.30	0.29	0.92	3.35

From Bus	To Bus	Volt. (kV)	Length (km)	R1 Ω/km	X1 Ω/km	B1 Mho-km	R0 Ω/km	X0 Ω/km	B0 Mho-km
18	33	230	109.90	0.04	0.40	4.30	0.29	0.92	3.34
18	58	230	50.05	0.04	0.48	3.48	0.37	1.33	2.25
18	83	230	29.80	0.04	0.48	3.48	0.37	1.33	2.25
19	32	230	94.50	0.07	0.49	3.37	0.34	1.34	2.20
19	48	230	2.30	0.09	0.50	3.98	0.36	1.44	2.92
22	71	230	9.20	0.07	0.52	3.34	0.29	0.92	2.70
22	75	230	11.58	0.07	0.54	3.21	0.43	1.36	2.19
23	21	230	42.00	0.06	0.53	3.30	0.36	1.42	2.05
24	86	230	92.90	0.08	0.52	3.19	0.45	1.26	2.35
26	31	230	63.10	0.06	0.48	3.43	0.33	1.46	1.95
26	53	230	28.93	0.05	0.48	3.47	0.32	1.45	1.96
26	54	230	26.40	0.06	0.48	3.43	0.33	1.46	1.95
27	40	230	24.00	0.21	0.54	3.72	0.56	1.70	2.23
27	45	230	23.90	0.06	0.48	3.46	0.24	1.10	2.19
27	45	230	23.90	0.06	0.48	3.46	0.24	1.10	2.19
27	87	230	193.30	0.05	0.46	3.49	0.40	1.33	2.17
27	87	230	193.30	0.05	0.46	3.49	0.40	1.33	2.17
28	24	230	47.10	0.08	0.52	3.19	0.45	1.26	2.35
28	73	230	86.00	0.08	0.53	3.32	0.53	1.72	1.89
28	73	230	86.00	0.08	0.53	3.32	0.53	1.72	1.89
29	25	230	8.80	0.06	0.49	3.37	0.32	1.46	2.03
29	53	230	81.20	0.05	0.48	3.44	0.32	1.45	1.95
30	23	230	95.00	0.08	0.53	3.32	0.53	1.72	1.86
30	23	230	95.00	0.08	0.53	3.32	0.53	1.72	1.86
30	73	230	92.00	0.08	0.53	3.32	0.53	1.72	1.95
30	73	230	92.00	0.08	0.53	3.32	0.53	1.72	1.95
31	35	230	18.80	0.05	0.42	2.64	0.34	1.08	1.82
31	35	230	14.45	0.05	0.42	2.64	0.34	1.08	1.82
31	49	230	51.30	0.06	0.49	3.42	0.33	1.46	1.94
31	49	230	51.30	0.06	0.49	3.42	0.33	1.46	1.94
31	54	230	37.90	0.06	0.48	3.43	0.33	1.46	1.95
31	59	230	21.16	0.06	0.49	3.42	0.33	1.46	1.94
31	67	230	35.74	0.04	0.49	3.54	0.39	1.35	2.14
32	10	230	13.81	0.07	0.51	3.23	0.39	1.36	2.18
33	17	230	22.00	0.05	0.50	3.44	0.40	1.34	2.21
33	17	230	22.00	0.05	0.50	3.44	0.40	1.34	2.21
33	42	230	80.40	0.03	0.37	4.54	0.26	0.80	3.68
33	82	230	84.00	0.03	0.48	3.57	0.38	1.32	2.26

From Bus	To Bus	Volt. (kV)	Length (km)	R1 Ω/km	X1 Ω/km	B1 Mho-km	R0 Ω/km	X0 Ω/km	B0 Mho-km
33	82	230	84.00	0.03	0.48	3.57	0.38	1.32	2.26
33	83	230	155.10	0.03	0.37	4.55	0.26	0.80	3.68
34	41	230	86.40	0.05	0.48	3.47	0.39	1.37	2.18
34	41	230	86.40	0.05	0.48	3.47	0.39	1.37	2.18
36	66	230	188.00	0.06	0.46	3.51	0.41	1.34	2.14
36	66	230	188.00	0.06	0.46	3.51	0.41	1.34	2.14
37	55	230	34.00	0.06	0.48	3.49	0.32	1.17	2.20
37	57	230	22.90	0.06	0.49	3.47	0.51	1.53	2.40
37	64	230	63.10	0.06	0.49	3.47	0.51	1.53	2.40
37	70	230	21.45	0.05	0.48	3.48	0.34	1.28	2.19
38	27	230	31.20	0.05	0.49	3.47	0.25	1.13	2.19
38	69	230	65.62	0.05	0.49	3.49	0.24	1.15	2.21
39	41	230	5.00	0.04	0.48	3.48	0.37	1.34	2.23
39	41	230	5.00	0.04	0.48	3.48	0.37	1.34	2.23
39	58	230	7.50	0.04	0.48	3.48	0.37	1.33	2.26
39	58	230	7.50	0.04	0.48	3.48	0.37	1.33	2.26
43	60	230	60.16	0.07	0.55	3.33	0.36	1.51	1.94
43	61	230	99.96	0.05	0.47	3.48	0.35	1.25	2.18
44	8	230	16.00	0.06	0.49	3.37	0.32	1.46	2.03
45	13	230	18.10	0.06	0.49	3.46	0.25	1.13	2.19
45	40	230	26.95	0.05	0.48	3.43	0.25	1.08	1.93
45	70	230	166.84	0.02	0.32	5.21	0.36	1.11	3.12
45	70	230	165.75	0.04	0.32	5.23	0.33	0.97	3.13
46	32	230	30.80	0.06	0.48	3.40	0.28	1.20	2.20
46	81	230	79.43	0.05	0.52	3.29	0.29	1.04	2.22
47	35	230	70.10	0.06	0.53	3.26	0.43	1.30	2.21
47	60	230	7.53	0.06	0.53	3.26	0.43	1.30	2.21
50	41	230	39.70	0.05	0.50	3.42	0.27	1.10	2.22
50	82	230	19.50	0.05	0.48	3.42	0.25	1.06	2.20
50	82	230	19.50	0.05	0.48	3.42	0.25	1.06	2.20
51	62	230	45.60	0.08	0.53	3.32	0.55	1.71	1.91
51	62	230	44.00	0.06	0.48	3.43	0.23	1.09	2.14
51	62	230	44.00	0.06	0.48	3.43	0.23	1.09	2.14
51	76	230	23.50	0.08	0.53	2.35	0.55	1.71	1.82
52	46	230	160.53	0.06	0.52	3.30	0.29	1.07	2.20
53	44	230	23.06	0.05	0.48	3.47	0.32	1.45	1.96
54	59	230	54.75	0.06	0.49	3.42	0.33	1.46	1.94
57	64	230	49.20	0.06	0.49	3.47	0.51	1.53	2.40

From Bus	To Bus	Volt. (kV)	Length (km)	R1 Ω/km	X1 Ω/km	B1 Mho-km	R0 Ω/km	X0 Ω/km	B0 Mho-km
57	87	230	26.70	0.07	0.49	3.45	0.48	1.65	2.39
58	72	230	33.96	0.04	0.48	3.47	0.37	1.33	2.25
59	60	230	104.00	0.06	0.48	3.50	0.30	1.03	2.05
60	19	230	112.30	0.07	0.55	3.33	0.35	1.53	1.92
60	19	230	101.74	0.07	0.54	3.21	0.43	1.35	2.19
60	78	230	8.21	0.06	0.48	3.42	0.28	1.11	2.19
60	78	230	8.21	0.06	0.48	3.42	0.28	1.11	2.19
61	50	230	101.55	0.05	0.46	3.50	0.40	1.33	2.17
61	50	230	101.55	0.05	0.46	3.50	0.40	1.33	2.17
62	28	230	92.60	0.08	0.52	3.16	0.43	1.27	2.26
62	28	230	90.20	0.07	0.48	3.54	0.34	1.05	2.54
62	80	230	80.00	0.08	0.53	3.32	0.53	1.71	1.91
62	80	230	80.00	0.08	0.53	3.32	0.53	1.71	1.91
63	16	500	183.00	0.03	0.33	4.93	0.30	0.96	2.83
63	16	500	185.00	0.02	0.33	5.14	0.26	0.99	3.38
65	81	230	44.64	0.07	0.53	3.23	0.30	1.05	2.19
66	55	230	116.00	0.06	0.48	3.51	0.37	1.30	2.16
67	82	230	104.50	0.05	0.50	3.42	0.24	1.11	2.20
67	27	230	193.76	0.05	0.50	3.44	0.26	1.13	2.18
67	27	230	193.76	0.05	0.50	3.44	0.26	1.13	2.18
67	43	230	66.01	0.05	0.47	3.48	0.33	1.20	2.19
67	45	230	212.92	0.02	0.32	5.21	0.36	1.11	3.12
67	45	230	212.24	0.03	0.33	5.22	0.27	0.84	3.13
67	61	230	91.33	0.05	0.46	3.49	0.40	1.33	2.16
69	27	230	97.42	0.05	0.49	3.49	0.24	1.15	2.20
69	41	230	78.82	0.05	0.49	3.46	0.25	1.13	2.19
69	41	230	78.82	0.05	0.49	3.46	0.25	1.13	2.19
71	20	230	68.50	0.11	0.42	4.51	0.34	1.53	2.20
71	20	230	68.50	0.11	0.42	4.51	0.34	1.53	2.20
71	52	230	120.23	0.06	0.51	3.33	0.29	1.08	2.20
71	75	230	18.30	0.07	0.49	3.34	0.29	0.92	2.70
72	32	230	150.00	0.07	0.51	3.23	0.41	1.33	2.19
72	83	230	14.89	0.04	0.48	3.55	0.37	1.33	2.30
74	32	230	158.16	0.05	0.47	3.44	0.30	1.17	2.02
74	56	230	5.25	0.04	0.47	3.48	0.29	1.20	2.22
74	56	230	5.25	0.04	0.47	3.48	0.29	1.20	2.22
75	46	230	100.12	0.07	0.53	3.24	0.41	1.34	2.20
76	62	230	38.50	0.08	0.53	3.32	0.53	1.71	1.91

From Bus	To Bus	Volt. (kV)	Length (km)	R1 Ω/km	X1 Ω/km	B1 Mho-km	R0 Ω/km	X0 Ω/km	B0 Mho-km
76	62	230	38.50	0.08	0.53	3.32	0.53	1.71	1.91
76	62	230	38.50	0.08	0.53	3.32	0.53	1.71	1.91
77	12	230	3.40	0.08	0.53	3.32	0.53	1.71	1.90
77	12	230	3.40	0.08	0.53	3.32	0.53	1.71	1.90
77	80	230	3.20	0.08	0.53	3.32	0.53	1.71	1.90
77	80	230	3.20	0.08	0.53	3.32	0.53	1.71	1.90
79	51	230	7.40	0.08	0.53	2.35	0.55	1.71	1.82
79	51	230	7.40	0.08	0.53	2.35	0.55	1.71	1.82
83	42	230	74.70	0.03	0.37	4.56	0.26	0.80	3.70
84	85	230	48.80	0.06	0.52	3.35	0.36	1.44	1.89
86	23	230	114.00	0.08	0.52	3.19	0.45	1.26	2.35
87	66	230	122.60	0.05	0.48	3.51	0.38	1.35	2.15
87	70	230	6.15	0.06	0.48	3.46	0.24	1.10	2.19

Appendix B: Dip Frequency Results

Site performance obtained via method of fault positions is presented. Symmetrical and unsymmetrical faults are considered.

Cumulative dip frequency										
Bus	Name	0.55	0.6	0.65	0.7	0.75	0.8	0.85	0.9	0.95
1	ALTOANCHICAYA	0.1	0.5	0.6	0.6	1.2	1.6	2.1	3.3	9.5
2	ANCONSUR	1.5	2.1	2.7	4.0	5.4	10.1	13.9	24.1	49.0
3	ANCONSURISA	1.5	2.0	2.7	4.0	5.7	10.1	13.9	24.2	49.3
4	BALSILLAS	1.5	1.6	2.0	3.1	4.3	6.2	11.6	18.9	32.2
5	BANADIA	7.4	8.6	10.0	11.4	13.4	16.2	17.9	19.8	23.3
6	BARBOSA	1.0	1.0	1.4	2.3	3.1	3.4	5.4	9.2	15.3
7	BARRANCA	0.2	0.3	0.5	0.5	0.6	1.0	1.8	3.5	9.2
8	BELLO	0.8	0.9	1.5	1.7	1.9	2.5	4.1	6.7	12.4
9	BETANIA	0.2	0.7	0.8	0.9	1.5	2.1	3.5	6.6	14.5
10	BUCARAMANGA	3.5	4.8	5.5	7.4	9.4	11.9	13.9	18.0	23.4
11	CANOLIMON	7.6	8.8	10.1	11.6	13.6	16.4	17.9	19.8	23.3
12	CARTAGENA	0.3	0.3	0.7	0.8	0.9	1.4	2.8	4.6	9.2
13	CARTAGO	3.9	6.0	7.5	10.7	14.7	21.1	30.0	43.1	57.1
14	CERROMATOSO230	3.8	5.1	5.7	7.5	12.2	15.3	16.8	21.4	31.0
15	CERROMATOSO500	10.9	11.8	12.9	14.0	15.7	16.0	17.2	18.7	30.1
16	CHINU500	6.8	8.2	10.6	12.0	15.2	16.0	16.6	17.7	24.5
17	CHIVOR	0.3	0.5	1.4	1.5	1.6	2.6	5.4	11.5	21.6
18	CIRCO	2.5	3.6	5.4	6.3	7.7	10.4	12.3	15.6	23.5
19	COMUNEROS	0.2	0.3	0.5	0.9	1.0	1.9	2.7	5.4	9.5
20	COROZO	2.6	2.8	3.0	3.2	3.5	4.0	5.0	8.7	11.9
21	CUATRICENTENARIO	4.7	5.4	6.0	7.2	8.9	12.5	14.6	15.7	20.9
22	CUCUTABELEN	0.8	1.2	1.3	2.2	2.8	3.7	4.5	6.4	11.4
23	CUESTECITAS	4.7	5.4	6.0	7.2	8.9	12.5	14.6	15.7	20.9
24	ELCOPEY	5.5	7.0	9.2	11.2	15.0	17.3	19.3	21.3	31.5
25	ELSALTO	0.2	0.2	0.6	0.7	1.2	1.9	2.9	4.5	7.9
26	ENVIGADO	1.2	1.9	2.5	2.9	4.2	4.9	7.2	11.4	22.7
27	ESMERALDA	4.1	5.1	7.2	9.4	13.2	20.9	35.1	43.3	58.6
28	FUNDACION	4.9	5.9	6.8	8.0	11.0	14.3	19.2	22.0	32.2
29	GUADALUPEIV	0.2	0.4	0.6	0.7	1.1	2.0	2.8	4.9	8.3
30	GUAJIRA	0.2	1.0	1.2	1.3	2.4	3.9	7.0	11.4	17.1
31	GUATAPE	0.2	0.4	0.4	0.8	2.0	2.3	4.5	7.5	16.1
32	GUATIGUARA	3.5	4.4	6.0	8.1	10.7	11.9	14.0	18.1	24.5
33	GUAVIO	0.6	1.3	1.8	2.3	3.1	5.3	11.2	16.4	20.8
34	IBAGUEMIROLINDO	3.4	3.5	4.4	5.0	5.9	7.6	9.1	13.2	30.2
35	JAGUAS	0.4	0.4	0.4	0.4	0.7	1.1	2.7	5.1	10.6

Cumulative dip frequency										
Bus	Name	0.55	0.6	0.65	0.7	0.75	0.8	0.85	0.9	0.95
36	JAMONDINO	10.4	12.7	13.6	14.1	14.5	15.6	17.3	21.8	34.7
37	JUANCHITO	1.5	2.0	2.4	3.8	4.8	6.9	10.2	20.0	37.0
38	LAENEA	4.0	6.0	6.9	9.7	12.9	17.4	27.6	41.6	59.2
39	LAGUACA	0.2	0.2	0.3	0.9	1.5	2.7	4.8	9.8	27.4
40	LAHERMOSA	4.5	5.3	7.5	9.2	14.4	22.4	33.2	43.3	58.5
41	LAMESA	0.3	0.8	1.2	2.0	2.6	4.5	7.0	12.2	30.5
42	LAREFORMA	2.5	3.2	4.4	5.9	9.1	10.6	12.4	16.1	22.0
43	LASIERRA	0.2	0.5	0.8	0.9	1.3	1.8	2.7	3.7	11.0
44	LATASAJERA	0.3	0.6	0.6	0.7	0.9	1.8	3.7	6.9	13.1
45	LAVIRGINIA	4.6	6.0	7.0	10.1	14.4	21.8	32.5	43.2	58.0
46	LOSPALOS	4.1	4.9	6.8	8.5	10.6	13.6	16.7	19.6	23.1
47	MALENA	0.5	0.6	1.2	1.6	2.1	3.1	4.4	6.7	8.9
48	MERILECTRICA	0.2	0.2	0.3	0.5	0.9	1.1	2.0	4.2	8.7
49	MIRAFLORES	1.3	1.9	2.6	3.4	4.4	6.5	9.4	16.9	31.4
50	NOROESTE	1.9	2.2	3.3	3.6	5.2	9.3	13.1	20.4	31.3
51	NUEVABARRANQUILLA	0.7	1.3	1.7	2.0	2.8	4.3	6.0	7.6	20.2
52	OCANA	4.6	5.5	6.6	7.1	9.2	11.4	14.0	17.5	20.5
53	OCCIDENTE	1.0	1.2	1.6	1.7	3.0	5.0	9.4	14.9	25.8
54	ORIENTE	1.3	1.7	2.2	2.8	3.5	4.2	6.1	9.2	18.3
55	PAEZ	2.4	2.7	3.6	4.7	6.5	10.9	14.9	27.2	37.8
56	PAIPA	0.2	0.3	1.0	1.2	1.8	2.2	4.0	7.8	12.1
57	PANCE	1.2	1.7	2.3	3.0	3.7	5.6	7.2	12.5	29.3
58	PARAISO	0.2	0.3	0.5	0.7	0.9	2.3	3.9	8.0	22.8
59	PLAYAS	0.3	0.4	0.8	0.8	0.9	1.5	2.6	4.9	9.6
60	PRIMAVERA	0.3	0.7	1.1	1.4	1.9	3.0	4.3	6.9	8.4
61	PURNIO	2.8	4.5	5.8	6.6	7.1	8.1	9.2	16.6	35.5
62	SABANALARGA230	0.4	0.9	2.1	3.7	4.8	6.8	8.4	17.6	28.4
63	SABANALARGA500	7.1	8.5	9.9	10.9	12.2	15.0	18.0	21.2	26.6
64	SALVAJINA	0.3	0.6	0.6	0.9	1.2	2.1	2.8	3.7	9.3
65	SAMORE	7.4	8.4	9.9	11.3	13.4	16.2	17.8	19.8	23.3
66	SANBERNARDINO	6.1	8.7	10.9	13.8	14.3	15.4	17.2	21.4	34.0
67	SANCARLOS230	0.2	0.4	0.7	2.3	3.6	5.5	8.6	19.2	45.7
68	SANCARLOS500	1.9	2.7	3.6	5.3	8.5	11.7	13.2	18.5	30.4
69	SANFELIPE	4.0	5.2	5.8	6.0	8.8	11.1	15.3	28.0	59.4
70	SANMARCOS	1.0	1.3	1.8	3.2	4.5	7.5	14.7	21.7	41.0
71	SANMATEOCENS	1.2	2.0	2.0	3.2	3.5	4.0	5.0	8.7	11.9
72	SANMATEOEEB	1.5	2.1	2.9	4.1	6.6	9.6	12.1	15.1	24.0
73	SANTAMARTA	5.4	6.1	6.9	8.4	9.3	10.8	15.5	20.2	28.1
74	SOCHAGOTA	0.8	1.0	1.2	1.7	2.1	3.1	5.0	8.5	13.7

Cumulative dip frequency										
Bus	Name	0.55	0.6	0.65	0.7	0.75	0.8	0.85	0.9	0.95
75	TASAJERO	0.5	0.5	0.5	0.8	1.5	1.9	3.3	4.9	10.4
76	TEBSA	0.2	0.5	1.3	1.5	2.5	4.3	5.5	7.4	19.9
77	TERMOCANDELARIA	0.3	0.7	0.7	0.8	1.3	1.9	3.0	5.1	10.0
78	TERMOCENTRO	0.2	0.3	0.3	0.8	1.2	1.9	3.1	5.6	7.7
79	TERMOFLORES	0.3	0.3	0.4	1.3	2.0	2.9	5.1	6.7	17.1
80	TERNERA	0.7	0.7	0.8	1.3	1.4	2.2	3.1	5.6	11.1
81	TOLEDO	6.8	8.3	9.8	11.3	13.0	16.2	17.7	19.8	23.3
82	TORCA	1.9	2.2	4.0	5.1	7.0	8.8	12.6	19.1	30.3
83	TUNAL	2.4	3.6	4.9	7.5	9.6	10.6	12.0	15.6	23.6
84	URABA	5.7	6.3	6.4	8.0	12.4	15.4	16.8	21.4	31.1
85	URRA	5.7	6.3	6.4	8.0	12.4	15.4	16.8	21.4	31.1
86	VALLEDUPAR	6.9	8.5	10.4	12.6	15.0	15.4	17.2	20.8	28.5
87	YUMBO	0.2	0.3	1.0	2.2	2.8	4.5	8.3	18.6	34.1